

**EFFECTS OF ENDOCANNABINOIDS IN ACUTE
CEREBRAL ISCHAEMIA AND WHOLE BLOOD
PLATELET AGGREGATION IN THE RAT**

Jennifer Shearer

A thesis presented in fulfilment of the requirements for the degree of
Doctor of Philosophy.

2012

STRATHCLYDE INSTITUTE OF PHARMACY AND
BIOMEDICAL SCIENCES

UNIVERSITY OF STRATHCLYDE

DECLARATION

This thesis is the result of the author's original research. It has been composed by the author and has not been previously submitted for examination which has led to the award of a degree.

The copyright of this thesis belongs to the author under the terms of the United Kingdom Copyright Acts as qualified by University of Strathclyde Regulation 3.50. Due acknowledgement must always be made of the use of any material contained in, or derived from, this thesis.

Signed:

Date:

CONTENTS

Title	i
Declaration	ii
Contents	iii-ix
Acknowledgements	x
Publications	xi-xii
Communications	xiii-xv
Abstract	xvi
Abbreviations	xvii-xviii

CHAPTER 1

GENERAL INTRODUCTION

1.1 Cannabinoids	
1.1.1 Cannabinoid Overview	
1.1.1.1 Receptors and Signalling Pathways	2-4
1.1.1.2 Endocannabinoid Ligands	4-6
1.1.1.3 Endocannabinoid Metabolism: Release, Uptake and Inactivation	6-8
1.1.2 Physiological Role of Cannabinoids in the Central Nervous System	
1.1.2.1 Effects of Cannabinoids in the Central Nervous System	8-9
1.1.2.2 Effects of Cannabinoids on Microglia	9-10
1.1.3 Physiological Role of Cannabinoids in the Cardiovascular System	
1.1.3.1 Effects of Cannabinoids in the Cardiovascular System	11-12
1.1.3.2 Effects of Cannabinoids on Platelet Aggregation	12-14
1.2 Cerebral Ischaemia	14-15
1.2.1 Pathophysiology of Cerebral Ischaemia	15
1.2.1.1 Energy Failure	16
1.2.1.2 Elevation of Intracellular Calcium (Ca ²⁺) Level	16-17
1.2.1.3 Excitotoxicity	17-18
1.2.1.4 Oxidative Stress	18-19

1.2.1.5 Cell Death	19-20
1.2.1.6 Inflammation	20-21
1.2.1.7 Platelets	21-22
1.2.2 Models of Cerebral Ischaemia	22-24
1.2.3 Models of Platelet Aggregation	24-28
1.3 Cannabinoids and Cerebral Ischaemia	28-30
1.4 Hypothesis and Objectives	30-31

CHAPTER 2

ESTABLISHMENT OF AN INTRALUMINAL THREAD MODEL OF MIDDLE CEREBRAL ARTERY OCCLUSION IN RATS

2.1 Introduction	33
2.2 Aim	33
2.3 Methods	
2.3.1 Source of Materials	33
2.3.2 Animal Source	34
2.3.3 Animal Preparation	34-35
2.3.4 Laser Doppler Flowmetry	35-36
2.3.5 Intraluminal Filament Preparation	36
2.3.6 Intraluminal Thread Model	36-41
2.3.7 Protocols	41
2.3.7.1 Study 1: Permanent Middle Cerebral Artery Occlusion	41-43
2.3.7.2 Study 2: Transient Middle Cerebral Artery Occlusion	43-44
2.3.7.3 Study 3: Transient Middle Cerebral Artery Occlusion	44
2.3.7.4 Study 4: Transient Middle Cerebral Artery Occlusion	44
2.3.7.5 Study 5: Transient Middle Cerebral Artery Occlusion	44
2.3.7.6 Study 6: Transient Middle Cerebral Artery Occlusion	45
2.3.8 Inclusion Criteria	45
2.3.9 Neurological Deficit Score	45-47
2.3.10 Tissue Processing	47-49
2.3.11 Haematoxylin and Eosin Staining	49-52

2.3.12 Infarct Quantification	52
2.3.13 Oedema Quantification	53
2.3.14 Drug Preparation	53
2.4 Results	
2.4.1 Survival	53-56
2.4.2 Neurological Deficits	56
2.4.3 Infarct Volume	58
2.4.4 Oedema	58-62
2.4.5 Laser Doppler Flowmetry	62-66
2.4.6 Complications	66-67
2.5. Discussion	68-76

CHAPTER 3

EFFECT OF ANANDAMIDE AND URB597 ON INJURY AND MICROGLIAL RESPONSE AFTER 4 HOUR CEREBRAL ISCHAEMIA IN RATS

3.1 Introduction	78
3.2 Aim	78-79
3.3 Methods	
3.3.1 Source of Materials	79
3.3.2 Animal Source	79
3.3.3 Animal Preparation	79
3.3.4 Physiological Monitoring	80
3.3.5 Laser Doppler Flowmetry	80-81
3.3.6 Intraluminal Filament Preparation	81
3.3.7 Intraluminal Thread Model	81
3.3.8 Experimental Protocol	81-82
3.3.9 Inclusion Criteria	82-85
3.3.10 Tissue Processing	85
3.3.11 Haematoxylin and Eosin Staining	85
3.3.12 Lesion Quantification	85-88

3.3.13 Immunofluorescence	88-89
3.3.14 Confocal Microscopy	90
3.3.15 Microglia Analysis	90-91
3.3.16 Drug Preparation	92
3.3.17 Statistical Analysis	92-93
3.4 Results	
3.4.1 Physiological Variables	93-95
3.4.2 Laser Doppler Flowmetry	95
3.4.3 Infarct Volume	95-102
3.4.4 Microglia Number and Activation	102-110
3.5 Discussion	110-115

CHAPTER 4

EFFECT OF 2-ARACHIDONOYL GLYCEROL (2-AG) AND JZL184 ON INJURY AND MICROGLIAL RESPONSE AFTER 4 HOUR CEREBRAL ISCHAEMIA IN RATS

4.1 Introduction	117
4.2 Aim	118
4.3 Methods	
4.3.1 Source of Materials	118
4.3.2 Animal Source	118
4.3.3 Animal Preparation	
4.3.3.1 Pilot Study: Haemodynamic Study	118-119
4.3.3.2 Main Study: Middle Cerebral Artery Occlusion Study	119
4.3.4 Laser Doppler Flowmetry	119
4.3.5 Intraluminal Filament Preparation	119-120
4.3.6 Intraluminal Thread Model	120
4.3.7 Experimental Protocol	
4.3.7.1 Pilot Study: Haemodynamic Study	120-122
4.3.7.2 Main Study: Middle Cerebral Artery Occlusion Study	122-125
4.3.8 Inclusion Criteria	125

4.3.9 Tissue Processing	125
4.3.10 Haematoxylin and Eosin Staining and Lesion Quantification	126
4.3.11 Immunofluorescence	126
4.3.12 Confocal Microscopy and Microglia Analysis	126
4.3.13 Drug Preparation	126-127
4.3.14 Statistical Analysis	127-128
4.4 Results	
4.4.1 Pilot Study	
4.4.1.1 Haemodynamic Measurements	128-133
4.4.2 Main Study: Middle Cerebral Artery Occlusion	
4.4.2.1 Physiological Variables	133-136
4.4.2.2 Laser Doppler Flowmetry	136-140
4.4.2.3 Infarct Volume	140
4.4.2.4 Microglia Number and Activation	140-146
4.5 Discussion	146-158

CHAPTER 5

CHARACTERISATION OF 2-ARACHIDONOYL GLYCEROL (2-AG)-INDUCED PLATELET AGGREGATION IN RAT WHOLE BLOOD

5.1 Introduction	160-161
5.2 Aim	161
5.3 Methods	
5.3.1 Source of Materials	161
5.3.2 Animal Source	161
5.3.3 Animal Preparation	162
5.3.4 Surgical Procedure	162
5.3.5 Whole Blood Aggregometry	162-163
5.3.6 Experimental Protocol	
5.3.6.1 Ethanol Vehicle	163
5.3.6.2 Agonist Response	163-164
5.3.6.3 Cannabinoid Receptors	164

5.3.6.4	Role of Metabolism	164-165
5.3.6.5	Agonist Interaction	165-166
5.3.7	Drug Preparation	166-168
5.3.8	Statistical Analysis	168-169
5.4	Results	
5.4.1	Ethanol Vehicle	169
5.4.2	Agonist Response	169-172
5.4.3	Cannabinoid Receptors	172-175
5.4.4	Role of Metabolism	176
5.4.5	Agonist Interaction	176-181
5.5	Discussion	181-192

CHAPTER 6

GENERAL DISCUSSION

6.1	Novel Findings	194
6.2	Was a Model of Transient Cerebral Ischaemia Established?	194-196
6.3	Do Endocannabinoids Modify Injury Development in Acute Cerebral Ischaemia?	196-197
6.4	Do Endocannabinoids Modify Haemodynamic Measurements and Cerebral Blood Flow in Acute Cerebral Ischaemia?	197
6.5	Do Endocannabinoids Modify the Microglia Response following Injury in Acute Cerebral Ischaemia?	198-199
6.6	Do Endocannabinoids Produce Platelet Aggregation in Rat Whole Blood?	199
6.7	Potential Limitations	199-202
6.8	Future Work	202-204
6.9	Clinical Relevance	204-207
	REFERENCES	209-243

APPENDICES

Appendix A: Equipment and Materials	245-246
Materials for <i>In Vivo</i> Experiments	247
Appendix B: Suppliers of Drugs	248-250

ACKNOWLEDGEMENTS

I would like to express my gratitude to my supervisors, Dr Hilary Carswell, Dr Susan Coker and Professor Kathy Kane, for giving me the opportunity to perform this work. Over the years I have come to appreciate their words of wisdom and their patience and resilience in the face of all the difficulties which have occurred along the way.

I would like to thank the BBSRC Capacity Building Award in Integrative Mammalian Biology for providing the funding for my project. This work has allowed me to gain new skills and expertise which I am sure I will continue to be grateful for in the future.

During the completion of this work I have received assistance from a number of important individuals who I would also like to thank; the technical staff, including Tony Preston, David Blatchford and all of the staff in the BPU who have provided help on numerous occasions; Lindsay Gallagher, Professor Mhairi Macrae and everyone at the Wellcome Surgical Institute who helped develop the surgical model; the cardiovascular and neuroscience lab groups for their insightful input and the many other students who have shared a lab or office with me over the past 3 years and spent considerable time listening to me complain about my latest bad day.

Finally, I would like to thank my family: my mother; father; my sister, Gillian; and my grandmother, who continue to support me as I write the final sentence in this thesis and always make the days brighter. Their patience and support has made this work possible.

Thank you.

PUBLICATIONS

Work completed during PhD:

Shearer JA, Kane KA, Coker SJ and Carswell HV. Characterisation of 2-arachidonoyl glycerol induced platelet aggregation in rat whole blood. *Manuscript in preparation.*

Shearer J, Coker S and Carswell H (2011). Effect of anandamide on early injury development and microglia response following 4 hr cerebral ischaemia in rats. Proceedings of the International Society for Cerebral Blood Flow and Metabolism at <http://kenes.com/brain2011/abstracts/pdf/548.pdf> (Abstract from International Symposium on Cerebral Blood Flow, Metabolism and Function and Quantification of Brain Function with PET 2011).

Shearer J, Kane K, Carswell H and Coker S (2009). Endocannabinoids and platelet aggregation: effects of 2-arachidonoyl glycerol in rat whole blood. Proceedings of the British Pharmacological Society at <http://www.pA2online.org/abstracts/Vol7Issue3abst024P.pdf> (Abstract from 7th James Black Conference 2009).

Shearer J, Kane K, Carswell H and Coker S (2009). Characterisation of 2-arachidonoyl glycerol-induced platelet aggregation in rat whole blood. Proceedings of the British Pharmacological Society at <http://www.pA2online.org/abstracts/Vol7Issue1abst022P.pdf> (Abstract from New Drugs in Cardiovascular Research Meeting 2009).

Work completed during Masters in Research (MRes):

Shearer J, Kane K, Carswell H and Coker S (2009). Does gender modify the effect of 2-arachidonoyl glycerol on platelet aggregation in rat whole blood? Proceedings of the British Pharmacological Society at <http://www.pa2online.org/abstracts/volume7issue021p.pdf> (Abstract from Summer Meeting 2009).

COMMUNICATIONS

Work completed during PhD:

Glasgow Neuroscience Group Meeting, Glasgow, UK (2012)

Oral communication: Effect of endocannabinoids on acute cerebral ischaemia and microglia response. *J Shearer, S Coker and H Carswell.*

Scottish neuroscience Group Meeting, Aberdeen, UK (2011)

Poster communication: Effect of anandamide on injury development and microglia response following 4 hr cerebral ischaemia in rats. *J Shearer, S Coker and H Carswell.*

Integrative Mammalian Biology Centre: Animal Welfare (3Rs) Meeting, Manchester, UK (2011)

Poster communication: Effect of anandamide on early injury development and microglia response following 4 hr cerebral ischaemia in rats. *J Shearer, S Coker and H Carswell.*

International Symposium on Cerebral Blood Flow, Metabolism and Function and Quantification of Brain Function with PET, Barcelona, Spain (2011)

Poster communication: Effect of anandamide on early injury development and microglia response following 4 hr cerebral ischaemia in rats. *J Shearer, S Coker and H Carswell, PP548.*

Glasgow Neuroscience Group Meeting, Glasgow, UK (2011)

Poster communication: Effect of anandamide on early injury development and microglia response following 4 hr cerebral ischaemia in rats. *J Shearer, S Coker and H Carswell.*

Joint Meeting of British Pharmacological and Physiological Societies (7th James Black Conference), London, UK (2009)

Poster communication: Endocannabinoids and platelet aggregation: effects of 2-arachidonoyl glycerol in rat whole blood. *J Shearer, K Kane, H Carswell and S Coker, PP024.*

Joint Meeting of British Pharmacology Society and German Societies for Pharmacology and Clinical Pharmacology (New Drugs in Cardiovascular Research), Dresden, Germany (2009)

Poster communication: Characterisation of 2-arachidonoyl glycerol-induced platelet aggregation in rat whole blood. *J Shearer, K Kane, H Carswell and S Coker, PP022.*

Work completed during Masters in Research (MRes):

British Pharmacological Society Summer Meeting. Edinburgh, UK (2009)

Poster communication: Does gender modify the effect of 2-arachidonoyl glycerol on platelet aggregation in rat whole blood? *J Shearer, K Kane, H Carswell and S Coker, PP021.*

Scottish Cardiovascular Forum, Inverness, UK (2009)

Poster communication: Gender differences in the effect of 2-arachidonoyl glycerol on platelet aggregation in rat whole blood. *J Shearer, K Kane, H Carswell and S Coker.*

ABSTRACT

Cerebral ischaemia causes an increase in the endocannabinoid anandamide and expression of cannabinoid receptors in the brain. Endocannabinoids are known to exert anti-inflammatory effects and may reduce injury in cerebral ischaemia through modulation of the immune response. The aims of this study were to examine the effect of endocannabinoids, anandamide and 2-AG, in acute cerebral ischaemia and investigate the mechanisms involved, including characterising the microglia response. Endocannabinoids exert pro-aggregatory effects in human platelets and may affect cerebral ischaemia through actions on platelets. As such, it was decided to characterise the effects of endocannabinoids on platelet aggregation in rat whole blood.

Anaesthetised rats underwent 4 hour permanent middle cerebral artery occlusion and received either: anandamide (10mg/kg, s.c.); 2-AG (6mg/kg, i.v.); metabolism inhibitors, URB597 (0.3mg/kg, s.c.) or JZL184 (10mg/kg, i.v.); or appropriate vehicle. Whole blood aggregometry was performed to examine the aggregatory effect of 2-AG (19-300 μ M) alone and in the presence of cannabinoid receptor antagonists and metabolism inhibitors.

Anandamide and URB597 did not affect total injury volume but modified injury topography with reduced cortical and increased subcortical injury. In contrast, 2-AG and JZL184 increased cortical injury volume (111.7 \pm 9.4mm³ and 121.3 \pm 10.1mm³ vs. 82.3 \pm 3.5mm³) and JZL184 increased total injury (167.9 \pm 13.5mm³ vs. 134.7 \pm 5.7mm³). Neither anandamide nor 2-AG significantly affected microglia number or activation. The detrimental effect of 2-AG and JZL184 may be related to a reduction in cerebral blood flow (20.2 \pm 8.8% and 22.7 \pm 6.4 at 4 hours vs. 56.4 \pm 12.1% with vehicle). In rat whole blood 2-AG produced aggregation at micromolar concentrations through CB₂ receptors and COX metabolism to form thromboxane A₂. Addition of 2-AG and ADP in combination potentiated the ADP response. Endocannabinoids modified injury development in acute cerebral ischaemia but did not affect the microglia response. The effects of 2-AG on injury may be related to changes in cerebral blood flow and platelet aggregation.

ABBREVIATIONS

2-AG	–	2-Arachidonoyl glycerol
5-HT	–	5-Hydroxytryptamine
ACA	–	Anterior cerebral artery
ADP	–	Adenosine diphosphate
AMPA	–	α -Amino-3-hydroxy-5-methyl-4-isoxazolepropionic acid
ANOVA	–	Analysis of variance
ATP	–	Adenosine triphosphate
BA	–	Basilar artery
BPM	–	Beats per minute
BPU	–	Biological procedures unit
Ca ²⁺	–	Calcium ions
cAMP	–	Cyclic adenosine monophosphate
CB	–	Cannabinoid receptor
CCA	–	Common carotid artery
CCAO	–	Common carotid artery occlusion
COX	–	Cyclooxygenase
DAPI	–	4',6-diamidino-2-phenylindole
DMSO	–	Dimethyl sulfoxide
ECA	–	External carotid artery
ETCO ₂	–	End-tidal carbon dioxide
FITC	–	Fluorescein isothiocyanate
GABA	–	γ -Aminobutyric acid
H ⁺	–	Hydrogen ions
HIF-1	–	Hypoxia inducible factor 1
HPLC	–	High pressure liquid chromatography
Iba-1	–	Ionised calcium binding adaptor molecule 1
ICA	–	Internal carotid artery
ID	–	Internal diameter
IL	–	Interleukin
i.p	–	Intraperitoneal
IP3	–	Inositol trisphosphate
i.v	–	Intravenous
K ⁺	–	Potassium ions
Ling	–	Lingual artery
LPS	–	Lipopolysaccharide
Max	–	Maxillary artery
MCA	–	Middle cerebral artery
MCAO	–	Middle cerebral artery occlusion
MLC	–	Myosin light chain
MLCK	–	Myosin light chain kinase
MMP	–	Matrix metalloproteinase
mPTP	–	Mitochondrial permeability transition pore
N ₂ O	–	Nitrous oxide
Na ⁺	–	Sodium ions
NaOH	–	Sodium hydroxide
NF- κ B	–	Nuclear factor- κ B

NMDA	–	N-Methyl-D-aspartate
NOS	–	Nitric oxide synthase
O ₂	–	Oxygen
OccA	–	Occipital artery
OD	–	Outer diameter
PAF	–	Platelet activating factor
PBS	–	Phosphate buffered saline
PCA	–	Posterior cerebral artery
PCR	–	Polymerase chain reaction
PEG	–	Polyethylene glycol
PI3-K	–	Phosphatidyl inositol-3-kinase
PLA	–	Phospholipases A ₂
PLC	–	Phospholipase C
PTA	–	Pterygopalatine artery
RhoA	–	Ras homolog gene family, member A
ROS	–	Reactive oxygen species
s.c	–	Subcutaneous
S.E.M	–	Standard error of the mean
SO ₂	–	Oxygen saturation
STA	–	Superior thyroid artery
STAIR	–	Stroke therapy academic and industry roundtable
STAT-3	–	Signal transducer and activator of transcription-3
Δ ⁹ -THC	–	Δ ⁹ -Tetrahydrocannabinol
TNF-α	–	Tumour necrosis factor-α
Tpa	–	Tissue plasminogen activator
TRPV	–	Transient potential vanilloid receptor
TXA ₂	–	Thromboxane A ₂

CHAPTER 1

GENERAL INTRODUCTION

1.1 Cannabinoids

1.1.1 Cannabinoid Overview

Cannabis (*Cannabis sativa*) is one of the most widely used drugs in the world which has been utilised for centuries for recreational and medicinal purposes (Pacher *et al.*, 2006). Cannabinoids are a group of pharmacologically active compounds which can be extracted from the cannabis plant. Cannabis can exert a diverse range of physiological effects, including neurological and behavioural changes, immunomodulation and potent cardiovascular effects (Pacher *et al.*, 2006). Δ^9 -Tetrahydrocannabinol (Δ^9 -THC) is the main active component of the cannabis plant and its physiological and pharmacological properties have been studied extensively. Increasing fear of abuse led to the prohibition of cannabis for recreational purposes in the United Kingdom in 1928 and prescription for medicinal use was banned in 1973 (Sleator and Allen, 2000). The illegal status of cannabis and the subsequent social stigma have significantly limited research into the effects of cannabinoids.

1.1.1.1 Receptors and Signalling Pathways

Pharmacological studies with Δ^9 -THC support the involvement of specific cannabinoid receptors in mediating the effects of these compounds. Inhibition of adenylyl cyclase activity by Δ^9 -THC was sensitive to pertussis toxin which inhibits G-protein signalling (Howlett *et al.*, 1986). Additionally, radiolabelled cannabinoids were shown to bind to rat brain homogenate in a stereoselective manner (Devane *et al.*, 1988). Molecular cloning studies identified two saturable high affinity cannabinoid receptors, known as CB₁ and CB₂. CB₁ receptors are predominantly expressed in the central nervous system (Svíženská *et al.*, 2008) and have been

associated with the behavioural effects of cannabinoids (Ashton and Glass, 2007). CB₁ receptors have also been identified in peripheral organs; including spleen, small intestine, myocardium and vascular smooth muscle cells (Pacher *et al.*, 2005). CB₂ receptors exhibit 44% amino acid homology with CB₁ and are predominantly expressed on immune cells (Munro *et al.*, 1993). CB₂ receptors have been identified on resident immune cells in the central nervous system, such as microglia and astrocytes, and peripheral blood cells, including neutrophils, lymphocytes, monocytes and mast cells (Svíženská *et al.*, 2008; Racz *et al.*, 2008; Galiègue *et al.*, 1995). CB₂ receptors are believed to be involved in modulation of the immune response. Activation of CB₂ receptors has been shown to suppress release of pro-inflammatory cytokines and augment anti-inflammatory cytokine release (Molina-Holgado *et al.*, 2003; Berdyshev *et al.*, 2000).

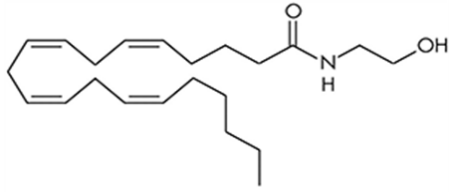
Several studies have utilised selective receptor antagonists and CB₁/CB₂ knockout mice to elucidate the receptors involved in mediating the various effects of cannabinoids. Evidence from these studies has suggested that cannabinoids can exert their effects through additional receptor types, including vanilloid receptors, orphan GPR55 and a novel, as yet unidentified, non-CB₁/CB₂ receptor (Pacher *et al.*, 2006; Járai *et al.*, 1999; Ryberg *et al.*, 2007; Pertwee *et al.*, 2010). A range of potent synthetic cannabinoids and selective inhibitors for CB₁ and CB₂ receptors have been developed to study the cannabinoid system. Unfortunately, the use of cannabinoid receptor antagonists is complicated by lack of absolute receptor specificity and inverse agonism at cannabinoid receptors (Pertwee, 2005).

Both cannabinoid receptors, CB₁ and CB₂, are coupled to a G_{i/o} protein and contain seven-transmembrane domains (Felder *et al.*, 2006). Activation of cannabinoid receptors directly inhibits adenylyl cyclase activity to reduce cAMP, activates mitogen activated protein kinase and phosphatidyl inositol-3-kinase and can also affect ion channel function (Pacher *et al.*, 2006). Cannabinoid receptor agonists cause inhibition of L-type calcium (Ca²⁺) channels and activation of inwardly rectifying potassium (K⁺) channels (Pacher *et al.*, 2006). Modulation of the function of these ion channels produces hyperpolarisation and inhibits activity of the cell.

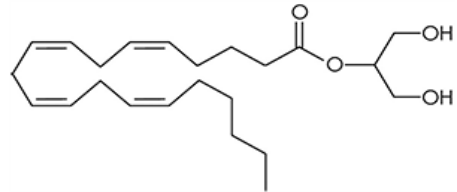
1.1.1.2 Endocannabinoid Ligands

Endogenous cannabinoids, known as endocannabinoids, are a group of lipid mediators which can bind to and activate cannabinoid receptors. Endocannabinoids are involved in several important physiological functions; including nervous and cardiovascular function and the immune response. The main endocannabinoid mediators are anandamide and 2-arachidonoyl glycerol (2-AG). These mediators were first discovered in porcine and rat brain by Devane *et al.* (1992) and Sugiura *et al.* (1995), respectively. The chemical structures of the main endogenous, plant-derived and synthetic cannabinoids are shown in **figure 1.1**. Endocannabinoids have been identified in plasma, brain and peripheral tissues (Pacher *et al.*, 2006). Each endocannabinoid mediator exhibits different receptor binding properties. Anandamide acts a partial agonist at CB₁ and CB₂ receptors, with higher affinity at CB₁, and as a full agonist at the vanilloid receptor, TRPV₁ (transient potential vanilloid receptor), in certain conditions (Pacher *et al.*, 2006). 2-AG is the most abundant endocannabinoid in brain tissue, 170 times greater than anandamide (Stella

A. Endogenous Cannabinoids

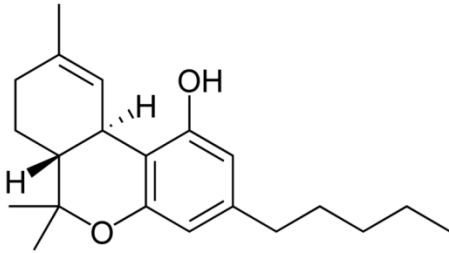


Anandamide

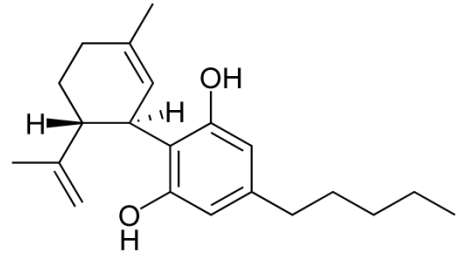


2-Arachidonoyl glycerol (2-AG)

B. Plant-Derived Cannabinoids



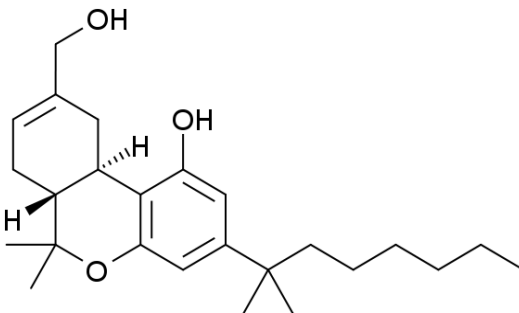
Δ^9 -tetrahydrocannabinol (Δ^9 -THC)



Cannabidiol

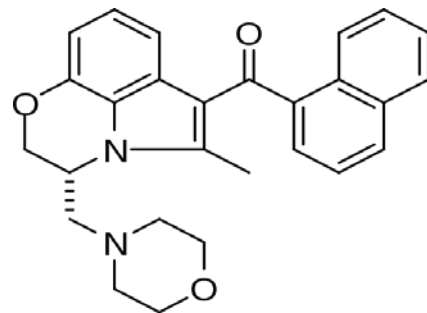
C. Synthetic Cannabinoids

Classical



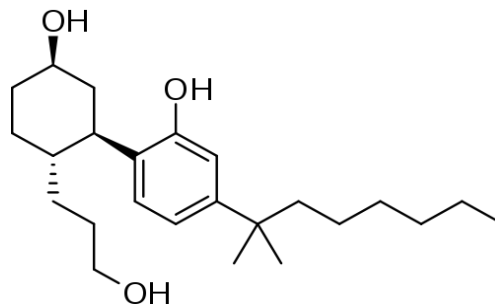
HU-210

Non-Classical



WIN 55-212,2

Aminoalkylindol



CP 55,940

Figure 1.1: Chemical structure of selected A) endogenous, B) plant-derived and C) synthetic cannabinoids.

et al., 1997). 2-AG acts as a full agonist at both CB₁ and CB₂ receptors with a lower potency than anandamide (Felder *et al.*, 2006; Hillard *et al.*, 2000).

1.1.1.3 Endocannabinoid Metabolism: Release, Uptake and Inactivation

Endocannabinoids are synthesised “on demand” by certain cell types in response to increased intracellular Ca²⁺ (Hillard *et al.*, 2000). Intracellular endocannabinoid concentrations are very low under basal conditions and are increased following nerve depolarisation or receptor activation (Hillard *et al.*, 2000). Endocannabinoids are structurally related to arachidonic acid and are produced through stimulated hydrolysis of phospholipid precursors. Synthesis and inactivation pathways for anandamide and 2-AG are shown in **figure 1.2**. Anandamide is predominantly synthesised through Ca²⁺-activated hydrolysis of N-arachidonoyl phosphatidylethanolamide (NAPE) by phospholipase D (Pacher *et al.*, 2006). In platelets, anandamide may also be synthesised by condensation of arachidonic acid and ethanolamine via reverse activity of the metabolism enzyme fatty acid amide hydrolase (Maccarrone *et al.*, 2002). Following receptor activation, the intracellular messenger, diacylglycerol, is released from membrane phospholipids by phospholipase C (PLC) (Pacher *et al.*, 2006). 2-AG is generated from diacylglycerol by diacylglycerol lipase (Pacher *et al.*, 2006).

Endocannabinoids are inactivated by a 2 step process; involving uptake into the cell and hydrolysis by several enzymes. Circulating anandamide can be taken into cells by a saturable nitric oxide-dependent bi-directional membrane carrier (De Petrocellis *et al.*, 2004) or through passive diffusion driven by metabolism (Fasia *et al.*, 2003).

The mechanism of anandamide uptake varies between cell types. 2-AG can enter cells through a specific saturable membrane carrier (Maccarrone *et al.*, 2001). Anandamide and 2-AG are primarily metabolised by fatty acid amide hydrolase and monoacylglycerol lipase, respectively, in neurones (Pacher *et al.*, 2006). 2-AG can also be degraded by fatty acid amide hydrolase in leukocytes and platelets (Di Marzo *et al.*, 1999; Maccarrone *et al.*, 2001). Fatty acid amide hydrolase and monoacylglycerol lipase metabolise anandamide and 2-AG to form arachidonic acid and ethanolamine or arachidonic acid and glycerol, respectively (Sugiura *et al.*, 2006). Endocannabinoid metabolism forms free arachidonic acid which may subsequently be used for cyclooxygenase (COX)-dependent prostanoid production. Generation of prostanoids through COX metabolism may be involved in mediating some of the effects of endocannabinoids. Anandamide and 2-AG are also substrates for direct metabolism by COX-2 to form prostaglandin ethanolamine and prostaglandin glycerol ester, respectively, which can undergo further metabolism to form prostanoids (Kozak *et al.*, 2001; 2004).

1.1.2 Physiological Role of Cannabinoids in the Central Nervous System

1.1.2.1 Effects of Cannabinoids in the Central Nervous System

As stated previously, CB₁ receptors are widely expressed throughout the central nervous system with highest expression in the basal ganglia, cerebellum and cortex (Pettit *et al.*, 1998; Mackie, 2005). Activation of CB₁ receptors has been associated with the typical neurological effects of cannabinoids; catalepsy (rigid mobility), sedation, analgesia and hypothermia (Long *et al.*, 2009). CB₁ receptors are expressed on the axon terminals of pre-synaptic neurones, primarily cholecystinin-positive

interneurons which release γ -aminobutyric acid (GABA) (Katona *et al.*, 2000; Freund *et al.*, 2003). Anandamide and 2-AG are released from post-synaptic neurones and activate pre-synaptic CB₁ receptors in a process known as “retrograde signalling” (Pacher *et al.*, 2006). Activation of pre-synaptic CB₁ receptors causes cell depolarisation and suppresses the release of inhibitory or excitatory neurotransmitters, including GABA, acetylcholine, 5-hydroxytryptamine (5-HT), noradrenaline and cholecystokinin (Freund *et al.*, 2003). This process, known as depolarisation-induced suppression of inhibition or excitation, is a cannabinoid-specific effect which can be observed using *in vitro* electrophysiology. Activation of CB₁ receptors is believed to reduce neurotransmitter release through inhibition of N-type voltage-gated Ca²⁺ channels which prevents Ca²⁺ influx and subsequent initiation of vesicle formation and release of stored neurotransmitters. Endocannabinoids can influence cell function by reducing the influx of extracellular Ca²⁺ via P/Q-type voltage-sensitive Ca²⁺ channels (Twitchell *et al.*, 1997) and release of stored intracellular Ca²⁺ through ryanodine receptors (Zhuang *et al.*, 2005). Endocannabinoids also activate Ca²⁺-activated K⁺ channels and inwardly rectifying conductance K⁺ channels to promote K⁺ efflux and membrane hyperpolarisation (Romano and Lograno, 2006)

1.1.2.2 Effects of Cannabinoids on Microglia

CB₂ receptors have been identified on resident immune cells in the central nervous system, such as microglia. Under normal circumstances, microglia express low levels of CB₁ and CB₂ receptors (Cabral and Marciano-Cabral, 2005). However, CB₂ receptors are highly expressed in primed and activated microglia which also release

anandamide and 2-AG (Cabral and Marciano-Cabral, 2005; Walter *et al.*, 2003).

Activated microglia can exhibit multiple phenotypes; including phagocytosis, release of cytotoxic mediators (including proteinases and nitric oxide) and pro- and anti-inflammatory cytokines and secretion of growth factors (Lalancette-Hébert *et al.*, 2007). It has been proposed that microglia may be detrimental in cerebral ischaemia by contributing to the inflammatory response (Gehrmann *et al.*, 1995). Alternatively, microglia may protect injured neurons by release of anti-inflammatory cytokines and secretion of growth factors (Neumann *et al.*, 2006). Previous studies have demonstrated that endocannabinoids can influence the phenotype of microglia *in vitro*. Activation of CB₂ receptors on lipopolysaccharide (LPS)-activated microglia inhibited microglial migration in response to adenosine diphosphate (ADP) (Romero-Sandoval *et al.*, 2009) and reduced release of the pro-inflammatory cytokines; tumour necrosis factor- α (TNF- α), interleukin-1 (IL-1) and interleukin-6 (IL-6) (Puffenbarger *et al.*, 2000). CB₁ activation inhibited the production of nitric oxide in LPS-activated microglia (Waksman *et al.*, 1999). The endocannabinoid, 2-AG, increased proliferation of cultured microglia (Carrier *et al.*, 2004) and induced concentration-dependent migration via CB₂ receptor activation (Walter *et al.*, 2003). Both endocannabinoids, anandamide and 2-AG, reduced the release of TNF- α from LPS-activated microglia (Facchinetti *et al.*, 2003). Exposure to anandamide increased release of the anti-inflammatory cytokine, IL-10, from LPS-activated microglia (Correa *et al.*, 2010). As such, it is possible that endocannabinoids could exert a beneficial effect on microglia *in vivo* following cerebral ischaemia.

1.1.3 Physiological Role of Cannabinoids in the Cardiovascular System

1.1.3.1 Effects of Cannabinoids in the Cardiovascular System

Endogenous cannabinoids are released from endothelial cells, activated platelets and macrophages in the vasculature (Maccarrone *et al.*, 2002; Varga *et al.*, 1998; Di Marzo *et al.*, 1999). Cannabinoids can bind to CB₁ receptors in the myocardium and on the endothelium and vascular smooth muscle throughout the vasculature (Pacher *et al.*, 2008). CB₂ receptors are also expressed in the myocardium and coronary blood vessels (Pacher *et al.*, 2008). The endocannabinoids, anandamide and 2-AG, exert potent vasodilatory effects in isolated vessels from several tissues and *in vivo* administration is associated with the development of widespread hypotension (reviewed in Pacher *et al.*, 2005). Anandamide produced vasodilation in cat cerebral arteries and rat coronary arteries by inhibition of L-type Ca²⁺ channels (Gebremedhin *et al.*, 1999) and activation of Ca²⁺-activated K⁺ channels (White *et al.*, 2001), respectively.

In other preparations, anandamide has been shown to produce vasodilation in various vessel types through activation of TRPV₁ receptors (Peroni *et al.*, 2007) or metabolism via COX (Grainger and Boachie-Ansah, 2001; Pratt *et al.*, 1998). 2-AG can produce vasodilation of rat middle cerebral and bovine coronary arteries through CB₁ activation (Hillard *et al.*, 2007) and metabolism of 2-AG via COX to form prostanoids (Gauthier *et al.*, 2005), respectively. Anandamide treatment produced vasodilation of rat cerebral blood vessels *in vivo* and increased cerebral blood flow through activation of vascular CB₁ receptors (Wagner *et al.*, 2001).

Systemic anandamide administration produced a triphasic haemodynamic response with transient hypotension (phase I) and a brief non-sympathetic pressor response (phase II) followed by prolonged hypotension and bradycardia (5-10 minutes) (phase III) (Lake *et al.*, 1997). 2-AG administration produced systemic hypotension and tachycardia (Járai *et al.*, 2000). 2-AG-induced hypotension was inhibited by the CB₁ antagonist SR141716A in rats (Varga *et al.*, 1998) but not in mice (Járai *et al.*, 2000). The hypotensive effect of 2-AG in mice was sensitive to the COX inhibitor, indomethacin. However, the stable 2-AG analogue, 2-arachidonyl glycerol ether, produced similar hypotension via activation of CB₁ receptors (Járai *et al.*, 2000). Endocannabinoids are released from the endothelium and activated platelets or macrophages. These mediators have been shown to produce vasodilation in isolated blood vessels and hypotension *in vivo* through binding to vascular CB₁ receptors.

1.1.3.2 Effects of Cannabinoids on Platelet Aggregation

Platelets are an important site of endocannabinoid production and metabolism within the vasculature (Randall, 2007). Recent studies in human platelets have identified several components of the endocannabinoid system; including CB₁ and CB₂ receptors and the metabolism enzyme fatty acid amide hydrolase (Randall, 2007). 2-AG is the primary endocannabinoid released from activated platelets. Human platelets have been shown to contain 1.4 mM 2-AG, 20-fold greater than anandamide (Maccarrone *et al.*, 2002).

Anandamide has been shown to activate washed human platelets at a supraphysiological concentration (1.3mM), however, no activation was observed in

platelet-rich plasma (Maccarrone *et al.*, 1999). As high anandamide concentrations are required to activate platelets it is unlikely that anandamide exerts pro-aggregatory effects *in vivo*. In human platelet-rich plasma, anandamide reduced secretion of 5-HT from ADP-activated platelets at nanomolar concentrations (Maccarrone *et al.*, 2002). 2-AG has been shown to produce platelet activation in human platelet-rich plasma (Maccarrone *et al.*, 2001) and cause aggregation in human and rat whole blood at high micromolar concentrations, maximal at 200 μ M (Keown *et al.*, 2010; Shearer *et al.*, 2009 (abstract)).

There is controversy over the mechanisms involved in mediating the aggregatory response to 2-AG. 2-AG produced aggregation in human whole blood through metabolism by monoacylglycerol lipase and COX with no involvement of cannabinoid receptors (Keown *et al.*, 2010). In contrast, the response to 2-AG in human platelet-rich plasma was mediated through a cannabinoid receptor sensitive to both CB₁ and CB₂ antagonists with no involvement of COX metabolism (Maccarrone *et al.*, 2001). In human platelet-rich plasma, 2-AG was shown to interact with physiological agonists to modify the platelet response (Maccarrone *et al.*, 2001). In these experiments in human platelet-rich plasma, 2-AG-induced platelet activation was reduced by ADP and collagen and the interaction of 5-HT and 2-AG enhanced the platelet response in a synergistic manner and increased release of 2-AG (Maccarrone *et al.*, 2001; 2003). These studies demonstrated that human platelets express cannabinoid receptors and synthesise and degrade endocannabinoids. Both anandamide and 2-AG can produce platelet aggregation in human platelets and modify the response to other aggregatory agents. However, the

mechanisms involved in mediating these effects are unclear.

1.2 Cerebral Ischaemia

Stroke is a major cause of death worldwide resulting in 10-12% of all deaths in industrialised countries and accounts for more than 4% of healthcare costs (Donnan *et al.*, 2008). Stroke is the leading cause of long-term disability in adults with one third of sufferers being dependent on others at 6 months after initial injury (Durukan and Tatlisumak, 2007). Disability following stroke varies between individuals depending on the severity of the infarct and region of the brain affected and can produce impairments in memory, communication and movement, such as partial paralysis (Lakhan *et al.*, 2009).

Stroke can be classified as haemorrhagic or ischaemic (Donnan *et al.*, 2008). Ischaemic stroke is the most common type of stroke and occurs in 80% of patients (Donnan *et al.*, 2008). Ischaemic stroke involves the blockage of an artery supplying blood to a specific area of the brain by a thrombus or embolus (Donnan *et al.*, 2008). The extent of injury is dependent on the duration and severity of ischaemia and presence of collateral blood flow to maintain oxygenation of the penumbral tissue (Lakhan *et al.*, 2009). The main treatment for ischaemic stroke in the acute stage is tissue reperfusion using thrombolytic drugs such as tissue plasminogen activator (tPA) (Donnan *et al.*, 2008). Thrombolytic therapy can reduce infarct size and improve functional recovery following stroke (Donnan *et al.*, 2008). However, the benefit of this treatment is limited by the short therapeutic window (4.5 hours from onset) and risk of intracerebral haemorrhage (Hatcher and Starr, 2011; Derex and

Nighoghossian, 2008).

1.2.1 Pathophysiology of Cerebral Ischaemia

Within minutes of onset, ischaemia initiates a complex injury process, known as the ischaemic cascade, which ultimately leads to cell death (Lakhan *et al.*, 2009). Following occlusion of a cerebral artery, blood flow to the area supplied by this vessel is significantly reduced. If cerebral blood flow is reduced below a certain threshold, 20% of the contralateral hemisphere, then cell death can occur within several minutes (Lo *et al.*, 1996; González, 2006). In this area, cells are irreversibly damaged by ischaemia and form the core of the infarct. In areas peripheral to the occluded vessel the tissue may be partially perfused by collateral vessels which allow cell function to be preserved (cerebral blood flow of 40-70% contralateral hemisphere) (Lo *et al.*, 1996). In this “penumbra” the cells are reversibly injured and can survive if the tissue is reperfused (González, 2006). However, over time this penumbral tissue will succumb to the detrimental effects of reduced blood flow and excitotoxicity resulting in expansion of the infarct (Lo *et al.*, 1996). It is considered that in rats most of the affected cells will be irreversibly injured by 4 hours post-occlusion and are certain to become apoptotic at a later time-point (Park *et al.*, 1988). Therefore, at 4 hours post-occlusion the injury boundary can be reliably identified by microscopy (Park *et al.*, 1988). In contrast, in humans the reversibly injured cells may remain salvageable for a longer period (Phan *et al.*, 2002; Heiss, 2000).

1.2.1.1 Energy Failure

The ischaemic insult reduces cerebral blood flow and causes oxygen and glucose deprivation in cells supplied by the occluded vessel. In the absence of oxygen, the main source of adenosine triphosphate (ATP) production for cell metabolism is lost (Hertz, 2008). These cells then undergo anaerobic glycolysis which is associated with low energy production. Anaerobic glycolysis produces lactate and hydrogen (H^+) ions resulting in acidosis. H^+ ions are removed from the cell through increased activity of the Na^+/H^+ exchanger which results in an influx of sodium (Na^+) into the cell (Hertz, 2008). Failure of energy production causes a disturbance in ATP-dependent ion channels; Na^+/K^+ -ATPase and Ca^{2+}/H^+ -ATPase, and reversal of the Na^+/Ca^{2+} transporter in an attempt to remove excess Na^+ (Phan *et al.*, 2002; Hertz, 2008). The result is an increase in intracellular Ca^{2+} and Na^+ leading to a loss of ionic homeostasis and excessive depolarisation of the cell membrane.

1.2.1.2 Elevation of Intracellular Calcium (Ca^{2+}) Level

During ischaemia, Ca^{2+} can enter cells through reversal of the Na^+/Ca^{2+} transporter and via opening of voltage and storage-operated Ca^{2+} channels and N-methyl-D-aspartate (NMDA) and α -amino-3-hydroxy-5-methyl-4-isoxazole propionic acid (AMPA)-type glutamate channels (Dirnagl *et al.*, 1999). Ca^{2+} can also be released from intracellular organelles, such as mitochondria and the endoplasmic reticulum. Ca^{2+} overload causes an increase in mitochondrial Ca^{2+} which promotes formation of the mitochondrial permeability transition pore (mPTP) (Sims and Muyderman, 2010). The mPTP allows efflux of Ca^{2+} ions to the cytosol and influx of water resulting in mitochondrial swelling and release of cytochrome C (Szydlowska

and Tymianski, 2010).

High intracellular Ca^{2+} can damage cells through overactivation of Ca^{2+} -dependent enzymes, including kinases, phosphatases, COX and Ca^{2+} -dependent nitric oxide synthase (NOS). These Ca^{2+} -mediated effects cause free radical formation and irreversible mitochondrial damage (Dirnagl *et al.*, 1999). High intracellular Ca^{2+} can also increase osmotic load resulting in cytotoxic oedema (Durukan and Tatlisumak, 2007).

1.2.1.3 Excitotoxicity

High intracellular Ca^{2+} and Na^+ in injured pre-synaptic neurones can cause excessive Ca^{2+} -dependent release of excitatory transmitters, such as glutamate, and reverse transport of Na^+ by glutamate transporters. Under normal physiological conditions, glutamate transporters are involved in removing glutamate and Na^+ ions from the extracellular space (Nishizawa, 2001). However, in response to high intracellular Na^+ the activity of these transporters is reversed with transport of Na^+ and glutamate out of the cell (Nishizawa, 2001). Glutamate can activate two receptor types; ionotropic (NMDA- and AMPA-/kainate receptors) and metabotropic receptors (Durukan and Tatlisumak, 2007). Activation of NMDA receptors and AMPA receptors that contain a glutamate receptor 2 subunit will stimulate Ca^{2+} influx (Morley *et al.*, 1994). Activation of NMDA and AMPA receptors also increases influx of Na^+ and K^+ ions resulting in cell depolarisation (Morley *et al.*, 1994). Glutamate can activate pre-synaptic kainite receptors as part of a feed forward mechanism which stimulates further glutamate release (Kimura *et al.*, 1998). Excessive neurotransmitter release

from injured neurones can damage viable cells in the surrounding area by a process known as excitotoxicity. Excitotoxicity is a continuous process involving the development of recurrent waves of depolarisation originating in the infarct core and spreading outwards. This process is energy-dependent and will eventually exhaust the ATP supply of affected cells resulting in necrosis. Excitotoxicity can promote irreversible injury of surrounding neurones through Ca^{2+} -mediated activation of pro-apoptotic pathways and metabolic dysfunction (Durukan and Tatlisumak, 2007).

1.2.1.4 Oxidative Stress

Reactive oxygen species (ROS) are highly reactive cytotoxic molecules produced in injured tissue during ischaemia. There are several types of ROS which cause oxidative stress; including superoxide, hydroxyl radicals and hydrogen peroxide (Lakhan *et al.*, 2009). In injured neurones ROS can be generated through Ca^{2+} -mediated effects on the electron transport chain in the mitochondrial membrane (Peng and Jou, 2010). ROS can also be released by upregulation of NOS in endothelial cells and granule secretion from infiltrating neutrophils and macrophages (Kaminski *et al.*, 2002). ROS can damage surrounding viable cells through oxidation of essential cell components; including membrane lipids, proteins and nucleic acids (Crack and Taylor, 2005; Durukan and Tatlisumak, 2007). ROS cause lipid peroxidation and subsequent membrane damage (Durukan and Tatlisumak, 2007). Peroxidation of structural proteins can affect their function, such as altering ion channel permeability (Crack and Taylor, 2005; Matalon *et al.*, 2003). These modified proteins can accumulate in the cell due to saturation of proteolytic degradation mechanisms (Cadenas and Davies, 2000). Oxidation of nucleic acids can cause

genetic mutations (Durukan and Tatlisumak, 2007). ROS can also induce transcription factors, including nuclear factor- κ B (NF- κ B), hypoxia inducible factor 1 (HIF-1) and signal transducer and activator of transcription-3 (STAT-3), which up-regulate pro-inflammatory genes and expression of adhesion molecules and promote cell proliferation or apoptosis (Lakhan *et al.*, 2009; Hancock *et al.*, 2001). Activation of pro-inflammatory genes potentiates the inflammatory response by increasing cytokine production and enhancing expression of adhesion molecules (Lakhan *et al.*, 2009). Additional deleterious effects can be exerted through peroxynitrite formation by the reaction of superoxide and nitric oxide (Gürsoy-Özdemir *et al.*, 2000). Peroxynitrite is believed to be highly cytotoxic and its synthesis from nitric oxide reduces the protective vasodilatory and anti-inflammatory effects associated with endothelial release of nitric oxide (Gürsoy-Özdemir *et al.*, 2000).

1.2.1.5 Cell Death

The deleterious effects of ischaemia and reperfusion; including excitotoxicity, oxidative stress, mitochondrial dysfunction and release of cytochrome C, will individually contribute to irreversible injury and cell death. Cell death can occur through two processes; apoptosis or necrosis. Apoptosis is a process of programmed cell death which involves shrinkage of the cytoplasm, condensation of chromatin and fragmentation of the cell, whereas, necrosis is characterised by cell swelling, cytoskeletal breakdown and eventual disruption of the plasma membrane (Durukan and Tatlisumak, 2007). In the absence of ATP, cells in the ischaemic core will undergo necrosis (Nicotera *et al.*, 1998). Apoptosis is an energy-dependent process

which occurs in the ischaemic penumbra (Nicotera *et al.*, 1998). Apoptotic cells are removed by phagocytosis and do not promote an inflammatory response. In injured cells, Ca^{2+} overload activates Ca^{2+} -dependent pathways, including calpain and cathepsin, which can degrade the cytoskeleton and activate pro-apoptotic caspases (Chaitanya and Babu, 2008). Caspases are also activated in response to pro-apoptotic proteins, such as Bax, and activation of death receptors and downregulation of the anti-apoptotic protein Bcl-2 (Mergenthaler *et al.*, 2004). Caspases are protein cleavage enzymes which cause DNA damage and cleavage of structural proteins (Mergenthaler *et al.*, 2004).

1.2.1.6 Inflammation

Inflammation is one of the primary mechanisms of tissue injury in cerebral ischaemia. The brain contains resident immune cell populations; including tissue specific macrophages, known as microglia, which are activated during the acute inflammatory response (Lakhan *et al.*, 2009). Microglia are among the first cells to respond to injury following cerebral ischaemia. Activated microglia have been detected in ischaemic tissue as early as 30 minutes after cerebral ischaemia with a significant increase at 4-6 hours reaching a peak at 48 hours post-occlusion (Rupalla *et al.*, 1998; Mabuchi *et al.*, 2000). Regional ischaemia up-regulates transcription of pro-inflammatory genes and production of cytokines; including $\text{TNF-}\alpha$, IL-1 and IL-6, by injured neurones and activated microglia (Wang *et al.*, 2007). Cytokines promote activation and migration of leukocytes to the site of injury (Wang *et al.*, 2007). Activated microglia can also release other cytotoxic mediators, such as ROS and prostanoids, which damage surrounding neurones (Wang *et al.*, 2007).

Infiltration of peripheral leukocytes into the brain is delayed for several hours to days after cerebral ischaemia. Neutrophils are the first peripheral leukocyte to enter the ischaemic tissue (4-6 hours after injury) followed by macrophage and lymphocyte infiltration a few days later (Wang *et al.*, 2007; Durukan and Tatlisumak, 2007). Infiltrating leukocytes adhere to the luminal surface of the vessel and undergo degranulation with release of pro-inflammatory mediators and proteolytic enzymes; such as proteases, matrix metalloproteases (MMPs) and collagenase (Heo *et al.*, 2005). Release of MMPs, especially MMP-2 and MMP-9, has been associated with increased blood brain barrier permeability (Harris *et al.*, 2005). Leukocyte degranulation can cause direct injury to the endothelium leading to release of vasoconstrictors and pro-aggregatory mediators which can reduce local blood flow (Forman *et al.*, 1989).

1.2.1.7 Platelets

Cerebral ischaemia is considered to produce a pro-thrombotic vascular environment. Previous studies have demonstrated an increase in platelet aggregation in response to ADP, arachidonic acid and platelet-activating factor in patients following cerebral ischaemia (Uchiyama *et al.*, 1983). Following ischaemia, there is increased release of ADP and 5-HT from dense granules in activated platelets (Tohgi *et al.*, 1991; Joseph *et al.*, 1989). An elevated concentration of the inert thromboxane A₂ metabolite, thromboxane B₂, and increased expression of the platelet adhesion molecules, p-selectin and CD63, were also identified following ischaemia (Fisher *et al.*, 1985; Zeller *et al.*, 1999). Thrombus development in the cerebral vasculature may block other cerebral arteries near to the injury site exacerbating injury development and

increasing the risk of further stroke.

1.2.2 Models of Cerebral Ischaemia

Cerebral ischaemia is a highly variable condition which can be affected by the duration and severity of ischaemia (permanent or transient) and the region affected (global or focal). As such, several different models have been developed to study cerebral ischaemia. *In vitro* studies using primary neuronal and organotypic cultures can be performed to allow simple high throughput studies of the effects of oxygen and glucose deprivation (Hossmann, 2008). However, *in vitro* models do not allow the study of complex networks of interactions, including neuronal, immunological and cerebrovascular effects, on the response to ischaemic insult.

Animal models have been developed to allow cerebral ischaemia to be studied in a physiological setting, including cardiovascular and inflammatory effects, and assessment of the functional deficits produced by ischaemia. In animal models of cerebral ischaemia the pathophysiology should resemble the clinical situation as closely as possible and result in reproducible and measurable outcomes for injury development and functional deficits. Rats are commonly used as a model of cerebral ischaemia due to the low cost of these animals and relative ease of surgery and tissue processing (Durukan and Tatlisumak, 2007). Additionally, rats and humans have a similar cerebrovascular anatomy, including the circle of Willis, and high collateral blood flow in the cortex (Macrae, 1992). There is also relatively high homogeneity between animals due to the use of inbred rat strains which reduces the influence of individual variation.

Animal models of global ischaemia involve cardiac arrest or bilateral common carotid artery occlusion, with or without occlusion of the vertebral arteries and hypotension (Hossmann, 2008). Focal ischaemia models have been developed that involve localised occlusion of the middle cerebral artery which is commonly observed in humans with ischaemic stroke (Hossmann, 2008). Permanent occlusion of the middle cerebral artery using the intraluminal thread model can produce primary injury in the lateral caudoputamen and frontoparietal cortex (Garcia *et al.*, 1993). Infarct in these regions produces a complex pattern of motor, sensory and cognitive deficits (Carmichael, 2005). There are 2 main animal models of middle cerebral artery occlusion. The Tamura model involves performing a craniectomy to expose the middle cerebral artery which can be occluded permanently by electrocoagulation or temporarily using an artery clip (Tamura *et al.*, 1981). The intraluminal thread model was first introduced by Koizumi *et al.* (1986) and later modified by Longa *et al.* (1989). This model involves permanent or transient occlusion of the middle cerebral artery by insertion of a filament through the internal carotid artery which is either secured in position (permanent) or removed after a specified period of occlusion (transient). The intraluminal thread model is one of the most extensively used models of cerebral ischaemia. This technique is easier to perform and relatively non-invasive as it does not involve a craniectomy which can damage small blood vessels and change intracranial pressure (Nagasawa and Kogure, 1989).

The intraluminal thread model has several disadvantages, including spontaneous reperfusion and the risk of subarachnoid haemorrhage (Schmid-Elsaesser *et al.*,

1998). Coated filaments have been used to reduce the risk of subarachnoid haemorrhage, 44% rate of haemorrhage with uncoated filaments reduced to 12% with silicone-coated filaments (Schmid-Elsaesser *et al.*, 1998). Coated filaments may also increase the success of occlusion by adherence of the coating to the luminal surface of the vessel which will reduce residual blood flow through the internal carotid artery (Belayev *et al.*, 1996). It has been suggested that filament insertion may damage the endothelial lining and promote thrombus formation (Schmid-Elsaesser *et al.*, 1998). Models of cerebral ischaemia can be affected by multiple factors; including species, animal strain and supplier and physiological variables. Infarct size can vary significantly between rat strains and different suppliers (Herz *et al.*, 1996; Oliff *et al.*, 1997). Hyperthermia can increase injury, whereas, hypothermia can confer neuroprotection (McIlvoy, 2005). Systemic blood pressure can affect evolution of the infarct in acute cerebral ischaemia (Jørgensen *et al.*, 1994; Rordorf *et al.*, 1997). Blood gases should be measured as high PCO_2 levels can exert a vasodilatory effect on cerebral blood vessels through increased release of H^+ (Olah *et al.*, 2000). As such, it is important to limit possible sources of variation by maintaining animals within normal physiological parameters.

1.2.3 Models of Platelet Aggregation

Platelets are anuclear cells which are involved in haemostasis. The intact endothelium is anti-thrombotic and releases potent anti-aggregatory mediators, such as nitric oxide and prostacyclin. Following injury, platelets can be activated by adherence to exposed collagen in the damaged vessel wall or through binding of soluble pro-aggregatory mediators (Li *et al.*, 2010). Platelet aggregation can occur

through several mechanisms depending on the aggregatory mediator involved (**figure 1.3**). Platelet activation produces increased cytosolic Ca^{2+} and reduced cAMP levels resulting in shape change with formation of pseudopodia and increased expression of the integrin GP IIb/IIIa (Li *et al.*, 2010). Platelet activation is amplified by secretion of pro-aggregatory mediators, such as ADP and 5-HT, and adhesion molecules from dense and alpha granules, respectively, and production of thromboxane A_2 from arachidonic acid (Li *et al.*, 2010). Pseudopodia formation and interaction of the integrin GP IIb/IIIa and fibrin contributes to the formation of a stable platelet aggregate (Lefkovits *et al.*, 1995).

Platelet function can be assessed *in vitro* using several different preparations; washed platelets, platelet-rich plasma and whole blood. Aggregometry studies can be performed in humans and laboratory animals, such as rats, guinea pigs and rabbits. The aggregation response to physiological agonists can vary depending on the species studied (Kurata *et al.*, 1995; Pelagalli *et al.*, 2002). In laboratory animals the volume of blood that can be taken is limited by the size of the animal. The response of platelets to different agonists can be examined in washed platelets and platelet-rich plasma by light transmission aggregometry which was first developed by Born in 1962. In this technique a light is passed through a cuvette containing the platelet preparation and light transmission is detected by a photoelectric cell (Born, 1962a and b). During aggregation, platelets clump together reducing the volume of the cuvette that they occupy resulting in an increase in light transmission (Born, 1962a and b). In light transmission aggregometry both phases of the aggregation response, primary (reversible) and secondary (irreversible; granule secretion), can be

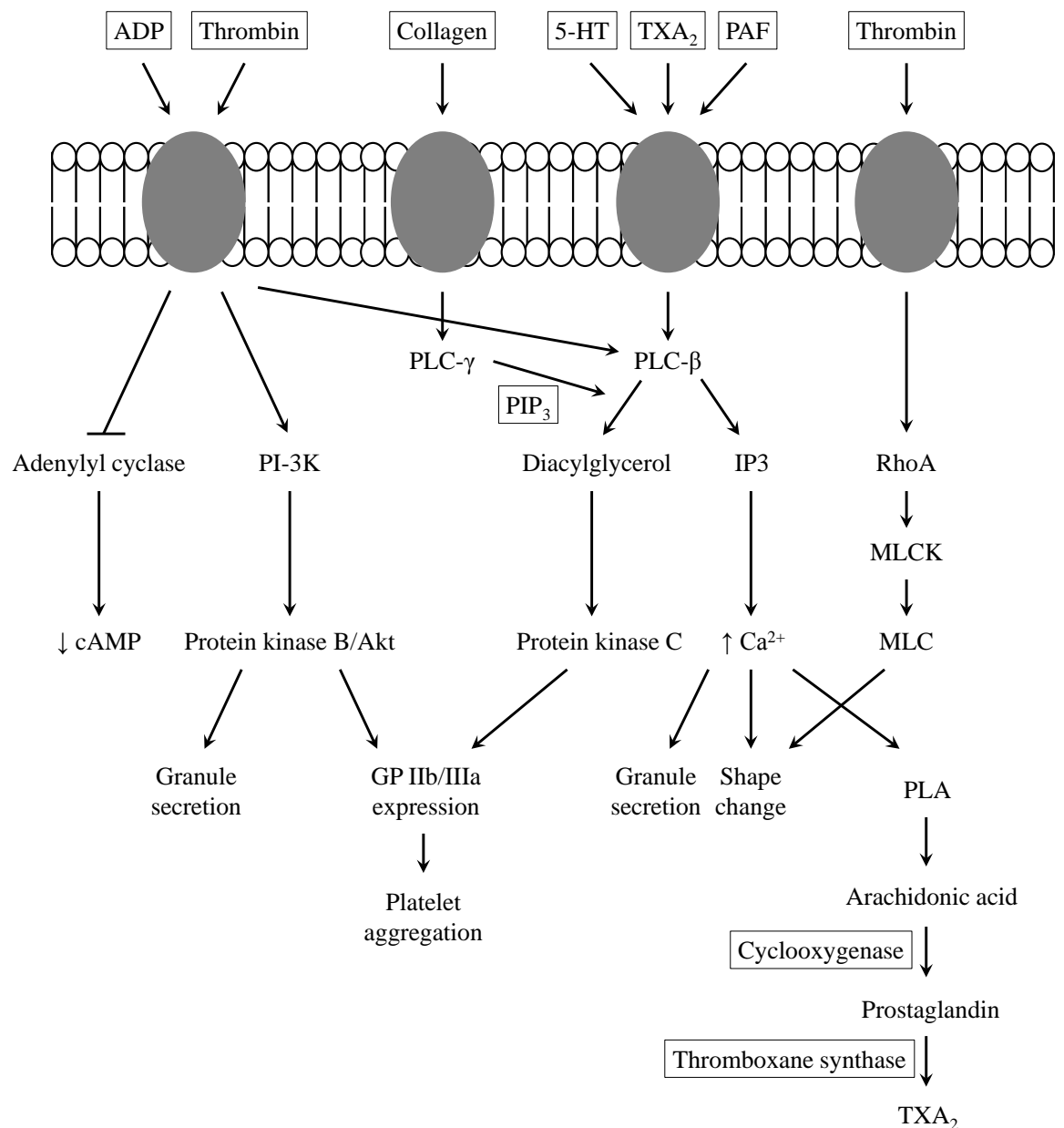


Figure 1.3: Schematic of the signalling pathways involved in mediating platelet aggregation in response to several physiological agonists. 5-HT; 5-hydroxytryptamine, ADP; adenosine diphosphate, Ca²⁺; calcium, cAMP; cyclic adenosine monophosphate, IP₃; inositol trisphosphate, MLC; myosin light-chain, MLCK; myosin light-chain kinase, PAF; platelet activating factor, PI-3K; phosphatidylinositol 3-kinase, PLA; phospholipases A releases fatty acids from the plasma membrane, PLC; phospholipase C, RhoA; Ras homolog gene family, TXA₂; thromboxane A₂.

clearly observed. There are several disadvantages associated with the use of this technique. The use of this technique is limited to translucent preparations, such as platelet-rich plasma, and cannot be performed in whole blood (Cardinal and Flower, 1980). Platelet-rich plasma is prepared through gentle centrifugation of blood which can be time and labour intensive (Cardinal and Flower, 1980; Dyszkiewicz-Korpanty *et al.*, 2005). The physiological agonist, platelet-activating factor, was less potent in platelet-rich plasma compared to washed platelets due to the buffering effect of plasma proteins on lipophilic agonists (Floch and Caverio, 1990)

Platelet aggregation can be assessed in whole blood and platelet-rich plasma by impedance aggregometry. This technique was first described by Cardinal and Flower in 1980. Impedance aggregometry records changes in electrical current between 2 electrodes (Cardinal and Flower, 1980). In the absence of aggregation a platelet monolayer will coat the electrodes, however, conductance of the electrical current will remain constant. Following addition of an aggregatory agent activated platelets will adhere to the platelet monolayer and impede conductance of the electrical current between the electrodes (Cardinal and Flower, 1980). In platelet-rich plasma impedance aggregometry is more sensitive to aggregation produced by ADP and collagen compared to light transmission aggregometry (Mannucci *et al.*, 1988). However, no difference was observed in the response to other agonists. Whole blood aggregometry allows quick assessment of platelet function, within minutes of blood withdrawal, and requires a relatively small volume of blood compared to platelet-rich plasma (Cardinal and Flower, 1980; Dyszkiewicz-Korpanty *et al.*, 2005). The primary advantage of using whole blood is the ability to study platelet function in the

presence of other blood cells, including red blood cells and leukocytes, at physiological concentrations (Dyszkiewicz-Korpanty *et al.*, 2005). It is known that red blood cells and leukocytes can affect platelet function *in vivo*. Higher concentrations of ADP are required to produce 50% maximal aggregation in whole blood compared to platelet-rich plasma (Mannucci *et al.*, 1988). This difference in potency may be due to degradation of ADP by red blood cells and leukocytes via ADPase and 5-nucleotidase (Dyszkiewicz-Korpanty *et al.*, 2005). In contrast, the aggregation response to collagen, platelet-activating factor and adrenaline was similar in whole blood and platelet-rich plasma (Mannucci *et al.*, 1988). It has been demonstrated that red blood cells can degrade the anti-aggregatory agonist, prostacyclin (Dyszkiewicz-Korpanty *et al.*, 2005), whereas, leukocytes are able to generate prostacyclin (Blackwell *et al.*, 1978). Taken together, impedance aggregometry can provide a quick and reliable method of measuring platelet aggregation. The use of whole blood provides more physiologically relevant information on the pro-aggregatory effects of different agonists as other blood cells can influence platelet aggregation *in vivo*.

1.3 Cannabinoids and Cerebral Ischaemia

The endocannabinoid system has been shown to have a role in the pathophysiology of cerebral ischaemia. In animal models cerebral ischaemia increased the expression of both CB₁ and CB₂ receptors in the ischaemic hemisphere. Expression of CB₁ receptors increased in the first hour following ischaemia with maximal expression at 6 hours (Zhang *et al.*, 2008). CB₂ receptor expression decreased in the 3 hours after insult followed by a gradual increase with maximal expression observed at 24 hours

(Zhang *et al.*, 2008). The anandamide concentration increased in the ipsilateral hemisphere within 30 minutes of cerebral ischaemia (Muthian *et al.*, 2004). In contrast, the concentration of 2-AG was unaffected following ischaemia (Muthian *et al.*, 2004).

Endogenous and synthetic cannabinoids promoted the survival of neuronal cultures exposed to neurotoxic stimuli, including oxygen and glucose deprivation (up to 8 hours) and glutamate-induced excitotoxicity (Nagayama *et al.*, 1999; van der Stelt *et al.*, 2002). Pre-treatment with synthetic cannabinoids reduced infarct volume following permanent cerebral ischaemia via activation of CB₁ receptors (Leker *et al.*, 2003; Nagayama *et al.*, 1999; Mauler *et al.*, 2002). In contrast, administration of CB₁ antagonists, SR 141716A and LYS 320135, in transient cerebral ischaemia has been shown to reduce infarct volume and improve neurological function (Muthian *et al.*, 2004). Recently, CB₂ receptors have been implicated in the neuroprotective effect of cannabinoids in cerebral ischaemia. Pre-treatment with the CB₂ agonist, O-1966, increased cerebral blood flow during occlusion, reduced infarct size and improved motor function following transient cerebral ischaemia in mice (Zhang *et al.*, 2008). Interestingly, the greatest beneficial effect was observed when the CB₂ agonist was administered in combination with a CB₁ antagonist, SR141716A (Zhang *et al.*, 2008). Administration of the endocannabinoids anandamide and palmitoylethanolamide during transient occlusion of the middle cerebral artery reduced infarct volume at 24 hours post-occlusion (Schomacher *et al.*, 2008). However, the mechanisms involved in mediating this protective effect have not been investigated. 2-AG has been shown to exert a neuroprotective effect in animal

models of traumatic brain and spinal cord injury (Panikashvili *et al.*, 2001; Arevalo-Martin *et al.*, 2010). However, the effect of 2-AG in cerebral ischaemia has not been studied.

1.4 Hypothesis and Objectives

The endocannabinoid system is modified following cerebral ischaemia and may have a role in the pathophysiology of this condition. The hypothesis being tested in this thesis is that the endocannabinoids anandamide and 2-AG will be neuroprotective in acute cerebral ischaemia and will reduce injury volume at 4 hours post-occlusion. Endocannabinoids are known to exert anti-inflammatory effects *in vivo*; however, the effects of these mediators on microglia may be beneficial or detrimental in cerebral ischaemia. As such, it is important to characterise the effect of endocannabinoids on the microglia response following injury. It is also hypothesised that endocannabinoids may have effects on platelet aggregation which could affect the outcome following cerebral ischaemia. Thus, the effect of the endocannabinoid 2-AG on platelet aggregation in rat whole blood was characterised.

In order to test these hypotheses the following aims were set:

- To establish a reproducible model of transient cerebral ischaemia in rats.

- To investigate the effect of exogenously administered and increased endogenous anandamide by inhibition of metabolism by fatty acid amide hydrolase using URB597 on acute cerebral ischaemia. Haemodynamic measurements and

cerebral blood flow were recorded throughout the occlusion period and injury volume and microglia number and activation were measured at 4 hours post-occlusion.

- To investigate the effect of exogenous and enhanced endogenous 2-AG through inhibition of monoacylglycerol lipase metabolism by JZL184 on acute cerebral ischaemia. Continuous monitoring of haemodynamic measurements and cerebral blood flow was performed during occlusion and injury volume and microglia number and activation were assessed at 4 hours post-occlusion.
- To characterise the effect of 2-AG alone and in combination with ADP on platelet aggregation in rat whole blood. Cannabinoid receptor antagonists and COX metabolism inhibitors were used to examine the mechanisms involved in mediating the aggregation response to 2-AG.

CHAPTER 2

ESTABLISHMENT OF AN INTRALUMINAL THREAD MODEL OF MIDDLE CEREBRAL ARTERY OCCLUSION IN RATS

2.1 Introduction

The intraluminal thread model is one of the most extensively used animal models of cerebral ischaemia. In this technique, the origin of the middle cerebral artery is occluded by a filament advanced through the internal carotid artery. This technique can be used to produce permanent or transient occlusion of varying duration. The intraluminal thread model has the advantage of being less invasive than other techniques. However, this model can be affected by multiple variables; for example physiological parameters, such as blood gases (Olah *et al.*, 2000), blood pressure (Kaliszewski *et al.*, 1988) and temperature (McIlvoy, 2005); and the type of filament used. Several filament types, heat blunted and silicon or poly-L-lysine coated, have been developed in an attempt to limit variability and reduce the risk of subarachnoid haemorrhage (Schmid-Elsaesser *et al.*, 1998).

2.2 Aim

The aim of this work was to establish an intraluminal thread model of transient middle cerebral artery occlusion in rats. The optimal model would produce reproducible infarction with low rates of mortality and morbidity in animals that were allowed to recover from anaesthesia.

2.3 Methods

2.3.1 Source of Materials

Details of suppliers for all equipment, drugs and reagents are given in Appendix A and B, respectively.

2.3.2 Animal Source

All animal experiments were carried out in accordance with UK Home Office Guidelines on the Operation of the Animals (Scientific Procedures) Act 1986 (Project Licence No. PPL 60/3775; Personal Licence No. PIL 60/11356). Adult male outbred Sprague Dawley rats (8-10 weeks; 275-350g) were sourced from an in-house breeding colony in the Biological Procedures Unit (BPU) of the University of Strathclyde. Animals were originally sourced from Harlan laboratories and bred in-house using a harem system; 1 male to 3 females. Rats were housed in the BPU and had free access to food and water, room temperature was held at 21 °C and light and dark cycles were rotated twelve hourly. Prior to each experiment, animals were housed in groups (4 rats per cage) and provided with environmental enrichment. Following surgery animals were housed individually for the duration of the recovery period and provided with a soft diet.

2.3.3 Animal Preparation

Male Sprague-Dawley rats weighing 275-350g were placed in an anaesthetic box and anaesthesia was induced by inhalation of 5% isoflurane in 100% oxygen at 1 l/min.

Once anaesthetised, animals were either connected to a nose cone or the trachea was intubated and anaesthesia was maintained with 2.25-2.5% isoflurane. In procedures using a nose cone isoflurane was delivered in 100% oxygen at 0.5 l/min. In intubated animals isoflurane was delivered in either 100% oxygen or 30% oxygen:70% nitrous oxide at 0.5 or 1 l/min, respectively. Intubated animals were artificially ventilated using a stroke volume of 2.8 ml at a rate of 62 strokes per minute. Suitable depth of

anaesthesia was assessed by lack of a pedal withdrawal response and corneal reflex and this depth of anaesthesia was maintained throughout the procedure.

Anaesthetised rats were placed in a supine position. Skin was shaved around the area of the incision and 0.5 ml atropine (600 µg/ml) was administered subcutaneously (s.c.) at the side of the neck, where indicated in the results, to reduce the build-up of secretions in the trachea. Further doses were administered every 1½ hours or when required due to rasping or laboured breathing. Body temperature was monitored continuously by a rectal probe throughout the procedure and maintained within 36.5-37.5 °C using a homeothermic blanket and heat lamp.

2.3.4 Laser Doppler Flowmetry

The animal was rolled on to its right side and an incision was made in the skin on the left side of the head midway between the corner of the eye and the ear. The temporalis muscle was dissected and the skull was thinned using a small drill. The laser Doppler probe was positioned on the skull level with the coronal suture (0 mm bregma) and above the somatosensory cortex which is perfused by the middle cerebral artery. Laser Doppler flowmetry was used to monitor cerebral blood flow during the procedure and confirm successful middle cerebral artery occlusion (>60% reduction in signal). In laser Doppler flowmetry cerebral blood flow was measured in arbitrary units. The baseline laser Doppler signal was taken as the mean of three separate measurements recorded over the first hour following placement of the probe and before occlusion of the middle cerebral artery. Laser Doppler flowmetry measurements were expressed as a percentage of the baseline value. Cerebral blood

flow values were recorded every 30 minutes during the surgery, immediately prior to filament insertion and at 15 minute intervals throughout the occlusion period.

2.3.5 Intraluminal Filament Preparation

In studies 1-5, an uncoated heat blunted 3-0 nylon filament was used to occlude the middle cerebral artery (**figure 2.1A**). The tip of the filament was rounded to form a bulb (200-300 μ M diameter) using a low temperature cautery pen. Bulbs of varying sizes were used in each experiment based on the body weight of the animal. In study 6, a commercially available silicon rubber coated filament was used (50-3033; Docol Corporation; **figure 2.1B**). The profiles of these filaments are illustrated in **figure 2.1**.

2.3.6 Intraluminal Thread Model

The intraluminal thread model is based on the modified surgical technique described by Longa *et al.* (1989). A schematic of the cerebrovascular anatomy and intraluminal thread placement is shown in **figure 2.2** and the surgical technique, described below, is illustrated in **figure 2.3**. A midline incision was made at the neck and the connective tissue was dissected. Using a surgical microscope, carotid pulsing was visible beneath the sternohyoid muscle. This muscle was dissected to expose the left common carotid artery and bifurcation of the external and internal carotid branches (**figure 2.3a**). The vagus nerve was gently dissected and separated from the carotid artery. The branches of the external carotid artery; the superior thyroid artery, maximal and lingual arteries, were dissected and electrocoagulated and the superior thyroid

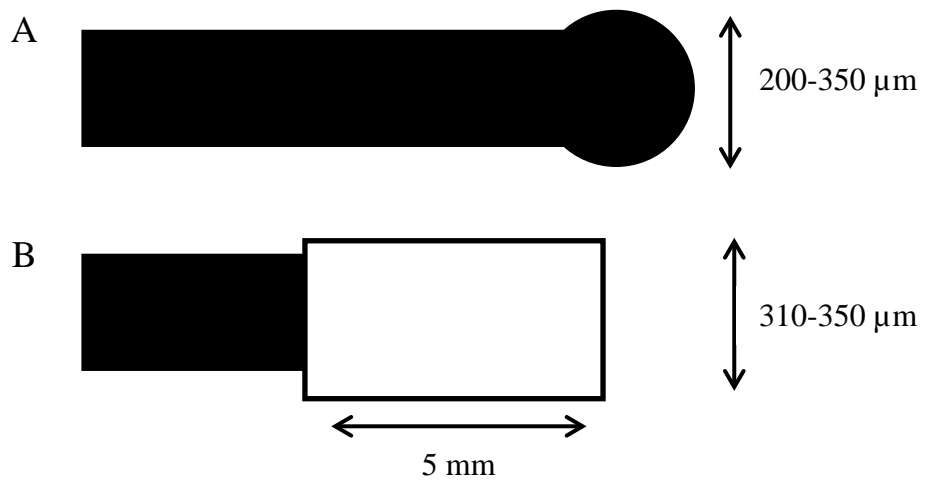


Figure 2.1: Diagram of **A)** traditional heat blunted and **B)** silicon coated Doccol filament.

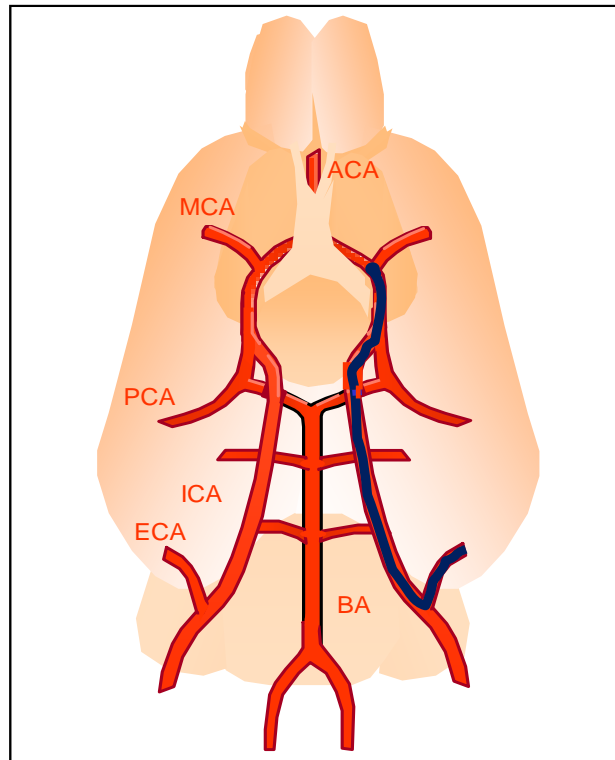


Figure 2.2: Schematic of intraluminal thread placement at the origin of the middle cerebral artery (Adapted from Kitagawa *et al.* 1997).

— Intraluminal filament

ACA = Anterior cerebral artery; MCA = Middle cerebral artery;

PCA = Posterior cerebral artery; ICA = Internal cerebral artery;

ECA = External cerebral artery; BA = Basilar artery

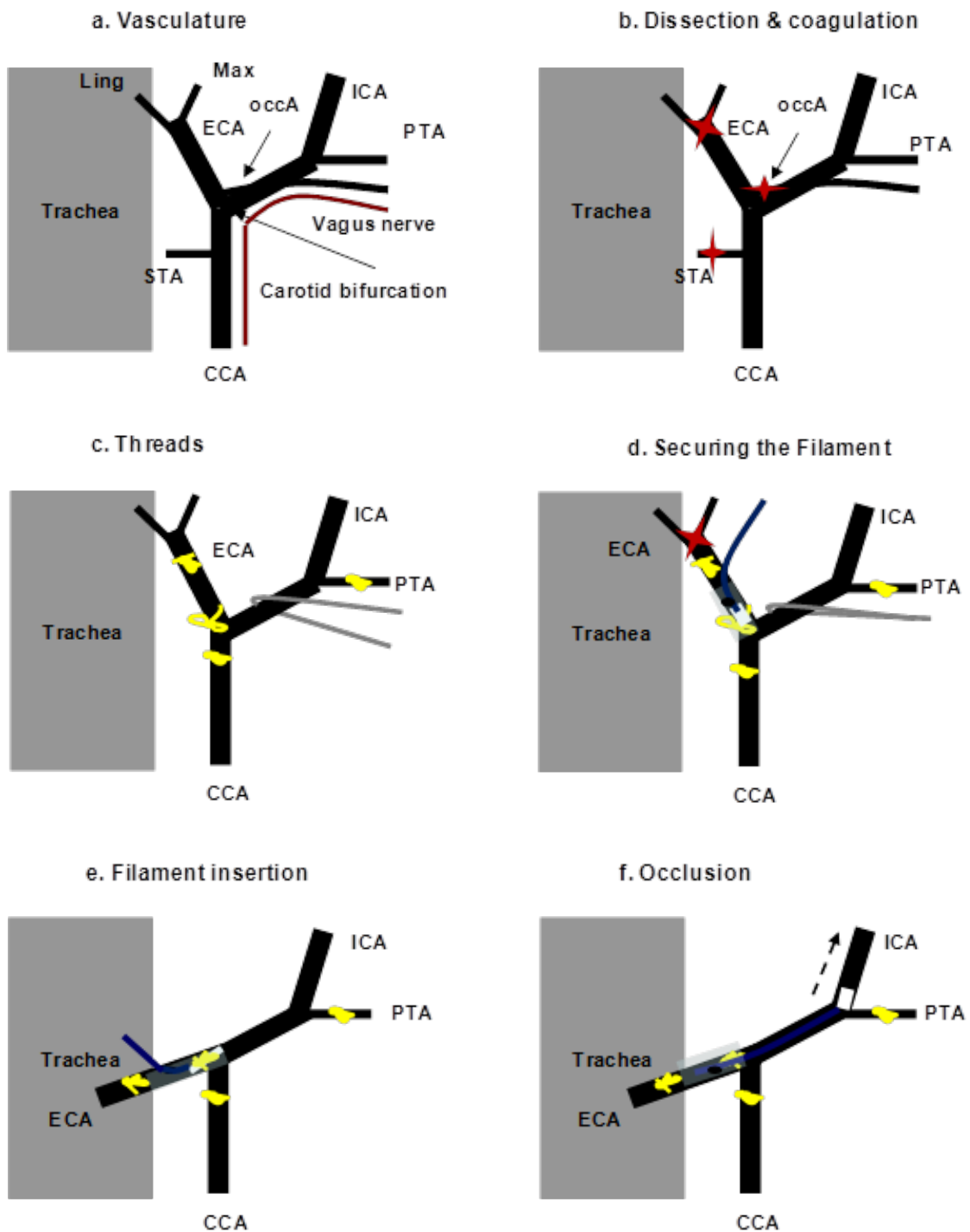


Figure 2.3: Diagram of the surgical procedure used for the intraluminal thread model of middle cerebral artery occlusion. CCA = Common carotid artery; STA = Superior thyroid artery; ECA = External carotid artery; OccA = Occipital artery; Max = Maxillary artery; Ling = Lingual artery; ICA = Internal carotid artery; PTA = Pterygopalatine artery; ★ = Electrocoagulation; ✂ = Ligatures; — = Filament. Figure adapted from an original image by Dr. Shalmali Patkar.

artery was cut (**figure 2.3b**). A thread (4-0 silk) was tied around the external carotid artery proximal to the maximal and lingual arteries and a loose tie was positioned near to the bifurcation of the common carotid artery. The occipital branch was separated from surrounding connective tissue and the internal carotid artery and then electrocoagulated and cut. The common carotid artery was occluded by tying a tight thread below the bifurcation of the external and internal carotid branches. The internal carotid artery was dissected from the surrounding connective tissue and a loose tie was placed around the vessel. Pressure was applied to this tie to retract the internal carotid artery and improve access to the bifurcation with the pterygopalantine branch. This part of the procedure was added to the final protocol to improve success of the surgery, it was not performed in the initial permanent middle cerebral artery occlusion experiments (study 1a; n=12). The pterygopalantine branch was occluded by tying a thread around it to prevent advancement of the filament into this vessel instead of the internal carotid artery (**figure 2.3c**). The maximal and lingual branches were cut to free the external carotid artery. An incision was made near the base of the external carotid artery stump and the filament was inserted to the bifurcation and secured by tightening the loose tie around the external carotid artery (**figure 2.3d**). The external carotid artery then was turned to advance the filament into the internal carotid artery (**figure 2.3e**), approximately 22 mm or until resistance was felt, to occlude the origin of the middle cerebral artery. The filament was secured in position by tightening the ligature around the external carotid artery (**figure 2.3f**).

In transient middle cerebral artery occlusion models the filament remained in

position for a variable length of time. After the occlusion period the filament was withdrawn from the internal carotid artery to allow reperfusion of the middle cerebral artery. Once the filament entered the external carotid artery stump, pressure was applied to the internal carotid artery tie to occlude blood flow and the filament was removed. The ligature around the external carotid artery stump was tightened to prevent bleeding and the vessel was electrocoagulated. Finally, the ligature around the common carotid artery was removed.

The wound was sutured, cleaned with betadine and 1 ml of saline was administered s.c. to prevent dehydration. Anaesthesia was stopped and the animal was allowed to regain consciousness. Once fully conscious, the animal was placed in a warm cage, heated by a homeothermic blanket and lamp, and provided with moistened chow and water. The animal's condition was monitored regularly throughout the recovery period.

2.3.7 Protocols

Several experimental protocols (studies 1-6) were examined during the establishment of the middle cerebral artery occlusion model. The protocols used in each study are shown in **table 2.1**.

2.3.7.1 Study 1: Permanent Middle Cerebral Artery Occlusion

Permanent middle cerebral artery occlusion was performed using the intraluminal thread model to establish the surgical technique and confirm correct filament placement at the origin of the middle cerebral artery. In this model, the filament was

Table 2.1: Experimental protocol used in each stroke study.

Study	Surgery	Occlusion period	Reperfusion period	Filament type	Type of ventilation	Delivery gases	Flow rate (l/min)	Laser Doppler
1 (n=18) <i>1a (n=12)</i> <i>1b (n=6)</i>	Permanent MCAO	24 h	–	Heat blunted	Spontaneous breathing	100% O ₂	0.5	No
2 (n=12)	Transient MCAO	90 min	22 h 30 min	Heat blunted	Spontaneous breathing	100% O ₂	0.5	No
3 (n=5)	Transient MCAO	2 h	70 h	Heat blunted	Artificial ventilation	100% O ₂	0.5	Yes
4 (n=12)	Transient MCAO	2 h	70 h	Heat blunted	Artificial ventilation	30% O ₂ :70% N ₂ O	1	Yes
5 (n=4)	Transient MCAO	90 min	70 h	Heat blunted	Artificial ventilation	30% O ₂ :70% N ₂ O	1	Yes
6 (n=2)	Transient MCAO	90 min	22 h 30 min	Silicon coated	Artificial ventilation	30% O ₂ :70% N ₂ O	1	Yes

MCAO; middle cerebral artery occlusion, O₂; oxygen, N₂O; nitrous oxide.

advanced to occlude the middle cerebral artery origin and secured in position for 24 hours. In initial experiments (study 1a; n=12) the procedure varied from the stated surgical protocol as atropine was not administered and there were minor differences in the technique used to expose and occlude the branches of the external and internal carotid arteries.

In later experiments (study 1b; n=6) the surgical protocol was modified to reduce damage to the vagus nerve during dissection of the vasculature. These changes are detailed below:

1. Atropine (0.5 ml; 600 µg/ml) was administered s.c. at the neck to reduce airway secretions.
2. The sternohyoid muscle was dissected lateral to the midline above the visible pulsing of the carotid artery. This reduced the time required to expose the carotid vasculature.
3. A loose thread was placed around the internal carotid artery to retract this vessel and improve access to the bifurcation. This made it easier to place a ligature around the pterygopalantine branch and reduced the length of time required for this part of the procedure.

2.3.7.2 Study 2: Transient Middle Cerebral Artery Occlusion

In study 2, the surgical technique established in the permanent ischaemia study was used to produce a model of transient ischaemia. In this study, the middle cerebral artery was occluded for 90 minutes and subsequently reperfused for 22 hours

30 minutes.

2.3.7.3 Study 3: Transient Middle Cerebral Artery Occlusion

In study 3, the protocol was modified to attempt to reduce the inter-animal variability. Tracheal intubation was performed to improve ventilation. The duration of occlusion was increased to 2 hours and the reperfusion period extended to 70 hours to allow complete injury development and produce a more consistent infarct. Doppler flowmetry was also introduced in this study to monitor cerebral blood flow throughout the procedure and confirm successful occlusion.

2.3.7.4 Study 4: Transient Middle Cerebral Artery Occlusion

In study 4, the ventilation settings were changed from 100% oxygen to 30% oxygen:70% nitrous oxide as during study 3 it had been difficult to control respiration in ventilated animals. An experiment was performed to assess the blood gases in one animal with the ventilation settings used in study 3. Use of 100% oxygen as a delivery gas was associated with a high PO_2 , over 500 mmHg, and low PCO_2 of 20-25 mmHg. Physiologically abnormal blood gases, such as those observed in this animal, can affect infarct development following cerebral ischaemia.

2.3.7.5 Study 5: Transient Middle Cerebral Artery Occlusion

In study 5, the duration of occlusion was reduced from 2 hours to 90 minutes to decrease the severity of the injury as the protocol in study 4 was associated with high post-operative mortality.

2.3.7.6 Study 6: Transient Middle Cerebral Artery Occlusion

In study 6, the filament type was modified with the introduction of a commercially available silicon coated Docol filament to replace the heat blunted filament.

2.3.8 Inclusion Criteria

Animals were only included in the data analyses if they fulfilled the following criteria:

1. No sign of haemorrhage of the internal carotid artery was present on the base of the brain.
2. If Doppler flowmetry was used, a >60% reduction in cerebral blood flow was observed following placement of the filament.

2.3.9 Neurological Deficit Score

In each animal, neurological deficits were assessed at multiple time-points after cerebral ischaemia. Following cerebral ischaemia, the severity of deficits in neurological function was quantified using two 28-point scores to assess general and focal deficits. These tests were initially developed by Clark *et al.* (1997) in mice and have been used more recently to examine deficits in rats (Pignataro *et al.*, 2004; Cuomo *et al.*, 2007).

To assess these general deficits, animals were placed on a flat surface (4 ft² surface area) and observed without interference or any external stimulation (**table 2.2**). Seizures and hyperactive behaviour observed at any time-point following surgery

Table 2.2: Scoring system used to measure general deficits following middle cerebral artery occlusion.

Score	Fur	Ears	Eyes
0	Clean and tidy	Ears stretch latero-posteriorly and respond to noises	Open, clean and follow movements quickly
1	Localised piloerection and dirt around nose and eyes	One or both ears are lateral	Open with watery dirt and follow movements slowly
2	Piloerection and dirty fur in more than two areas	One or both ears are lateral and do not respond to noise	Open with dark mucosal dirt
3			Oval opening with mucosal dirt
4			Shut

Score	Posture	Spontaneous Activity
0	Upright with back parallel to desk and keeping balance on four legs	Alert and explores continuously
1	Animal stooped when walks and lowers itself to gain balance	Alert but calm and listless
2	Head or part of trunk lies on desk	Starts and stops exploring slowly and iteratively
3	Animal lies on side, but can straighten up with effect	Lethargic, numb and moves on-site
4	Animal lies on side unable to straighten up	Still, moving occasionally on-site

Score	Seizures
0	Absence of seizures
3	Hyperactive and tend to climb cage walls
6	Aggressive and nervous
9	Extremely excitable, frenzy, seizures after stimulation
12	Seizures, breathing variations and loss of consciousness

General deficits were examined after cerebral ischaemia and quantified on a scale of 0-4 for all parameters, except seizures, and 0-12 for seizures only.

were recorded and scored as described in **table 2.2**.

Focal deficits were examined by different techniques depending on the parameter being assessed. Body symmetry, walking and circling were assessed in animals at rest or walking, where appropriate, without external stimulation and scored as shown in **table 2.3**. To assess slope climbing, animals were placed at the bottom of a coarse 45° sloping surface and their ability to climb the slope was examined. Forelimb symmetry was examined by suspending the animal by its tail and observing extension of the forelimbs. In the mandatory circling test, the animal was held by its tail with its forelimbs touching the desk and circling of the animal was observed. This test was repeated 3 times in each animal and the average response was recorded. The response of whiskers to stimulation on the ipsilateral and contralateral side was examined.

2.3.10 Tissue Processing

For studies 1, 2, 3 and 5, the animal was euthanised at the end of the experiment by an overdose of carbon dioxide. In study 6, the animals were euthanised by cervical dislocation and exsanguination. Rats were then decapitated and the brain was removed immediately.

In study 4, rats were euthanised by an overdose of sodium pentobarbital (200 mg/ml) administered as an intraperitoneal (i.p.) bolus. The rats then underwent a process known as perfusion fixation. Once the animal was very deeply anaesthetised, the chest cavity was opened and a small needle inserted into the left ventricle. The right

Table 2.3: Scoring system used to measure focal deficits following middle cerebral artery occlusion.

Score	Body Symmetry	Walking	Circling Behaviour
0	Body raised from desk, legs symmetrical under body, tail is straight	Normal walking, quick and symmetrical	Turns equally to both sides
1	Body lies on ipsilateral side, tail is bent	Stooped, slow and mechanical walking.	Turns preferentially to one side
2	Body lies on ipsilateral side, legs on ischemic side extend laterally, tail is bent	Slight limp and asymmetrical movements	Turns to one side, although inconstantly
3	Body is bent and ischemic side lies on the desk	Severe limp and clear walking deficits	Turns constantly to one side
4	Body and tail bent, ischemic side lies constantly on desk	Limited movement after stimulation	Swings slowly on-site or remains still

Score	Sloping Desk Climbing	Forelimb Symmetry	Mandatory Circling
0	Climbs quickly	Both forelimbs extended, vigorously moving	Both forelimbs equally extended
1	Climbs slowly with a lot of effort	Ipsilateral forelimb not completely extended	Both forelimbs extended, starts to circle from one side
2	Can only keep position on sloping desk.	Ipsilateral forelimb not extended. Mild contortion of body to ipsilateral side	Turns slowly to one side
3	Falls slowly towards the bottom	Ipsilateral forelimb adheres to trunk. Contortion of body to ipsilateral side.	Turns slowly to one side without completing a circle
4	Falls immediately to the bottom	Slow or no movement of forelimb. Contortion of body to ipsilateral side	Little movement of forelimbs, trunk lies on desk.

Score	Whisker Response
0	Symmetrical response. Animal moves away from source of stimulation
1	Delayed response on ipsilateral side and normal response on the contralateral side
2	No response on ipsilateral side and normal response on the contralateral side
3	No response on ipsilateral side and delayed on the contralateral side
4	No response on either side

Focal deficits were examined after cerebral ischaemia and quantified on a scale of 0-4.

atrium was cut and the vasculature flushed with saline to remove the blood. The saline infusion was maintained until fluid leaving the right atrium was clear. The animal was then infused with 4% paraformaldehyde for 15 minutes until all tissues were fixed. The animal was then decapitated and the head placed in 4% paraformaldehyde for 24 hours. The next day the brain was removed and placed in 4% paraformaldehyde for another 24 hours. On the second day, the brain was placed in 30% sucrose solution until it sank.

In all studies, brains were frozen by immersion in isopentane at -42 °C for 10 minutes and coated in embedding matrix. Frozen brains were stored at -20 °C prior to sectioning in a cryostat. Coronal sections (20 µM) were taken on to polarised or gelatin coated slides at 8 pre-determined levels based on Osborne *et al.* (1987). The 8 coronal sections were taken at the level of the olfactory tract, nucleus accumbens, septal nuclei, globus pallidus, anterior hypothalamus, lateral habenula, medial geniculate and the aqueduct. The coronal sections were taken based on known physiological landmarks (detailed in **figure 2.4**); including the presence of olfactory tract and forceps of the corpus callosum, anterior commissure, ventral hippocampal commissure, progressive hippocampal development (over 3 sections) and the aqueduct.

2.3.11 Haematoxylin and Eosin Staining

Haematoxylin and eosin staining is commonly used to identify ischaemic injury. Haematoxylin stains the cell nuclei dark blue and eosin will stain the cell cytoplasm pink.

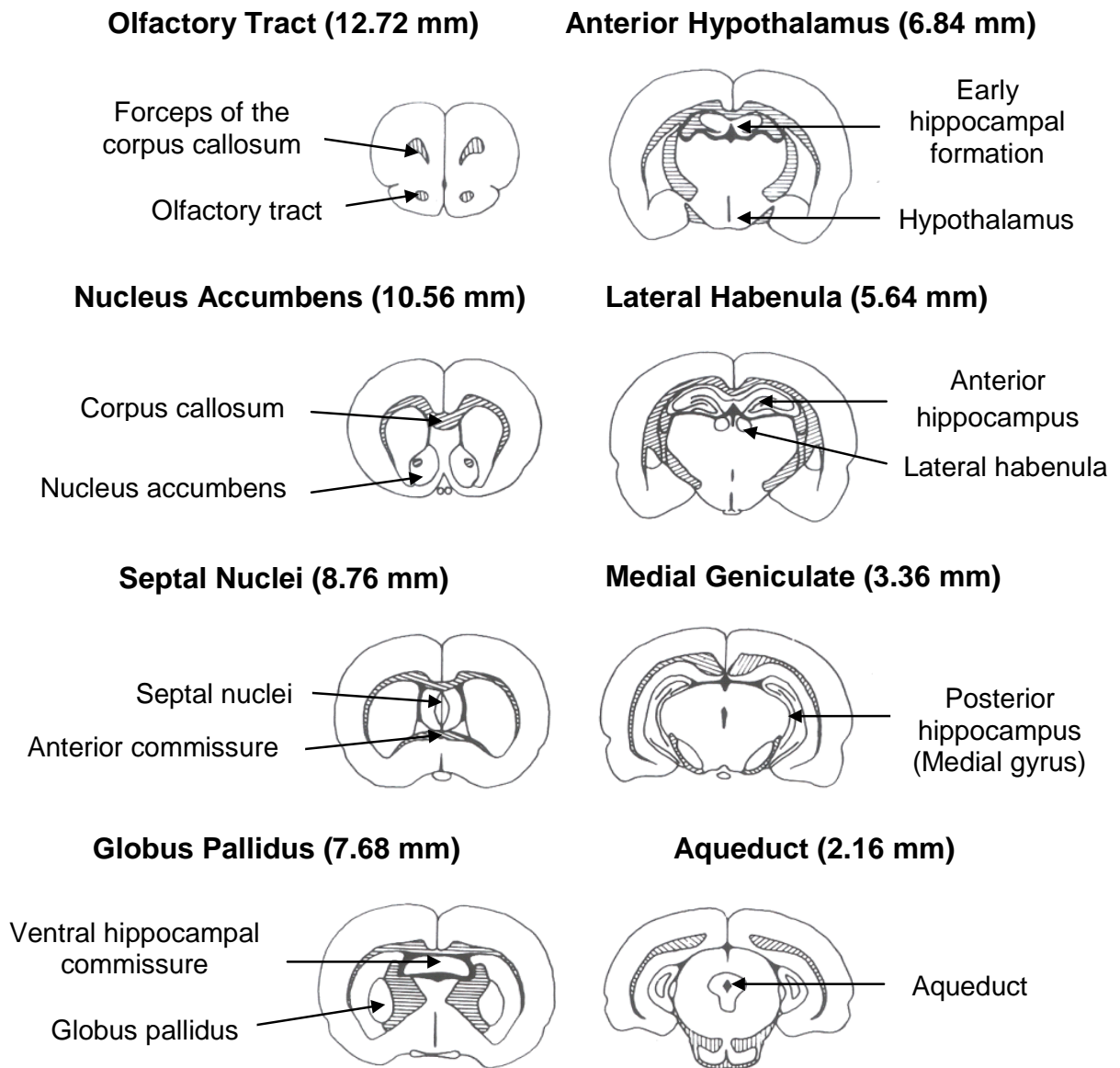


Figure 2.4: Line diagrams illustrate the 8 coronal sections, including stereotaxic coordinates based on the distance from the intra-aural line, taken to calculate infarct volume and the main anatomical landmarks used to identify each coronal level (Adapted from Osborne *et al.*, 1987).

The technique used for haematoxylin and eosin staining of this tissue is described below:

1. Coronal sections were fixed in 10% formal saline for 10 minutes. This step was only performed in non-perfusion fixed tissue.
2. The sections were rinsed in water for 3 minutes.
3. The tissue was dehydrated by placing the sections in 70% ethanol for 2 minutes and then 100% ethanol for a further 2 minutes.
4. The tissue was rehydrated by returning the sections to 70% ethanol for 2 minutes and then rinsed by dipping the sections in water several times.
5. The sections were stained with haematoxylin for 3 minutes. The sections were then rinsed in water and the strength of the stain checked under the microscope. If the staining was considered to be weak the tissue was re-stained with haematoxylin for ~30 seconds and the staining checked again.
6. The stained sections were then placed in 1% hydrochloric acid (1M) in alcohol for 2 minutes which removes the haematoxylin stain from the tissue. This step will reduce non-specific (non-nuclear) staining in the tissue.
7. The sections were rinsed in water.
8. The sections were then transferred to a solution of Scott's tap water for 2 minutes which stops the action of the 1% acid alcohol solution.
9. The tissue was then rinsed in water.
10. The sections were stained in aqueous eosin for 3 minutes and then rinsed in water.

11. The tissue was dehydrated by being placed in 70% ethanol for 1 minute and then transferred into 90% ethanol and then 100% ethanol for 1 minute each.
12. The tissue was then placed in histoclear for 1 minute to remove any stain remaining on the sections.
13. A coverslip was then positioned over the tissue using histomount mounting medium.

2.3.12 Infarct Quantification

Areas of infarct were identified by pallor of the tissue in stained sections. Stained sections were visualised using image analysis (MCID, InterFocus Imaging Ltd.). This software was then used to delineate and quantify the area of infarct in each section. Stained sections were also viewed under a light microscope to verify the border of the infarct in tissue without visible pallor. Irreversibly damaged neurons were pyknotic (shrunken or triangular in shape) and the surrounding neuropil was disrupted and displayed pallor.

Infarct and hemispheric volumes was calculated by multiplying the area in each section by the known distance between the levels based on the stereotactic coordinates. The total volume was taken as the sum of these individual volumes. The volume measurements were taken between the stereotactic coordinates 12.72 mm anterior and 0 mm posterior in relation to the inter-aural line. Infarct volume was expressed as a percentage of the ipsilateral hemispheric volume.

2.3.13 Oedema Quantification

In studies 1-3, 5 and 6, tissue oedema was calculated as the difference between the ipsilateral and contralateral hemisphere volume expressed as a percentage of the contralateral hemisphere volume. Oedema was not measured in perfusion fixed sucrose sunk tissue from study 4 as submersion in sucrose removes water from the tissue causing shrinkage. The extent of tissue shrinkage is not consistent throughout the tissue which prevents the accurate measurement of oedema.

2.3.14 Drug Preparation

The following drugs were used in this study and were prepared as described below:

- *Saline*: 0.9% sodium chloride (w/v) dissolved in distilled and stored at room temperature.
- *Atropine sulphate*: Dissolved in saline each day to form a 600 µg/ml solution.

2.4 Results

2.4.1 Survival

Table 2.4 shows the success of filament insertion and survival to the experimental end-point with each protocol as a percentage of the total number of animals that underwent the procedure. The initial surgical protocol used in the permanent ischaemia study (study 1a; n=12) was associated with poor success of filament insertion. In this study, several animals exhibited breathing difficulties while under anaesthesia and the animals that survived to 24 hours exhibited rasping and labored breathing. Modification of the surgical protocol (study 1b; n=6) increased the success

Table 2.4: Experimental protocol used and the success of filament insertion and post-operative survival in each study.

Study	Protocol	Occlusion period	Recovery period	Filament type	Filament placement (%)	Survival to end-point (%)
1a (n=12)	Permanent MCAO	24 h	–	Bulb	42	17
1b (n=6)	Permanent MCAO (Modified protocol)	24 h	–	Bulb	67	50
2 (n=12)	Transient MCAO	90 min	22 h 30 min	Bulb	83	58
3 (n=5)	Transient MCAO	2 h	70 h	Bulb	100	100
4 (n=12)	Transient MCAO	2 h	70 h	Bulb	83	42
5 (n=4)	Transient MCAO	90 min	70 h 30 min	Bulb	100	25
6 (n=2)	Transient MCAO	90 min	22 h 30 min	Silicon coated	100	100

MCAO; middle cerebral artery occlusion.

of filament insertion and prevented the breathing difficulties observed previously in animals during the recovery period. Two animals were excluded from analysis as one animal died before the 24 hour end-point and the other animal exhibited signs of rupture of the internal carotid artery (animals included in analysis; n=4).

In study 2 (n=12) there was a higher success of filament insertion compared to the permanent ischaemia study (studies 1a and 1b). Operative mortality (n=5) in this model was associated with reperfusion which resulted in haemorrhage due to an inability to properly seal the external carotid artery stump or damage to the common carotid artery when removing the ligature. All of the animals in study 2 that were allowed to recover from anaesthesia survived to the 24 hour end-point (n=7). Three animals were excluded from the analysis due to incomplete reperfusion, rupture of the internal carotid artery or lack of infarct development (animals included in analysis; n=4).

In study 3 (n=5) there was 100% survival to 72 hours with all of the animals undergoing successful surgery. However, it was shown in a separate experiment that the use of 100% oxygen as a delivery gas produced abnormal blood gases, high PO_2 and low PCO_2 , which has been shown to reduce infarct development in cerebral ischaemia. As such, the protocol used in this study does not represent an acceptable model for studying cerebral ischaemia under normal physiological conditions. It was decided to change the delivery gas used in study 4 from 100% oxygen to 30% oxygen:70% nitrous oxide. This change in the delivery gas had a detrimental effect on the survival rate. In study 4 (n=12) there was a high mortality rate as 33% of the

animals (n=4) that were allowed to recover from anaesthesia died within 24 hours. Three animals died during surgery due to blockage of the intubation tube or problems with anaesthesia. One of the animals that survived to 72 hours was excluded due to rupture of the internal carotid artery (animals included in analysis; n=4). Due to the high mortality rate the duration of the occlusion period was reduced from 2 hours to 90 minutes to limit the severity of the insult. The reduction in the occlusion period in study 5 (n=4) did not improve post-operative mortality compared to study 4. In this study, all 4 animals were allowed to recover following the procedure, however, due to poor physical condition 3 of the animals were euthanised at various points before the 72 hour end-point; at 4, 24 and 48 hours, respectively (animals included in analysis; n=3). In study 6 (n=2) the experimental protocol remained unchanged, however, silicon coated filaments were used instead of heat blunted nylon filaments. In this study, both of the animals that underwent 90 minutes occlusion survived to 24 hours post-occlusion.

2.4.2 Neurological Deficits

The general and focal deficit scores for animals in studies 3-6 at 24 and 72 hours is shown in **figure 2.5**. The different delivery gases used in studies 3 and 4 did not affect the general and focal deficits at 72 hours post-occlusion. In study 5 severe neurological deficits were observed at 24 hours despite the reduction in the duration of occlusion vs. study 4. Use of silicon coated filaments in study 6 was associated with an apparent reduction in the severity of the neurological deficits at 24 hours vs. study 5.

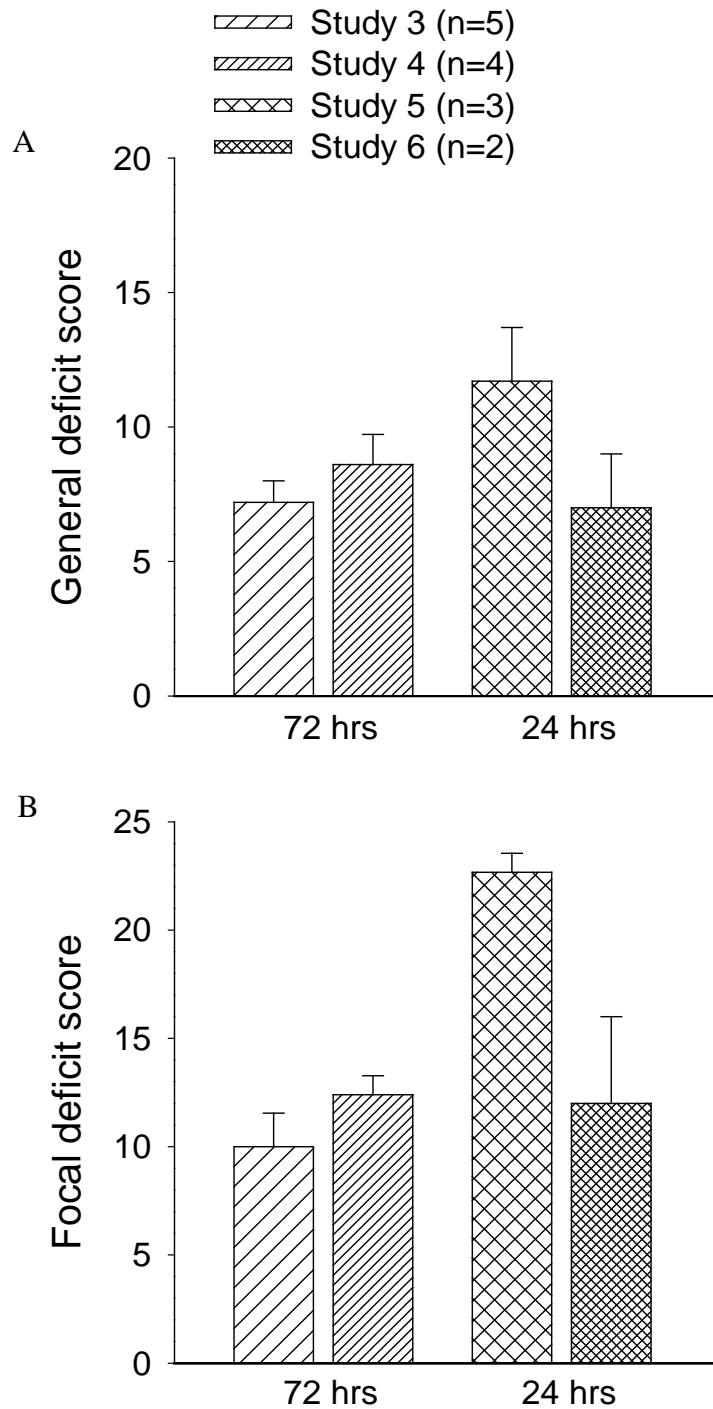


Figure 2.5: **A)** General and **B)** focal deficit scores assessed at 72 hours in studies 3 and 4 and 24 hours in studies 5 and 6. Neurological deficits were assessed on a scale ranging from 0 (healthy) to 28 (severe). Data are expressed as mean \pm standard error of the mean (s.e.m.).

2.4.3 Infarct Volume

In study 1, infarct development was present in all animals that survived to 24 hours after permanent ischaemia. A representative infarct from one of these animals is shown in **figure 2.6**. Infarct volume from animals in this study was not quantified as the aim of this work was to establish the surgical protocol. Mean infarct volume from animals that survived to 24 hours in studies 2-6 is shown in **figure 2.7**. In study 2, transient ischaemia produced a small infarct primarily affecting subcortical regions. The introduction of artificial ventilation with 100% oxygen in study 3 resulted in a very small infarct at 72 hours in most animals. However, one animal in this group had a much larger infarct resulting in a large standard error. Use of nitrous oxide/oxygen mixture as a delivery gas in study 4 resulted in a larger infarct in animals that survived to 72 hours vs. study 3. In study 4 greater infarct development was present in animals that died before the experimental end-point. Higher infarct volume was observed in study 5 in comparison to study 4. As in study 4, greater infarct volume was observed in animals that were euthanised at 24 and 48 hours. In study 6, there was a large infarct volume observed at 24 hours post-occlusion.

2.4.4 Oedema

There was visible oedema of the ipsilateral hemisphere at 24 hours after permanent ischaemia, as seen in the representative sections in **figure 2.6**. Oedema development was not assessed in study 1. Oedema development in animals that survived to 24 hours in studies 2-6 is shown in **figure 2.8**. There was little oedema development in spontaneously breathing animals (study 2) and those artificially ventilated with 100% oxygen (study 3) (**Figure 2.8**). Oedema could not be measured in study 4 as

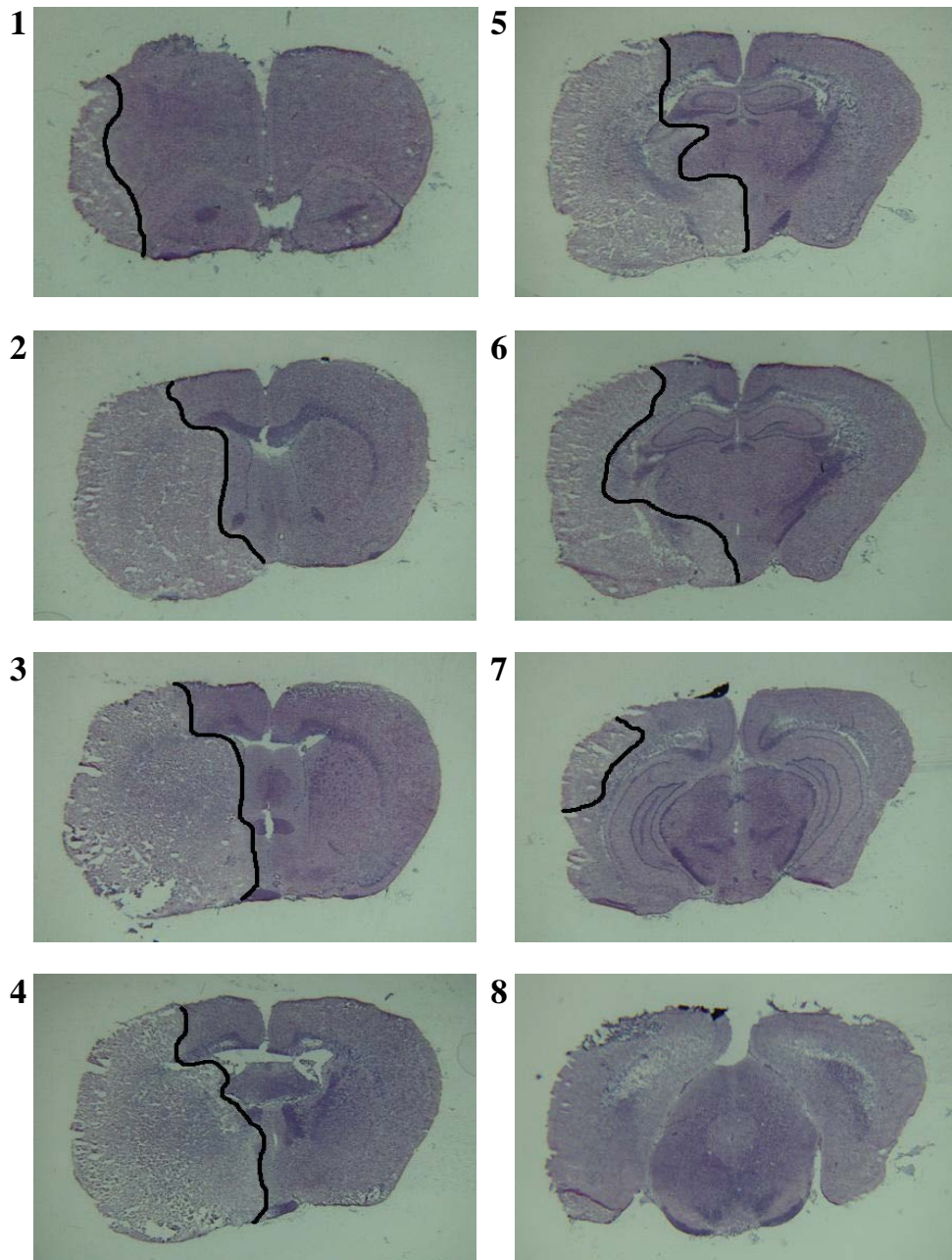


Figure 2.6: Study 1. Representative infarct observed at 24 hours after permanent middle cerebral artery occlusion in haematoxylin and eosin stained coronal sections. Sections were taken at 8 coronal levels based on Osborne *et al.*, 1987 (described in section 2.3.10).

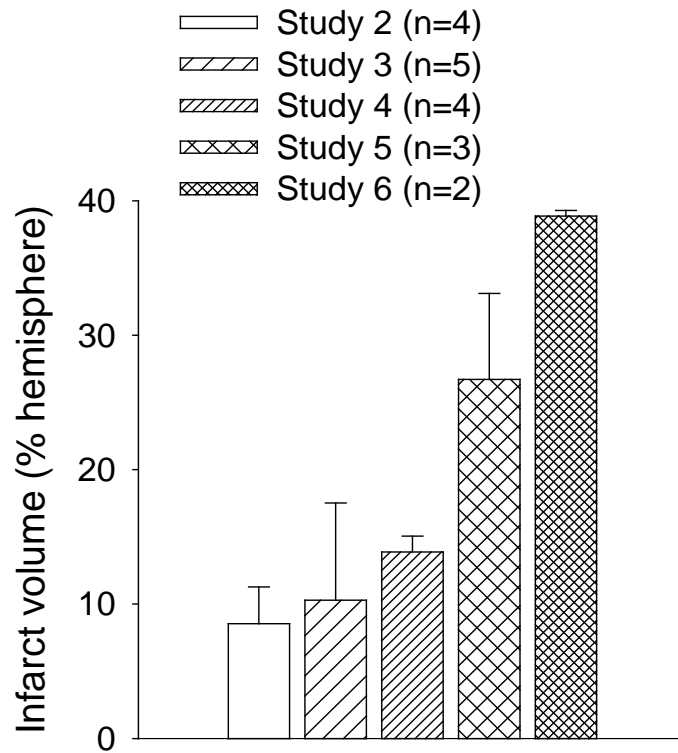


Figure 2.7: Infarct volume in animals that survived to at least 24 hours post-occlusion in studies 2-6. Infarct volumes were measured at different end-points in each study: study 2 (24 h), studies 3 and 4 (72 h), study 5 (24, 48 and 72 h) and study 6 (24 h). Data are expressed as mean \pm s.e.m.

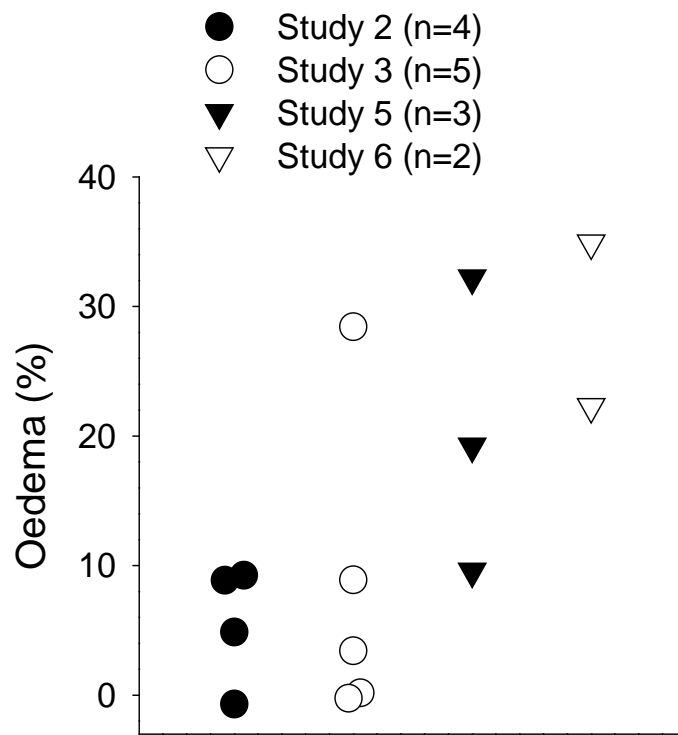


Figure 2.8: Oedema development in individual animals that survived to at least 24 hours post-occlusion in studies 2-6. Oedema was measured at different end-points in each study: study 2 (24 h), study 3 (72 h), study 5 (24, 48 and 72 h) and study 6 (24 h).

brains were immersed in sucrose prior to freezing which caused tissue shrinkage and prevented accurate oedema measurement. In study 5 the level of oedema varied between animals. There was little tissue oedema in the animal that survived to 72 hours, however, severe oedema was observed in the 3 animals that were euthanised at 4, 24 and 48 hours. Greatest oedema development was observed in study 6 (**figure 2.8**).

2.4.5 Laser Doppler Flowmetry

Doppler flowmetry was not used to monitor cerebral blood flow in studies 1 and 2. Mean cerebral blood flow monitored during the experimental period in animals that survived to 24 hours in studies 3-6 is shown in **figure 2.9**. In studies 3-5, the common carotid artery was occluded at the beginning of the surgical procedure resulting in a 30-40% decrease in cerebral blood flow. Middle cerebral artery occlusion caused a similar decrease in cerebral blood flow (~70% of baseline) in animals that survived to 24 hours in all groups. Reperfusion produced an increase in cerebral blood flow, however, this did not return to the baseline value in any group. In study 6, there was a greater increase in cerebral blood flow following reperfusion (~85% of baseline). In study 4, there was a greater decrease in cerebral blood flow during occlusion in animals that died before 24 hours compared to those that survived to the 72 hours (**figure 2.10**). In study 5 the decrease in cerebral blood flow following occlusion varied between animals. A greater reduction in cerebral blood flow was observed in the animals that died at 4 and 24 hours post-occlusion (**figure 2.11**). Following reperfusion there tended to be a smaller increase in cerebral blood flow in animals that died before 72 hours compared to the animal that survived

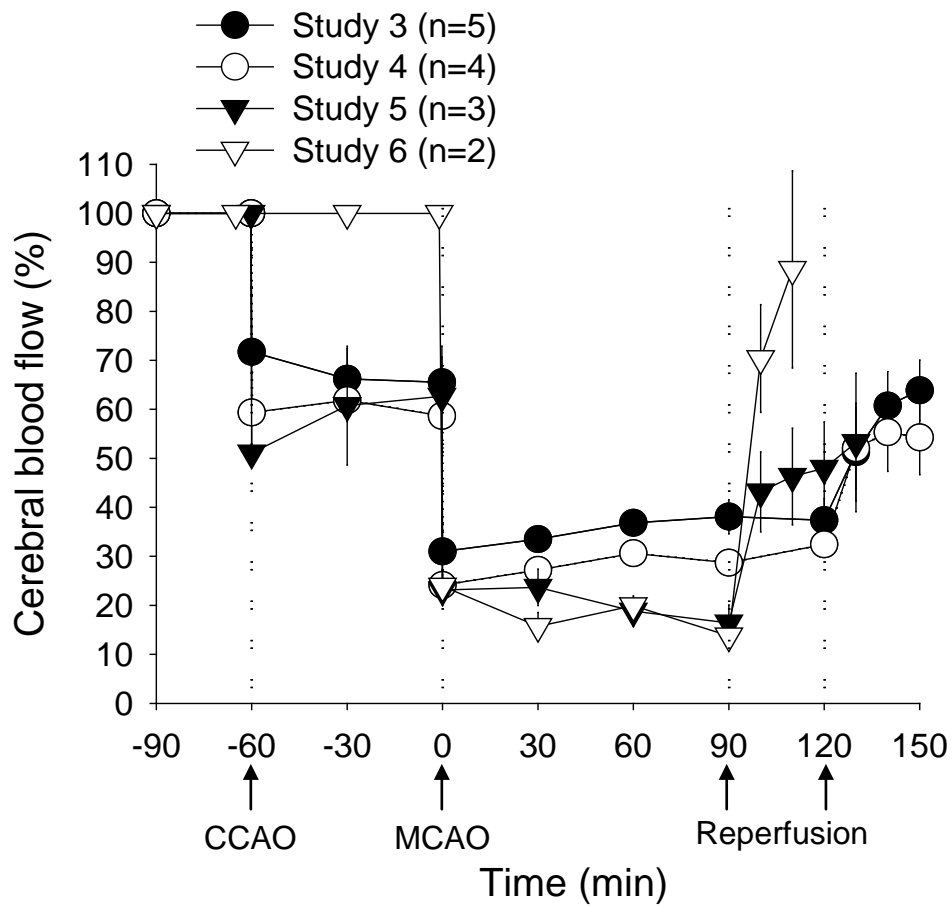


Figure 2.9: Cerebral blood flow measurements recorded throughout the experimental period in animals that survived to at least 24 hours post-occlusion in studies 3-6. Data are expressed as mean \pm s.e.m. CCAO; common carotid artery occlusion, MCAO; middle cerebral artery occlusion.

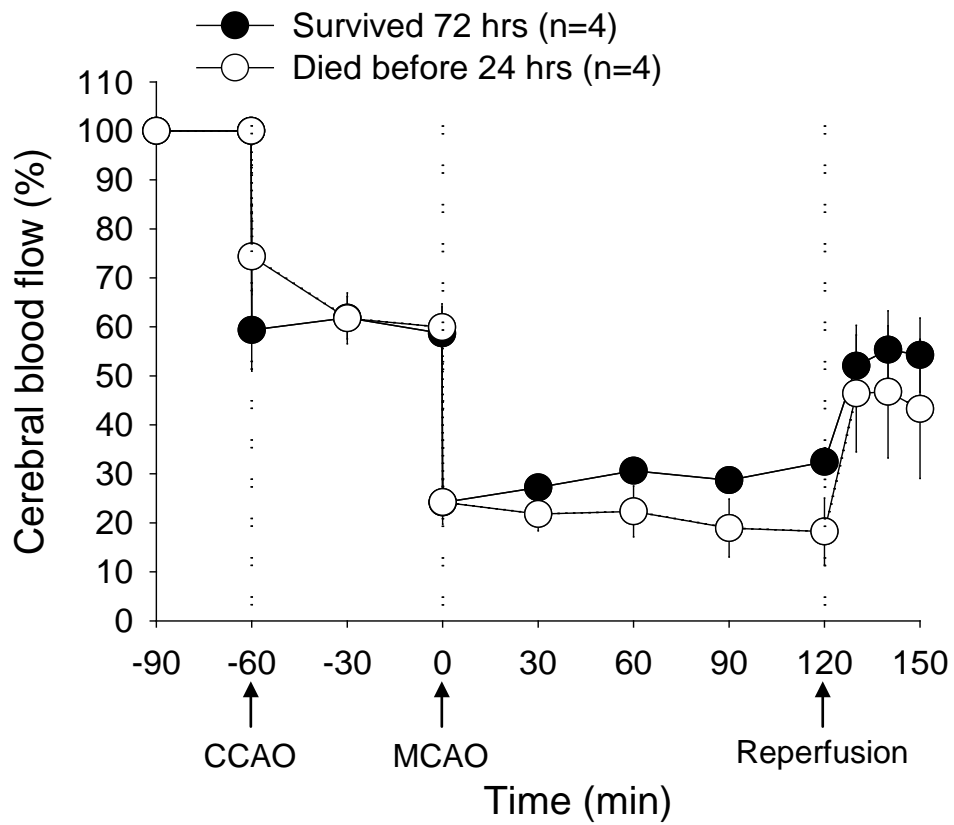


Figure 2.10: Study 4. Cerebral blood flow measurements recorded throughout the experimental period in animals that survived to 72 hours post-occlusion and those that died before the experimental end-point. Data are expressed as mean \pm s.e.m. CCAO; common carotid artery occlusion, MCAO; middle cerebral artery occlusion.

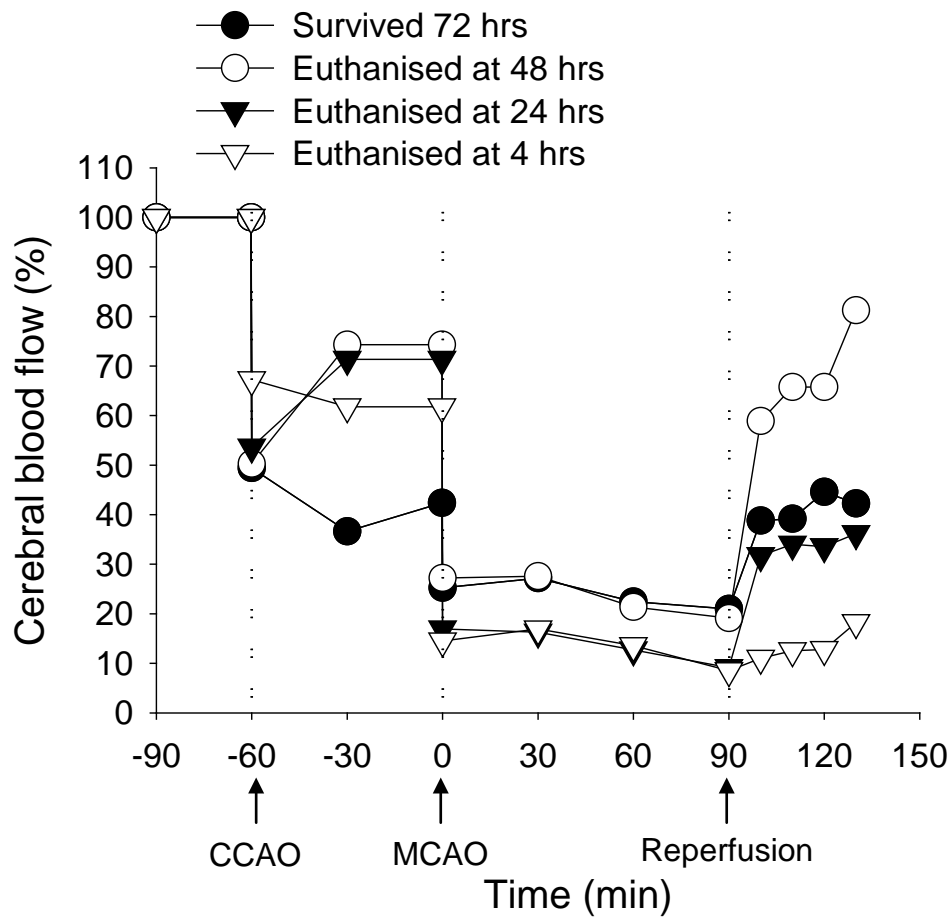


Figure 2.11: Study 5. Cerebral blood flow measurements recorded throughout the experimental period in each animal that underwent the experimental protocol (n=4). Data are expressed as mean \pm s.e.m. CCAO; common carotid artery occlusion, MCAO; middle cerebral artery occlusion.

to this time-point. There was little change in cerebral blood flow following reperfusion in the animal that died within 4 hours of the procedure.

2.4.6 Complications

The initial surgical protocol used in study 1 resulted in high surgical mortality and poor recovery of animals at 24 hours. Breathing problems were present in these animals during surgery and the recovery period. It is likely that these problems were caused by damage to the vagus nerve during dissection of the carotid vasculature. Breathing difficulties were reduced by modification of the surgical technique to limit contact with the vagus nerve. In transient ischaemia studies, the main complication was the presence of small bleeds, known as haemorrhagic transformations, caused by the rupture of small cerebral blood vessels. A typical pattern of bleeding observed in a frozen brain is shown in **figure 2.12**. In study 3 haemorrhagic transformation was present in 2 animals which both survived to 72 hours. Haemorrhagic transformation was extremely common in study 4 with bleeding identified in 89% of animals allowed to recover from anaesthesia (n=9 animals that recovered from anaesthesia). In study 4, haemorrhagic transformation was present in all of the animals that survived to 72 hours and 3 of the 4 animals that died within 24 hours of the procedure. Haemorrhagic transformation was less prevalent in study 5 following a reduction in the occlusion period vs. study 4. Bleeding was observed in 2 of the 4 animals in this study; one animal that survived to 72 hours and the animal euthanised within 4 hours. As such, haemorrhagic transformation did not cause the severe neurological deficits observed in the animals that were euthanised at 24 hours and 48 hours.

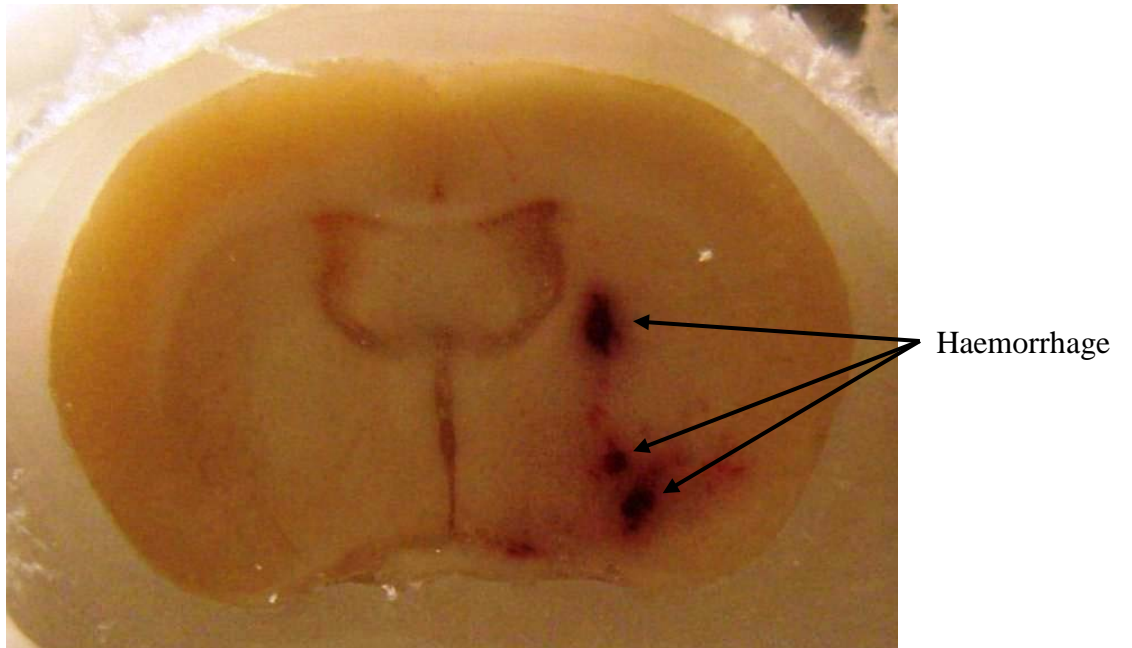


Figure 2.12: Study 4. Photograph of haemorrhagic transformation in a partially sectioned frozen brain.

2.5. Discussion

The intraluminal thread model is useful in the study of cerebral ischaemia as it allows the induction of permanent or transient middle cerebral artery occlusion using a non-invasive technique. However, the benefit of using this model may be limited by variability in the extent of injury development. The aim of this work was to develop the intraluminal thread technique and establish a reproducible model of transient middle cerebral artery occlusion.

In study 1, the intraluminal thread technique was used to produce permanent middle cerebral artery occlusion. The initial surgical technique was associated with high operative mortality and poor physical condition of animals allowed to recover from anaesthesia. Surgical mortality was related to the difficulties associated with learning a new technique; for example damage to surrounding tissue during exposure of the vasculature and prolonged use of anaesthesia. Several of the animals stopped breathing during the surgery and animals which recovered from anaesthesia exhibited severe breathing difficulties at 24 hours, this suggests that there may have been damage to the vagus nerve. Damage to the vagus nerve is a common complication of this technique due to the proximity of the carotid vasculature to the nerve. Vagus nerve damage can cause a build-up of mucus secretions in the trachea which can obstruct the airway and result in breathing difficulties. In the revised surgical technique administration of atropine to reduce tracheal secretions was effective in improving breathing during surgery and in the recovery period. Breathing problems may have been exacerbated by prolonged use of anaesthesia and the reduction in the length of the procedure with increased surgical experience may

have contributed to this beneficial effect.

In the first transient middle cerebral artery occlusion model (study 2) animals underwent 90 minute occlusion with 24 hour recovery. This protocol resulted in a relatively small and variable infarct, $9 \pm 3\%$, with a coefficient of variation of 64%. Six animals underwent this protocol, 2 of these animals had to be excluded due to subarachnoid haemorrhage or absence of infarct. These issues are common in this model due to the non-invasive nature of the surgical technique and inability to directly confirm successful filament insertion during the surgery (Durukan and Tatlisumak, 2007). Laser Doppler flowmetry was introduced to monitor cerebral blood flow in the ipsilateral hemisphere and was used to confirm successful middle cerebral artery occlusion in later studies. The addition of laser Doppler flowmetry to the protocol improved the rate of successful middle cerebral artery occlusion. Since its introduction in study 3 there have been no animals that have not shown an infarct following filament insertion and only one animal has been identified with subarachnoid haemorrhage.

Tracheal intubation and artificial ventilation were also incorporated into the protocol to control blood gases during surgery and attempt to reduce inter-animal variation. Blood gases can exert direct effects on the cerebral vasculature. Carbon dioxide can cause potent vasodilation of cerebral vessels due to increased release of H^+ ions (Olah *et al.*, 2000). In cerebral ischaemia this effect can be detrimental as blood vessels in the ischaemic tissue show a decreased response to the vasodilatory effects of carbon dioxide and dilation of other vessels in the non-ischaemic tissue may cause

a further reduction in tissue perfusion (Olah *et al.*, 2000; Dirnagl and Pulsinelli, 1990). The benefit of intubation in studies 3-5 is unclear as due to a lack of access to the necessary equipment it was not possible to measure blood gases or haemodynamics in these animals. Prior to the introduction of artificial ventilation an experiment was performed to establish the correct pump settings to maintain normal blood gases and blood pressure and these settings were maintained between animals.

Duration of occlusion is one of the main factors affecting infarct severity. However, when 100% oxygen was used as the delivery gas the increase in the occlusion period from 90 minutes to 2 hours caused little change in infarct development. In a single experiment it was shown that the use of 100% oxygen as a delivery gas in intubated animals resulted in supraphysiological PO_2 values, 5 times higher than normal, and a low PCO_2 of 20-25 mmHg. It is likely that the use of 100% oxygen caused a high PO_2 value in all of the animals in this study. The effect of these blood gases on infarct development in this model is unclear due to high variability of the infarct volume in this study, coefficient of variation of 157%. However, the marked deterioration in post-operative survival from 100% to 42% with the change from using 100% oxygen to 30% oxygen:70% nitrous oxide does suggest that these abnormal blood gases did affect infarct development. This observation agrees with previous studies which have shown that 100% oxygen delivered via a facemask or tracheal cannula during occlusion or reperfusion can reduce infarct size following transient cerebral ischaemia (Singhal *et al.*, 2002; Shin *et al.* 2007). Several mechanisms of action have been suggested, including increased blood oxygenation and improving cerebral blood flow (Shin *et al.*, 2007).

The use of an oxygen/nitrous oxide mixture was associated with an increase in the incidence of haemorrhagic transformation, 89% of animals that were allowed to recover from anaesthesia following 2 hour transient middle cerebral artery occlusion (**figure 2.13**). Haemorrhagic transformation was very common in this study and the presence of small bleeds in animals that survived to the experimental end-point suggests that haemorrhagic transformation itself was not the cause of the poor survival rate. A study in human stroke patients has suggested that haemorrhagic transformation is not directly detrimental and poor recovery is only associated with larger bleeds that exert a space-occupying effect and exacerbate oedema development (Molina *et al.*, 2002). In human stroke patients the development of haemorrhagic transformation was associated with tissue reperfusion, the duration of ischaemia before reperfusion, high blood pressure and high blood glucose (Lansberg *et al.*, 2007). The reduction in the duration of occlusion from 2 hours to 90 minutes resulted in a reduction in the incidence of haemorrhagic transformation (50% vs. 89%). This observation is in agreement with data from human patients which suggests that the risk of haemorrhagic transformation increases with the length of time from the onset of ischaemia until thrombolytic treatment is administered.

There was poor post-operative recovery and survival to the experimental end-point in study 5, despite the reduction in the duration of occlusion and decreased incidence of haemorrhagic transformation. Poor recovery in these animals may be associated with the presence of a large infarct volume and severe oedema. A correlation analysis demonstrated a relationship between infarct volume and oedema development (**figure 2.14**). Infarct volume and oedema are related to the severity of ischaemic

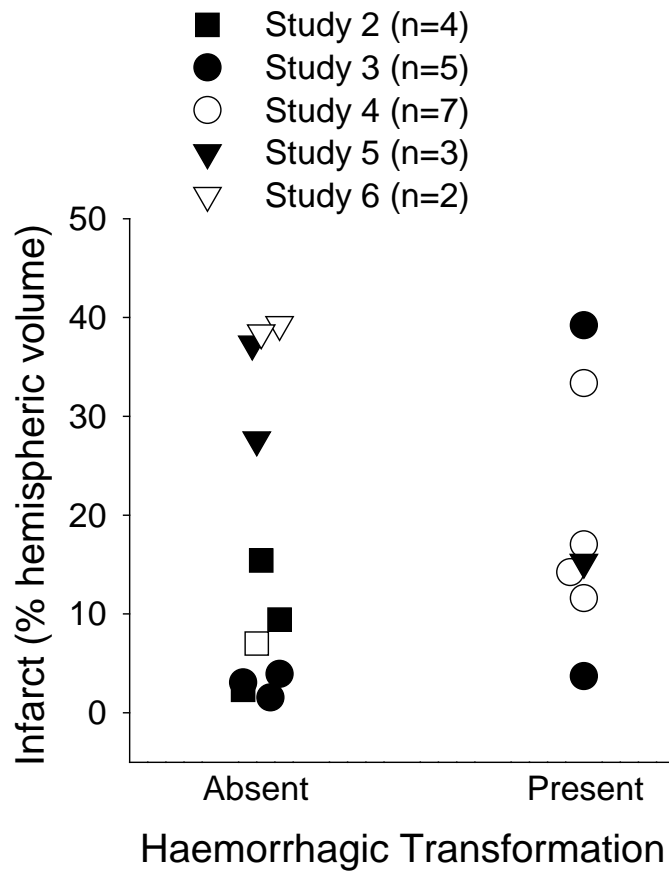


Figure 2.13: Comparison of infarct volume and the presence of haemorrhagic transformation in animals that survived to 24 hours post-occlusion in each study.

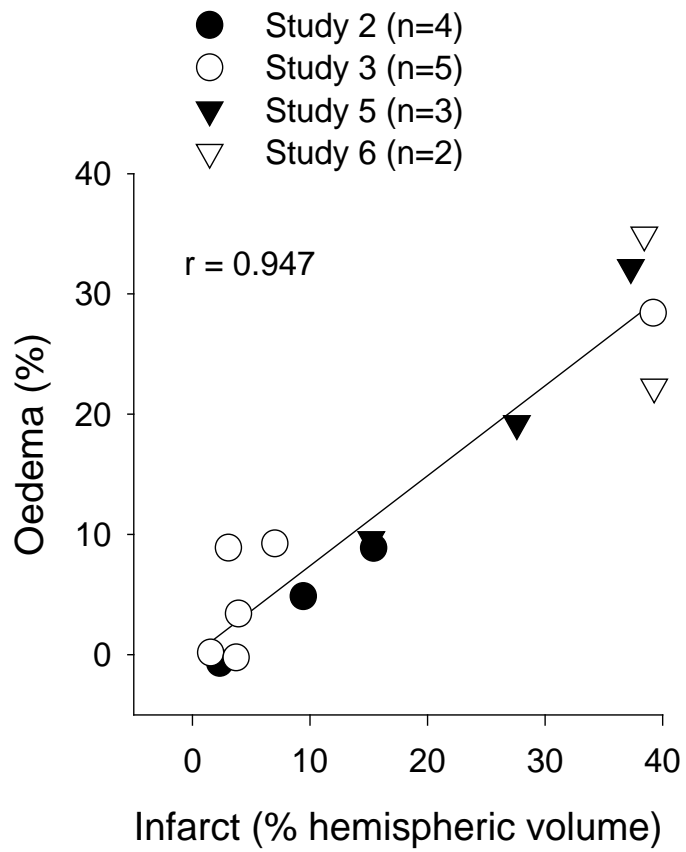


Figure 2.14: Correlation between infarct volume and oedema development was examined by performing a Pearson's correlation analysis.

injury as with a large infarct there are a greater number of injured cells causing greater cytotoxic oedema and severe injury is associated with breakdown of the blood brain barrier and subsequent vasogenic oedema. The relationship between the extent of ischaemic injury and infarct development may explain why animals which did not survive to the experimental end-point in studies 4 and 5 often showed a greater or more sustained reduction in cerebral blood flow following middle cerebral artery occlusion. However, this explanation is contradicted by the results from study 6 where the presence of a large infarct and severe oedema was not associated with post-operative mortality. Despite the large injury observed in study 6 these animals recovered well following surgery and exhibited fewer neurological deficits compared to study 5. The reason for the difference in survival and functional outcomes between these studies is unclear. The improved recovery of animals in study 6 may be related to more successful restoration of cerebral blood flow in these animals following reperfusion ($89 \pm 20\%$ of baseline in study 6 vs. $48 \pm 10\%$ in study 5).

Taken together, these studies demonstrate the difficulty involved in developing a reproducible model of transient middle cerebral artery occlusion and the multiple factors which can affect injury development and functional recovery. Following the poor survival and recovery outcomes in study 5 the decision was taken to halt attempts to develop a model of transient middle cerebral artery occlusion.

To examine the effect of endocannabinoids it was decided to use a model of acute cerebral ischaemia produced by 4 hour permanent middle cerebral artery occlusion. In this model haemodynamics and physiological parameters, including oxygen

saturation, end-tidal carbon dioxide and blood gases, can be monitored continuously throughout the surgery and occlusion period. The physiological data gathered using this model can be used to optimise ventilation settings and ensure animals are maintained within normal parameters. This information can be used to further develop the transient middle cerebral artery occlusion model and attempt to improve the experimental outcome.

The experiments in study 6 were performed as part of an unrelated pilot study which examined cerebral arteries taken from animals following transient middle cerebral artery occlusion. These experiments were started after the 4 hour permanent middle cerebral artery occlusion studies described in chapters 3 and 4 had been performed. The protocol used in this study was established using information gained from the 4 hour permanent middle cerebral artery occlusion experiments. This protocol was successful in producing a large infarct without the severe neurological deficits and high post-operative mortality observed in study 5. Unfortunately, due to external factors (time and cost) it was decided not to complete this study and only 2 animals underwent this protocol.

In conclusion, the surgical technique for the intraluminal thread model of middle cerebral artery occlusion has been successfully established. Attempts to establish a model of transient middle cerebral artery occlusion were complicated by high post-operative mortality which may be associated with large infarct size and severe oedema development. The introduction of coated filaments reduced post-operative mortality and improved neurological outcome during recovery. However, the small

number of animals included in study 6 prevents a conclusion from being drawn on whether this protocol would provide a reproducible model of transient middle cerebral artery occlusion. The protocol used in study 6, 90 minute middle cerebral artery occlusion using a silicon coated Doccol filament in artificially ventilated animals, does, however, represent a good starting point for the development of a rat model of transient middle cerebral artery occlusion.

CHAPTER 3

EFFECT OF ANANDAMIDE AND URB597 ON INJURY AND MICROGLIAL RESPONSE AFTER 4 HOUR CEREBRAL ISCHAEMIA IN RATS

3.1 Introduction

As described in the previous chapter, the development of a rat model of transient middle cerebral artery occlusion was complicated by high mortality. As such, it was decided to examine the effects of endocannabinoids in a model of 4 hour permanent middle cerebral artery occlusion. In this model the effects of endocannabinoids on haemodynamic measurements and cerebral blood flow can be monitored continuously following treatment and the microglia response can be assessed at the end of the experiment. This will provide greater information on the mechanisms involved in mediating the effects of endocannabinoids in cerebral ischaemia.

As detailed in chapter 1, anandamide has been shown to promote an anti-inflammatory phenotype in LPS-activated microglia through decreased release of the pro-inflammatory cytokine TNF- α (Facchinetti *et al.*, 2003) and enhanced release of the anti-inflammatory cytokine IL-10 (Correa *et al.*, 2010). Administration of exogenous anandamide has been shown to reduce infarct size at 24 hours after transient cerebral ischaemia (Schomacher *et al.*, 2008). The mechanisms involved in mediating this protective effect have not been examined. The hypothesis of the present study is that anandamide and the fatty acid amide hydrolase inhibitor URB597 are neuroprotective in acute cerebral ischaemia and may reduce injury development through effects on the microglia response.

3.2 Aim

The aim of this work was to examine the effect of exogenously administered anandamide and the fatty acid amide hydrolase inhibitor URB597 on injury volume

and microglia number and activation at 4 hours after middle cerebral artery occlusion.

3.3 Methods

3.3.1 Source of Materials

Details of suppliers for equipment, drugs and reagents are included in the Appendices.

3.3.2 Animal Source

All animals used in these experiments were sourced and housed as detailed in **section 2.3.2**.

3.3.3 Animal Preparation

Male Sprague-Dawley rats weighing 275-350g underwent middle cerebral artery occlusion. Anaesthesia was induced as described in **section 2.3.3**.

Once anaesthetised, the trachea was intubated and animals were artificially ventilated using a stroke volume of 1.5 ml per 100 g body weight at a rate of 50-55 strokes per minute. Anaesthesia was maintained with 2.25-2.5% isoflurane delivered in 30% oxygen:70% nitrous oxide at 1 l/min. The suitability of the depth of anaesthesia was assessed by the lack of a pedal withdrawal response and corneal reflex. Following induction, the animals were prepared for surgery as detailed in **section 2.3.3**.

3.3.4 Physiological Monitoring

A Medair Life-Sense™ Vet pulse-oximeter / capnograph was used to monitor oxygen saturation and end-tidal carbon dioxide. Oxygen saturation (%) was monitored by a clip placed on the hind paw. A carbon dioxide line was attached to the ventilation set-up to collect expired air and measure end-tidal carbon dioxide (mmHg). Oxygen saturation and end-tidal carbon dioxide values were recorded every 15 minutes throughout the experimental period.

For blood pressure measurement, a femoral artery was dissected free of connective tissue and cannulated with polythene tubing (0.40 mm internal diameter (ID) and 0.80 mm outer diameter (OD)) containing heparinised saline (20 units/ml). The cannula was connected to a pressure transducer and Gould bridge amplifier. Blood pressure signals were measured using a Gould paper chart recorder. At the start of every day, a mercury sphygmomanometer was used to calibrate the transducer for blood pressure measurement. Blood pressure was recorded continuously and measurements taken every 15 minutes during the experimental period. Mean arterial blood pressure was calculated from systolic and diastolic blood pressure measurements as shown below:

$$\text{Mean arterial Blood Pressure} = \text{Diastolic pressure} + \frac{1}{3} (\text{Systolic pressure} - \text{Diastolic pressure})$$

3.3.5 Laser Doppler Flowmetry

In each animal, laser Doppler flowmetry was used to monitor cerebral blood flow throughout the experimental period as described in **section 2.3.4**. Values were

recorded every 30 minutes during surgery, immediately prior to filament insertion and every 15 minutes following occlusion.

3.3.6 Intraluminal Filament Preparation

An uncoated heat blunted 3-0 nylon filament was used to occlude the middle cerebral artery. Preparation of each filament was previously described in **section 2.3.5**.

3.3.7 Intraluminal Thread Model

The intraluminal thread surgery was performed as detailed in **section 2.3.6**. The animal was maintained under anaesthesia for the duration of the 4 hour occlusion period and euthanised by anaesthetic overdose and decapitation at the end of the experiment.

3.3.8 Experimental Protocol

18 rats were placed into 3 treatment groups (n=6 in each group):

1. Group 1: Animals received both vehicles; 5% dimethyl sulfoxide (DMSO) at occlusion and 50% Tocrisolve at 30 minutes post-occlusion.
2. Group 2: Animals received the URB597 vehicle, 5% DMSO, at occlusion and anandamide (10 mg/kg, s.c.) at 30 minutes post-occlusion.
3. Group 3: Animals received the fatty acid amide hydrolase metabolism inhibitor, URB597 (0.3 mg/kg, s.c.), at occlusion and the anandamide vehicle, 50% Tocrisolve, at 30 minutes post-occlusion.

All treatments were administered s.c. at 2 ml/kg. Animals received either treatment or vehicle in a randomised and blinded manner. The treatment protocol is illustrated in **figure 3.1**. The treatment protocol for anandamide, dose and timing of administration, was decided based on a previous study by Schomacher *et al.*, 2008 who demonstrated that anandamide at 10 mg/kg (i.p.) given at 30 minutes post-occlusion reduced infarct size at 24 hours following 90 minute transient cerebral ishaemia. The treatment protocol for the fatty acid amide hydrolase metabolism inhibitor, URB597, was determined based on characterisation data published by Fegley *et al.* (2005). In the characterisation study, administration of URB597 at 0.3 mg/kg (i.p.) resulted in a significant increase in the anandamide concentration in the brain at 30 minutes post-administration which peaked at 1 hour.

3.3.9 Inclusion Criteria

Animals were only included in the data analyses if they fulfilled the following criteria:

1. No sign of haemorrhage of the internal carotid artery was present on the base of the brain.
2. Laser Doppler signal reduced by more than 60% following insertion of the filament.
3. Animals were successfully maintained within normal physiological parameters and oxygen saturation remained above 90%. Normal ranges for each of the physiological parameters are shown in **table 3.1**. These parameters were used based on guidelines from Hall L *et al.* (2002) and Flecknell (1996).

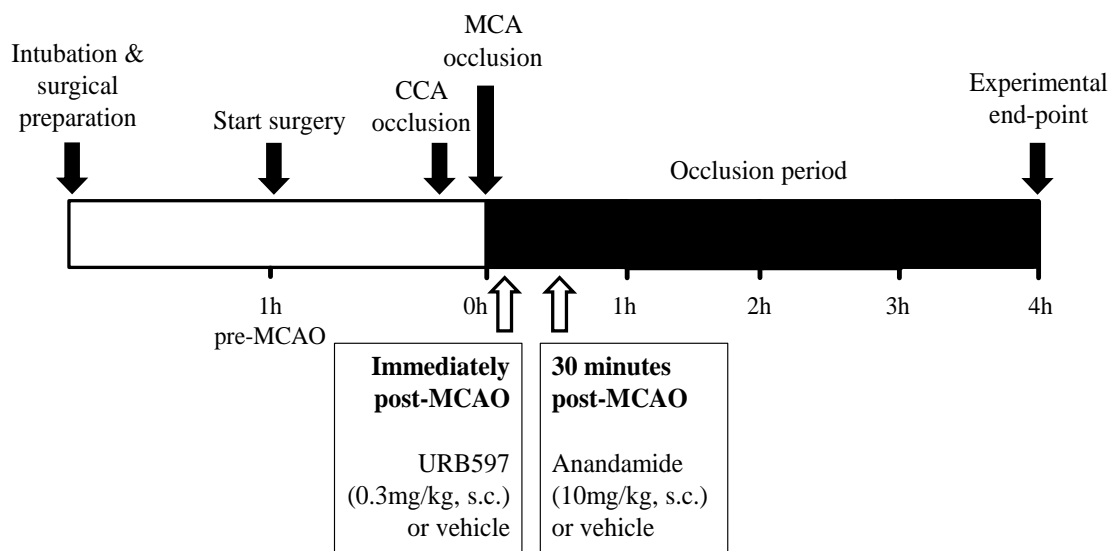


Figure 3.1: Experimental and treatment protocol. Following surgery the middle cerebral artery was occluded and animals received URB597 (0.3 mg/kg, s.c.) immediately after occlusion or anandamide (10 mg/kg, s.c.) at 30 minutes post-MCAO. Animals also received one or both of the vehicles, where appropriate. CCA; common carotid artery, MCA; middle cerebral artery, MCAO; middle cerebral artery occlusion.

Table 3.1: Normal range for physiological parameters monitored during each experiment.

<u>Parameter</u>	<u>Normal Range</u>	
	Minimum	Maximum
Heart rate (beats per minute (bpm))	350	450
Mean arterial blood pressure (mmHg)	60	100
SO ₂ (%)	90	100
ETCO ₂ (mmHg)	35	45
Temperature (°C)	36.5	37.5

SO₂; oxygen saturation, ETCO₂; end-tidal carbon dioxide.

3.3.10 Tissue Processing

Animals were killed by overdose of anaesthetic and decapitation at the end of the experimental period. The brains were removed immediately and frozen in isopentane. The tissue was sectioned at 20 μ M as described in **section 2.3.9**.

3.3.11 Haematoxylin and Eosin Staining

Sections were stained with haematoxylin and eosin to identify injured cells as described in **section 2.3.10**.

3.3.12 Lesion Quantification

In stained sections, light microscopy was used to confirm the injury boundary based on the presence of irreversibly injured cells. These cells were identified based on the presence of pyknotic nuclei and cytoplasmic degradation (**figure 3.2**). The injury was transcribed on to line diagrams of 8 coronal levels taken from the rat brain stereotaxic atlas (Paxinos and Watson, 6th edition; **figure 3.3** (actual size shown)). The injury boundary was transcribed based on its relation to anatomical landmarks shown on the line diagrams. The use of line diagrams prevented quantification of injury volume from being influenced by tissue oedema. Each line diagram was calibrated prior to use by confirming that the area of each coronal section was measured accurately. The injury area in each section was quantified using MCID image analysis software. In this study all animals received treatment in a blinded manner. As such, injury quantification was performed by an individual who was blind to the treatment administered without the need for re-coding of the animals.

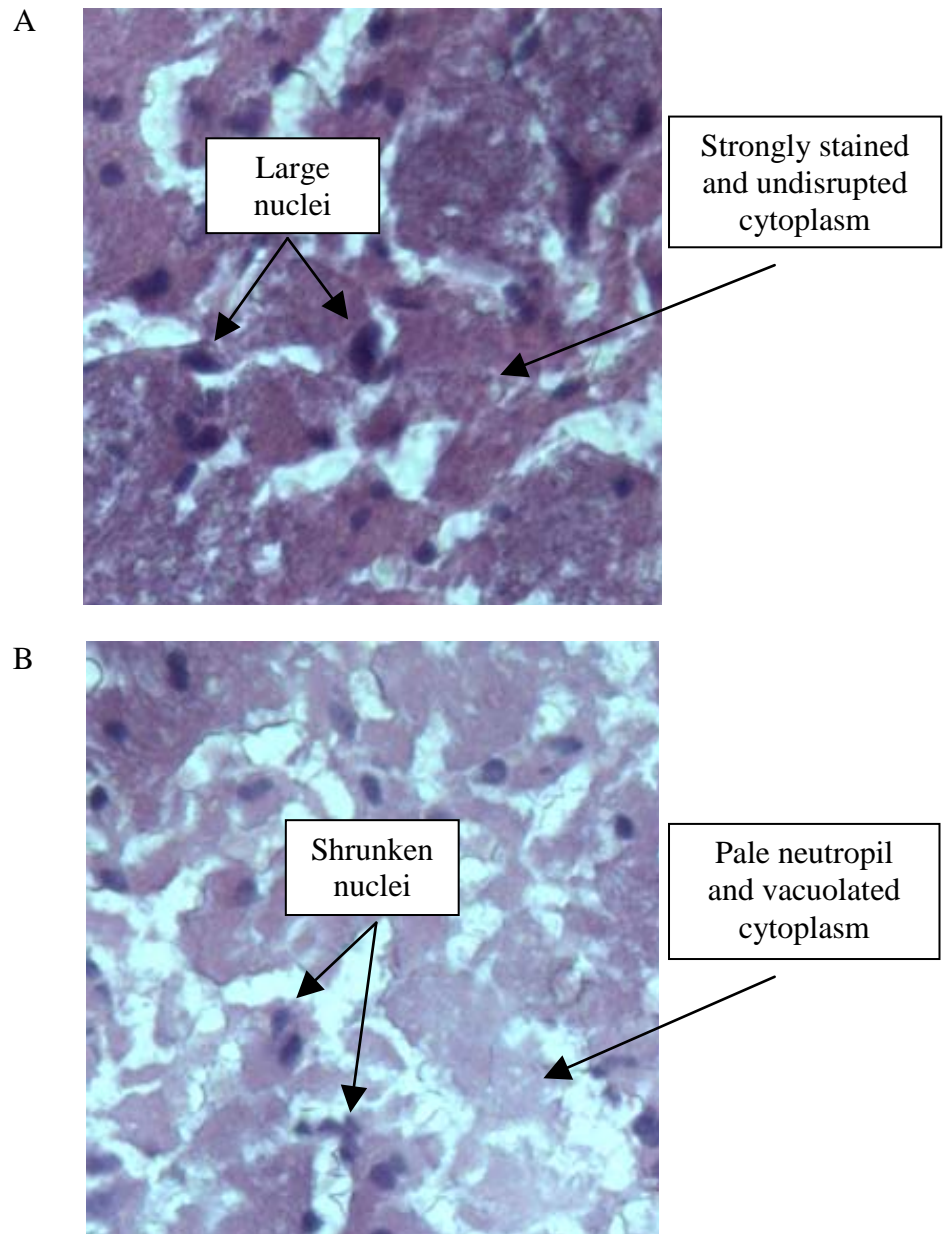


Figure 3.2: Images showing **A)** viable and **B)** irreversibly injured tissue taken using a light microscope (x200 magnification).

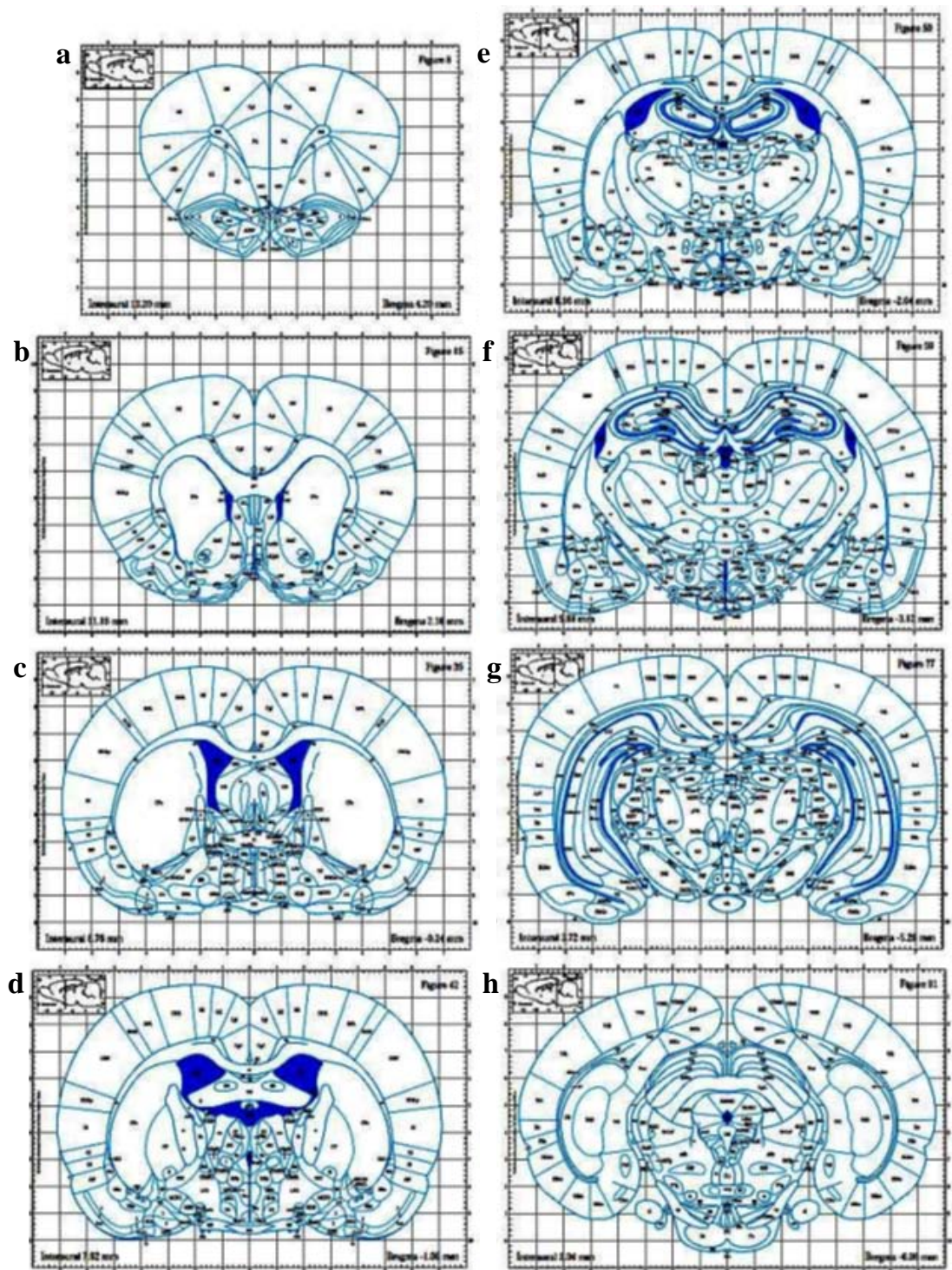


Figure 3.3: Line diagrams taken from a rat stereotaxic atlas showing the 8 coronal levels used to quantify injury volume.

Total volume was calculated by multiplying the area in each section by the known distance between the levels based on the stereotactic coordinates. The total volume was taken as the sum of these individual volumes and expressed as mm³. The volume measurements were taken between the stereotactic coordinates 12.72 mm anterior and 0 mm posterior in relation to the inter-aural line.

3.3.13 Immunofluorescence

Immunofluorescence was performed to examine microglia distribution and activation in coronal sections at the level of globus pallidus (**figure 3.3d**) and anterior hippocampus (**figure 3.3f**) which is normally perfused by the middle cerebral artery. Resting and activated microglia were stained using a polyclonal antibody raised in goat against ionised Ca²⁺ binding adaptor molecule-1 (Iba-1). Iba-1 is highly and specifically expressed in monocytic cell lines; including peripheral macrophage and both resting and activated microglia in several different subpopulations (Ito *et al.*, 1998). This antigen was not present on other cell types in the brain, such as neurons and astrocytes (Ito *et al.*, 1998). Expression of Iba-1 was shown to be strongly upregulated in activated microglia *in vivo* following nerve injury (Ito *et al.*, 1998) and cerebral ischaemia (Ito *et al.*, 2001).

Prior to immunofluorescence staining, frozen tissue was removed from the freezer and stored overnight at 4 °C to allow tissue to defrost slowly. The immunofluorescence protocol used is described below:

1. Sections were fixed in 2% paraformaldehyde for 1 hour at room temperature.

2. Sections were washed 3 times in phosphate buffered saline (PBS) 0.05 M (pH 7.4) for 5 minutes. The tissue was rinsed in PBS and 1% triton X-100 for 5 minutes to increase cell membrane permeability. Sections were then washed in PBS for a further 5 minutes.
3. The slides were dried and the tissue was encircled by a hydrophobic barrier pen.
4. To reduce background staining, non-specific binding sites were saturated by incubation with 20% normal rabbit serum in 0.5% triton X-100 in PBS for 30 minutes.
5. To identify microglia the tissue was stained by overnight incubation at 4 °C with a polyclonal primary antibody for Iba-1 (raised in goat) diluted to 1:250 in 20% normal serum.
6. Sections were washed in PBS for 5 minutes and then rinsed in PBS and 1% triton X-100 for a further 5 minutes.
7. Stained cells were labelled by incubation with a fluorescein isothiocyanate (FITC)-conjugated anti-goat secondary antibody at a concentration of 1:200 for 1 hour in the dark.
8. The sections were rinsed twice in PBS for 5 minutes.
9. The stained tissue was covered by a glass coverslip using vectashield aqueous mounting medium containing the fluorescent nucleic acid stain, 4',6-diamidino-2-phenylindole, commonly known as DAPI.

Negative controls were included in each batch by omitting the primary antibody and using 20% normal serum for the overnight incubation step.

3.3.14 Confocal Microscopy

Stained sections were viewed by confocal microscopy (x40 oil objective). Multi-layer z-stack images were produced by taking a series of cross-sectional images (380 μ m x 380 μ m) at 1 μ m steps through the tissue. Images were taken at the injury boundary in 3 fields; 1 field in the cortex and 2 fields in subcortical regions, and in corresponding areas in the contralateral hemisphere.

3.3.15 Microglia Analysis

The multi-layer z-stacks were compressed to form a 2-dimensional image and analysed using Volocity image analysis software (Perkin Elmer, Cambridge, UK). Each compressed image represents a tissue volume of 0.003 mm³. Positively stained microglia cells were counted in each image and the cell count expressed as cells per mm³. Activated microglia cells were clearly identified by a skilled observer based on their morphology; including enlarged nucleus and shorter, thicker processes (**figure 3.4**). In each group the activation state (activated or resting) could not be determined for ~10-20% of the total number of microglia present. The number of activated microglia was expressed as a percentage of the total number of microglia in each image. For the subcortical regions, microglia number and activation was assessed in the 2 fields examined and the mean of these values was calculated to give a single value for the subcortical region. This mean value was then used to produce the figures in this thesis and for statistical analyses. All analysis was performed by a person who was blind to the treatment groups.

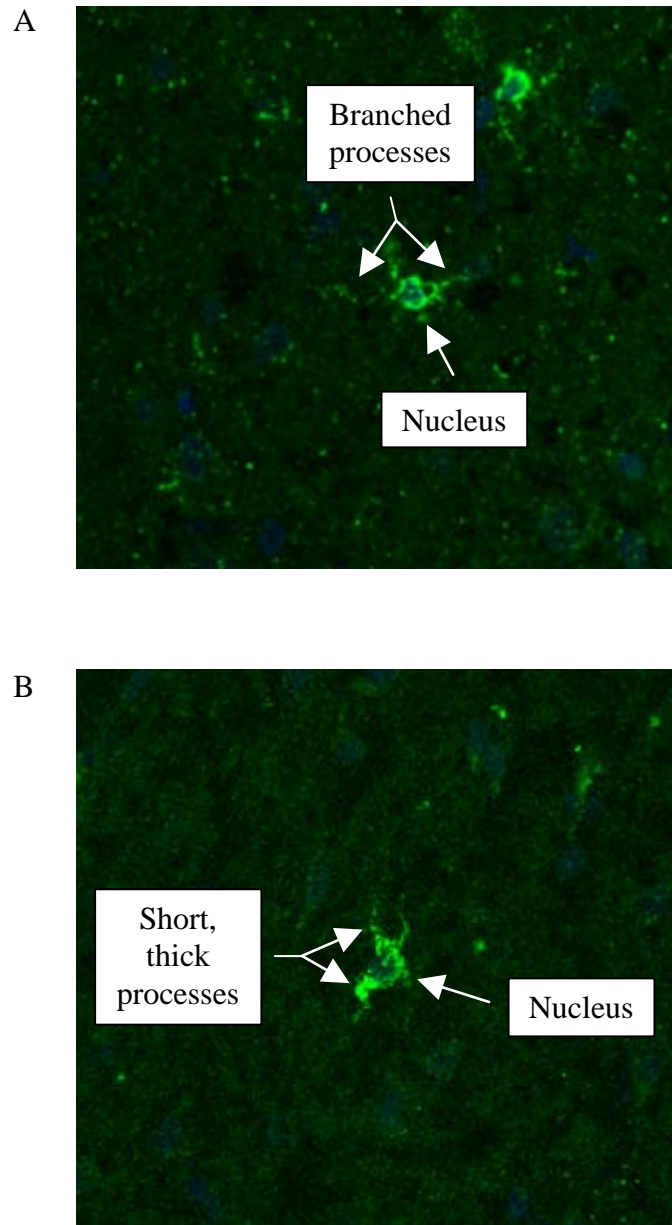


Figure 3.4: Confocal images showing a compressed z-stack series of **A)** resting and **B)** activated microglia (x400 magnification). The resting microglia has a small nucleus with thin, branching processes. Activated microglia can be identified by the presence of an enlarged nucleus and short, thick processes.

3.3.16 Drug Preparation

In this study, saline and atropine sulphate was prepared fresh each day as detailed in **section 2.3.14**. The following drugs were also used and were prepared as described below:

- *Heparinised saline*: Heparin (1000 units/ml) was added to saline to form a final concentration of 20 units/ml.

- *Anandamide*: Supplied in Tocrisolve, a water soluble emulsion, at 10 mg/ml, stored at 4 °C and diluted in saline to form a 5 mg/ml emulsion immediately before use.

- *URB597*: Dissolved in DMSO to form a 3 mg/ml solution, stored at -20 °C and diluted to 0.15 mg/ml in saline before use.

3.3.17 Statistical Analysis

Haemodynamic measurements and cerebral blood flow recorded immediately before occlusion and at 1 hour intervals post-occlusion were analysed using a mixed model repeated measures analysis of variance (ANOVA). Treatment groups were compared by a Dunnett's post-hoc test and the effect of time on these measurements was examined by performing one-way repeated measures ANOVA. The effect of anandamide on haemodynamic parameters was examined by comparing the percentage change in these measurements in anandamide and vehicle treated animals at 15 minutes post-administration using an unpaired t-test. One-way ANOVA followed by Dunnett's post-hoc test performed to compare total, subcortical and cortical injury volume and cortical:subcortical ratio. The number of microglia and

extent of activation in the ipsilateral and contralateral hemisphere were compared between groups using a one way ANOVA followed by a Dunnett's post-test and comparisons between hemispheres were performed using a paired t-test. To examine the effect of treatment microglia number and activation in the ipsilateral hemisphere in each animal were expressed as a percentage of the contralateral hemisphere values and compared with a one way ANOVA followed by Dunnett's post-test.

3.4 Results

3.4.1 Physiological Variables

One animal receiving anandamide was excluded from the analysis due to a progressive deterioration in oxygen saturation and cerebral blood flow during the occlusion period. In the 3rd hour of occlusion oxygen saturation fell below 90% and did not improve despite changes to ventilation settings in an attempt to improve oxygenation. As a result, this animal developed a much larger injury compared to others in the same treatment group (164 mm³ vs. 58 ± 7 mm³).

In all groups, physiological measurements remained within normal parameters throughout the experimental period except for end-tidal carbon dioxide which dropped periodically to ~34.5 mmHg across groups with lowest level of 33.7 mmHg (**table 3.2**). These values appeared similar in animals receiving anandamide, URB597 and vehicle. There was a gradual and significant decline in blood pressure in vehicle and URB597 treated animals over the experimental period. However, a decline in blood pressure which fell below 60 mmHg at the end of the experiment was observed in some animals in all groups. Anandamide produced a transient

Table 3.2: Physiological parameters recorded 1 hour before occlusion and repeated at several time-points throughout the occlusion period in animals that received anandamide, URB597 or both vehicles.

Time post-MCAO (hours)	Physiological parameters		
	SO ₂ (%)	ETCO ₂ (mmHg)	Temperature (°C)
Vehicle (n=6)			
-1	96.5 ± 1.1	34.5 ± 3.0	36.8 ± 0.1
0	94.2 ± 2.5	34.5 ± 2.1	36.9 ± 0.1
1	95.7 ± 0.7	37.2 ± 1.8	36.8 ± 0.1
2	94.7 ± 1.1	35.3 ± 1.3	37.0 ± 0.0
3	93.5 ± 1.4	34.3 ± 1.4	37.0 ± 0.1
4	94.0 ± 1.3	33.7 ± 1.7	36.9 ± 0.1
Anandamide (10 mg/kg; n=5)			
-1	96.0 ± 0.7	35.8 ± 0.9	36.8 ± 0.1
0	95.4 ± 0.9	34.8 ± 2.0	36.8 ± 0.2
1	95.0 ± 0.9	35.0 ± 1.1	37.0 ± 0.1
2	95.6 ± 0.5	36.0 ± 0.8	37.0 ± 0.1
3	95.2 ± 0.7	36.0 ± 0.8	37.3 ± 0.1
4	93.0 ± 0.8	35.2 ± 1.0	36.8 ± 0.1
URB597 (0.3 mg/kg; n=6)			
-1	95.3 ± 0.8	34.7 ± 1.0	37.1 ± 0.1
0	95.5 ± 1.2	35.2 ± 0.9	37.2 ± 0.1
1	94.2 ± 0.7	35.0 ± 1.2	37.1 ± 0.1
2	94.5 ± 0.9	34.7 ± 0.9	37.0 ± 0.1
3	95.0 ± 0.9	35.0 ± 0.8	37.1 ± 0.1
4	94.0 ± 0.6	36.2 ± 2.4	37.0 ± 0.1

All data are expressed as mean ± s.e.m. MCAO; middle cerebral artery occlusion, SO₂; oxygen saturation, ETCO₂; end-tidal carbon dioxide.

hypotensive effect with a reduction in blood pressure observed at 15 minutes after treatment compared to vehicle. There was no change in blood pressure following treatment with URB597 compared to the vehicle. Neither anandamide nor URB597 produced a significant change in heart rate or blood pressure in comparison to the vehicle treated group (**figure 3.5** and **figure 3.6**, respectively).

3.4.2 Laser Doppler Flowmetry

Cerebral blood flow measurements for each group recorded during surgery and the occlusion period are shown in **figure 3.7**. Occlusion of the middle cerebral artery caused a significant reduction in cerebral blood flow in all animals (mean $60.1 \pm 4.1\%$). Neither anandamide nor URB597 caused a significant difference in cerebral blood flow compared to vehicle.

3.4.3 Infarct Volume

Line diagrams showing injury topography from an individual animal in each group (median total injury volume) are shown in **figure 3.8**. The effect of anandamide and URB597 on injury volume compared to vehicle in **figure 3.9**. Anandamide and URB597 did not significantly affect total, subcortical or cortical injury volume compared to vehicle, however, both anandamide and URB597 modified the topography of the injury. In vehicle treated animals, the injury was equally distributed between cortical and subcortical region. Despite the absence of any effect of treatment on cortical or subcortical injury volume when injury volume in these regions was normalised by expressing these values as a percentage of total injury volume a significant effect was observed. Treatment with anandamide and URB597

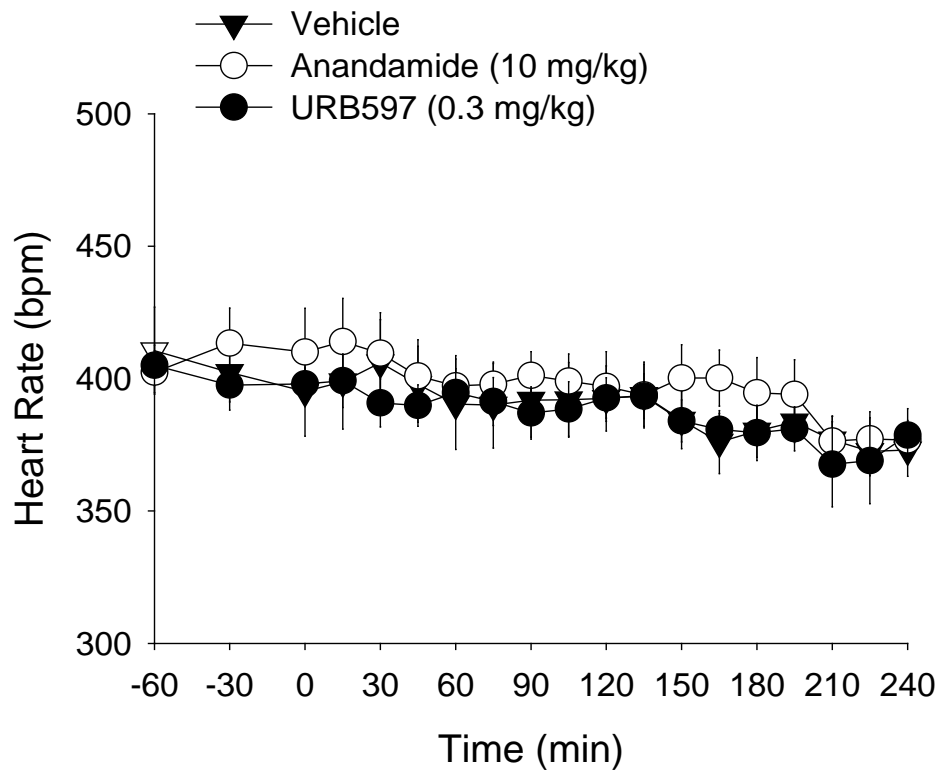
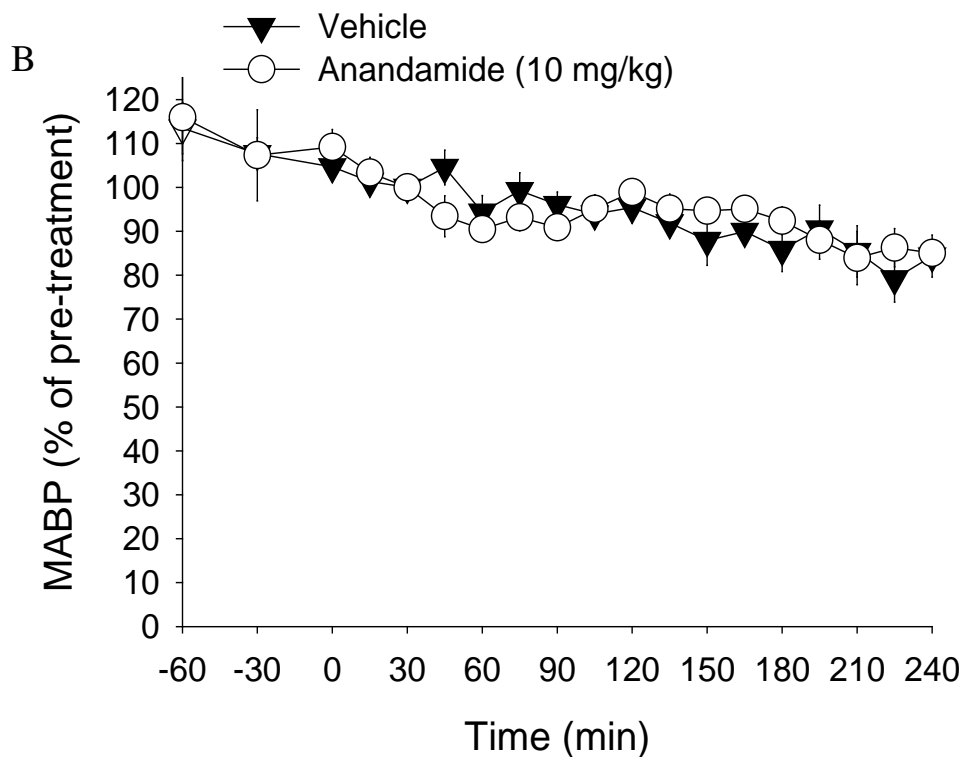
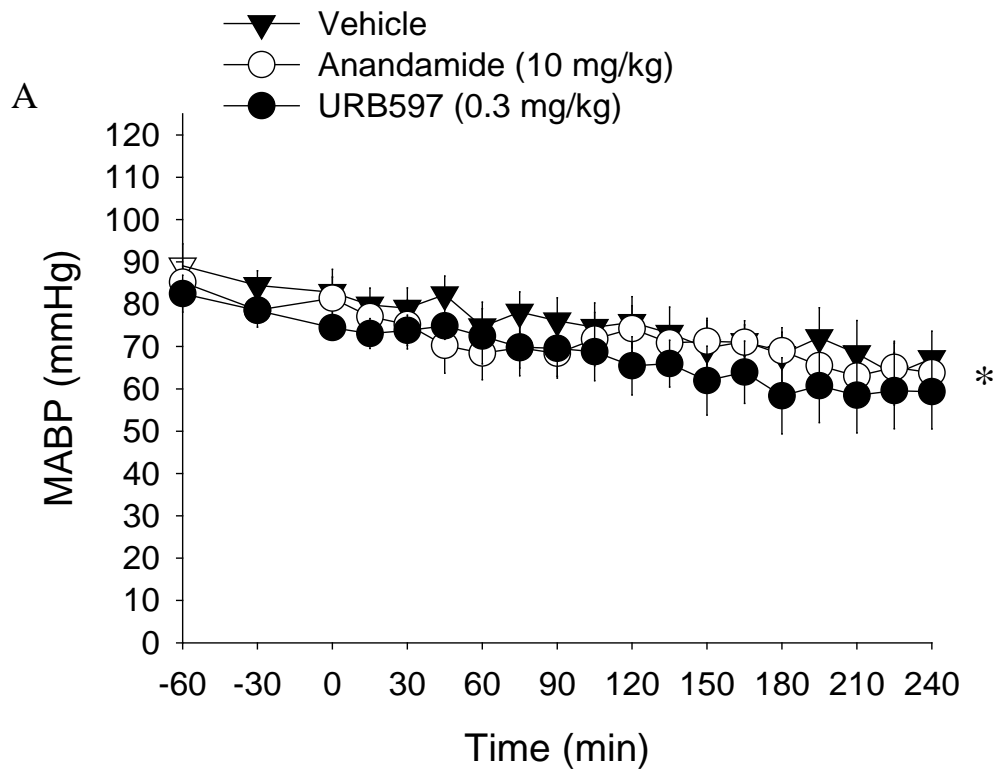


Figure 3.5: Heart rate in each treatment group (n=5 for anandamide, n=6 for vehicle and URB597). Data are expressed as mean \pm s.e.m. No significant difference at 4 hours post-MCAO vs. pre-MCAO or between treatment groups, mixed model ANOVA with post-hoc comparison between time-points and treatment groups performed by repeated measures ANOVA and Dunnett's test, respectively.



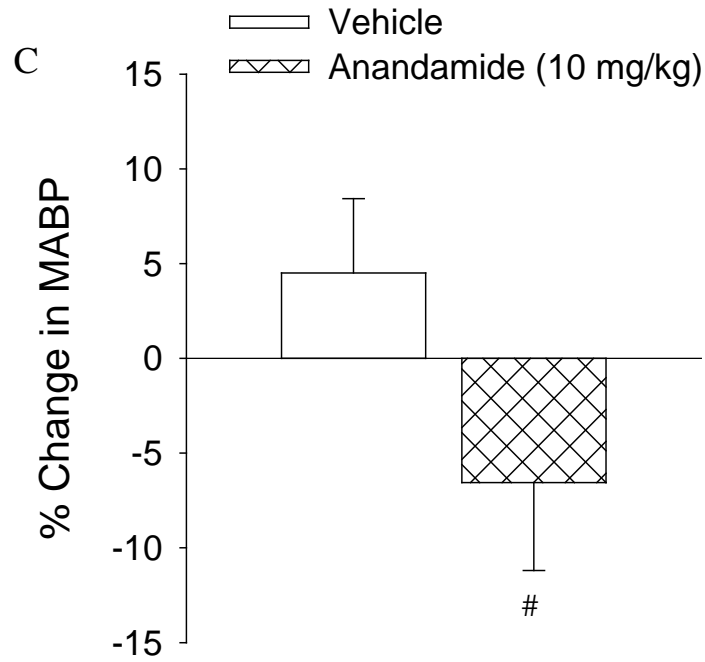


Figure 3.6: Mean arterial blood pressure expressed as **A)** mmHg and **B)** percentage of pre-treatment value in each treatment group and **C)** percentage change in blood pressure at 15 minutes after treatment with anandamide and tocrisolve vehicle (n=5 for anandamide, n=6 for vehicle and URB597). Data are expressed as mean \pm s.e.m. * $p < 0.05$ vs. pre-MCAO in vehicle and URB597 treated animals, mixed model ANOVA followed by Dunnett's test. Comparison of time-points; pre-MCAO and 1, 2, 3 and 4 hours post-MCAO, were performed using repeated measures ANOVA. # $p < 0.05$ for anandamide vs. vehicle at 15 minutes after treatment.

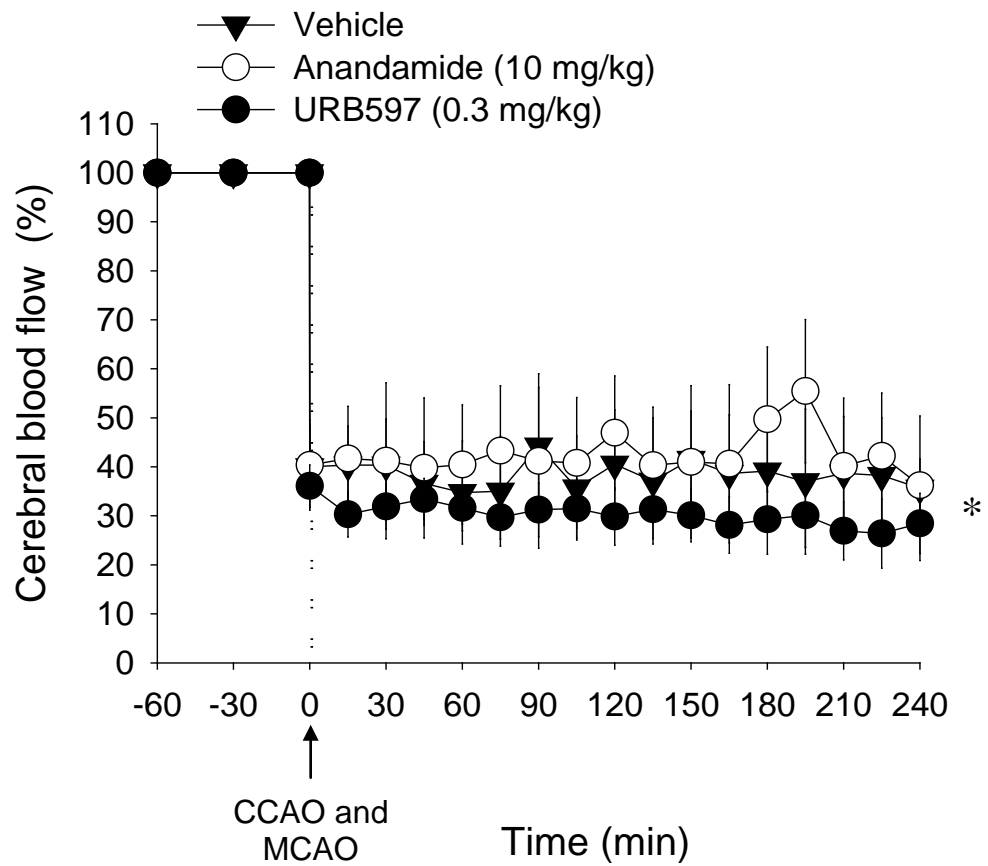


Figure 3.7: Cerebral blood flow measurements recorded in each treatment group throughout the experimental period (n=5 for anandamide, n=6 for vehicle and URB597). CCAO; common carotid artery occlusion, MCAO; middle cerebral artery occlusion. Data are expressed as mean \pm s.e.m. * $p < 0.05$ vs. pre-MCAO in all groups, mixed model ANOVA with Dunnett's test to compare treatment groups. Comparison of time-points; pre-MCAO and 1, 2, 3 and 4 hours post-MCAO, were performed using repeated measures ANOVA.

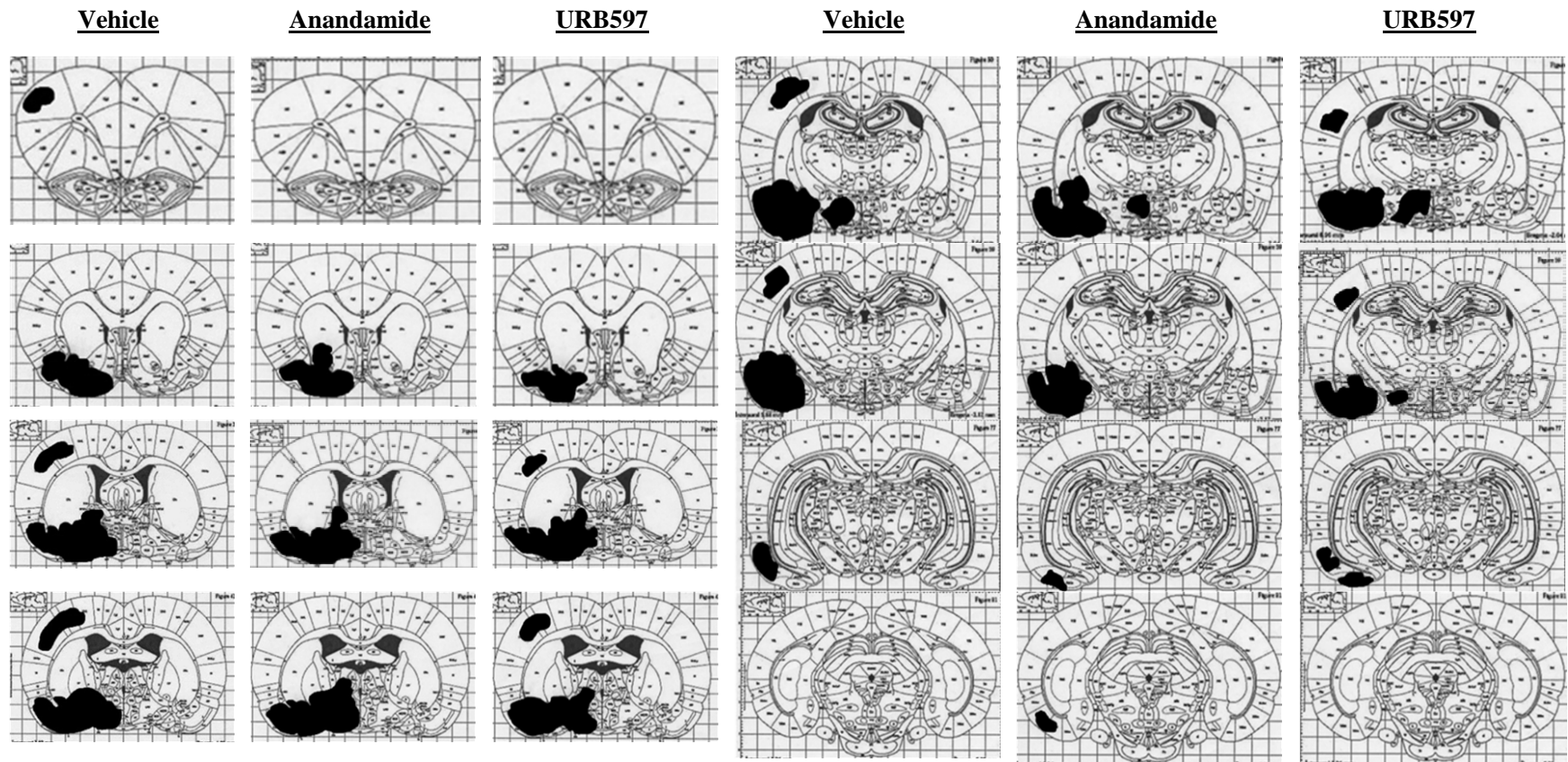


Figure 3.8: Representative line diagrams showing the injury topography observed in each treatment group.

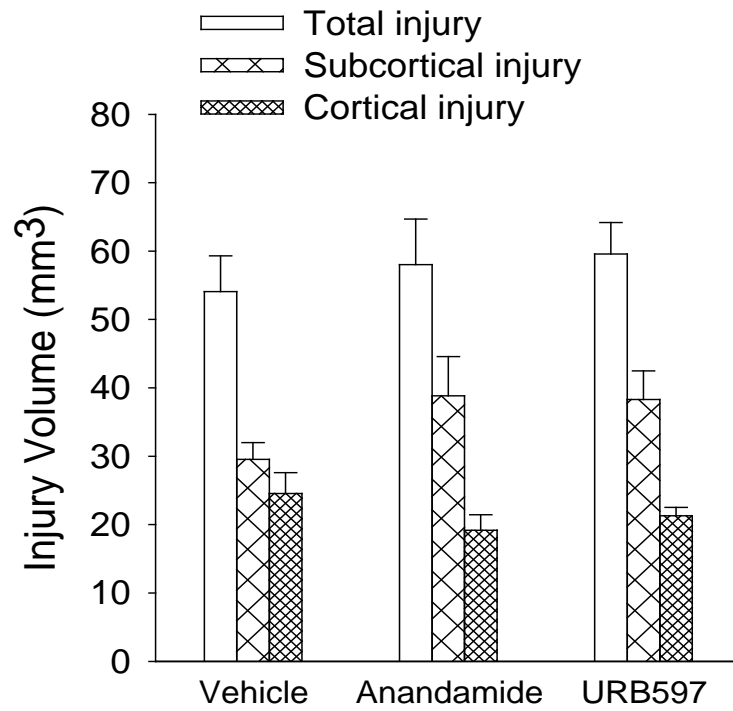


Figure 3.9: Total, subcortical and cortical injury volume in each treatment group at 4 hours post-MCAO (n=5 for anandamide, n=6 for vehicle and URB597). Data are expressed as mean \pm s.e.m. No significant difference between treatment groups, one way ANOVA followed by a Dunnett's post-hoc test.

reduced the extent of injury affecting the cortex and increased subcortical damage and also reduced the ratio of cortical:subcortical injury (**figure 3.10**).

3.4.4 Microglia Number and Activation

The numbers of microglia normally present in the field of view can vary between individual animals (**figure 3.11**). Microglia numbers were counted in cortical and subcortical regions in the ipsilateral and contralateral hemisphere in each group (**figure 3.12** and **figure 3.13**, respectively). Anandamide caused an increase in microglia number in the ipsilateral cortex at the level of the anterior hippocampus compared to vehicle (**figure 3.12**). However, when microglia number in the ipsilateral hemisphere was normalised to the contralateral tissue this effect failed to achieve significance ($p=0.0661$). In the subcortical area, treatment with URB597 and anandamide caused an increase in microglia number in the contralateral hemisphere compared to vehicle (**figure 3.13**). Injury in the ipsilateral hemisphere did not affect microglia number compared to the contralateral hemisphere in either cortical or subcortical regions in any treatment group.

Confocal images showing the range of microglia activation which can be observed is shown in **figure 3.14**. The extent of microglia activation in the ipsilateral and contralateral hemispheres in each group is shown in **figure 3.15** and **figure 3.16**. Greater microglia activation was observed in the ipsilateral hemisphere compared to contralateral in cortical and subcortical regions at the level of the globus pallidus following treatment with URB597 but not anandamide or vehicle (**figure 3.15** and **3.16**). In the cortex this effect was due to a significant decrease in

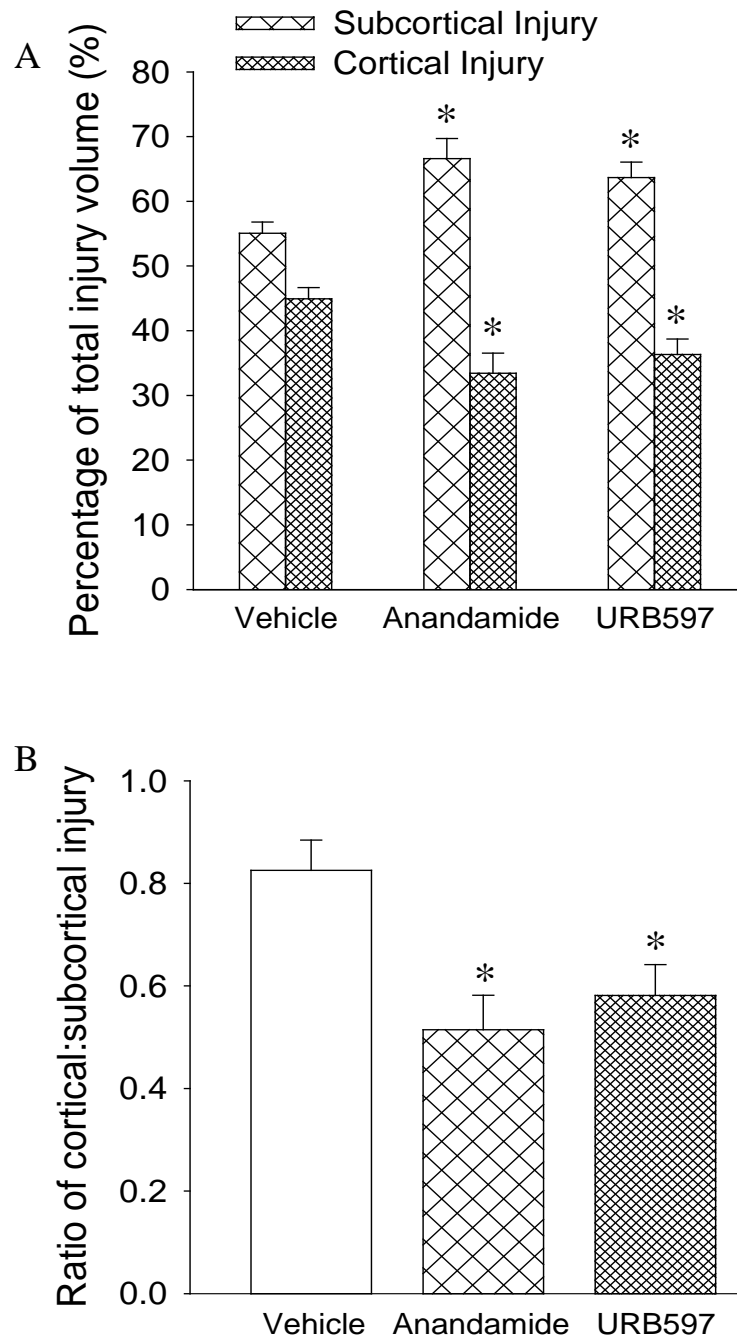
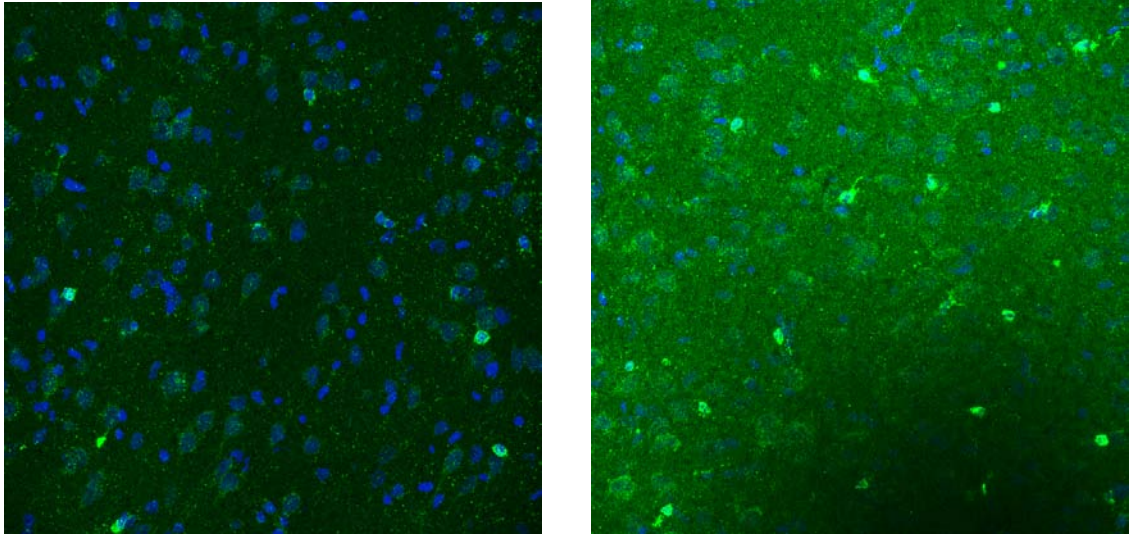


Figure 3.10: Distribution of injury in cortical and subcortical regions expressed as a **A)** percentage of total injury and **B)** the ratio of cortical:subcortical injury (n=5 for anandamide, n=6 for vehicle and URB597). Data are expressed as mean \pm s.e.m. * p<0.05 vs. vehicle treated group, one-way ANOVA followed by a Dunnett's post-hoc test.

Cortical area



Subcortical area

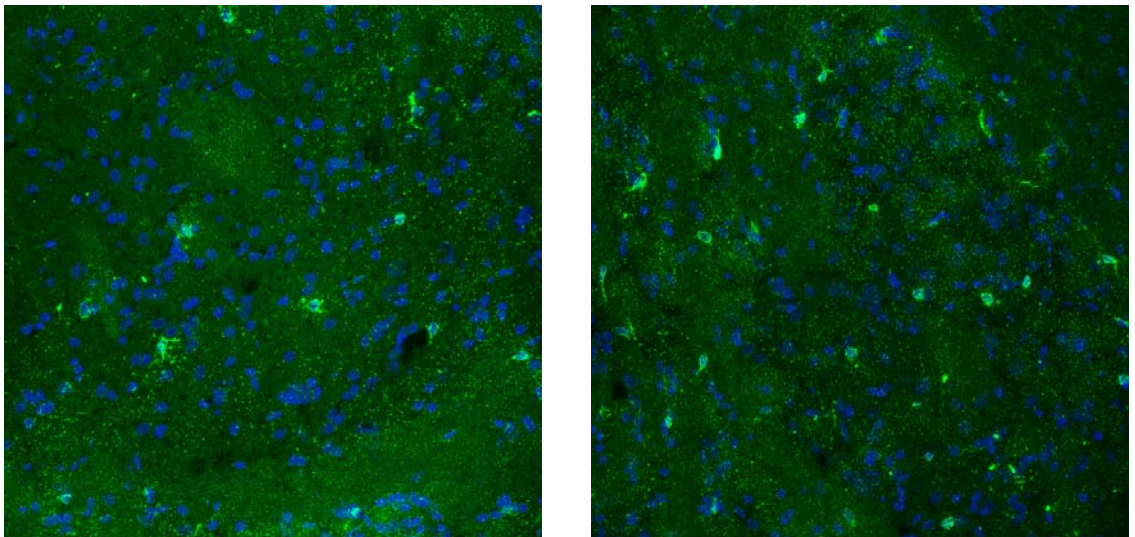


Figure 3.11: Confocal images (compressed z-stack) showing an example of low (left panels) and high (right panels) numbers of microglia present near the injury boundary in cortical and subcortical areas.

Cortical area

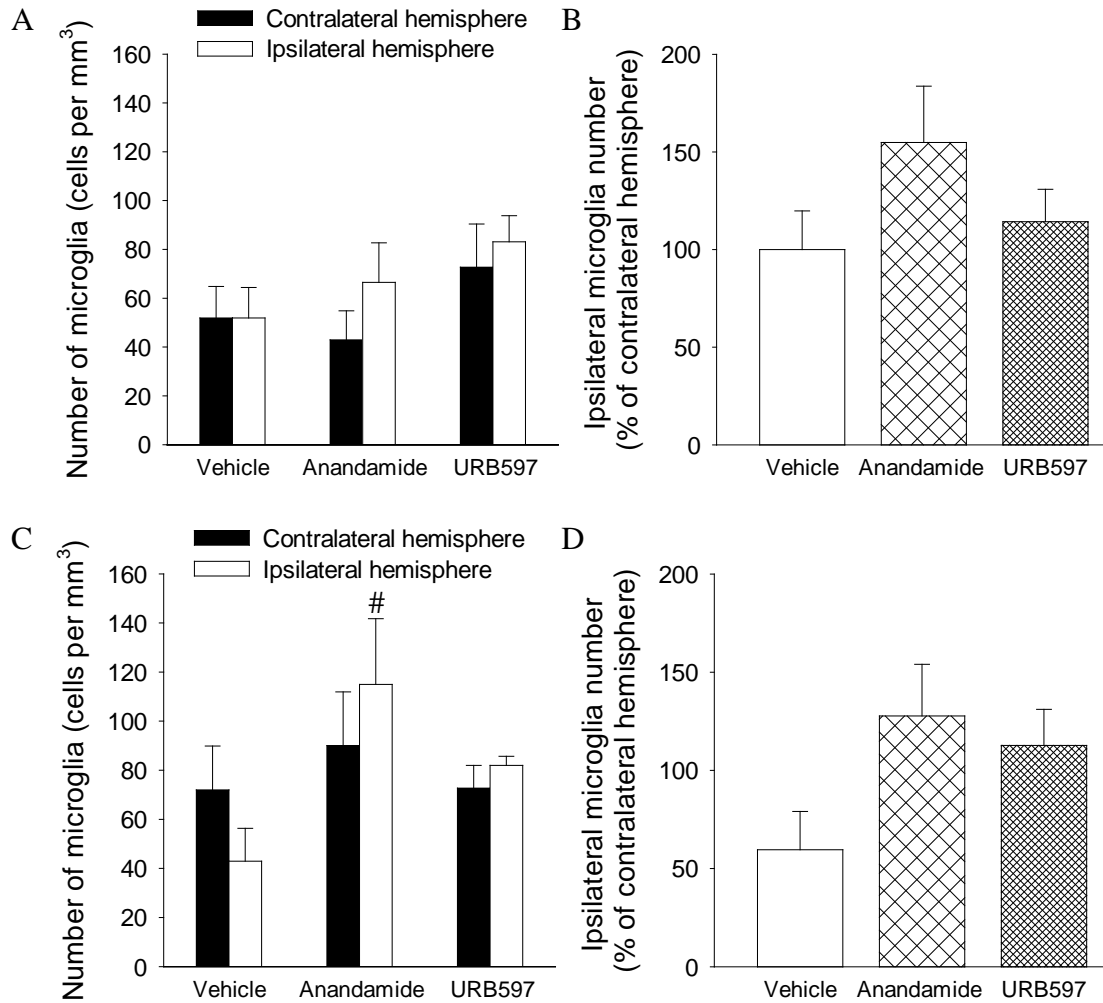


Figure 3.12: Number of microglia present in the cortex at the level of the **A and B)** globus pallidus and **C and D)** anterior hippocampus (n=5 for anandamide and n=6 for vehicle and URB597). **Panel A and C:** Total number of microglia in the cortex in the ipsilateral and contralateral hemispheres in all treatment groups. **Panel B and D:** Number of microglia in the ipsilateral hemisphere expressed as a percentage of the microglia number present in the contralateral hemisphere. Data are expressed as mean \pm s.e.m. Comparison of the ipsilateral and contralateral hemisphere, paired t-test. # p<0.05 vs. vehicle treated group, one way ANOVA followed by a Dunnett's post-hoc test.

Subcortical area

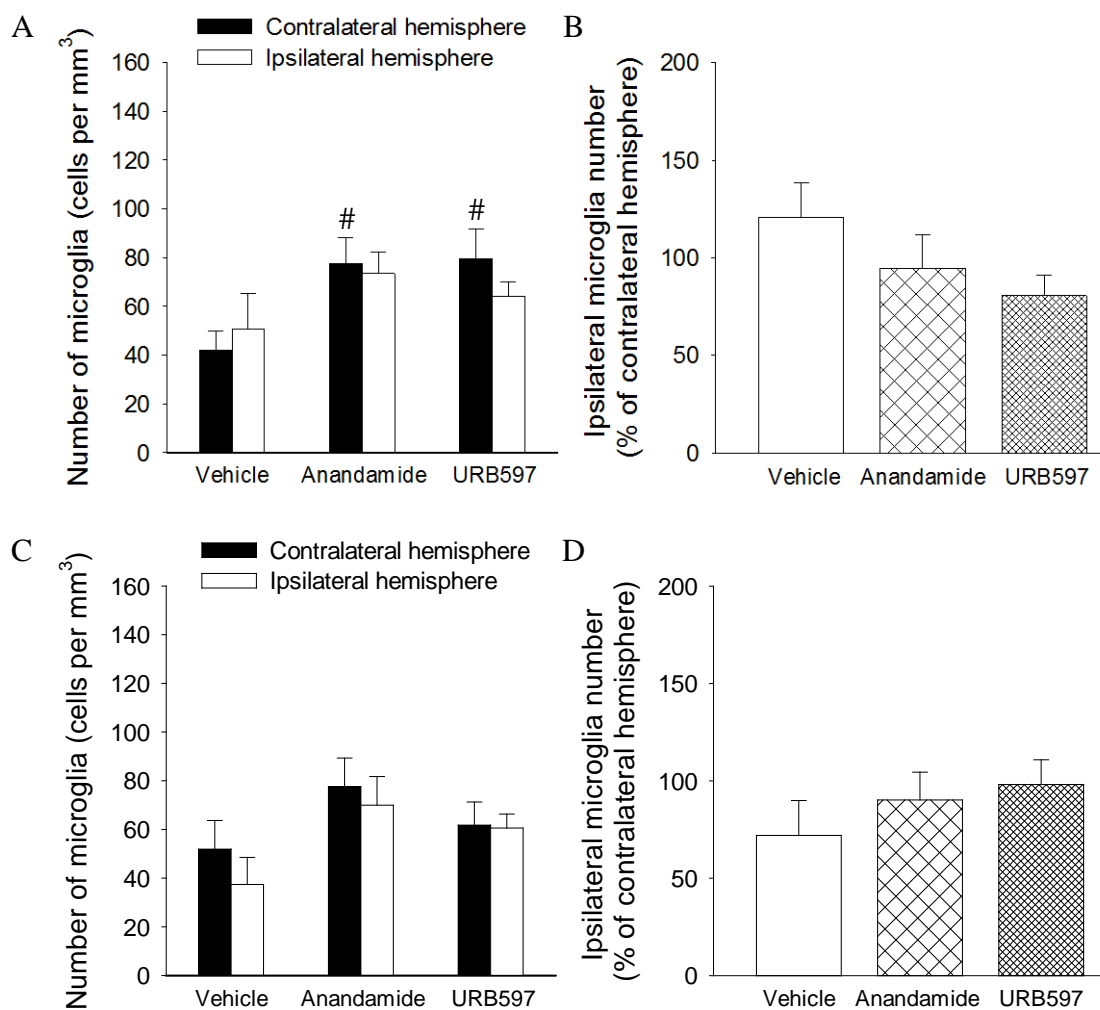
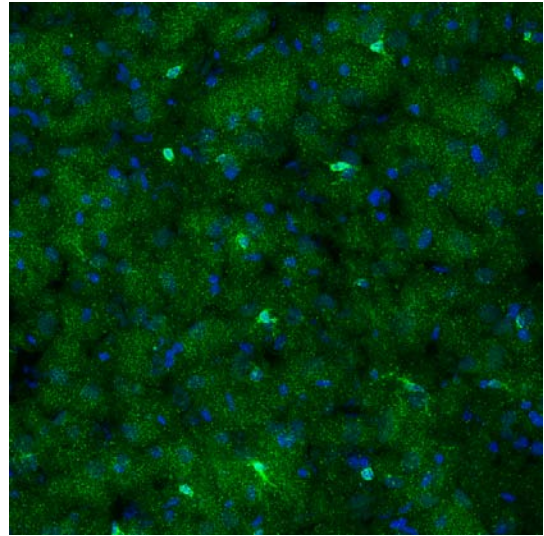
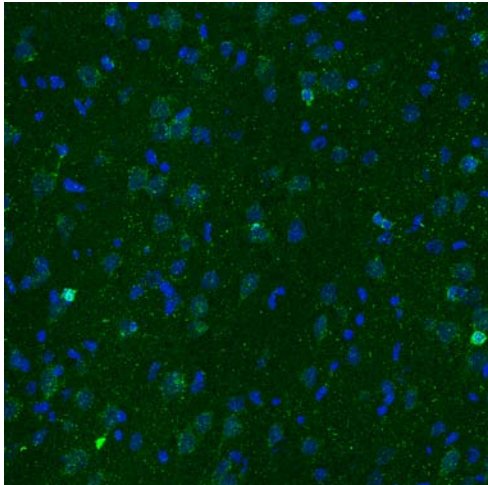


Figure 3.13: Number of microglia present in the subcortical area at the level of the **A and B)** globus pallidus and **C and D)** anterior hippocampus (n=5 for anandamide and n=6 for vehicle and URB597). **Panel A and C:** Total number of microglia in the cortex in the ipsilateral and contralateral hemispheres in all treatment groups. **Panel B and D:** Number of microglia in the ipsilateral hemisphere expressed as a percentage of the microglia number present in the contralateral hemisphere. Data are expressed as mean \pm s.e.m. Comparison of the ipsilateral and contralateral hemisphere, paired t-test. # p<0.05 vs. vehicle treated group, one way ANOVA followed by a Dunnett's post-hoc test.

Cortical area



Subcortical area

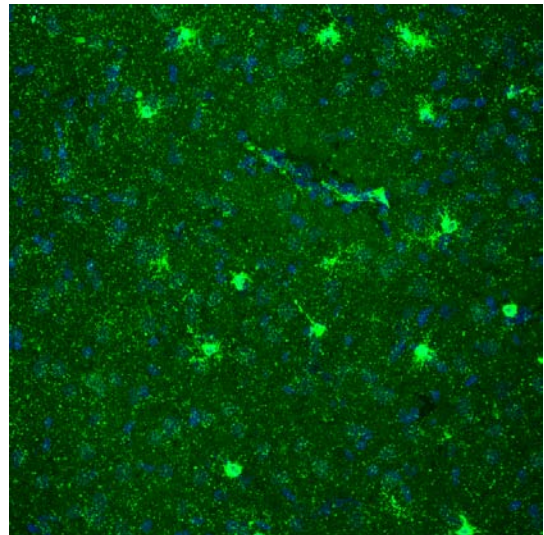
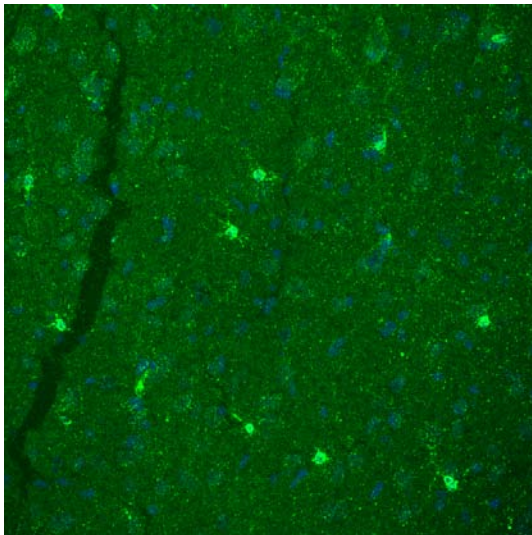


Figure 3.14: Confocal images (compressed z-stack) showing an example of low (left panels) and high (right panels) numbers of activated microglia present near the injury boundary in cortical and subcortical areas.

Cortical area

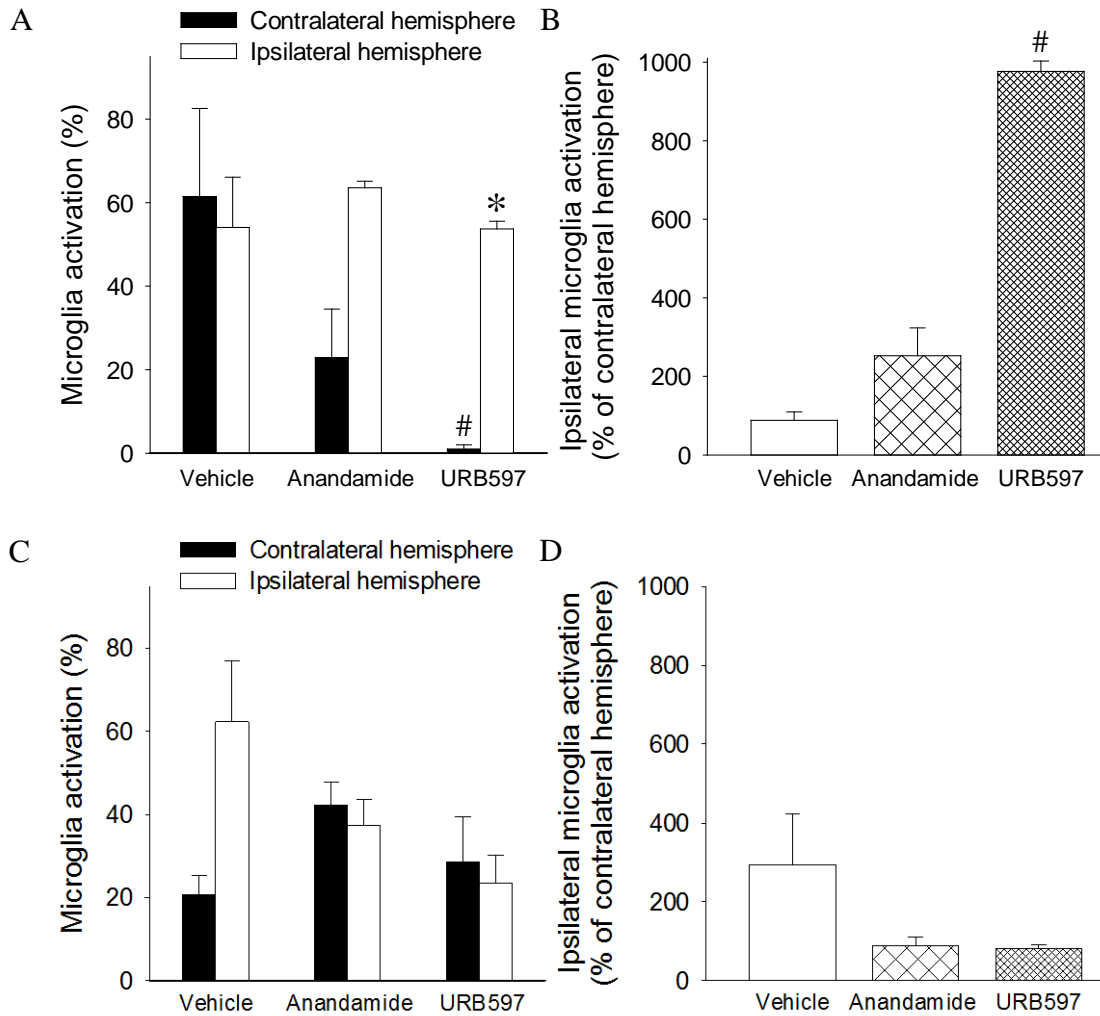


Figure 3.15: Extent of microglia activation in the cortex at the level of the **A and B)** globus pallidus and **C and D)** anterior hippocampus (n=5 for anandamide and n=6 for vehicle and URB597). **Panel A and C:** Number of activated microglia in the cortex in the ipsilateral and contralateral hemispheres in all treatment groups. **Panel B and D:** Number of activated microglia in the ipsilateral hemisphere expressed as a percentage of the activated microglia count present in the contralateral hemisphere. Data are expressed as mean \pm s.e.m. * $p < 0.05$ compared to the contralateral hemisphere, paired t-test. # $p < 0.05$ vs. vehicle treated group, one way ANOVA followed by a Dunnett's post-hoc test.

Subcortical area

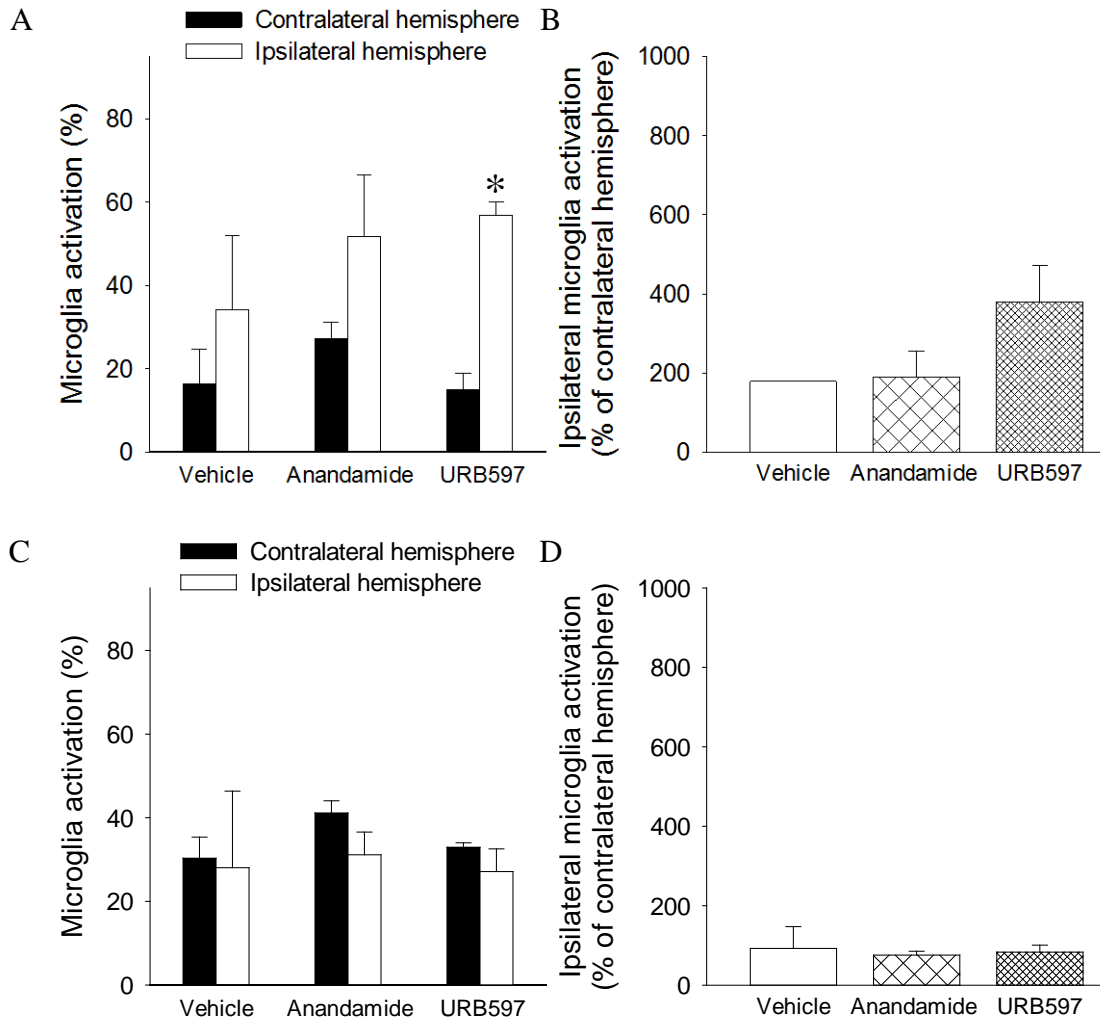


Figure 3.16: Extent of microglia activation in the subcortical area at the level of the **A and B)** globus pallidus and **C and D)** anterior hippocampus (n=5 for anandamide and n=6 for vehicle and URB597). **Panel A and C:** Number of activated microglia in the cortex in the ipsilateral and contralateral hemispheres in all treatment groups. **Panel B and D:** Number of activated microglia in the ipsilateral hemisphere expressed as a percentage of the activated microglia count present in the contralateral hemisphere. Data are expressed as mean \pm s.e.m. * $p < 0.05$ compared to the contralateral hemisphere, paired t-test. No significant difference between treatment groups, one way ANOVA followed by a Dunnett's post-hoc test.

microglia activation in the contralateral hemisphere compared to the vehicle group (**figure 3.15**). No effect of anandamide or URB597 treatment was observed at the level of the anterior hippocampus.

3.5 Discussion

The aim of this study was to examine the effect of anandamide and the metabolism inhibitor URB597 on early injury development and the microglial response at 4 hours after cerebral ischaemia induced by middle cerebral artery occlusion.

In this model anandamide treatment affected the topography of the injury with no change in total injury volume. In anandamide and URB597 treated animals there was significantly reduced injury in the cortex but a significant increase in injury in subcortical regions. These findings are not in agreement with previous work published by Schomacher *et al.* (2008) who demonstrated that administration of anandamide was neuroprotective in a model of 90 minute transient middle cerebral artery occlusion with a reduction in total infarct volume at 24 hours. The dosage and timing of anandamide and URB597 treatment used in the current study were based on previous studies published by Schomacher *et al.* (2008) and Fegley *et al.* (2005). The only deviation from the previous treatment protocols was the route of administration used; s.c. injection instead of i.p. Both routes of administration, s.c. and i.p., allow rapid absorption into the bloodstream. Comparison of these routes has shown that s.c. injection results in more rapid drug absorption, especially for administration of lipophilic drugs such as anandamide (Kalinichev *et al.*, 2008). The

similar effect of anandamide and URB597 treatment on injury topography in the present study suggests that drug administration via s.c. injection was successful.

The difference in the effect of anandamide on injury volume in the present study compared to that reported by Schomacher *et al.* (2008) is most likely related to the different middle cerebral artery occlusion models used (transient vs. permanent ischaemia). In the transient cerebral ischaemia model the filament is removed following a period of occlusion to allow reperfusion of the tissue. As such, anandamide may protect reversibly injured cells in the penumbra and allow a greater volume of tissue to be salvaged following reperfusion. In our permanent cerebral ischaemia model the ability of anandamide treatment to affect the site of injury is completely dependent on perfusion through collateral blood vessels. The cortical surface receives collateral blood flow from numerous small vessels supplied by the anterior communicating and anterior cerebral arteries. In contrast, subcortical regions are primarily perfused by the middle cerebral artery and have a comparatively poor collateral blood supply (Liebeskind, 2003; Scremin, 2004). This collateral blood flow may be responsible for the reduction in injury in the cortex observed in animals treated with anandamide and URB597 compared to vehicle. In this model the drug treatments would enter the ischaemic tissue through the ipsilateral anterior communicating artery and collateral blood vessels which perfuse the cortical surface. As such, it is possible that anandamide or URB597 could reach the cortex first and exert protective effects. However, these treatments may not reach the subcortical tissue at high enough concentrations to effectively protect the injured cells.

The mechanisms involved in mediating the reduction in cortical injury by anandamide and URB597 are not clear. Anandamide administration has previously been shown to cause vasodilation of cerebral blood vessels *in vivo* (Wagner *et al.*, 2001). In this study anandamide treatment produced a small transient hypotensive effect which was only observed at 15 minutes after administration. Treatment with URB597 did not affect blood pressure at any time-point measured. Neither anandamide nor URB597 produced a significant change in heart rate or cerebral blood flow as measured by laser Doppler flowmetry during the experimental period. The laser Doppler probe was placed above the region perfused by the middle cerebral artery and, as such, would be expected to record changes in collateral blood flow. However, it is not possible to exclude the suggestion that small changes in cerebral blood flow, which were not identified by laser Doppler flowmetry, could have been enough to affect injury development. Vasodilation of collateral blood vessels would increase blood supply to the injured cortex. As subcortical regions do not have a collateral blood supply vasodilation in the rest of the brain may divert blood away from the subcortical penumbra, which is still partly perfused, resulting in an increase in injury volume.

Anandamide can also induce hypothermia which has been shown to be neuroprotective in cerebral ischaemia (Crawley *et al.*, 1993; Deng *et al.*, 2003). In this model body temperature was tightly controlled and maintained between 36.5-37.5 °C in each animal using a heat lamp and homeothermic blanket. As such, it can be assumed that hypothermia could not have influenced injury development in this study. Another possible action of anandamide could be to exert direct cellular

effects through inhibition of Ca^{2+} channels which would reduce glutamate release from injured cells and limit the effects of excitotoxicity (Chemin *et al.*, 2001).

A significant part of this study focused on the possible role of microglia in mediating the effect of anandamide on injury development. Microglia are resident immune cells in the central nervous system and are one of the first cells to respond to injury following cerebral ischaemia. Activated microglia have been detected in ischaemic tissue as early as 30 minutes after middle cerebral artery occlusion and increase significantly at 4-6 hours following insult reaching a peak at 48 hours (Rupalla *et al.*, 1998; Mabuchi *et al.*, 2000). Microglia number was unaffected by injury in the ipsilateral hemisphere compared to the contralateral tissue. There was also little effect of either anandamide or URB597 on microglia number compared to the vehicle. At the level of the globus pallidus treatment with anandamide and URB597 was associated with greater microglia activation in the ipsilateral cortex and subcortical area compared to the contralateral hemisphere. In the cortex this effect was due to reduced microglia activation in the contralateral hemisphere compared to vehicle treated animals. The reason for this difference is unclear. Anandamide and URB597 did not significantly affect microglia activation in the ipsilateral hemisphere. As such, it is unlikely that the effect of anandamide and URB597 on injury topography is due to a difference in the microglia response. Additionally, due to the absence of untreated and sham animals in this study it is not possible to determine how cerebral ischaemia affects microglia number and activation in this model and exclude a possible effect of the vehicle on the microglia response. It is

possible that effects of the vehicle on the microglia response may contribute to observed differences in microglia activation between treatment groups.

As described in chapter 1, activated microglia have been shown to exhibit both pro- and anti-inflammatory phenotypes which may have a protective or detrimental effect in acute cerebral ischaemia. Activated microglia may reduce injury through the release of endocannabinoids; anti-inflammatory cytokines, such as IL-10; or growth factors; and phagocytosis. It is unlikely that secretion of growth factors or phagocytosis could exert a protective effect within the 4 hour time frame studied. Alternatively, activated microglia can also release pro-inflammatory cytokines and produce detrimental effects on injury development. Overall, increased microglia activation is unlikely to exert a protective effect on injury development in the cortex as this effect was only observed in one of the two levels examined. Further work is required to examine the phenotype of activated microglia, particularly expression of pro- and anti-inflammatory cytokines, in cortical and subcortical regions in each treatment group.

In the present study, the injury was relatively small and was primarily distributed at the base of the brain proximal to the origin of the middle cerebral artery. As such, it was decided to use silicon coated Doccol filaments in the next study instead of heat blunted filaments. The use of coated filaments has been shown to increase the success and reproducibility of middle cerebral artery occlusion (Schmid-Elsaesser *et al.*, 1998).

This study investigated the effect of exogenous and increased endogenous anandamide on injury development and the microglia response at 4 hours post-occlusion. In this study both anandamide and URB597 changed the injury topography with no effect on total injury volume. Anandamide and URB597 did produce a small change in microglia activation; however, as this effect was only observed at one coronal level it is unlikely that this change was involved in modifying injury development. As such, the mechanisms involved in mediating the effect of anandamide and URB597 on injury topography remain unresolved. As anandamide did not significantly affect injury volume or the microglia response at 4 hours after cerebral ischaemia it was decided to examine the effect of the other main endocannabinoid, 2-AG, in acute cerebral ischaemia.

In conclusion, treatment with both anandamide and URB597 modified injury topography at 4 hours post-occlusion with reduced cortical and increased subcortical injury but did not affect total injury volume. Anandamide treatment produced a small transient hypotensive effect; however, there was no change in blood pressure observed following treatment with URB597. Neither anandamide nor URB597 significantly affected heart rate or cerebral blood flow. Currently, the results of the microglia analysis are unclear. Anandamide and URB597 did produce a small increase in microglia activation in the ipsilateral hemisphere compared to the vehicle; however, this was a small effect which was only observed at one of the coronal levels studied. Further work is required to examine the effect of anandamide at a later time-point and fully elucidate the mechanisms involved.

CHAPTER 4

EFFECT OF 2-ARACHIDONOYL GLYCEROL (2-AG) AND JZL184 ON INJURY AND MICROGLIAL RESPONSE AFTER 4 HOUR CEREBRAL ISCHAEMIA IN RATS

4.1 Introduction

In the previous chapter it was shown that anandamide treatment did not affect total injury volume at 4 hours after middle cerebral artery occlusion. In this study exogenous anandamide and the fatty acid amide hydrolase inhibitor URB597 resulted in greater microglia activation in the ipsilateral hemisphere compared to the contralateral at the level of the globus pallidus but not at the level of the anterior hippocampus. In a previous study, the other endocannabinoid, 2-AG, was shown to be neuroprotective in an animal model of traumatic brain injury and reduced expression of pro-inflammatory cytokines (Panikashvili *et al.*, 2001). The effect of 2-AG has not been studied in cerebral ischaemia. As such, it was decided to examine the effect of the other main endocannabinoid, 2-AG, in acute cerebral ischaemia. Microglia have been shown to release 2-AG *in vitro* (Walter *et al.*, 2003). Exposure to 2-AG resulted in increased microglia proliferation and migration *in vitro* (Carrier *et al.*, 2004; Walter *et al.*, 2003). 2-AG also reduced release of the pro-inflammatory cytokine TNF- α from activated microglia (Facchinetti *et al.*, 2003). 2-AG is primarily metabolised *in vivo* by monoacylglycerol lipase as described in chapter 1. JZL184 is a potent inhibitor of monoacylglycerol lipase *in vivo* and can increase 2-AG in the brain with no effect on anandamide concentration (Long *et al.*, 2009). Therefore, the hypothesis of the present study is that exogenous 2-AG and the metabolism inhibitor JZL184 can reduce early injury development and may modify the microglia response to exert neuroprotective effects in acute cerebral ischaemia.

4.2 Aim

The aim of this work was to examine the effect of exogenously administered 2-AG and the monoacylglycerol lipase inhibitor JZL184 on injury volume and microglia number and activation at 4 hours after middle cerebral artery occlusion.

4.3 Methods

4.3.1 Source of Materials

Suppliers for all equipment, drugs and reagents are detailed in the Appendices.

4.3.2 Animal Source

For these experiments animals were sourced and housed as described in **section 2.3.2**. In the pilot study, haemodynamic experiments were performed in accordance with UK Home Office Guidelines on the Operation of the Animals (Scientific Procedures) Act 1986 (Project Licence No. PPL 60/3665; Personal Licence No. PIL 60/11356).

4.3.3 Animal Preparation

4.3.3.1 Pilot Study: Haemodynamic Study

Male Sprague-Dawley rats (260-315 g) were anaesthetised as described in **section 3.3.3**. The femoral artery and vein were dissected free of connective tissue and cannulated with polythene tubing (0.58 mm ID and 0.96 mm OD; 0.40 mm ID and 0.80 mm OD). The arterial cannula was connected to a pressure transducer (Bell and Howell type 4-422) to measure heart rate and arterial blood pressure. The pressure transducer was connected via an amplifier to a Ponemah data acquisition system.

Pulse-oximetry and capnography were performed to continuously monitor oxygen saturation and end-tidal carbon dioxide throughout the procedure.

4.3.3.2 Main Study: Middle Cerebral Artery Occlusion Study

Male Sprague-Dawley rats weighing 275-350 g underwent middle cerebral artery occlusion. Anaesthesia was induced and maintained as described in **section 3.3.3**. Following induction, the animals were prepared for surgery as detailed in **section 2.3.3**.

Physiological measurements were monitored by a pulse-oximeter / capnograph and femoral arterial cannulation as described in **section 3.3.4**. Arterial blood gases were measured prior to surgery to confirm correct ventilation of each animal. Repeat blood gases were taken prior to treatment or middle cerebral artery occlusion, where appropriate, and at 2 and 4 hours post-occlusion. For intravenous (i.v.) drug administration, the left femoral vein was dissected free of connective tissue and cannulated with polythene tubing (0.40 mm ID and 0.80 mm OD) containing heparinised saline (20 units/ml).

4.3.4 Laser Doppler Flowmetry

In each animal, laser Doppler flowmetry was used to monitor cerebral blood flow throughout the experimental period as described in **section 2.3.4**.

4.3.5 Intraluminal Filament Preparation

The middle cerebral artery was occluded using a silicon rubber-coated filament that

is available commercially from Docol (50-3033; California, US).

4.3.6 Intraluminal Thread Model

The intraluminal thread surgery was performed as detailed in **section 2.3.6**. In this study, a silicon-coated Docol filament was used instead of a heat blunted filament. The filament was secured in position for the 4 hour occlusion period.

4.3.7 Experimental Protocol

4.3.7.1 Pilot Study: Haemodynamic Study

Preliminary experiments were performed to assess the haemodynamic effects of 2-AG and JZL184 at several doses. In this study, 2-AG and JZL184 were administered as a short rapid i.v. infusion followed by a slower continuous infusion representing the first 30 minutes of the treatment protocol to give proposed total doses for the middle cerebral artery study.

Following surgery, animals were allowed to stabilise for 20 minutes before the first infusion was administered. Rats were divided into 2 groups (n = 3 or 4 for each) and received either 2-AG or JZL184 at a range of concentrations as detailed below:

Treatment Protocol: 2-AG

1. **Vehicle:** Animals received 10, 20 or 40% DMSO in saline; 90 µl, 180 µl and 360 µl DMSO administered over 30 minutes (n=3).
2. **2-AG:** Animals received initial infusion over 2 minutes followed by a continuous infusion.

- 2 mg/kg total dose (10% DMSO; n=4): Animals received 0.4 mg/kg infusion + 0.4 mg/kg/hr continuous infusion to give 0.6 mg/kg over 30 minutes.
- 3.5 mg/kg total dose (20% DMSO; n=4): Animals received 0.7 mg/kg infusion + 0.7 mg/kg/hr continuous infusion to give 1 mg/kg over 30 minutes.
- 7 mg/kg total dose (40% DMSO; n=3): Animals received 1.4 mg/kg infusion + 1.4 mg/kg/hr continuous infusion to give 2 mg/kg over 30 minutes.

Treatment Protocol: JZL184

1. **Vehicle:** Animals received polyethylene glycol (PEG-300) alone or PEG-300:tween-80 (4:1) (n=3).
2. **JZL184:** Animals received initial infusion over 5 minutes followed by a continuous infusion.
 - 5 mg/kg total dose (n=3): Animals received 2.4 mg/kg infusion + 0.6 mg/kg/hr continuous infusion to give 3 mg/kg over 30 minutes.
 - 9.5 mg/kg total dose (n=3): Animals received 4.8 mg/kg infusion + 1.2 mg/kg/hr continuous infusion to give 5.5 mg/kg over 30 minutes.
 - 19 mg/kg total dose (n=3): Animals received 9.6 mg/kg infusion + 2.4 mg/kg/hr continuous infusion to give 11 mg/kg over 30 minutes.

Both treatments were administered as an initial infusion at 0.6 ml/kg over 2 or 5 minutes, for 2-AG and JZL184, respectively, followed by continuous 0.6 ml/kg/hr infusion for the remaining period of observation. Haemodynamic measurements were recorded immediately prior to treatment, at one minute intervals during the initial infusion and at 5 minute intervals during the slower continuous infusion. There

was a 20 minute interval between completion of each treatment and initiation of the next infusion.

4.3.7.2 Main Study: Middle Cerebral Artery Occlusion Study

30 rats were randomised into 5 treatment groups (n=6 in each group):

1. **Group 1:** Animals underwent middle cerebral artery occlusion and did not receive either treatment or vehicle.
2. **Group 2:** Animals underwent middle cerebral artery occlusion and received the vehicle for both treatments, PEG-300 (i.v.), at 2 different rates (n=3 for each).
Vehicle administered as either:
 - 100 µl/kg i.v. infusion + 100 µl/kg per hour infusion
 - 250 µl/kg i.v. infusion + 62.5 µl/kg per hour infusion
3. **Group 3:** Animals underwent middle cerebral artery occlusion and received 2-AG (6 mg/kg in PEG-300, i.v.). Treatment was administered as a 1.2 mg/kg i.v. infusion over 2 minutes followed by a slower 1.2 mg/kg per hour infusion.
4. **Group 4:** Animals underwent middle cerebral artery occlusion and received the monoacylglycerol lipase metabolism inhibitor, JZL184 (10 mg/kg in PEG-300, i.v.). Treatment was administered as a 5 mg/kg i.v. infusion over 5 minutes followed by a 1.25 mg/kg per hour infusion.
5. **Group 5:** Animals underwent sham surgery without middle cerebral artery occlusion and did not receive either treatment or vehicle.

The sham surgery involved preparing the animal and performing the intraluminal thread surgical protocol, including occlusion of the common cerebral artery, as described in **sections 4.3.3.2 and 4.3.4** without middle cerebral artery occlusion.

Both treatments and vehicle were administered as a short infusion dose given 15 minutes before middle cerebral artery occlusion followed by a continuous slow infusion until the end of the experiment. All treatments were administered as a total volume of 500 μ l/kg in a randomised and non-blinded manner. The experimental protocol is illustrated in **figure 4.1**.

The timing and route of administration used was chosen to ensure successful drug administration throughout the experimental period. The treatment protocol was initiated before occlusion of the middle cerebral artery to ensure that both treatments were able to reach the affected area of the brain prior to injury onset. As 2-AG is highly labile in rat plasma (Kozak *et al.*, 2001), it was decided to administer both treatments as a continuous i.v. infusion to increase the likelihood of exogenous 2-AG reaching the ischaemic tissue. In this study, 2-AG and JZL184 were dissolved in PEG-300 as i.v. administration of this vehicle was associated with more stable haemodynamic measurements compared to DMSO.

The doses of 2-AG and JZL184 used in this study were chosen based on previously published work. 2-AG at 5 mg/kg (i.p. bolus) has been shown to exert neuroprotective effects in a model of traumatic brain injury (Panikashvili *et al.*, 2001). JZL184 is a potent and selective inhibitor of monoacylglycerol lipase and has

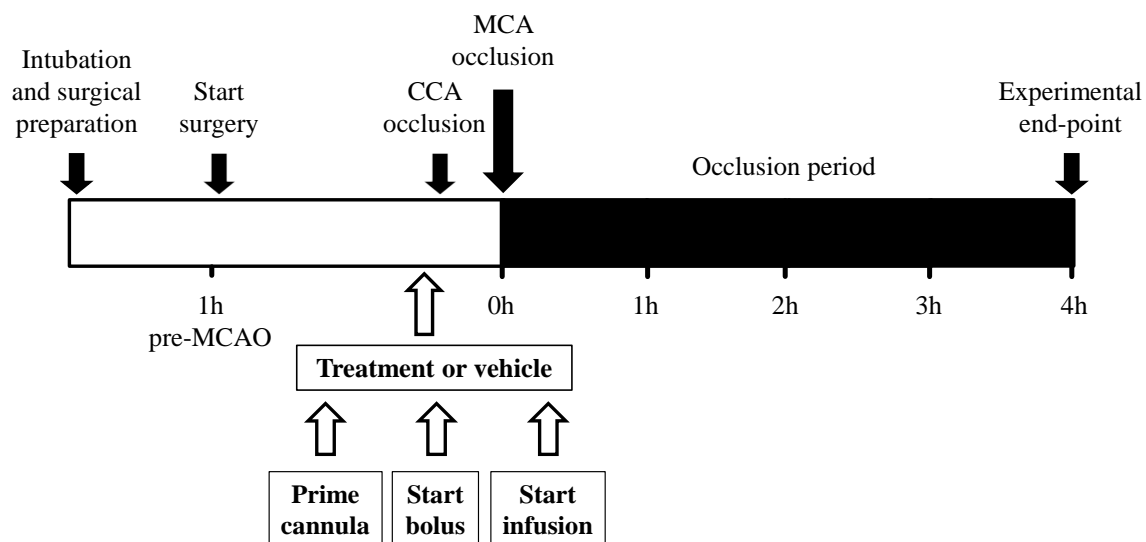


Figure 4.1: Experimental (top panel) and treatment protocol (bottom panel). Following surgery, animals received 2-AG (6 mg/kg), JZL184 (10 mg/kg) or vehicle as an i.v. bolus administered 15 minutes before middle cerebral artery occlusion followed by continuous infusion until end of the experiment. CCA; common carotid artery, MCA; middle cerebral artery, MCAO; middle cerebral artery occlusion.

been shown to increase endogenous 2-AG in the brain at 30 minutes post-administration. Long *et al.* (2009) characterized this inhibitor and demonstrated that JZL184 at 8 mg/kg (i.p. bolus) inhibits monoacylglycerol lipase activity by 80%. In this study, both 2-AG and JZL184 were administered as an initial fast infusion, 20% or 50% of total dose given over 2 or 5 minutes, respectively, followed by a slower continuous infusion until the end of the experiment. In this protocol, the total stated dose is not administered until the end of the occlusion period. As such, it was decided to administer an additional 20% of the 2-AG and JZL184 doses used previously to give a total dose of 6 mg/kg and 10 mg/kg, respectively.

4.3.8 Inclusion Criteria

Animals were included in the data analysis based on the criteria in **section 3.3.9**. For haemodynamic and pulse-oximetry / capnography measurements, the normal physiological parameters are detailed in **section 3.3.9**. In this study, blood gases were measured at several time-points throughout the procedure. For blood gases, normal ranges for PO_2 and PCO_2 were 90-130 mmHg and 35-45 mmHg, respectively.

4.3.9 Tissue Processing

The animals were killed by overdose of anaesthetic and decapitation at the end of the experiment. The brains were removed immediately and frozen in isopentane. The tissue was sectioned at 20 μ M as described in **section 2.3.9**.

4.3.10 Haematoxylin and Eosin Staining and Lesion Quantification

Sections were stained with haematoxylin and eosin to identify injured cells and the injury volume quantified by a person blind to treatment administered as described in **section 2.3.10** and **4.3.12**, respectively. Prior to injury quantification all of the animals were re-coded by a third party to allow the analysis to be performed in a blinded manner.

4.3.11 Immunofluorescence

Immunofluorescence was performed to identify resting and activated microglia in sections taken at the level of the globus pallidus and anterior hippocampus as detailed in the protocol in **section 3.3.13**. In these experiments, the protocol was changed to use a higher concentration of secondary antibody, 1:250 instead of 1:200, as this concentration was found to give optimal staining for the batch of antibody used in this study.

4.3.12 Confocal Microscopy and Microglia Analysis

Stained sections were viewed by confocal microscopy and microglia number and activation was analysed in each image in a blinded manner as described in **sections 3.3.14** and **3.3.15**.

4.3.13 Drug Preparation

Saline, atropine sulphate and heparinised saline were prepared freshly each day as detailed in **sections 2.3.14** and **3.3.16**. The following drugs were also used and were prepared as described below:

- *2-AG*: For haemodynamic experiments; dissolved in nitrogen-purged DMSO to form 30 mg/ml and stored at -20 °C. At the start of each day, working solutions were produced at 3, 6 and 12 mg/ml in 10, 20 and 40% DMSO, respectively.

For cerebral ischaemia study; supplied as colourless oil which was diluted in PEG-300 to form 12 mg/ml. Stored at -80 °C and warmed to room temperature before being administered.

- *JZL184*: For haemodynamic experiments; dissolved directly in 0.5 ml PEG-300 to form 20 mg/ml solution and stored at -20 °C. Working solutions of 4, 8 and 16 mg/ml were used for the initial infusions and 1, 2 and 4 mg/ml for the continuous infusion.

For cerebral ischaemia study; dissolved in PEG-300 to form a 20 mg/ml solution which underwent gentle heating and rapid vortexing to ensure good solubility of the drug. Stock solutions were stored at -20 °C and warmed to room temperature before being administered.

4.3.14 Statistical Analysis

Haemodynamic measurements and cerebral blood flow recorded immediately before occlusion and at 1 hour intervals post-occlusion were analysed using a mixed model repeated measures analysis of variance (ANOVA). Multiple comparisons were

performed between treatment groups; sham vs. untreated, untreated vs. vehicle and vehicle vs. 2-AG and JZL184, with a Bonferroni correction. The effect of time on these measurements was examined by performing one way repeated measures ANOVA. One way ANOVA was used to compare total, subcortical and cortical injury volume and cortical:subcortical ratio followed by multiple comparisons between treatment groups with a Bonferroni correction. The number of microglia and extent of activation in the ipsilateral and contralateral hemisphere were compared between groups using a one way ANOVA followed by multiple comparisons with a Bonferroni correction and comparisons between hemispheres were performed using a paired t-test. To examine the effect of treatment microglia number and activation in the ipsilateral hemisphere in each animal were expressed as a percentage of the contralateral hemisphere values and compared with a one way ANOVA followed by multiple comparisons between groups with a Bonferroni correction.

4.4 Results

4.4.1 Pilot Study

4.4.1.1 Haemodynamic Measurements

The effect of 2-AG, JZL184 and the corresponding vehicles on heart rate and blood pressure is shown in **figures 4.2-4.5**. Neither 2-AG nor the DMSO vehicle produced a significant change in heart rate or blood pressure compared to pre-treatment values (**figure 4.2** and **figure 4.3**). There was no difference in heart rate or blood pressure between the different doses of 2-AG and the corresponding DMSO vehicles. The JZL184 vehicle, PEG-300, did not affect heart rate or blood pressure when administered alone. In contrast, the administration of PEG-300:tween-80 mixture

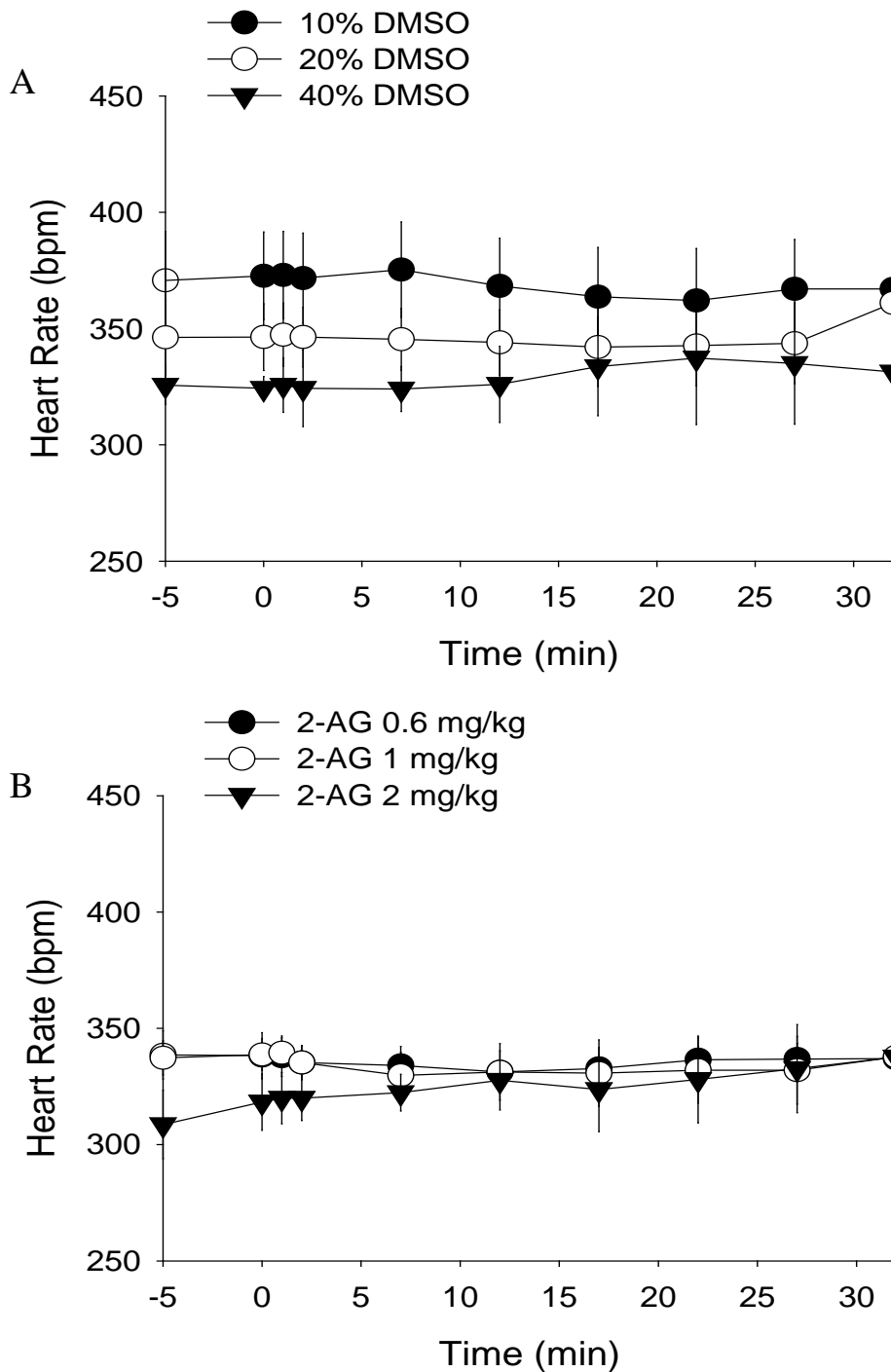


Figure 4.2: Heart rate in animals that received **A)** DMSO vehicle at 10, 20 and 40% and **B)** 2-AG at 0.6 mg/kg, 1 mg/kg or 2 mg/kg over 30 minutes (n=3-4). Data are expressed as mean \pm s.e.m. No significant difference between treatment groups, mixed model repeated measures ANOVA followed by post-hoc comparisons with Bonferroni correction.

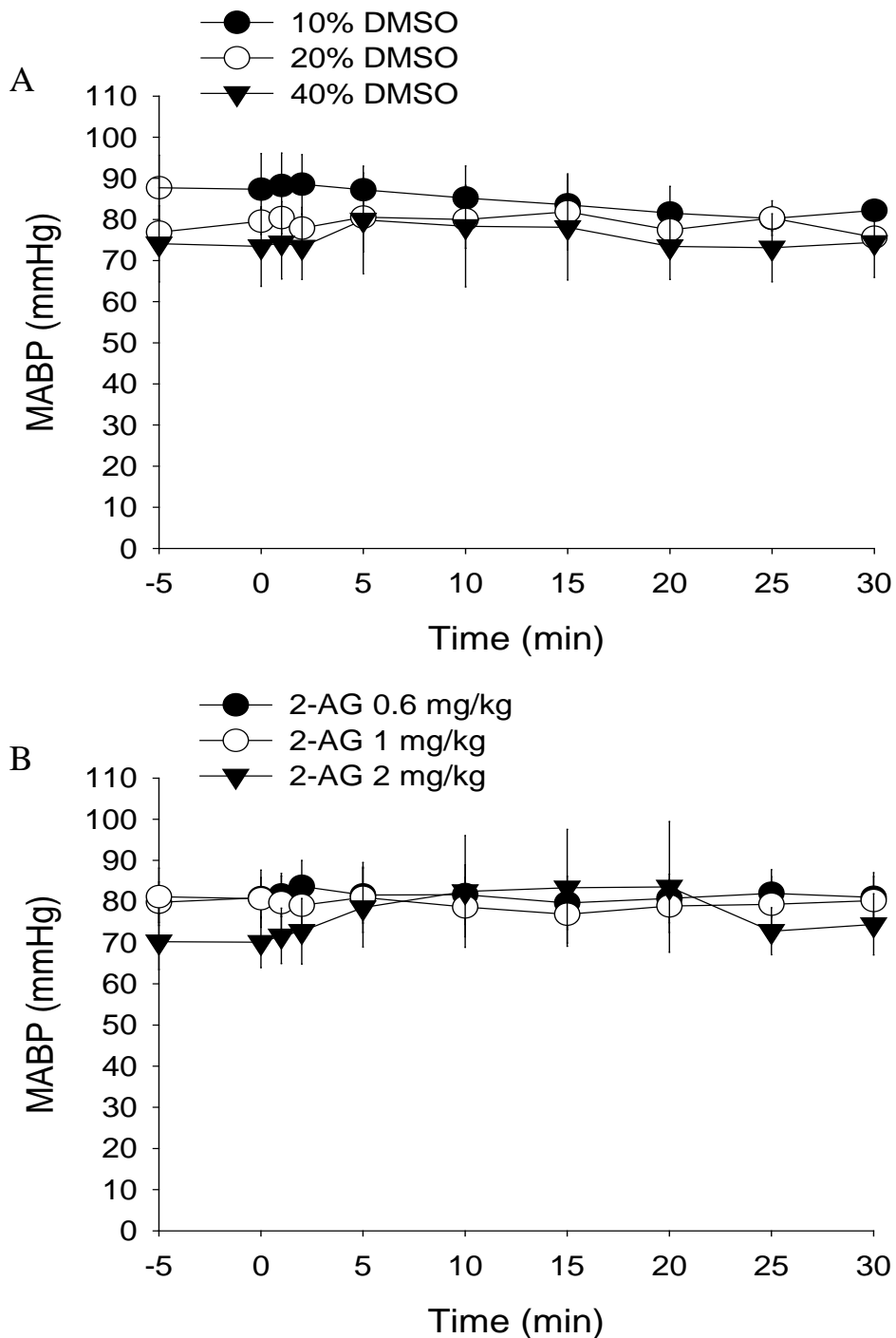


Figure 4.3: Mean arterial blood pressure in animals that received **A)** DMSO vehicle at 10, 20 and 40% and **B)** 2-AG at 0.6 mg/kg, 1 mg/kg or 2 mg/kg over 30 minutes (n=3-4). Data are expressed as mean \pm s.e.m. No significant difference between treatment groups, mixed model repeated measures ANOVA followed by post-hoc comparisons with Bonferroni correction.

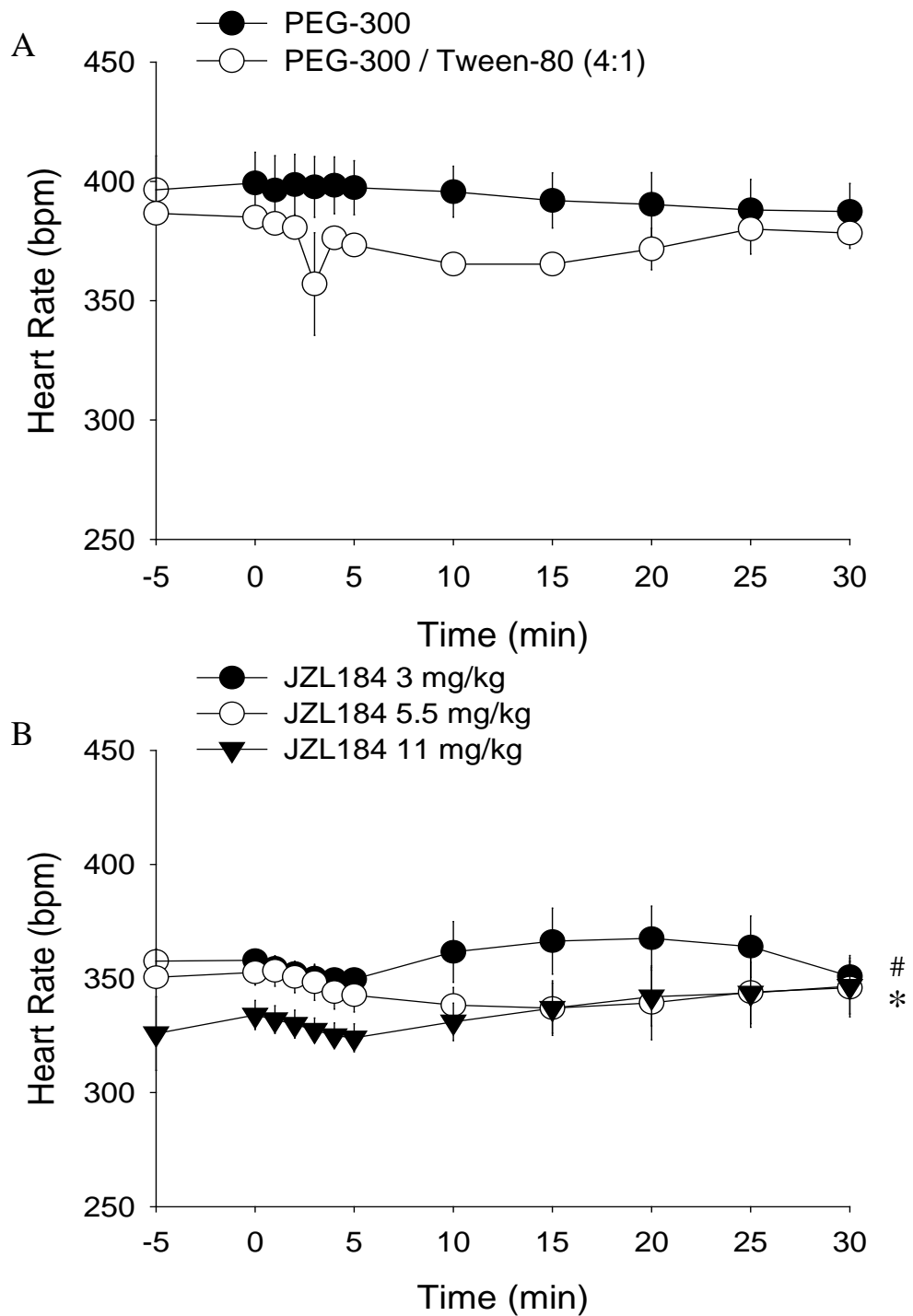


Figure 4.4: Heart rate in animals that received **A**) PEG-300 and PEG-300:tween-80 (4:1) and **B**) JZL184 at 3 mg/kg, 5.5 mg/kg or 11 mg/kg over 30 minutes (n=3). Data are expressed as mean \pm s.e.m. * $p < 0.05$ for JZL184 at 5.5 mg/kg and 11 mg/kg vs. PEG-300 alone and # $p = 0.056$ for JZL184 at 3 mg/kg vs. PEG-300 alone, mixed model repeated measures ANOVA followed by post-hoc comparisons with Bonferroni correction.

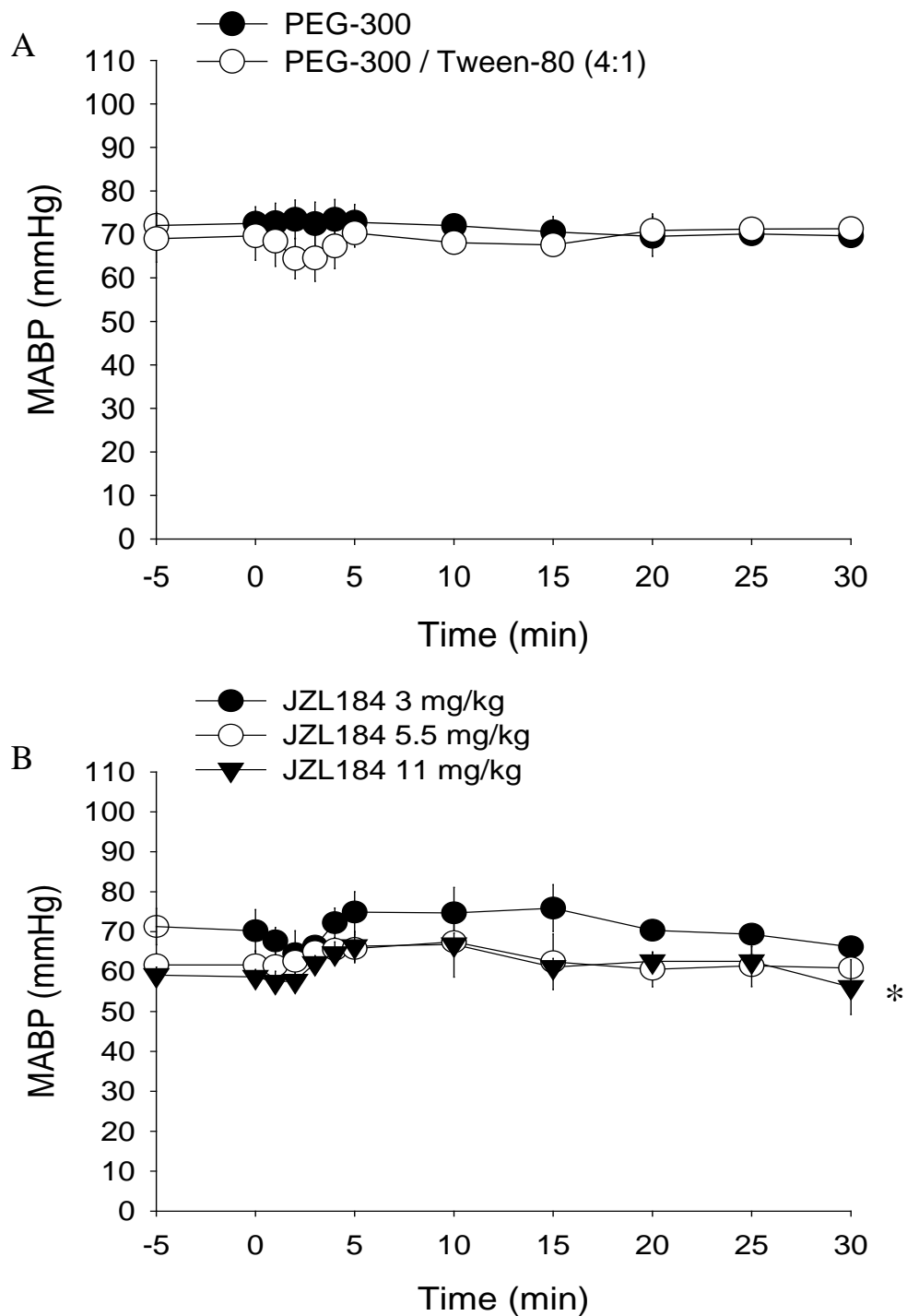


Figure 4.5: Mean arterial blood pressure in animals that received **A)** PEG-300 and PEG-300:tween-80 (4:1) and **B)** JZL184 at 3 mg/kg, 5.5 mg/kg or 11 mg/kg over 30 minutes (n=3). Data are expressed as mean \pm s.e.m. * p<0.05 for JZL184 at 11 mg/kg vs. PEG-300 alone, mixed model repeated measures ANOVA followed by post-hoc comparisons with Bonferroni correction.

(4:1) appeared to exert a greater effect of heart rate compared to PEG-300 alone, however, this effect was not significant (**figure 4.4A**). The non-significance of this result may be associated with the low power of this comparison (25%) due to the low number of animals used in this study. Baseline heart rates were lower in animals prior to treatment with the higher doses of JZL184 (5.5 and 11 mg/kg; **figure 4.4B**). There was a significant difference in blood pressure between animals that received JZL184 at 11 mg/kg and vehicle which may be due to differences in the baseline measurements (**figure 4.5B**). These lower baseline measurements may be the result of multiple doses of JZL184 producing a progressive increase in endogenous 2-AG which could have affected haemodynamic measurements.

In conclusion, these experiments demonstrated that neither 2-AG nor JZL184 caused significant haemodynamic effects at any of the concentrations examined. The vehicle, PEG-300, was associated with more stable and consistent haemodynamic measurements compared to PEG-300:tween-80 (4:1) and DMSO. As such, it was decided to use PEG-300 alone as the vehicle for both 2-AG and JZL184 in the main middle cerebral artery occlusion study.

4.4.2 Main Study: Middle Cerebral Artery Occlusion

4.4.2.1 Physiological Variables

Physiological measurements remained within normal parameters in most groups throughout the occlusion period (**table 4.1** and **table 4.2**). In some groups a low PCO₂, as low as 30.9 mmHg, was observed prior to occlusion, however, during the occlusion period PCO₂ increased to within normal parameters. Oxygen saturation

Table 4.1: Physiological parameters recorded 30 minutes before occlusion and repeated at several time-points throughout the occlusion period in animals that underwent sham surgery or middle cerebral artery occlusion without receiving treatment.

Time post-MCAO (hours)	Physiological parameters				
	SO ₂ (%)	PO ₂ (mmHg)	PCO ₂ (mmHg)	pH	Temperature (°C)
Sham (n=6)					
-0.5	97.5 ± 0.9	129.7 ± 10	31.7 ± 3.0	7.38 ± 0.02	37.1 ± 0.1
0	95.7 ± 1.4				37.1 ± 0.2
1	95.3 ± 1.5				37.0 ± 0.2
2	96.0 ± 1.3	104.5 ± 5.6	36.9 ± 1.2	7.35 ± 0.02	37.0 ± 0.1
3	93.7 ± 1.4				36.8 ± 0.1
4	94.0 ± 0.4	107 ± 8.7	34.6 ± 3.0	7.34 ± 0.02	36.9 ± 0.1
No treatment (n=6)					
-0.5	97.0 ± 0.6	103.5 ± 6.0	37.9 ± 3.3	7.36 ± 0.02	36.5 ± 0.2
0	95.8 ± 0.5				36.6 ± 0.2
1	94.5 ± 0.5				37.3 ± 0.1
2	93.3 ± 1.7	94.8 ± 3.1	35.7 ± 2.7	7.35 ± 0.01	37.0 ± 0.2
3	92.6 ± 1.3				37.2 ± 0.1
4	92.5 ± 1.1	87.5 ± 3.0	41.2 ± 1.9	7.32 ± 0.02	36.7 ± 0.1

Data are expressed as mean ± s.e.m. MCAO; middle cerebral artery occlusion, SO₂; oxygen saturation, ETCO₂; end-tidal carbon dioxide.

Table 4.2: Physiological parameters recorded 30 minutes before occlusion and repeated at several time-points throughout the occlusion period in animals that received 2-AG, JZL184 or vehicle.

Time post-MCAO (hours)	Physiological parameters				
	SO ₂ (%)	PO ₂ (mmHg)	PCO ₂ (mmHg)	pH	Temperature (°C)
Vehicle (n=6)					
-0.5	95.7 ± 1.3	125.7 ± 10.3	30.9 ± 2.7	7.39 ± 0.02	36.9 ± 0.2
0	94.0 ± 1.4				36.9 ± 0.1
1	92.8 ± 1.1				37.1 ± 0.1
2	92.3 ± 1.2	105.5 ± 9.8	34.0 ± 1.4	7.35 ± 0.02	37.0 ± 0.1
3	92.0 ± 1.2				36.9 ± 0.1
4	91.0 ± 0.8	98.5 ± 10.1	39.4 ± 1.3	7.34 ± 0.02	36.8 ± 0.2
2-AG (6 mg/kg; n=6)					
-0.5	93.3 ± 1.1	115.8 ± 6.0	34.7 ± 2.2	7.35 ± 0.02	36.8 ± 0.1
0	92.3 ± 0.6				36.9 ± 0.2
1	91.8 ± 1.2				36.9 ± 0.1
2	91.0 ± 1.2	99.0 ± 9.1	39.9 ± 4.0	7.35 ± 0.02	36.8 ± 0.3
3	89.2 ± 1.5				36.7 ± 0.2
4	90.3 ± 1.4	90.5 ± 4.9	45.3 ± 1.4	7.32 ± 0.02	36.9 ± 0.1
JZL184 (10 mg/kg; n=6)					
-0.5	95.2 ± 1.2	129.7 ± 8.4	33.0 ± 3.0	7.36 ± 0.02	37.0 ± 0.1
0	92.7 ± 2.0				37.1 ± 0.2
1	91.3 ± 2.1				36.9 ± 0.1
2	90.7 ± 2.0	98.5 ± 4.3	39.8 ± 1.5	7.35 ± 0.02	37.1 ± 0.2
3	89.3 ± 1.8				37.1 ± 0.2
4	88.7 ± 1.3	94.0 ± 3.8	45.1 ± 1.6	7.33 ± 0.02	37.1 ± 0.1

Data are expressed as mean ± s.e.m. MCAO; middle cerebral artery occlusion, SO₂; oxygen saturation, ETCO₂; end-tidal carbon dioxide.

and PO_2 values appeared to decrease in all groups over the course of the experiment with the lowest values of 88.7% and 87.5 mmHg, respectively. This decrease in oxygen saturation and PO_2 was associated with a corresponding increase in end-tidal carbon dioxide and PCO_2 . However, in most experiments oxygen saturation was above 90% and PO_2 did not fall below 90 mmHg. There was a gradual decline in heart rate in most groups that underwent middle cerebral artery occlusion (**figure 4.6**). In contrast, there was no significant reduction in heart rate observed in animals that underwent the sham surgery (**figure 4.6A**). Blood pressure did not decrease significantly in animals that underwent the sham surgery, middle cerebral artery without receiving treatment or those receiving vehicle or 2-AG (**figure 4.7A**). In some animals that underwent middle cerebral artery occlusion mean arterial blood pressure did decrease to below 60 mmHg at 4 hours post-occlusion. Treatment with JZL184 caused a significant reduction in blood pressure at 4 hours post-occlusion compared to pre-treatment values. However, neither 2-AG nor JZL184 treatment caused a significant difference in heart rate or blood pressure compared to vehicle.

4.4.2.2 Laser Doppler Flowmetry

Cerebral blood flow was measured in all animals throughout the experimental period and these results are shown in **figure 4.8**. Middle cerebral artery occlusion caused a significant reduction in cerebral blood flow in all animals that was maintained throughout the occlusion period. In sham animals, occlusion of the common cerebral artery caused a significant reduction in cerebral blood flow of ~15%. Middle cerebral artery occlusion caused a much greater reduction in cerebral blood flow compared to the sham protocol. Treatment with 2-AG and JZL184

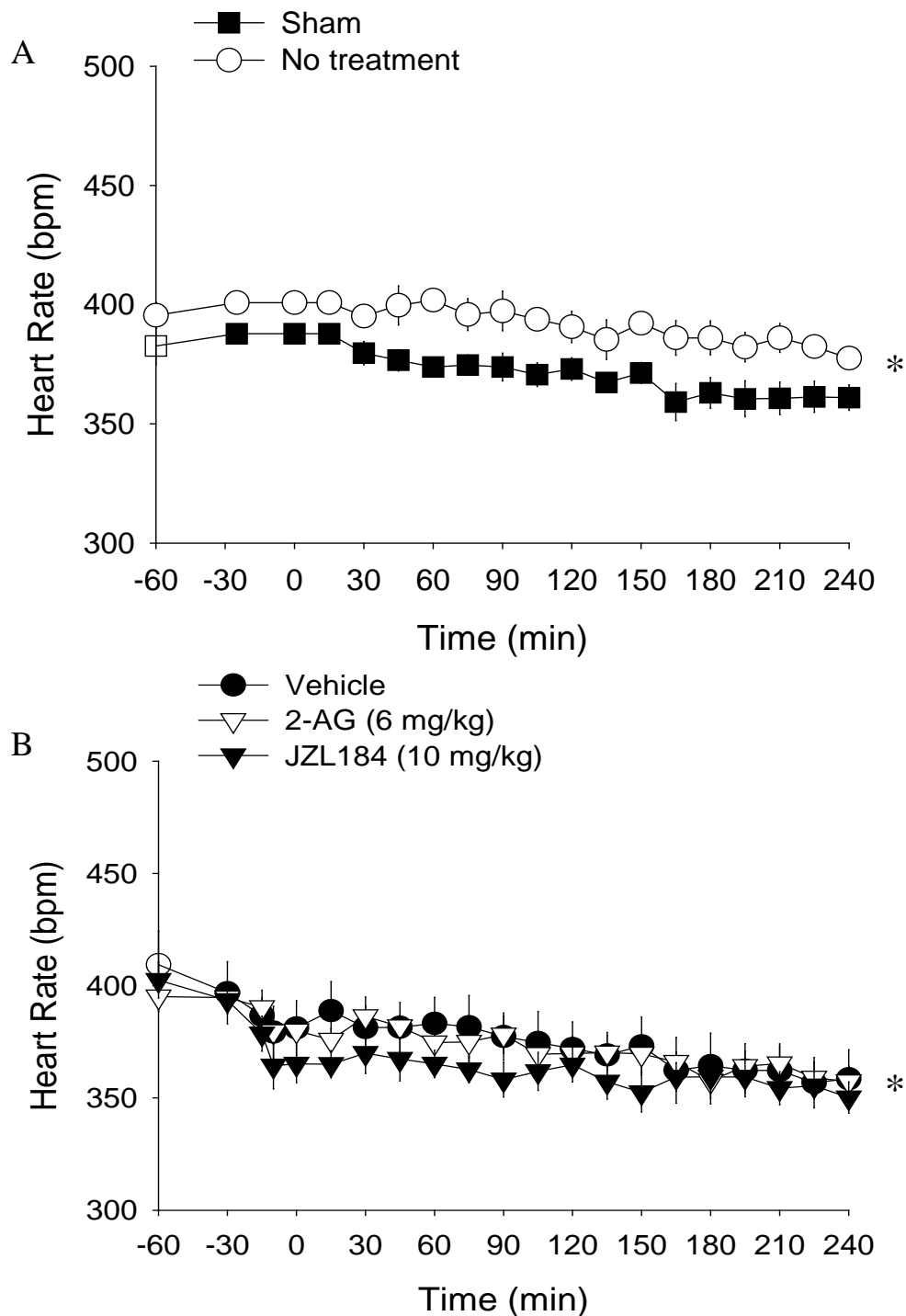


Figure 4.6: Heart rate in **A)** animals that underwent sham surgery or middle cerebral artery occlusion without treatment and **B)** animals receiving vehicle, 2-AG or JZL184 (n=6). Data are expressed as mean \pm s.e.m. * $p < 0.05$ for untreated, vehicle and JZL184 at 4 hours post-MCAO vs. pre-treatment, mixed model repeated measures ANOVA. Post-hoc analysis performed using one-way ANOVA followed by multiple comparisons with Bonferroni correction.

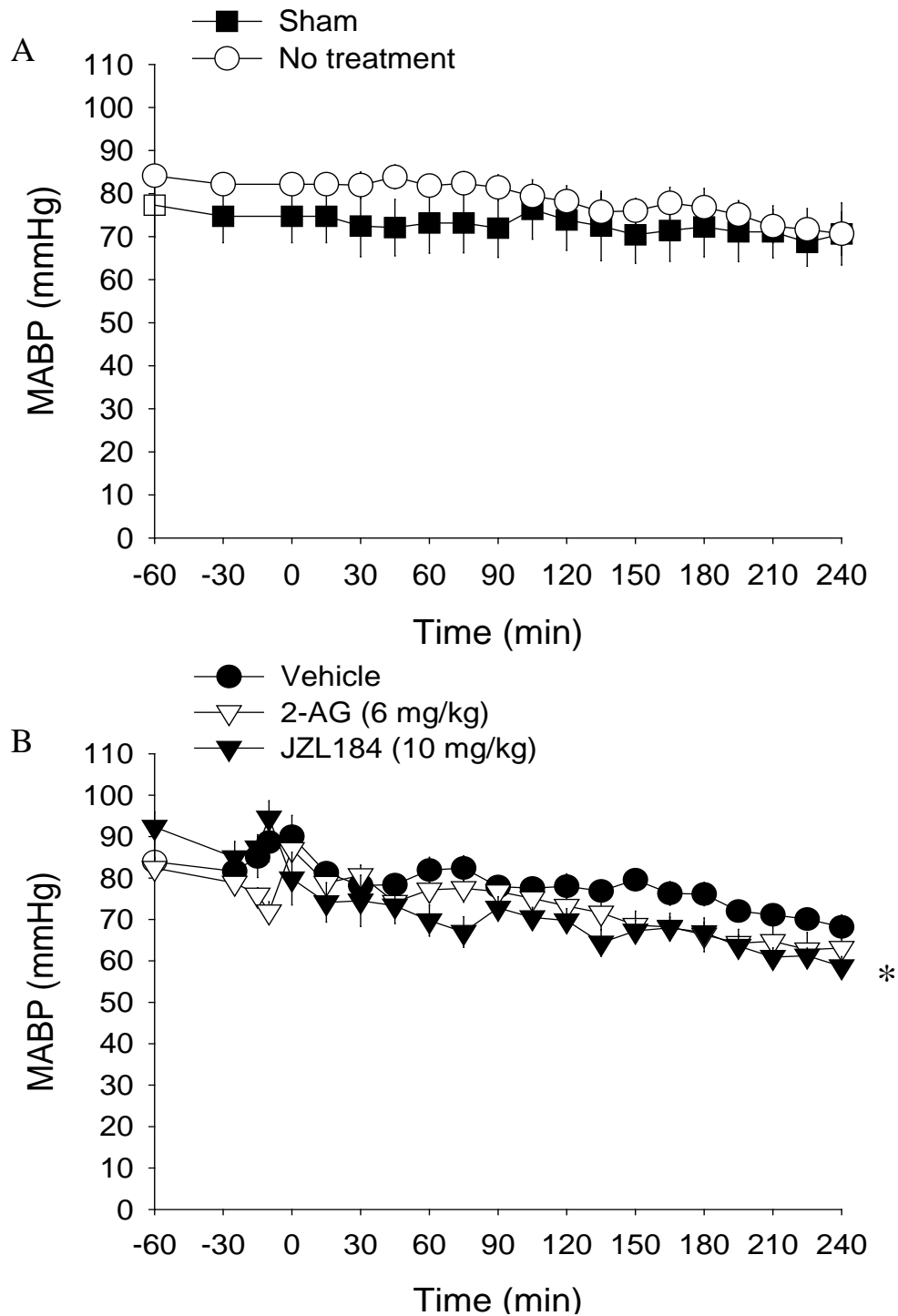


Figure 4.7: Mean arterial blood pressure in **A)** animals that underwent sham surgery or middle cerebral artery occlusion without treatment and **B)** animals receiving vehicle, 2-AG or JZL184 (n=6). Data are expressed as mean \pm s.e.m. * $p < 0.05$ for JZL184 at 4 hours post-MCAO vs. pre-treatment, mixed model repeated measures ANOVA. Post-hoc analysis performed using one-way ANOVA followed by multiple comparisons with Bonferroni correction.

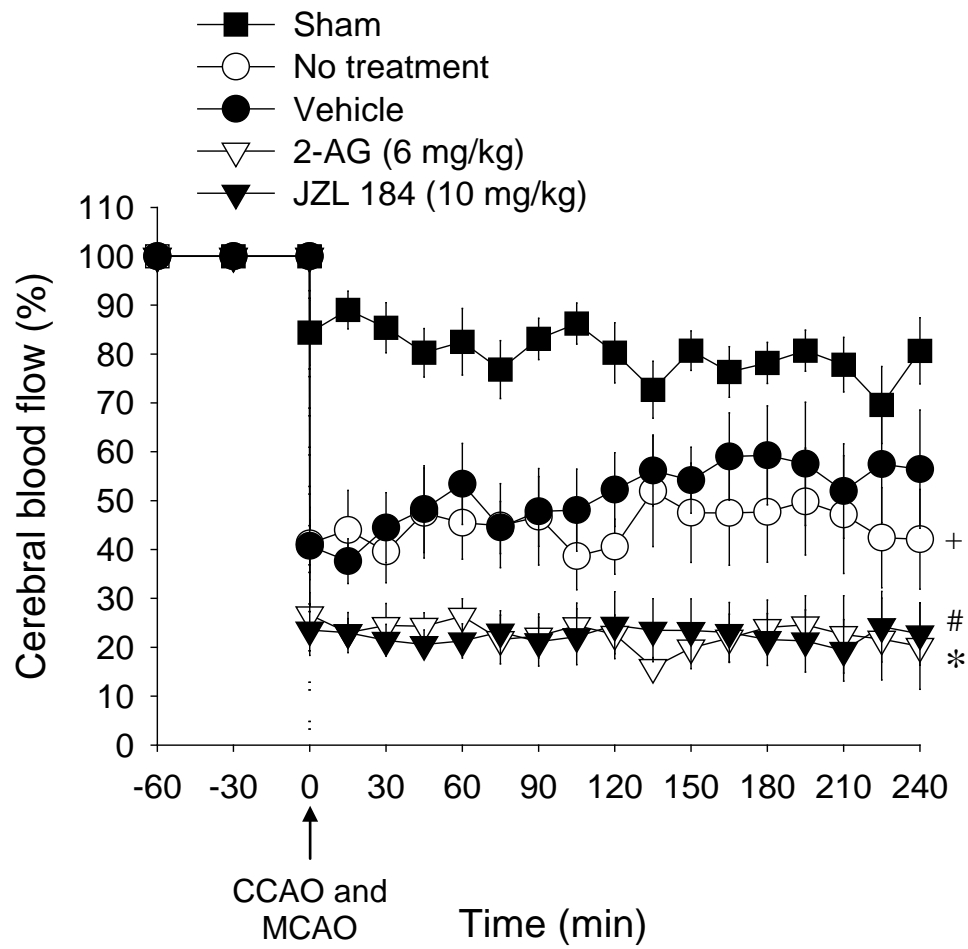


Figure 4.8: Cerebral blood flow measurements recorded in each group throughout the experimental period (n=6). Data are expressed as mean \pm s.e.m. + p<0.05 for untreated vs. sham, * p<0.05 for 2-AG vs. vehicle, # p<0.05 for JZL184 vs. vehicle treated group, mixed model repeated measures ANOVA followed by post-hoc comparisons with Bonferroni correction.

produced a greater reduction in cerebral blood flow during the occlusion period vs. vehicle (**figure 4.8**).

4.4.2.3 Infarct Volume

In sham animals, there was no visible tissue injury at 4 hours post-occlusion. Injury topography from individual animals receiving vehicle, 2-AG or JZL184 which represented the median total injury development in this group is shown in **figure 4.9**. Injury volume and topography was not significantly affected by the vehicle, PEG-300, in comparison to animals that did not receive treatment (**figure 4.10**). Cortical injury was significantly increased in animals that received 2-AG and JZL184 compared to vehicle, however, total injury volume was increased only in the JZL184 treated group (**figure 4.11**). In both 2-AG and JZL184 treated animals the percentage cortical injury was increased compared to vehicle with a corresponding reduction in subcortical injury (**figure 4.11A**). However, there was no significant change in the ratio of cortical:subcortical injury in either treatment group compared to vehicle treated animals (**figure 4.11B**).

4.4.2.4 Microglia Number and Activation

The number of microglia present in cortical and subcortical regions in each hemisphere following injury is shown in **figure 4.12**. Injury in the ipsilateral hemisphere resulted in an increase in the number of microglia in the cortex in untreated and vehicle groups at both coronal levels compared to contralateral regions (**figure 4.13**). At the level of the globus pallidus, a greater number of microglia was present in the ipsilateral cortex compared to contralateral tissue in animals that did

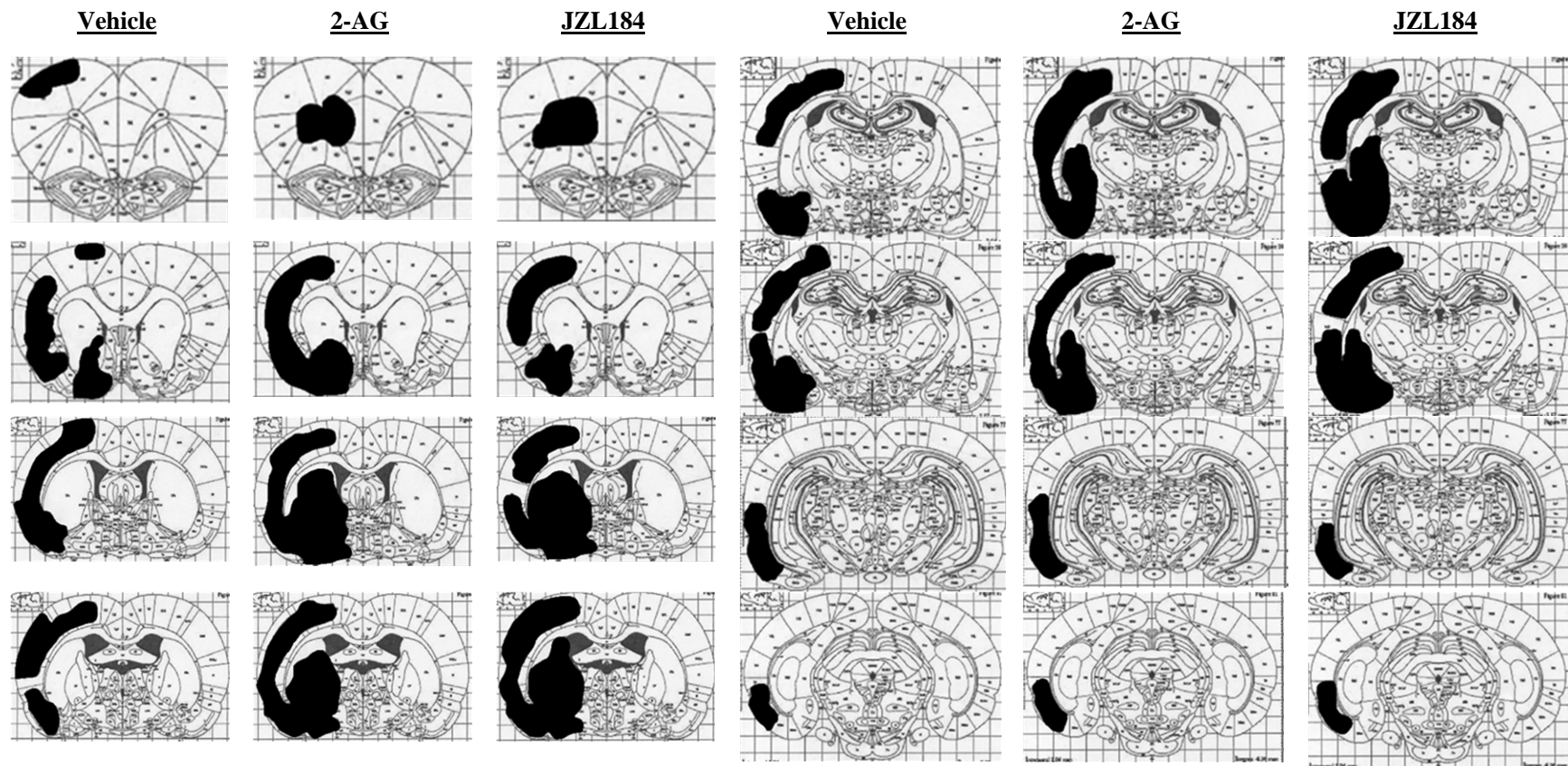


Figure 4.9: Representative line diagrams showing the injury topography observed in vehicle, 2-AG and JZL184 treated animals.

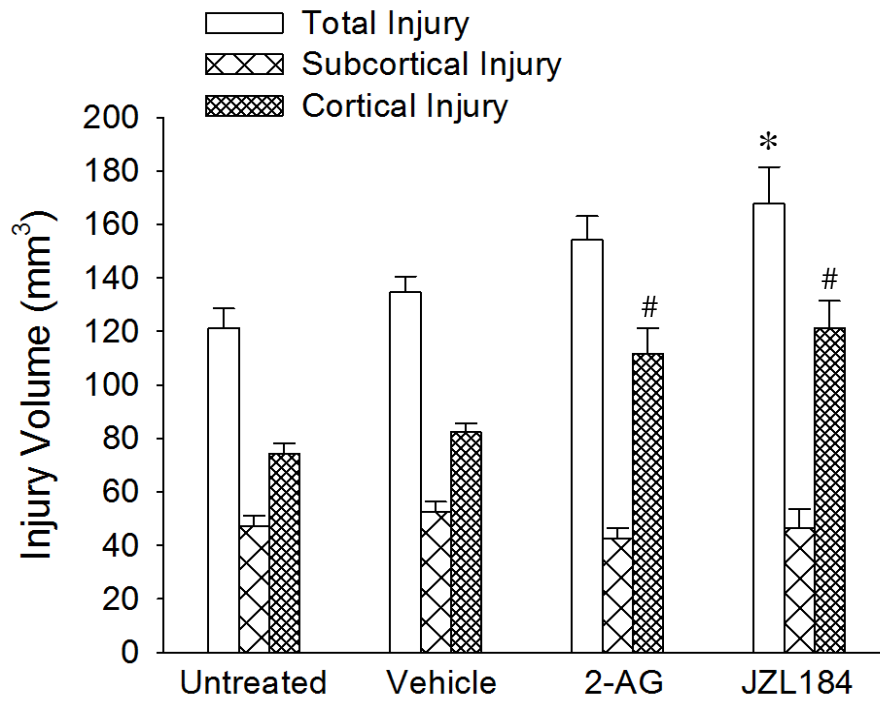


Figure 4.10: Total, subcortical and cortical injury volume in each group at 4 hours post-MCAO (n=6). Data are expressed as mean \pm s.e.m. * $p < 0.05$ for total injury vs. vehicle and # $p < 0.05$ for cortical injury vs. vehicle treated group, one way ANOVA followed by post-hoc tests with Bonferroni correction.

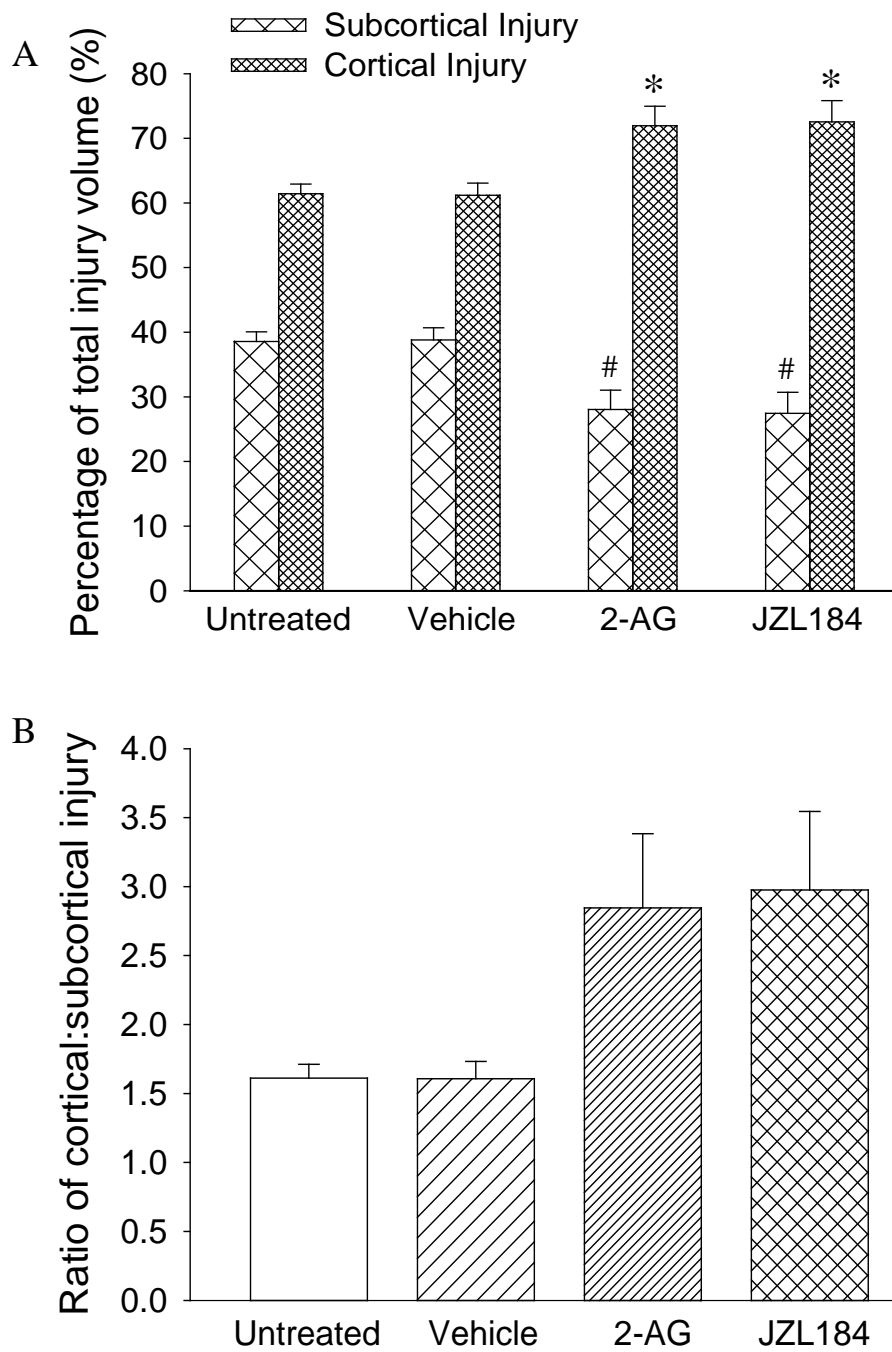
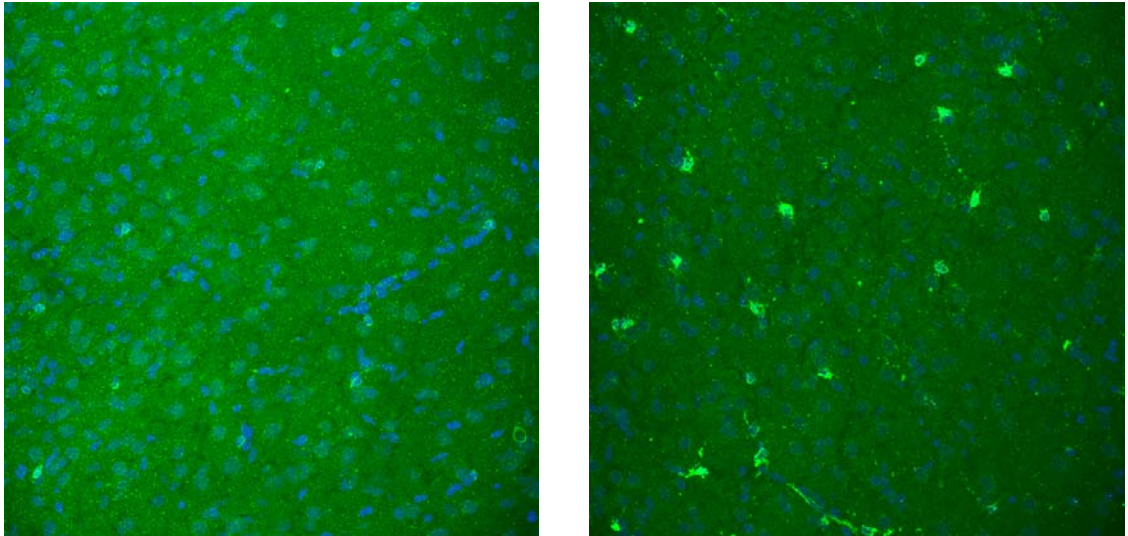


Figure 4.11: Distribution of injury in cortical and subcortical regions expressed as **A**) percentage of total injury and **B**) the ratio of cortical:subcortical injury (n=6). Data are expressed as mean \pm s.e.m. * $p < 0.05$ for cortical injury and # $p < 0.05$ for subcortical injury vs. vehicle treated group, one way ANOVA followed by post-hoc tests with Bonferroni correction.

Cortical area



Subcortical area

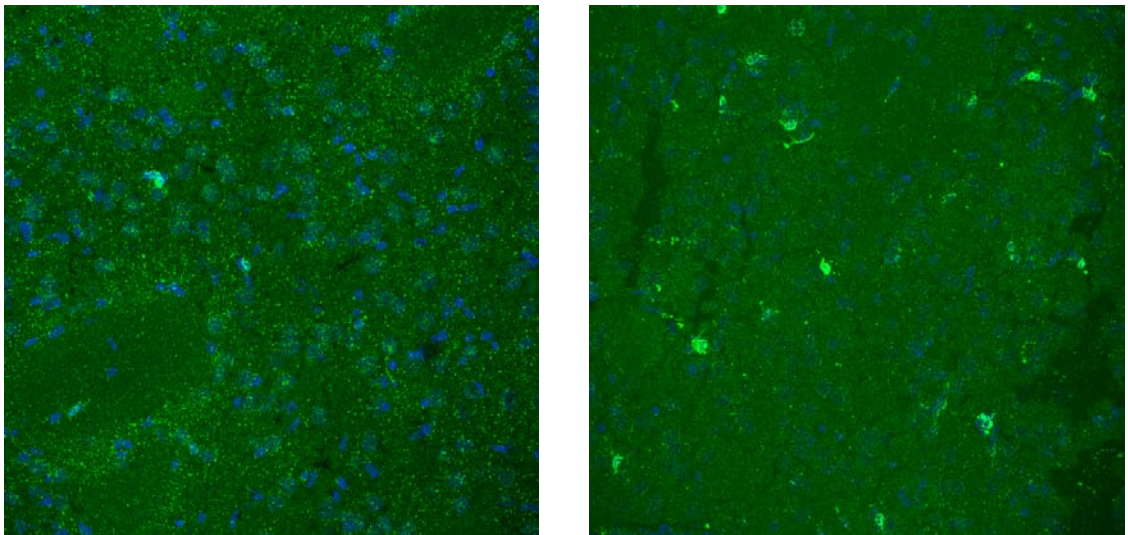


Figure 4.12: Confocal images (compressed z-stack) showing an example of low (left panels) and high (right panels) numbers of microglia present near the injury boundary in cortical and subcortical areas.

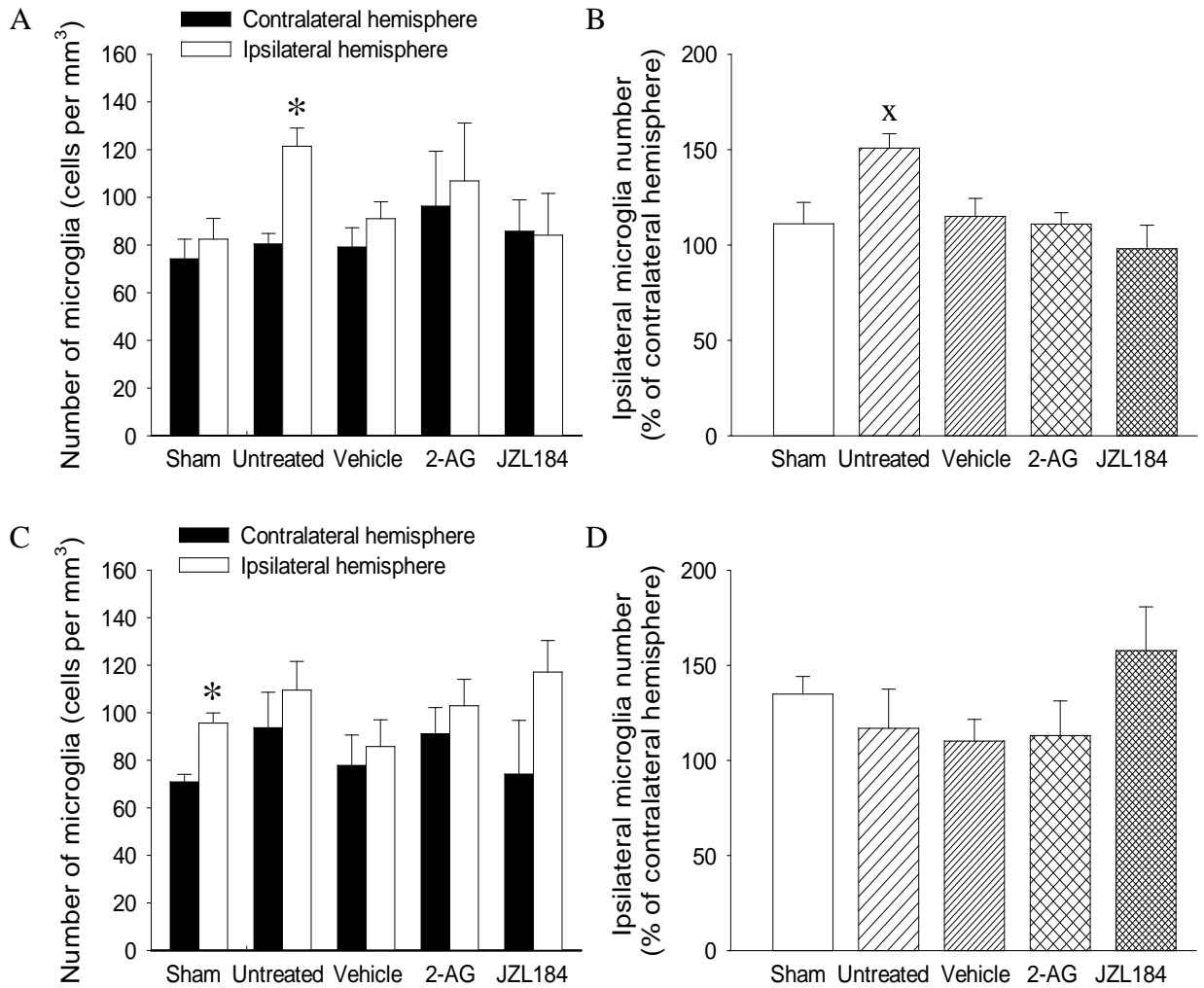


Figure 4.13: Number of microglia present in the cortex at the level of the **A and B)** globus pallidus and **C and D)** anterior hippocampus (n=5 for anandamide and n=6 for vehicle and URB597). **Panel A and C:** Total number of microglia in the cortex in the ipsilateral and contralateral hemispheres in all treatment groups. **Panel B and D:** Number of microglia in the ipsilateral hemisphere expressed as a percentage of the microglia number present in the contralateral hemisphere. Data are expressed as mean \pm s.e.m. * $p < 0.05$ compared to the contralateral hemisphere, paired t-test. ^X $p < 0.05$ vs. sham operated animals, one way ANOVA followed by multiple comparisons with Bonferroni correction.

not receive treatment (**figure 4.14**). In contrast, microglia number did not increase significantly in the ipsilateral hemisphere compared to the contralateral in animals that received 2-AG and JZL184 at either coronal level (**figure 4.13** and **figure 4.14**). There was no significant difference in the number of microglia present in the ipsilateral or contralateral hemisphere following 2-AG or JZL184 compared to vehicle.

An example of the difference in the extent of microglia activation between animals is shown in **figure 4.15**. Microglial activation was examined in the ipsilateral and contralateral hemisphere in each group and the results are shown in **figures 4.16** and **4.17**. Following middle cerebral artery occlusion, microglia activation was increased in the ipsilateral hemisphere in all treatment groups at cortical and subcortical regions compared to the contralateral hemisphere (**figure 4.16** and **figure 4.17**). Increased microglia activation was observed in cortical and subcortical regions in animals that underwent middle cerebral artery occlusion without treatment compared to sham operated animals. Neither 2-AG nor JZL184 treated caused any change in the extent of microglia activation following middle cerebral artery occlusion compared to vehicle.

4.5 Discussion

The aim of this study was to investigate the effect of 2-AG and the monoacylglycerol lipase inhibitor JZL184 on early injury development and the microglial response at 4 hours after middle cerebral artery occlusion.

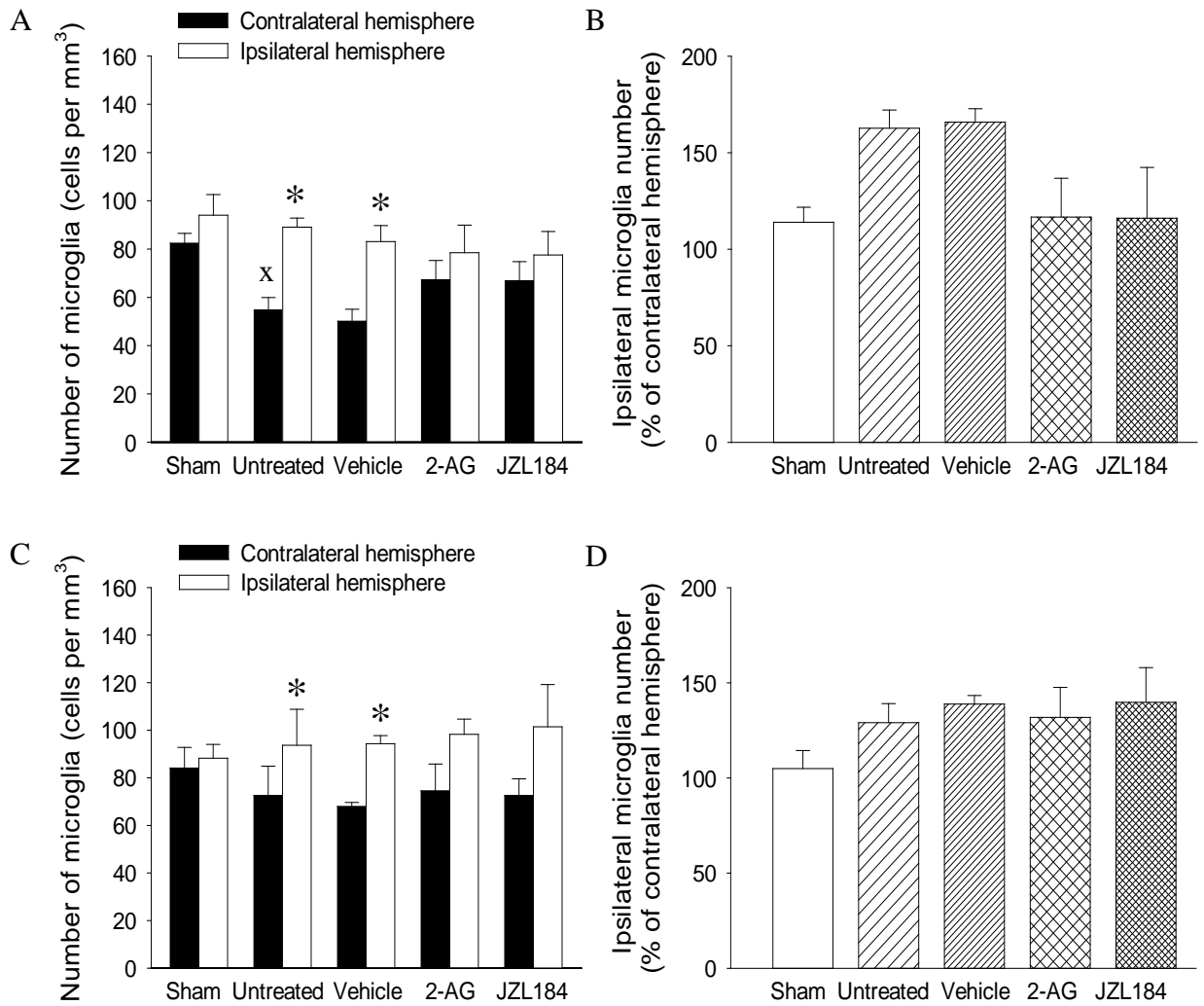
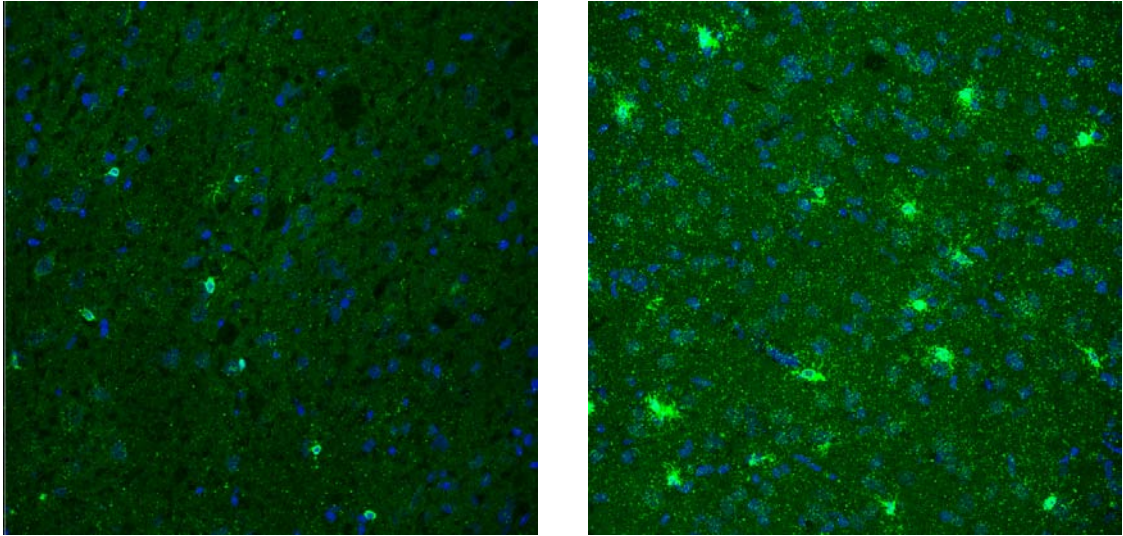


Figure 4.14: Number of microglia present in the subcortical area at the level of the **A and B**) globus pallidus and **C and D**) anterior hippocampus (n=5 for anandamide and n=6 for vehicle and URB597). **Panel A and C:** Total number of microglia in the cortex in the ipsilateral and contralateral hemispheres in all treatment groups. **Panel B and D:** Number of microglia in the ipsilateral hemisphere expressed as a percentage of the microglia number present in the contralateral hemisphere. Data are expressed as mean \pm s.e.m. * $p < 0.05$ compared to the contralateral hemisphere, paired t-test. x $p < 0.05$ vs. sham operated animals, one way ANOVA followed by multiple comparisons with Bonferroni correction.

Cortical area



Subcortical area

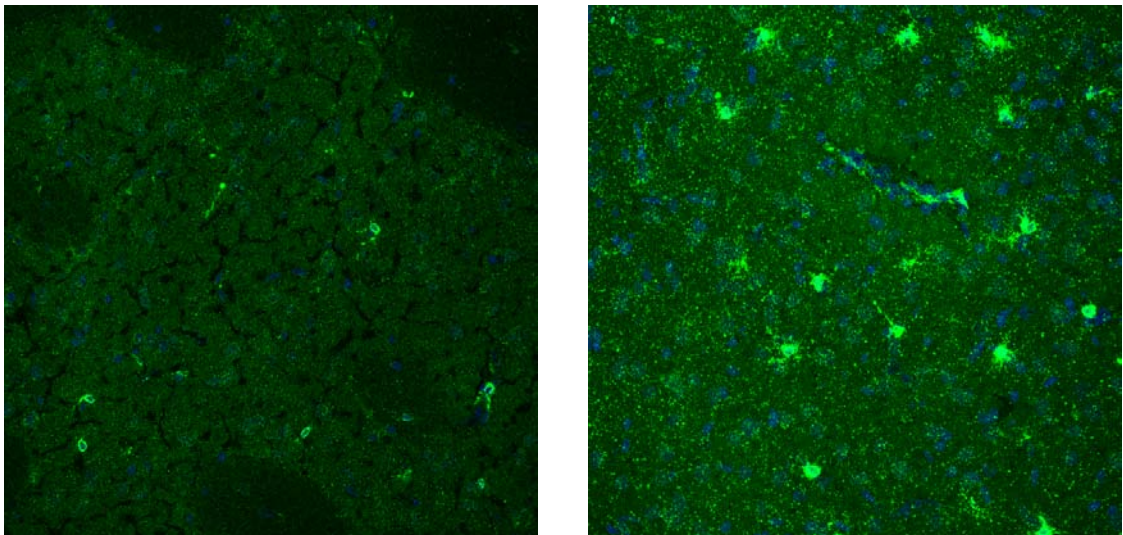


Figure 4.15: Confocal images (compressed z-stack) showing an example of low (left panels) and high (right panels) numbers of activated microglia present near the injury boundary in cortical and subcortical areas.

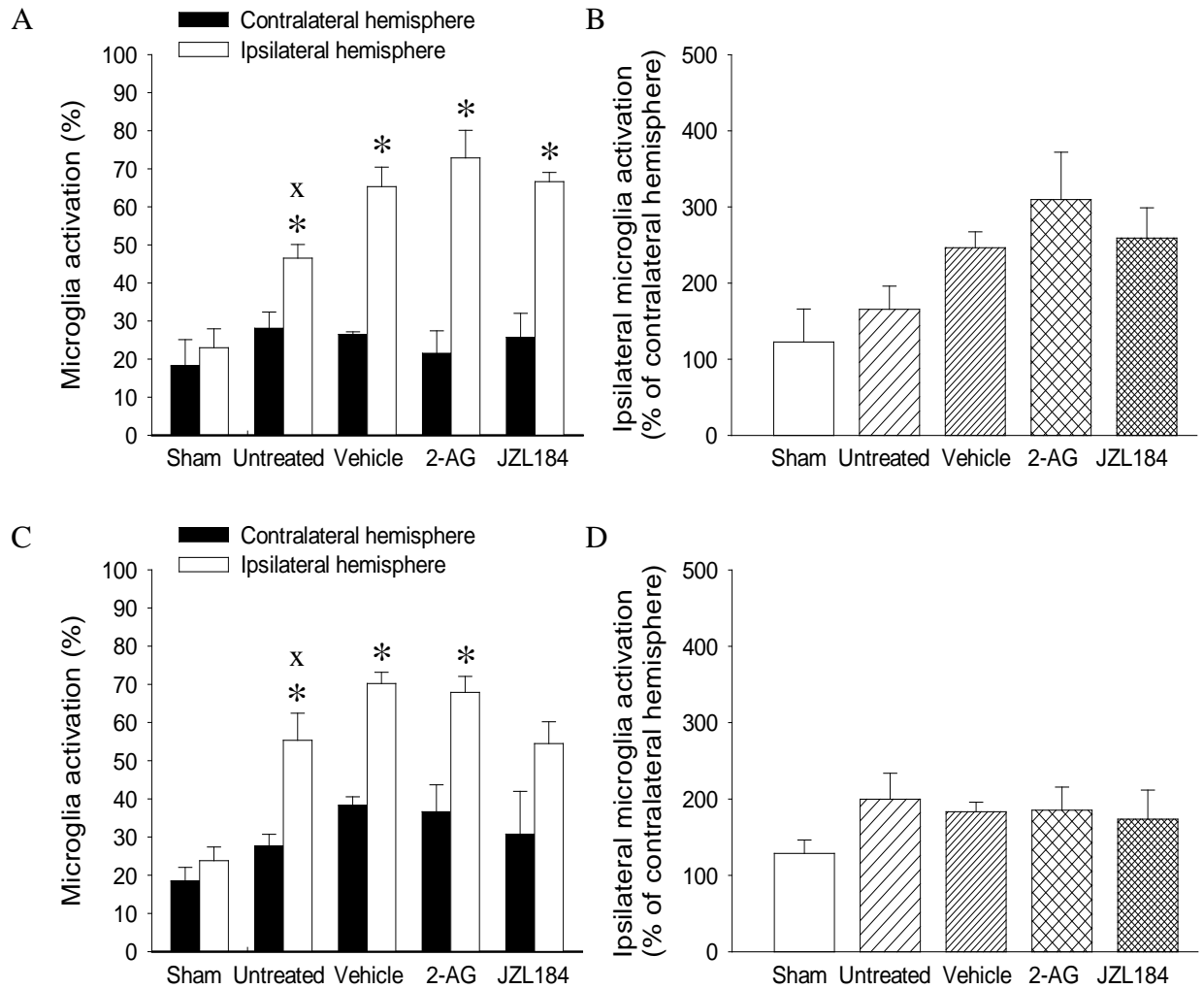


Figure 4.16: Extent of microglia activation in the cortex at the level of the **A and B)** globus pallidus and **C and D)** anterior hippocampus (n=5 for anandamide and n=6 for vehicle and URB597). **Panel A and C:** Number of activated microglia in the cortex in the ipsilateral and contralateral hemispheres in all treatment groups. **Panel B and D:** Number of activated microglia in the ipsilateral hemisphere expressed as a percentage of the activated microglia count present in the contralateral hemisphere. Data are expressed as mean \pm s.e.m. * $p < 0.05$ compared to the contralateral hemisphere, paired t-test. x $p < 0.05$ vs. sham operated animals, one way ANOVA followed by multiple comparisons with Bonferroni correction.

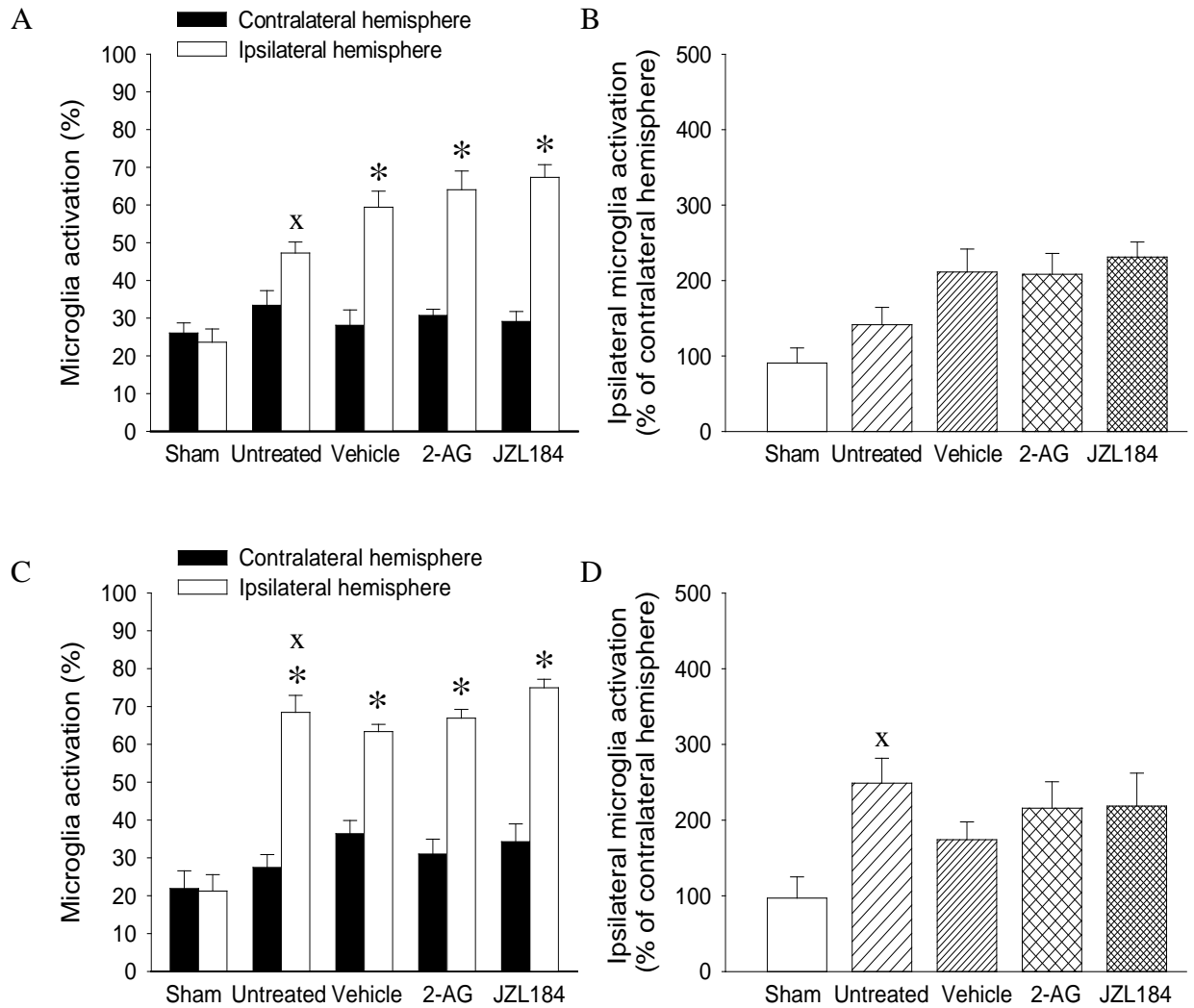


Figure 4.17: Extent of microglia activation in the subcortical area at the level of the **A and B)** globus pallidus and **C and D)** anterior hippocampus (n=5 for anandamide and n=6 for vehicle and URB597). **Panel A and C:** Number of activated microglia in the cortex in the ipsilateral and contralateral hemispheres in all treatment groups. **Panel B and D:** Number of activated microglia in the ipsilateral hemisphere expressed as a percentage of the activated microglia count present in the contralateral hemisphere. Data are expressed as mean \pm s.e.m. * p<0.05 compared to the contralateral hemisphere, paired t-test. # p<0.05 vs. vehicle treated group, one way ANOVA followed by a Dunnett's post-hoc test.

This work demonstrated that administration of JZL184 but not exogenous 2-AG caused an increase in total injury volume at 4 hours after middle cerebral artery occlusion. Cortical injury was increased in both 2-AG and JZL184 treated animals compared to the vehicle. This finding contradicts previous work by Panikashvili *et al.* (2001) and Arevalo-Martin *et al.* (2010) who have described neuroprotective effects of 2-AG in traumatic brain injury and spinal cord injury, respectively. Panikashvili *et al.* demonstrated that administration of 2-AG, 5 mg/kg (similar to the dose used in this study), resulted in reduced blood brain barrier permeability and decreased expression of pro-inflammatory cytokines (Panikashvili *et al.*, 2006), as well as, reduced infarct volume and improved functional recovery at 24 hours after traumatic brain injury (Panikashvili *et al.*, 2001).

The different results in our study compared to previous work in traumatic brain injury may be associated with the different injury models being studied. In traumatic brain injury oedema development is one of the early manifestations of injury with a transient increase in blood brain barrier permeability within 1 hour of insult (Barzó *et al.*, 1997). This disruption of normal blood brain barrier function is associated with the development of vasogenic oedema observed in the first few hours after injury (Barzó *et al.*, 1997). In contrast, oedema development in acute cerebral ischaemia primarily involves cytotoxic oedema (cell swelling) as a result of metabolic disturbance and ion imbalance (Solenski *et al.*, 2002). At 4 hours after permanent middle cerebral artery occlusion there is expression of activated MMP-2 and MMP-9 which are involved in breakdown of the blood brain barrier (Gasche *et al.*, 1999). Blood brain barrier permeability has been demonstrated at this time-point with

extravasation of evans blue (Gasche *et al.*, 1999) and inulin (Ennis and Keep, 2006) from cerebral blood vessels into the brain. In permanent cerebral ischaemia models significant cerebral oedema has been identified at 4 hours post-occlusion (Kawamura *et al.*, 1990). Following cerebral ischaemia there is progressive oedema formation which peaks at 24 hours post-occlusion and continues for up to 48 hours (Slivka *et al.*, 1995). As such, oedema development may not contribute significantly to injury development at the 4 hour time-point studied. Thus, 2-AG will not be able to exert neuroprotective effects through its actions on oedema development.

The different effects of 2-AG in these studies may also be related to the treatment protocol used. In previous studies 2-AG was administered as a single bolus i.p. injection given either immediately following injury (Panikashvili *et al.*, 2006) or at 30 minutes post-injury (Arevalo-Martin *et al.*, 2010). In the present study, it was decided to administer 2-AG as an i.v. bolus given at 15 minutes before middle cerebral artery occlusion followed by continuous infusion throughout the experimental period. This route was chosen to ensure successful administration of 2-AG into the brain before middle cerebral artery occlusion as this mediator has been shown to be rapidly metabolised in rat plasma (Kozak *et al.*, 2001). As such, 2-AG and JZL184 may exert greater cardiovascular effects in this study compared to i.p. administration due to a direct action on CB₁ receptors in the vasculature. Unfortunately, previous studies demonstrating 2-AG-induced neuroprotection in traumatic brain and spinal cord injury did not measure the cardiovascular effects of 2-AG following i.p. administration.

In the present study, larger injury was observed in untreated and vehicle treated animals compared to the anandamide study. This effect was likely due to the introduction of silicon coated Doccol filaments to occlude the middle cerebral artery instead of the heat blunted filaments used in the previous study. In comparison to the previous study, topography of the lesion also varied depending on the type of filament used with greater cortical injury produced using the Doccol filament. It has been proposed that coated filaments may result in more successful occlusion of the middle cerebral artery through increased adherence of the filament to the vessel lumen which will reduce residual blood flow in the internal carotid artery (Belayev *et al.*, 1996). Additionally, as there is a 5 mm long silicon coating present on the Doccol filaments these filaments will also occlude blood flow through branch vessels present on the internal carotid artery, such as the posterior cerebral artery. Occlusion of the posterior cerebral artery may produce greater injury as this vessel supplies blood to the posterior communicating artery which forms part of the collateral blood supply that perfuses tissue in the region of the middle cerebral artery (Lopez-Bresnahan *et al.*, 1993).

In the present study, sham operated animals were included to exclude a possible effect of anaesthesia or surgery on the microglia response. In sham operated animals the common carotid artery was occluded which caused a persistent reduction in cerebral blood flow of ~15%, however, this did not result in any visible tissue injury. This observation is in line with previous work which demonstrated that unilateral common carotid artery occlusion in normoxic and normotensive rats caused a 25% reduction in cerebral blood flow in both hemispheres and did not cause metabolic

dysfunction or tissue injury (De Ley *et al.*, 1985; Bronner *et al.*, 1998; Omae *et al.*, 2000). In the current study, injury development did not differ significantly between vehicle treated animals and those that did not receive any treatment. This lack of effect of the PEG vehicle in this model does not agree with previous studies which suggested that PEG can exert neuroprotective effects and improve functional recovery in animal models of spinal cord and traumatic brain injury (Baptiste *et al.*, 2009; Borgens and Bohnert, 2001; Koob *et al.*, 2008). In spinal cord injury systemic administration of fluorescently labelled PEG resulted in more intense staining at the site of injury compared to the surrounding tissue (Borgens and Bohnert, 2001). It was proposed that PEG may enter the central nervous system by crossing the compromised blood brain barrier in spinal cord and traumatic brain injury to act directly on injured cells. Previous studies have demonstrated that both 2-AG and the metabolism inhibitor JZL184 were capable of crossing the intact blood brain barrier to enter the brain following systemic administration (Darmani, 2002; Long *et al.*, 2009). In contrast, PEG is relatively inert and does not readily cross the blood brain barrier in healthy animals (Pardridge 2003; Spigelman, 1984). As such, it is possible that 2-AG and JZL184 were able to cross the blood brain barrier to enter the brain, whereas, either the permanent occlusion of the middle cerebral artery or limited permeability of the blood brain barrier may have prevented PEG from entering the tissue.

The effect of JZL184 on injury volume was most likely associated with the effect of this treatment on cerebral blood flow. Administration of 2-AG and JZL184 exacerbated the ischaemia-induced reduction in cerebral blood flow. A further

reduction in blood flow during cerebral ischaemia will have a detrimental effect. Reduced blood flow in the ischaemic cortex may have caused the increase in cortical injury observed in 2-AG and JZL184 treated animals. 2-AG is known to produce vasodilation of the middle cerebral artery *in vitro* and i.v. administration in mice caused potent hypotension and moderate tachycardia (Hillard *et al.*, 2007; Járai *et al.*, 2000). In the present study both the treatments and vehicle were administered prior to occlusion. As such, it is possible that cerebral blood vessels in the ipsilateral and contralateral hemispheres were already maximally dilated prior to occlusion of the middle cerebral artery. As there is a loss of autoregulation in cerebral blood vessels following cerebral ischaemia these vessels would be less able to constrict in order to maintain normal cerebral blood pressure and direct blood flow to the ischaemic cells (Dirnagl and Pulsinelli, 1990). Thus, pre-treatment with 2-AG and JZL184 may compromise the ability of cerebral blood vessels to respond to regional ischaemia and maintain perfusion of the penumbral tissue through collateral vessels.

Despite the similar effects of 2-AG and JZL184 on cerebral blood flow and cortical injury 2-AG did not significantly increase total injury volume at 4 hours post-occlusion. The reason for this difference in the effect of 2-AG and JZL184 on total injury volume is unclear. Treatment with JZL184 enhances the release of endogenous 2-AG from numerous cell types through inhibition of cellular metabolism by monoacylglycerol lipase. However, analysis has not been performed to determine the concentration of 2-AG present in the brain following administration of JZL184. The concentration of 2-AG in the brain produced by JZL184 treatment may be significantly higher than that achieved by exogenous 2-AG administration

due to metabolism of 2-AG *in vivo*. This difference in the 2-AG concentration achieved in the brain may explain the more potent effect of JZL184 on injury development in this study.

2-AG treatment *in vitro* can affect several aspects of the microglia response, including migration and cytokine expression (Walter *et al.*, 2003; Facchinetti *et al.*, 2003). The present study investigated the effect of 2-AG and JZL184 on the microglia response following middle cerebral artery occlusion to provide a greater understanding of the possible mechanisms involved in mediating the increase in cortical injury. In this study the number of microglia was increased in the ipsilateral hemisphere following injury compared to contralateral regions in untreated and vehicle treated animals but not in those receiving 2-AG and JZL184. Middle cerebral artery occlusion caused a significant increase in microglia activation in the ipsilateral hemisphere compared to the contralateral tissue. Microglia activation was not increased significantly in the ipsilateral hemisphere in sham operated animals. Treatment with 2-AG and JZL184 did not affect either microglia number or activation in the ipsilateral hemisphere at 4 hours after middle cerebral artery occlusion compared to vehicle treated animals.

As described previously, microglia may have several roles following cerebral ischaemia and can exhibit either a pro- or anti-inflammatory phenotype by releasing an array of different cytokines. 2-AG has been shown to increase microglia proliferation and migration *in vitro*, this effect may be considered to be detrimental during cerebral ischaemia. However, 2-AG may also promote an anti-inflammatory

phenotype by reducing release of the pro-inflammatory cytokine TNF- α from activated microglia. The present study did not identify an effect of 2-AG or JZL184 on microglia number or activation following 4 hour middle cerebral artery occlusion. However, it is possible that 2-AG may be able to affect the response of microglia in a manner which was not examined in this study, such as through modulation of cytokine expression in activated microglia. As such, it is necessary to perform further studies to examine the phenotype of microglia in the ipsilateral hemisphere following treatment with 2-AG and JZL184.

The findings in this study demonstrate that 2-AG, either exogenously administered or enhanced endogenously, reduced cerebral blood flow during cerebral ischaemia. The reason for this effect is unclear. Previous studies have demonstrated that 2-AG is released from activated platelets and can produce platelet aggregation in human whole blood (Keown *et al.*, 2010). Following middle cerebral artery occlusion the cerebral vasculature is considered to be a pro-thrombotic environment (Cherian *et al.*, 2003; Dougherty *et al.*, 1977). It is possible that 2-AG and JZL184 may affect cerebral ischaemia by causing platelet aggregation *in vivo* resulting in thrombi formation in the cerebral vasculature and a reduction in cerebral blood flow. As such, it was decided to investigate the effect of 2-AG on platelet aggregation in rat whole blood.

In conclusion, treatment with 2-AG and JZL184 caused an increase in cortical injury volume at 4 hours after middle cerebral artery occlusion. This effect is most likely due to the marked reduction in cerebral blood flow observed in animals receiving

these treatments. It is possible that vasodilation of cerebral blood vessels in the rest of the brain may divert blood away from the ischaemic tissue and exacerbate injury development. Treatment with 2-AG and JZL184 did not affect the microglia response following injury. Further work may be required to fully elucidate the role of 2-AG in cerebral ischaemia and identify the mechanisms involved.

CHAPTER 5

CHARACTERISATION OF 2-ARACHIDONOYL GLYCEROL (2-AG)-INDUCED PLATELET AGGREGATION IN RAT WHOLE BLOOD

5.1 Introduction

In the previous chapter it was demonstrated that the monoacylglycerol lipase inhibitor JZL184 caused an increase in total injury volume at 4 hours after middle cerebral artery occlusion. This effect may be related to the reduction in cerebral blood flow in JZL184 treated animals. However, the cause of this reduction in blood flow has not been established. Previous work has described pro-aggregatory effects of 2-AG in rat and human whole blood *in vitro* (Shearer *et al.*, 2009; Keown *et al.*, 2010). Treatment with 2-AG and JZL184 may have affected platelet function *in vivo* and influenced injury development following middle cerebral artery occlusion. As such, it is important to characterise the effect of 2-AG on platelet aggregation in the rat and identify the mechanisms involved.

Platelets express both CB₁ and CB₂ receptors and are an important site of endocannabinoid synthesis and metabolism in the vasculature (Randall, 2007). 2-AG is the primary endocannabinoid released from activated platelets (Maccarrone *et al.*, 2001). In previous studies 2-AG but not anandamide (up to 30 µM) produced platelet aggregation at micromolar concentrations in human and rat whole blood (Keown *et al.*, 2010; Shearer *et al.*, 2009). In human platelet-rich plasma, addition of 2-AG in combination with other physiological agonists modified the aggregation response to these agonists. Addition of 2-AG in combination with ADP or collagen abolished the aggregation response, whereas, 2-AG increased the response to 5-HT in a synergistic manner (Maccarrone *et al.*, 2001). The mechanisms involved in mediating 2-AG-induced aggregation in human platelets remain controversial. A recent study by Keown *et al.* (2010) in human whole blood demonstrated that 2-AG produced

aggregation through monoacylglycerol lipase and COX metabolism with no involvement of cannabinoid receptors. In contrast, Maccarrone *et al.* (2001) reported that 2-AG produced aggregation in human platelet-rich plasma through a cannabinoid receptor sensitive to both CB₁ and CB₂ antagonists. To date, 2-AG has been shown to produce aggregation in rat whole blood (Shearer *et al.*, 2009); however, the mechanisms involved in mediating this effect have not been fully elucidated. The hypothesis of this study is that 2-AG can produce platelet aggregation in rat whole blood through activation of cannabinoid receptors or COX metabolism to form pro-aggregatory prostanoids.

5.2 Aim

The aim of this study was to characterise the effect of 2-AG alone and in combination with ADP on platelet aggregation in rat whole blood. The involvement of cannabinoid receptors and cellular metabolism in mediating the aggregation response was also investigated.

5.3 Methods

5.3.1 Source of Materials

Details of suppliers for equipment, drugs and reagents are included in the Appendices.

5.3.2 Animal Source

Animals used in these experiments were sourced and housed as described in **section 2.3.2.**

5.3.3 Animal Preparation

Male Sprague-Dawley rats weighing 350-400g were anaesthetised as described in **section 3.3.3**.

Once anaesthetised, the animals were connected to a nose cone and anaesthesia was maintained with 2-2.75% isoflurane delivered in 100% oxygen at 0.5 l/min. Suitable depth of anaesthesia was assessed by lack of a pedal withdrawal response and corneal reflex. Body temperature was monitored continuously and maintained within 36.5-37.5 °C using a homeothermic blanket and heat lamp.

5.3.4 Surgical Procedure

Anaesthetised rats were placed in a supine position. A midline incision was made at the neck and the connective tissue and sternohyoid muscle were dissected. The common carotid artery was exposed, dissected free of connective tissue and cannulated with polythene tubing (0.58 mm ID and 0.96 mm OD) containing heparinised saline (10 units/ml). A 9-10 ml volume of arterial blood was withdrawn into heparinised syringes (20 units/ml of whole blood) and diluted 1:1 with saline. Diluted blood was pooled and stored at room temperature prior to performing aggregation studies.

5.3.5 Whole Blood Aggregometry

Prior to aggregation, blood was divided into 1 ml aliquots and warmed to 37 °C. Platelet aggregation was measured in whole blood by impedance aggregometry. First developed by Cardinal and Flower in 1980, this technique involves measuring

changes in an electrical current between two electrodes during aggregation. Initially a platelet monolayer will form on the electrodes and following addition of an aggregating agent platelets will adhere to the platelet monolayer and impede transmission of the electrical current. The rate and extent of impedance were used as a measure of the aggregation response. In these experiments, aggregation was measured using a two-channel Chrono-log 590 whole blood aggregometer. Studies were performed using a pair of matched electrodes that were used independently to measure aggregation. All drugs were added to whole blood in volumes of 1–10 μL using a positive displacement micropipette.

5.3.6 Experimental Protocol

5.3.6.1 Ethanol Vehicle

In preliminary experiments, the effect of ethanol on the peak response to ADP 1 μM was examined. In each experiment, a 10 μl volume of ethanol (10-40%) was added to 1 ml of blood to give the final concentration. In the first set of experiments, 10% and 40% ethanol in saline were added to blood 1 minute before ADP to produce final concentrations of 0.1% and 0.4%. In the second set of experiments, 20% and 40% ethanol were added 1 minute before ADP to give a final blood concentration of 0.2% and 0.4%, respectively.

5.3.6.2 Agonist Response

Whole blood aggregation in response to several agonists was studied at a range of concentrations; ADP (0.1-30 μM), collagen (0.3-10 $\mu\text{g/ml}$), 2-AG (19-300 μM), arachidonic acid (19-300 μM) and HU-210 (3-100 nM). The ADP response was

measured over 10 minutes and the peak response was recorded. For the other agonists, the maximal response was measured at 10 minutes or 15 minutes (collagen only) after addition of the aggregating agent. For 2-AG, the responses to the higher (75-300 μM) and lower (19-75 μM) concentrations were examined separately in different groups of animals to produce a complete concentration response curve. Responses to lower concentrations of 2-AG varied between individuals. As such, all of the data for 2-AG at 75 μM and 150 μM and arachidonic acid at 38 μM and 75 μM from 2 animal groups was combined to increase the total n number.

5.3.6.3 Cannabinoid Receptors

Antagonists at CB_1 (AM251) and CB_2 receptors (AM630) were used to examine the role of these receptors in the response to ADP (1 μM), 2-AG (150 μM) and arachidonic acid (75 μM). These concentrations of 2-AG and arachidonic acid were chosen as they produced consistent aggregation in all animals, ~80% of the maximal response for each agonist. AM251 and AM630 were added individually at 1 μM and 3 μM in combination with the appropriate vehicle for the other antagonist (0.03% ethanol for AM251 and 0.03% DMSO for AM630 as final blood concentration (f.b.c.)). The antagonist and vehicle or vehicles for both AM251 and AM630 were added to the blood 1 minute before each agonist. The peak response to ADP was recorded and the maximal response to 2-AG and arachidonic acid was measured at 10 minutes following addition of the agonist.

5.3.6.4 Role of Metabolism

The role of endocannabinoid metabolism and thromboxane A_2 production in the

aggregation response to ADP (1 μ M), 2-AG (150 μ M) and arachidonic acid (75 μ M) was investigated. COX inhibitors, indomethacin (3 and 10 μ M) and flurbiprofen (10 μ M), the thromboxane receptor antagonist, ICI 192,605 (1 μ M), or the appropriate vehicle were pre-incubated for 10 minutes prior to the addition of the agonist. This study was performed in 2 groups of animals, initial experiments examined the effect of indomethacin at 3 μ M and ICI 192,605. In the second set of experiments, a higher concentration of indomethacin (10 μ M) and flurbiprofen were used to examine the role of COX. For ADP, only the lower concentration of indomethacin (3 μ M) and ICI 192,605 were used. Inhibitors of fatty acid amide hydrolase and monoacylglycerol lipase, URB597 (0.3 μ M) and JZL184 (0.1 μ M), or vehicle were incubated alone and in combination with ICI 192,605 (1 μ M) or vehicle at 37 °C for 10 minutes before 2-AG or arachidonic acid. To confirm the role of monoacylglycerol lipase, a higher concentration of JZL184 (1 μ M) or appropriate vehicle was pre-incubated at 37 °C for 30 minutes prior to the addition of 2-AG or arachidonic acid. To investigate possible breakdown by plasma esterases, neostigmine (1 μ M) or vehicle was added to the blood 10 minutes before the addition of 2-AG or arachidonic acid. For all experiments the aggregation response was measured at the peak response to ADP and at 10 minutes after addition of 2-AG and arachidonic acid.

5.3.6.5 Agonist Interaction

The interaction of 2-AG and arachidonic acid with ADP was examined. Concentrations of 2-AG and arachidonic acid were chosen which produced a small aggregation response alone as this will allow the effect on the ADP response to be

clearly observed. 2-AG (75 μM), arachidonic acid (38 μM) or appropriate vehicle was added 1 minute before the addition of ADP (1 μM). The response was measured over 10 minutes and recorded at 1 minute intervals. The mechanisms involved in this interaction were studied using the COX inhibitors, indomethacin (3 μM and 10 μM) and flurbiprofen (10 μM), and the thromboxane receptor antagonist, ICI 192,605 (1 μM). Both the inhibitors and antagonist or appropriate vehicle were incubated for 10 minutes before addition of the first agonist.

5.3.7 Drug Preparation

In this study, heparinised saline was prepared fresh each day as detailed in **sections 2.3.14** and **3.3.16**. The following drugs were also used and were prepared as described below:

- *ADP*: Dissolved in saline each day to form a 1 mM solution.
- *Collagen*: Diluted in saline each day to form 0.3-1 ng/ml working solutions.
- *Arachidonic acid*: Supplied as an oil and dissolved in albumin solution (1 mg/ml in sterile saline) to form a 50 mM stock solution and stored in the dark at -80 °C. Prior to each experiment, aliquot was thawed and diluted in saline to 30 mM. Immediately before addition of arachidonic acid, varying concentrations of ethanol added to give a final blood concentration which matched that produced by corresponding concentrations of 2-AG.
- *2-AG*: Dissolved in ethanol to form a 100 mM (37.9 mg/ml) stock solution and

stored at -20 °C. In preliminary experiments, a 79.3 mM (30 mg/ml) stock solution was used for 2-AG experiments. Prior to each experiment, 2-AG was diluted in a saline:ethanol vehicle to form working solutions of 6.25 mM (9.5% ethanol), 12.5 mM (19% ethanol), 25 mM and 30 mM (38% ethanol). Final blood concentrations of 2-AG were achieved by adding varying concentrations of the prepared solutions to give 19, 38, 75, 150 and 300 µM (final blood concentration of 0.02%, 0.06%, 0.11%, 0.19% and 0.38% ethanol, respectively).

- *HU-210*: Dissolved in ethanol to form a 2.6 mM solution, stored at -20 °C and diluted 1:10 in saline before use (0.003% and 0.01% ethanol f.b.c.).
- *AM251*: Dissolved in ethanol to form a 10 mM solution and stored at -20 °C. Stock solution diluted in saline to form 1 and 3 mM (0.03% ethanol f.b.c.).
- *AM630*: Dissolved in DMSO to form a 10 mM solution and stored at -20 °C. Stock solution diluted in saline to form 1 and 3 mM solutions (0.03% DMSO f.b.c.).
- *Indomethacin*: Dissolved in ethanol to form 10 mM, stored at 4 °C and further diluted in saline to form 1 mM (0.03% and 0.1% ethanol f.b.c.).
- *ICI 192,605*: Dissolved in ethanol to form 10 mM, stored at 4 °C and further diluted in saline to form 1 mM (0.03% and 0.1% ethanol f.b.c.).
- *Flurbiprofen*: Supplied in acidic form and processed to form sodium salt prior to use in this study. Flurbiprofen (30 mg) dissolved in 0.5 ml of ethanol and 110 µl of sodium hydroxide (NaOH) solution (1 M; 4 grams per 100 ml of water) was added. Ethanol was evaporated using a jet of nitrogen and warming the solution to leave sodium salt residue. Sodium salt dissolved in 1 ml saline to form a

100 mM stock solution, stored at -20 °C and diluted 1:10 in saline prior to use.

- *URB597*: Dissolved in DMSO to give 10 mM solution, stored at -20 °C and diluted in saline to form 0.1 mM (0.001% and 0.003% DMSO f.b.c.) prior to use.
- *JZL184*: Dissolved in DMSO to give 10 mM stock solution, stored at -20 °C and diluted in saline to form a 0.1 mM solution (0.001% and 0.003% DMSO f.b.c.).

5.3.8 Statistical Analysis

Aggregation responses were expressed in ohms (Ω) as mean \pm s.e.m. Data distribution in each study was examined using a Shapiro-Wilk Test. As many of the responses were not normally distributed it was decided to perform non-parametric tests to analyse the data. The effect of ethanol vehicles on the ADP response was analysed using a Kruskal-Wallis test. Aggregation responses to each agonist in the presence and absence of cannabinoid receptor antagonists, COX inhibitors, indomethacin and flurbiprofen, thromboxane receptor antagonist, ICI 192,605, and metabolism inhibitors, URB597 and JZL184, added alone and in combination with ICI 192,605 were compared using a Kruskal-Wallis test. The effect of JZL184 (1 μ M) or neostigmine on the response to 2-AG and arachidonic acid in comparison to each agonist alone was examined using a Mann-Whitney test. For JZL184 (1 μ M) and neostigmine in combination with 2-AG or arachidonic acid the statistical power of these experiments was calculated by Statsdirect following comparison with an unpaired Student's t-test assuming unequal variances. The sample size required to give appropriate statistical power (80%) for these comparisons in an unpaired t-test

was calculated in Statsdirect using the difference between the mean values and standard deviation from these experiments.

For agonist interactions, the area under the curve was calculated for each response. Agonist interactions in the presence and absence of metabolism inhibitors and receptor antagonist were compared by performing Friedman tests to compare areas under the curve. As these experiments were performed in separate batches the aggregation response in the presence of each inhibitor or antagonist was compared against the agonist combination from the same batch to allow paired comparisons.

5.4 Results

5.4.1 Ethanol Vehicle

Ethanol alone did not cause aggregation at any concentration studied (n=5; results not shown). At lower concentrations (0.1% and 0.2% f.b.c.), ethanol did not significantly affect the response to ADP (**figure 5.1**). However, the highest concentration of ethanol studied (0.4% f.b.c.) caused a significant reduction in ADP-induced aggregation in both sets of experiments (**figure 5.1**).

5.4.2 Agonist Response

A typical trace for each agonist is shown in figure 5.2. ADP caused rapid aggregation which peaked at 1 minute and began to disaggregate (**figure 5.2A**). 2-AG produced a gradual increase in aggregation which peaked at 10 minutes (**figure 5.2B**). This gradual response was similar to that observed with arachidonic acid (**figure 5.2C**).

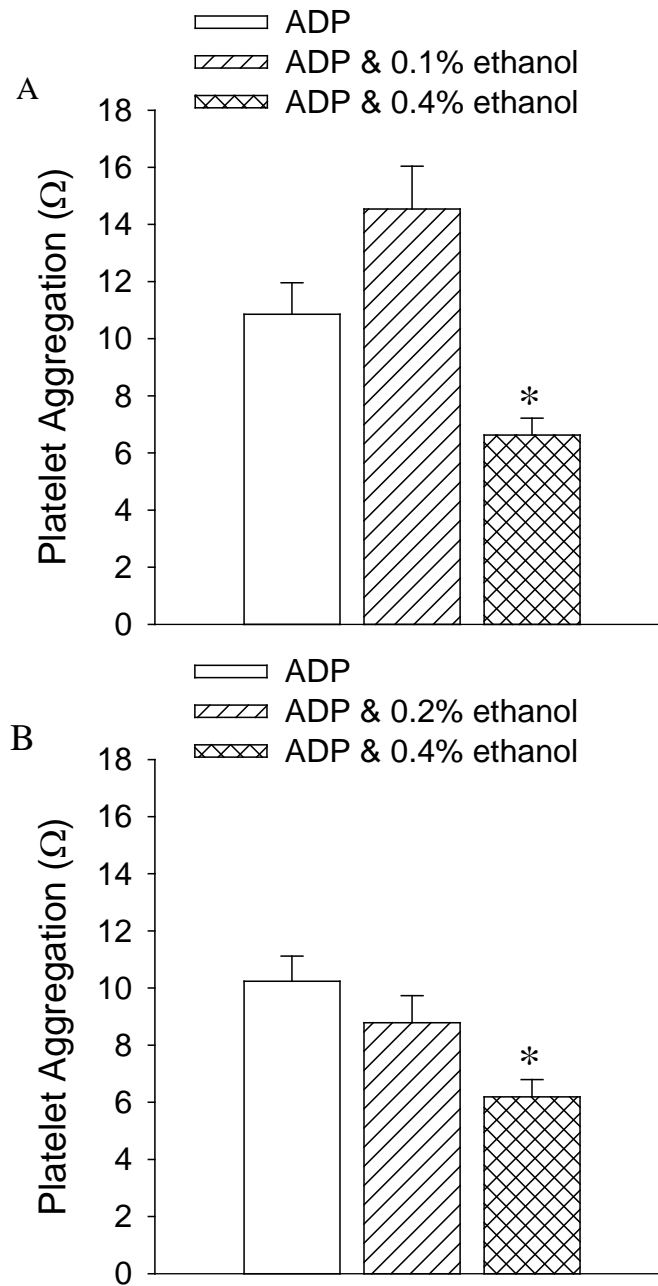


Figure 5.1: Effect of ethanol vehicle at **A**) 0.1% and 0.4% (f.b.c.) and **B**) 0.2% and 0.4% (f.b.c.) on the peak response to ADP at 1 μ M (n=6). Data are expressed as mean \pm s.e.m. * $p < 0.05$ vs. ADP alone, Kruskal-Wallis test.

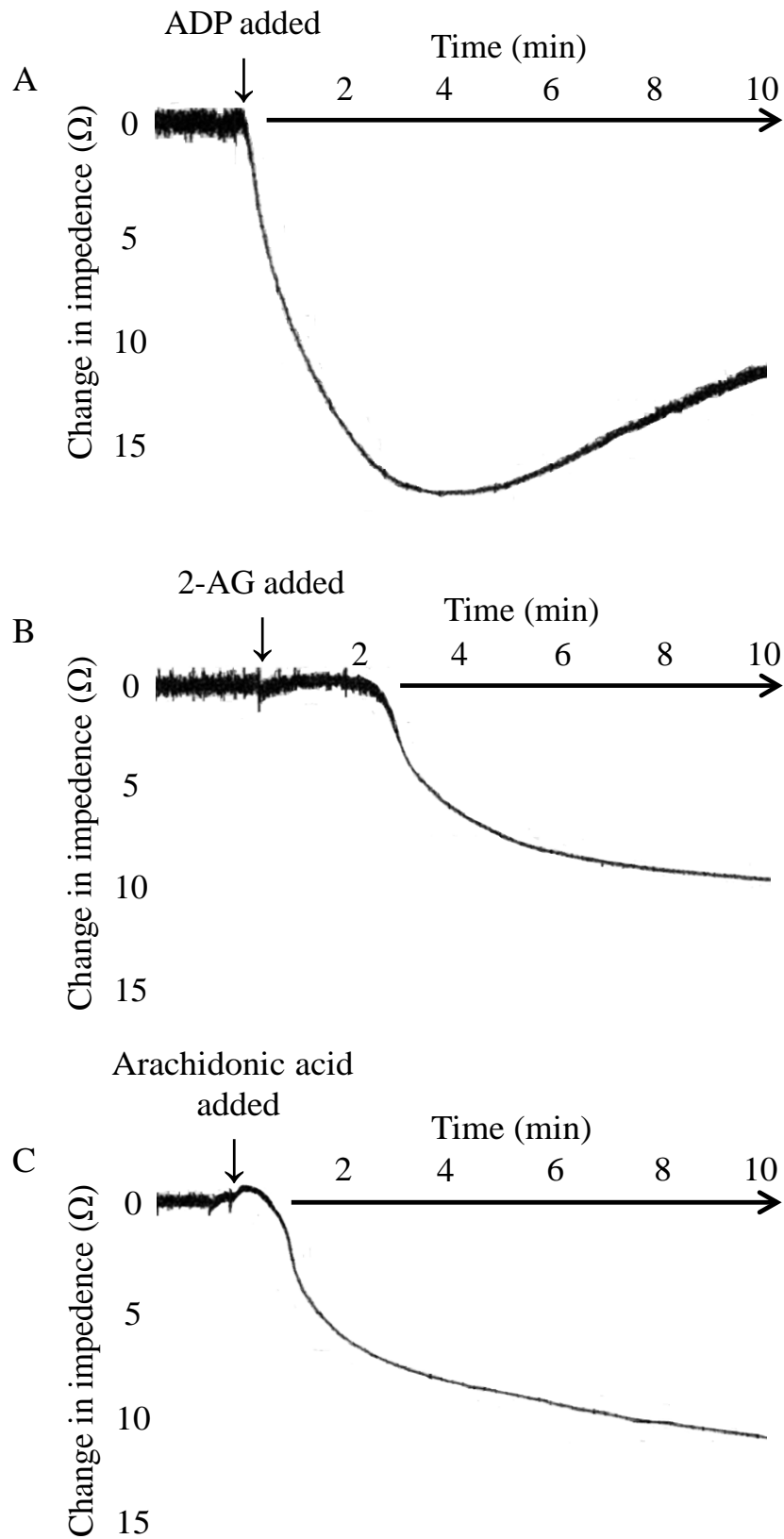


Figure 5.2: Original traces of typical platelet aggregation responses to **A)** ADP (1 μ M), **B)** 2-AG (150 μ M) and **C)** arachidonic acid (150 μ M) in rat whole blood.

Concentration-response curves for each agonist are shown in **figure 5.3**. ADP (0.1-30 μM) produced concentration-dependent aggregation with a maximal response of $18.5 \pm 0.9 \Omega$ at 3 μM . 2-AG and arachidonic acid at 19-300 μM produced a concentration-dependent increase in aggregation with maximal responses of $12.1 \pm 2.0 \Omega$ and $11.7 \pm 0.5 \Omega$ at 300 μM and 75 μM , respectively (**figure 5.3**). 2-AG-induced aggregation showed greater inter-individual variation compared to the same concentration of arachidonic acid (**figure 5.4A** and **5.4C**). 2-AG at 75 μM produced inconsistent aggregation with some animals showing strong aggregation and others not responding. At a higher 2-AG concentration (150 μM), all animals responded, although, the extent and rate of aggregation varied between individuals (**figure 5.4B**). As all animals responded to 2-AG at 150 μM it was decided to use this concentration to study the effects of receptor antagonists and metabolism inhibitors.

5.4.3 Cannabinoid Receptors

2-AG-induced aggregation was inhibited by the CB_2 antagonist, AM630, at both concentrations (**figure 5.5A**). The CB_1 antagonist, AM251, appeared to reduce the response to 2-AG, however, this effect did not reach significance at either concentration studied. In contrast to these findings, HU-210, a potent synthetic agonist at CB_1 and CB_2 receptors, did not cause any aggregation at concentrations up to 100 nM ($-0.9 \pm 0.3 \Omega$ at 100 nM; n=6). Neither AM251 nor AM630 had any effect on platelet aggregation responses to ADP or arachidonic acid (**figure 5.5B** and **5.5C**).

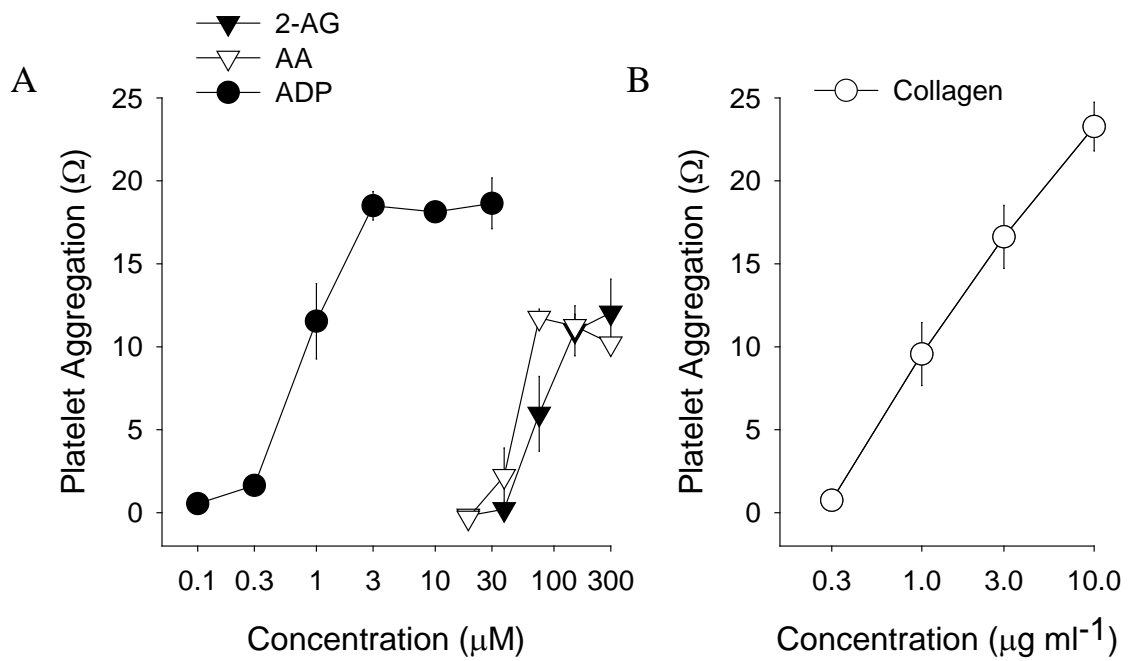


Figure 5.3: Concentration-response curve to **A)** 2-AG (19-300 μM ; $n=6-12$), arachidonic acid (19-300 μM ; $n=4-11$) and ADP (0.1-30 μM ; $n=5-6$) and **B)** collagen (0.3-10 $\mu\text{g/ml}$; $n=5-6$). AA; arachidonic acid. Aggregation measured at the peak response for ADP, at 10 minutes for 2-AG and arachidonic acid and at 15 minutes for collagen. Data are expressed as mean \pm s.e.m.

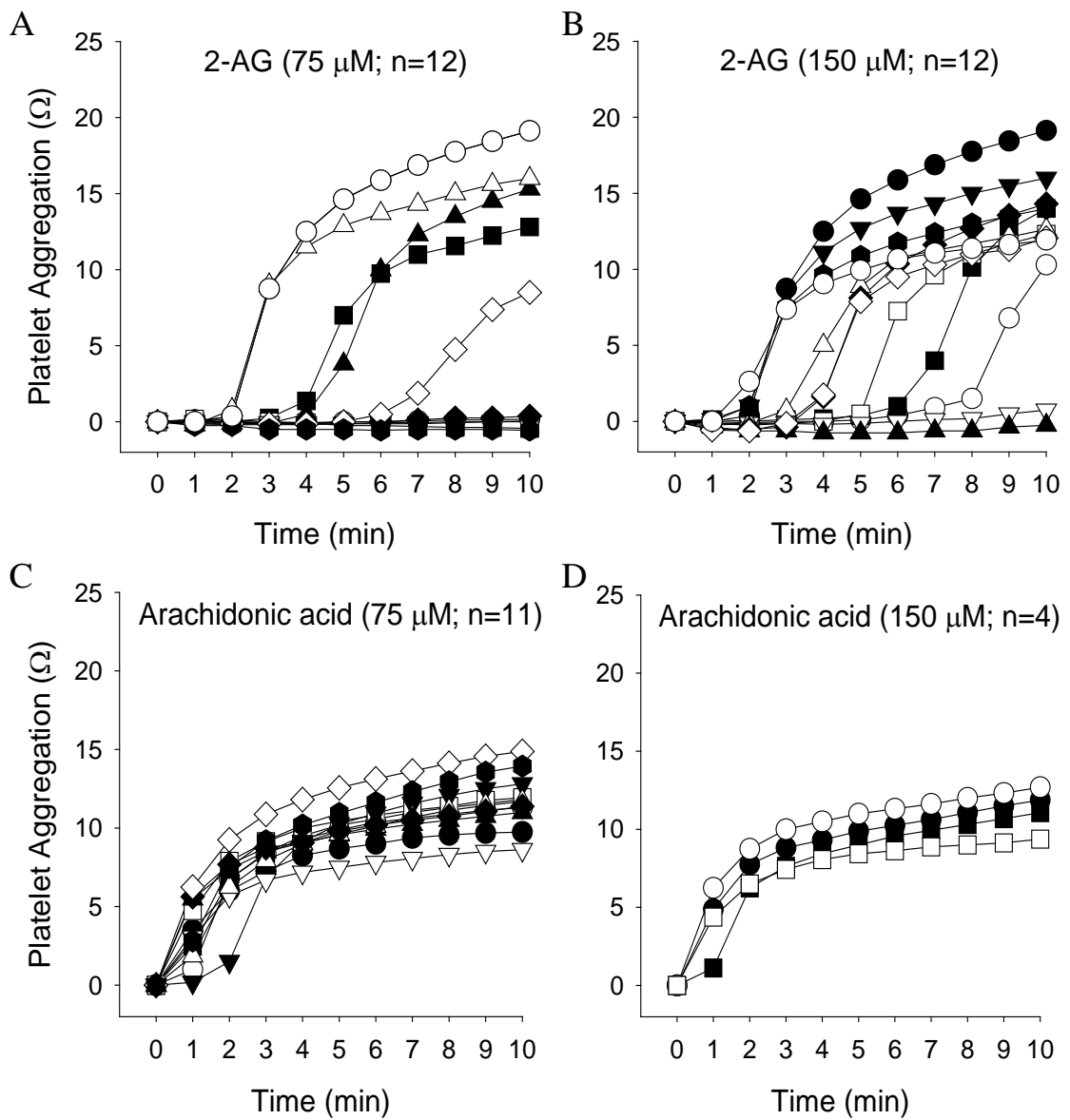


Figure 5.4: Individual aggregation responses to 2-AG at **A)** 75 μ M and **B)** 150 μ M and arachidonic acid at **C)** 75 μ M and **D)** 150 μ M.

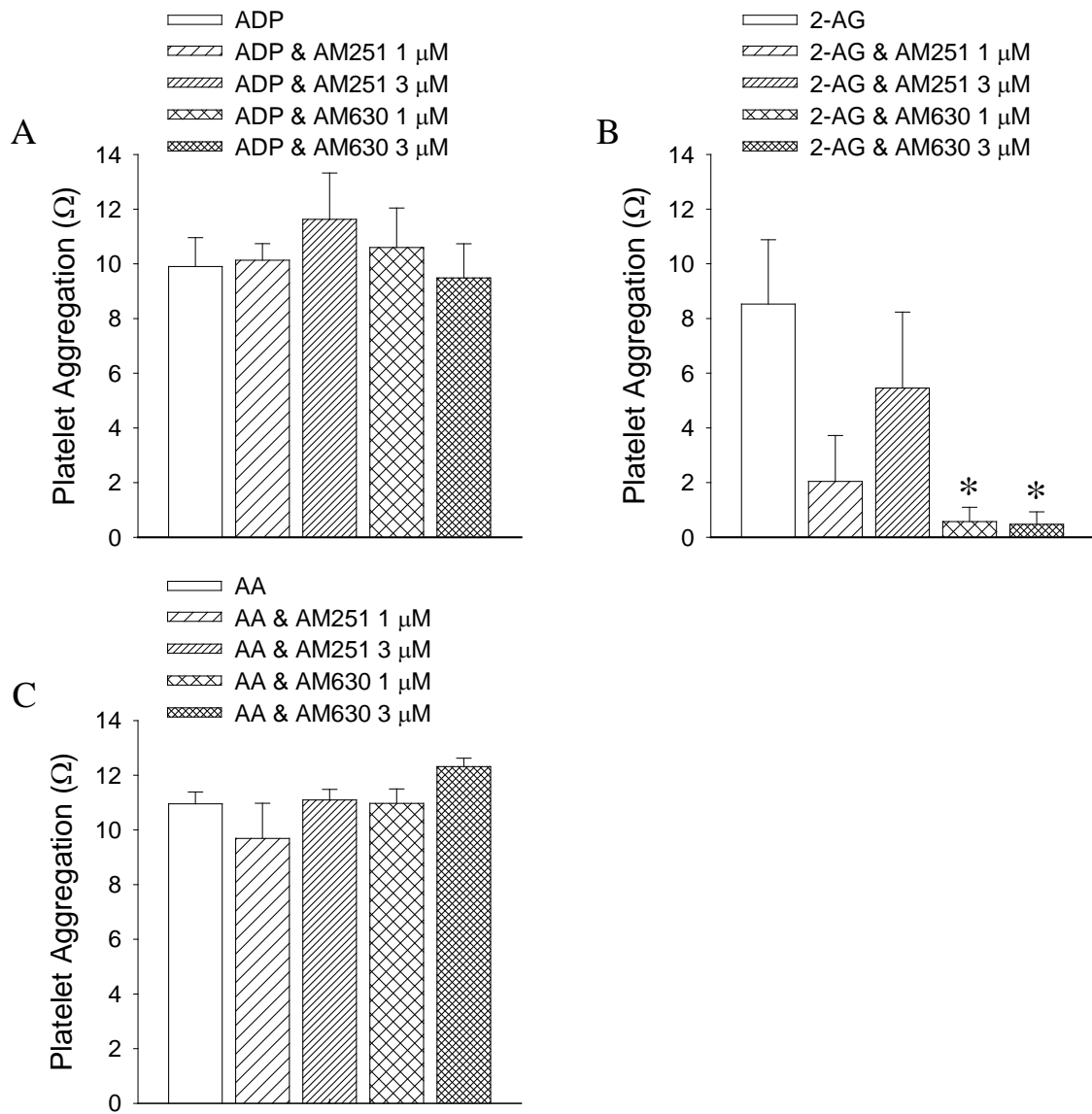


Figure 5.5: Effect of AM251 and AM630 at 1 and 3 μM on the aggregation response to **A)** ADP (1μM; n=6), **B)** 2-AG (150μM; n=7) and **C)** arachidonic acid (75 μM; n=4). AA; arachidonic acid. Aggregation measured at the peak response for ADP and at 10 minutes after addition of 2-AG and arachidonic acid. Data are expressed as mean ± s.e.m. * p<0.05 vs. agonist alone, Kruskal-Wallis test.

5.4.4 Role of Metabolism

The role of metabolism in the response to each agonist was studied using several inhibitors and a thromboxane receptor antagonist. Both COX inhibitors, indomethacin (10 μM) and flurbiprofen (10 μM), abolished the aggregation response to 150 μM 2-AG and 75 μM arachidonic acid (**figure 5.6A** and **5.6C**). 2-AG-induced aggregation was also reduced by indomethacin at 3 μM , however, this concentration did not affect the response to arachidonic acid. Aggregation induced by 2-AG and arachidonic acid was abolished by incubation with the thromboxane receptor antagonist, ICI 192,605 (**figure 5.6A** and **5.6C**). ADP-induced aggregation was not affected by either indomethacin (3 μM) or ICI 192,605 (**figure 5.6B**). Inhibition of fatty acid amide hydrolase and monoacylglycerol lipase by URB597 (0.3 μM) and JZL184 (0.1 μM), respectively, did not reduce the aggregation response to 2-AG or arachidonic acid (**figure 5.7**). Aggregation to 2-AG and arachidonic acid was inhibited following incubation of either URB597 or JZL184 added in combination with ICI 192,605 (**figure 5.7**). At a higher concentration, JZL184 (1 μM) reduced arachidonic acid-induced aggregation. In contrast, JZL184 appeared to reduce the response to 2-AG, however, this effect failed to achieve significance (**figure 5.8**). The plasma esterase inhibitor, neostigmine (1 μM), appeared to cause a reduction in the responses to 2-AG and arachidonic acid but these effects failed to achieve significance (**figure 5.9**). These experiments were performed in a small number of animals and had low statistical power.

5.4.5 Agonist Interaction

The interaction of 2-AG and arachidonic acid with ADP over 10 minutes is shown in

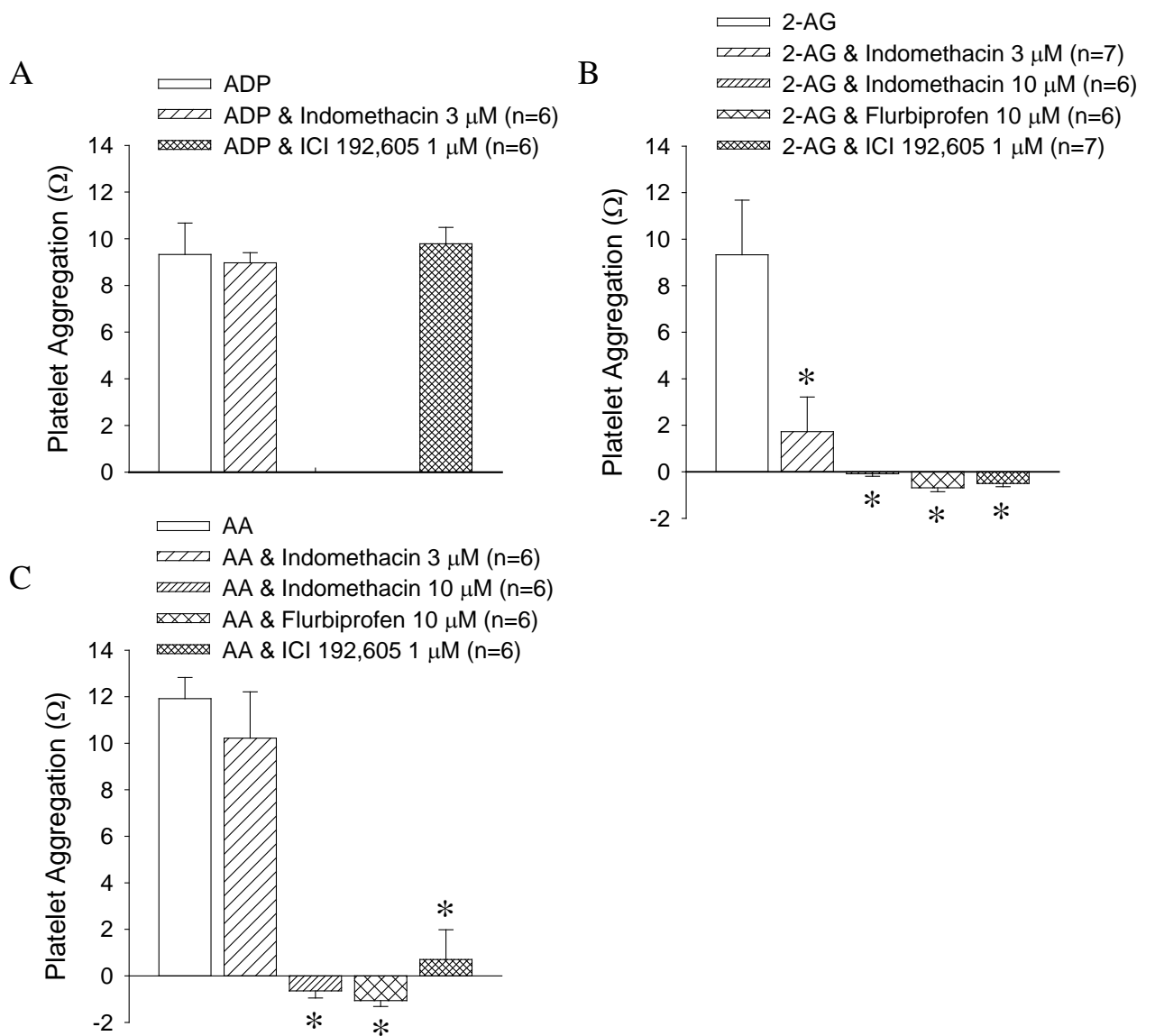


Figure 5.6: Effect of indomethacin (3 μM and 10 μM), flurbiprofen (10 μM) and ICI 192,605 (1 μM) on platelet aggregation induced by **A)** ADP (1 μM; n=6), **B)** 2-AG (150 μM; n=7) and **C)** arachidonic acid (75 μM). AA; arachidonic acid. Aggregation measured at the peak response for ADP and at 10 minutes after addition of 2-AG and arachidonic acid. Data are expressed as mean ± s.e.m. * p<0.05 vs. agonist alone, Kruskal-Wallis test.

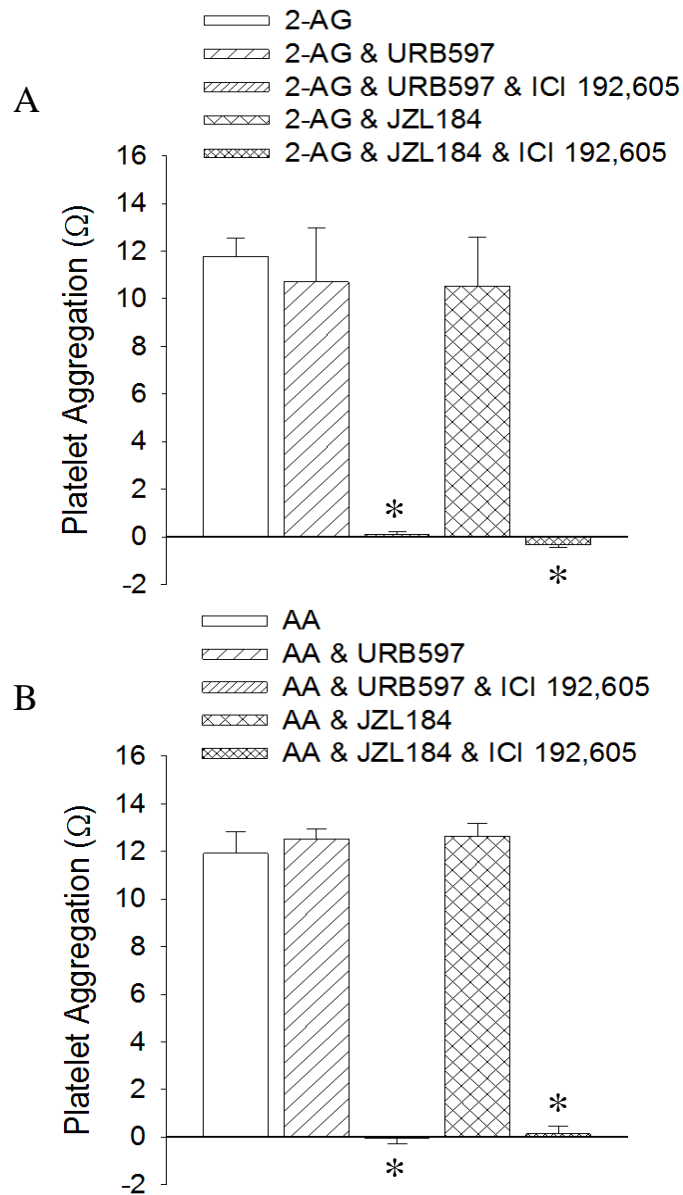


Figure 5.7: Effect of URB597 (0.3 μM) and JZL184 (0.1 μM) alone and in combination with ICI 192,605 (1 μM) on the aggregation response to **A**) 2-AG (150 μM ; n=6) and **B**) arachidonic acid (75 μM ; n=6). AA; arachidonic acid. Aggregation to 2-AG and arachidonic acid was measured at 10 minutes after addition of the agonist. Data are expressed as mean \pm s.e.m. * $p < 0.05$ vs. agonist alone, Kruskal-Wallis test.

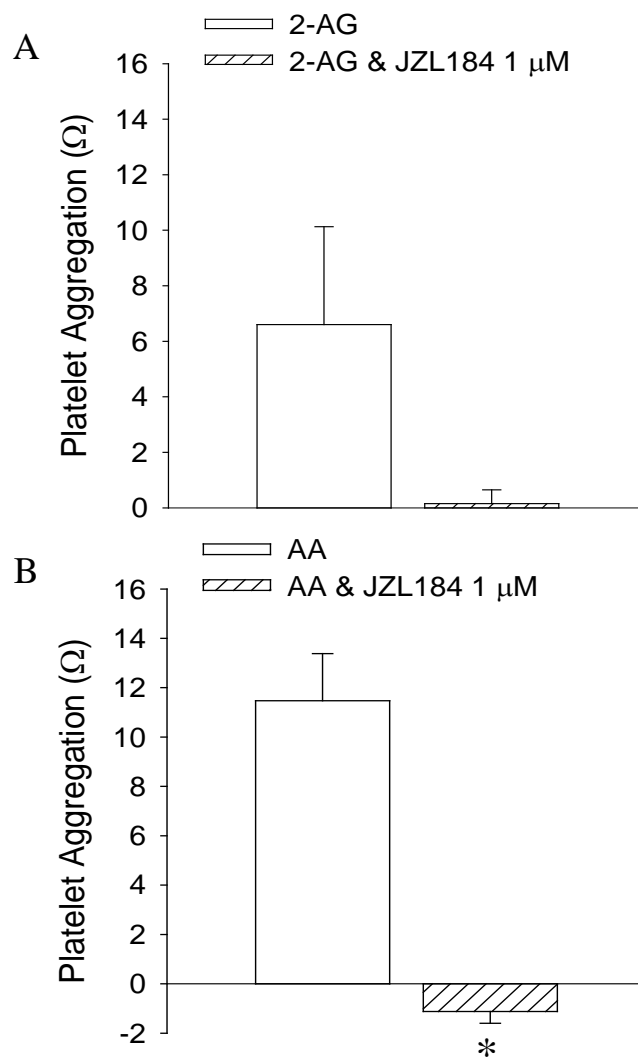


Figure 5.8: Effect of JZL184 (1 μM) on platelet aggregation induced by **A)** 2-AG (150 μM; n=5) and **B)** arachidonic acid (75 μM; n=4). AA; arachidonic acid. Aggregation to 2-AG and arachidonic acid was measured at 10 minutes after addition of the agonist. Data are expressed as mean ± s.e.m. * p<0.05 vs. agonist alone, Mann Whitney test.

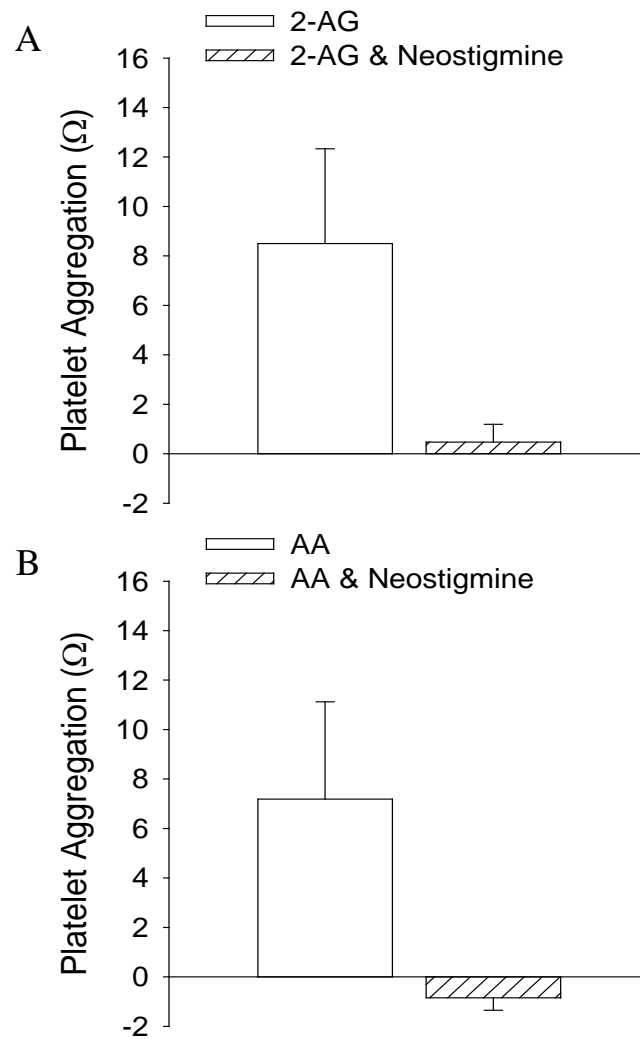


Figure 5.9: Effect of neostigmine (1 μM) on the aggregation response to **A**) 2-AG (150 μM ; n=4) and **B**) arachidonic acid (75 μM ; n=4). AA; arachidonic acid. Aggregation to 2-AG and arachidonic acid was measured at 10 minutes after addition of the agonist. Data are expressed as mean \pm s.e.m. Agonist response in presence and absence of inhibitor compared using Mann Whitney test.

figure 5.10. Arachidonic acid (38 μM) and 2-AG (75 μM) alone produced small aggregation responses. Combination of 2-AG or arachidonic acid with ADP (1 μM) caused significant potentiation of the ADP response.

Potentiation of the ADP response by 2-AG was prevented by flurbiprofen (10 μM) but was not significantly reduced by indomethacin at 10 μM (**figure 5.11A**). Incubation with indomethacin at 3 μM caused a small but statistically significant increase in the 2-AG response, however, a similar effect was not observed with the higher concentration of indomethacin. The thromboxane receptor antagonist, ICI 192,605, appeared to reduce the extent of potentiation of the ADP response by 2-AG at 10 minutes, however, this effect just failed to achieve significance ($p=0.0608$; **figure 5.11A**). Arachidonic acid potentiated the response to ADP at 10 minutes. This potentiation was prevented by flurbiprofen but was not significantly affected by either concentration of indomethacin or ICI 192,605 (**figure 5.11B**).

5.5 Discussion

The current study examined the effect of 2-AG and several physiological agonists; ADP, arachidonic acid and collagen, on platelet aggregation in rat whole blood. ADP (0.1-30 μM), arachidonic acid (19-300 μM) and collagen (0.3-10 $\mu\text{g/ml}$) produced concentration-dependent platelet aggregation with maximal responses at 3 μM for ADP, 75 μM for arachidonic acid and 10 $\mu\text{g/ml}$ for collagen. The concentration response curves for ADP and collagen are in agreement with previous data in rat whole blood (Kurata *et al.*, 1995; Lad *et al.*, 1987). Higher concentrations of arachidonic acid were required to produce platelet aggregation in this study

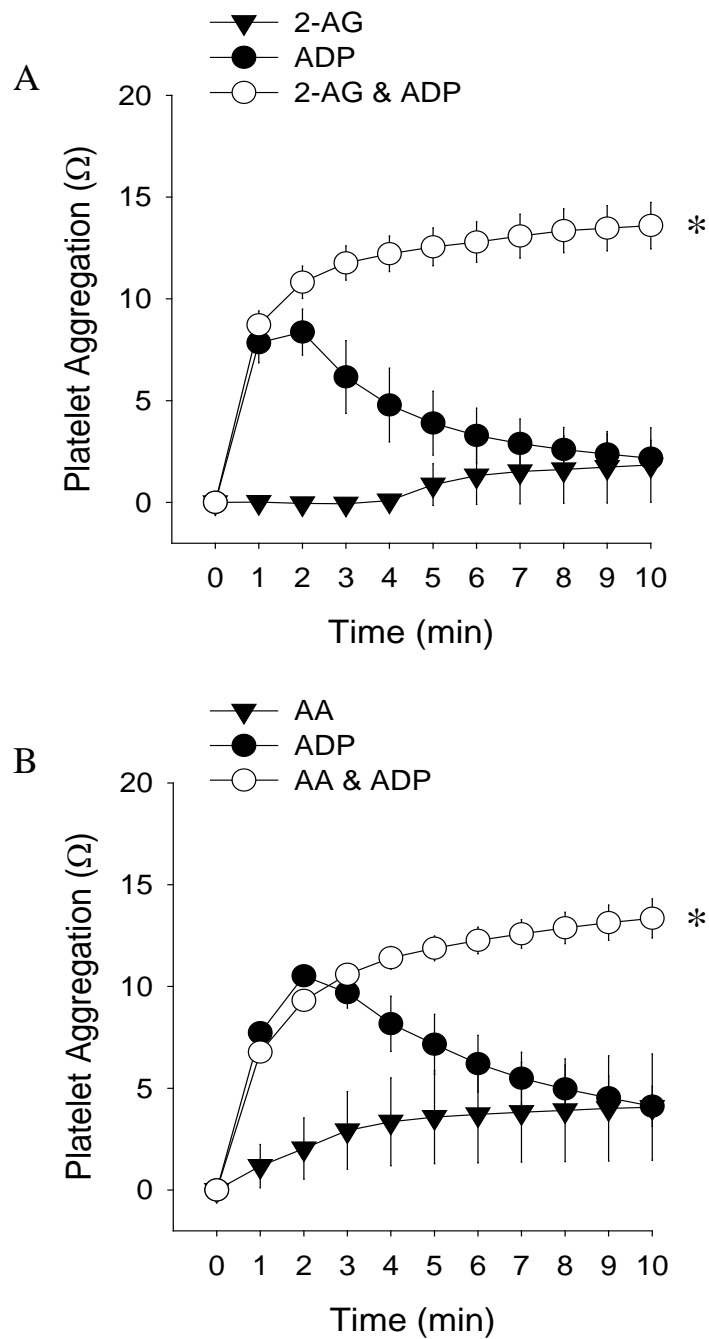


Figure 5.10: Aggregation induced by **A)** 2-AG (75 μM ; $n=7$) and **B)** arachidonic acid (38 μM ; $n=6$) added alone or in combination with ADP (1 μM). AA; arachidonic acid. Data are expressed as mean \pm s.e.m. * $p < 0.05$ vs. 2-AG, arachidonic acid and ADP alone, areas under the curve compared using Friedman analysis.

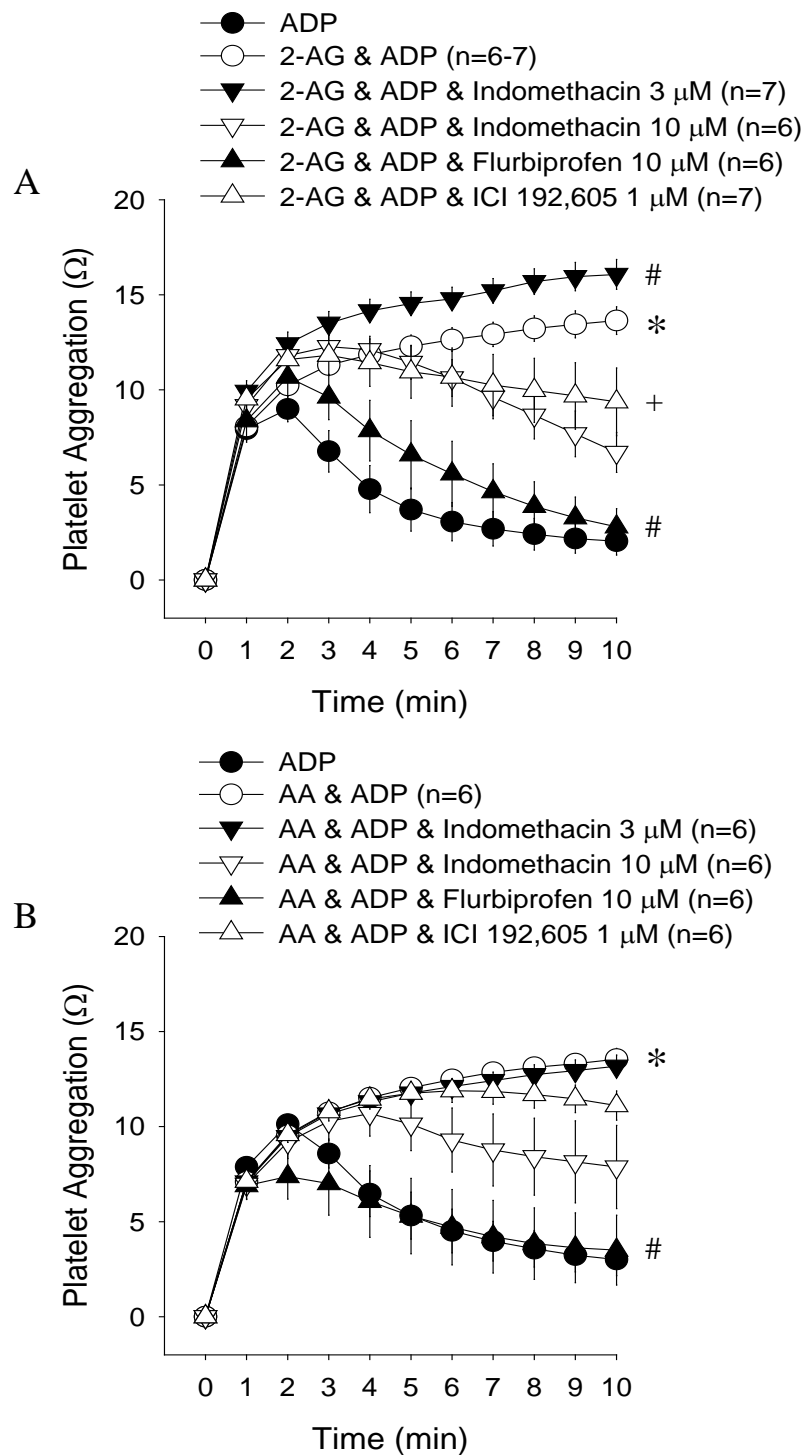


Figure 5.11: Effect of indomethacin (3 μ M and 10 μ M), flurbiprofen (10 μ M) and ICI 192,605 (1 μ M) on the interaction of **A**) 2-AG (75 μ M) and **B**) arachidonic acid (38 μ M; n=6) with ADP (1 μ M). AA; arachidonic acid. Data are expressed as mean \pm s.e.m. * p<0.05 vs. ADP alone, # p<0.05 vs. 2-AG or arachidonic acid in combination with ADP. + p=0.0608 vs. 2-AG and ADP in combination, areas under the curve compared using Friedman analysis.

compared to a previous study in rat whole blood (EC_{50} of $11.2 \pm 1.3 \mu\text{M}$) (Lad *et al.*, 1987). This difference in potency may be related to the methods used to measure platelet aggregation in these experiments. The previous study measured the extent of platelet aggregation by calculating the decrease in the platelet count following addition of the aggregating agent.

In the current study, 2-AG produced slowly developing platelet aggregation which peaked at 10 minutes. This gradual aggregation response is similar to that observed with arachidonic acid. In contrast, ADP produced rapid platelet aggregation which peaked at 1 minute and then began to disaggregate. This study also demonstrated that combination of 2-AG and ADP resulted in prolongation of the aggregation response to ADP. A similar interaction was observed between arachidonic acid and ADP. This effect of arachidonic acid and ADP in combination has not been described previously. 2-AG is likely to modify the aggregation response to ADP by enhancing the release of pro-aggregatory mediators which further amplify the response resulting in irreversible aggregation. The interaction of 2-AG and ADP in this study contradicts previous work in human platelet-rich plasma in which both 2-AG and ADP produced a reversible increase in platelet activation and combination of these agonists abolished the response (Maccarrone *et al.*, 2001). The difference in these results may be related to the preparation studied as whole blood contains other blood cells which may modify the platelet response.

The current study confirmed the previous finding (Shearer *et al.*, 2009) that 2-AG is pro-aggregatory in rat whole blood at micromolar concentrations (75-300 μM). In

contrast, it was previously demonstrated that the other main endocannabinoid, anandamide, does not produce platelet aggregation in rat whole blood at concentrations up to 30 μM and had no effect on the aggregation response to other agonists, such as ADP and 5-HT (Shearer *et al.*, 2009). 2-AG produced platelet aggregation in a concentration-dependent manner with maximal aggregation at 300 μM and little or no response at 19-38 μM . A similar concentration-response curve was observed with arachidonic acid. 2-AG-induced aggregation was highly variable with differences in the rate and extent of the response between individuals. 2-AG at 75 μM produced inconsistent platelet aggregation with some animals responding strongly, whereas, others showed no response. At higher concentrations all animals responded but there was variation in the rate and extent of the response. This variability was only observed with 2-AG, the physiological agonists, arachidonic acid and ADP, produced consistent platelet aggregation. The relatively high concentrations of 2-AG required to produce platelet aggregation in this study are similar to those used in human whole blood and platelet-rich plasma, in these preparations 2-AG produced a maximal response at 200 μM (Keown *et al.*, 2010; Maccarrone *et al.*, 2001). A previous study in human platelets identified a high intracellular concentration of 2-AG (up to 1.4 mM) (Maccarrone *et al.* 2001). As such, the high concentrations of 2-AG used in this study and in human whole blood and platelet-rich plasma may be considered physiologically relevant. In washed human platelets 2-AG produced platelet aggregation at lower concentrations with a maximal response at 10 μM (Baldassarri *et al.*, 2008). The lower potency of 2-AG in whole blood and platelet-rich plasma may be due to instability of 2-AG in plasma or a buffering effect of plasma proteins. 2-AG has been shown to be particularly labile

in rat plasma (half-life of 1 minute vs. 16 minutes in human plasma) due to rapid metabolism by plasma esterases (Kozak *et al.*, 2001). These findings emphasise the influence that platelet preparation and species can have on the aggregation response.

In this study 2-AG-induced platelet aggregation was sensitive to a CB₂ antagonist at 1 and 3 µM. However, the CB₁ antagonist AM251 did not reduce the response to 2-AG significantly at either concentration studied. These antagonists did not affect the response to ADP or arachidonic acid at either concentration. In contrast, in additional experiments the potent synthetic CB₁/CB₂ agonist HU-210 did not cause platelet aggregation at concentrations up to 100 nM. Interpretation of the effects of cannabinoid receptor antagonists can be difficult due to the complicated pharmacology of these compounds. AM251 and AM630 are potent antagonists which act as inverse agonists at CB₁ and CB₂ receptors, respectively (Pertwee, 2005; Ross *et al.*, 1999). At high micromolar concentrations these antagonists can bind non-selectively to both cannabinoid receptors and other receptor types, such as oestrogen receptors, to exhibit non-specific effects (Landsman *et al.*, 1998; New and Wong, 2003; Fiori *et al.*, 2011). There is conflicting data in the literature regarding the role of cannabinoid receptors in 2-AG-induced platelet aggregation. Previous work in human platelet-rich plasma showed equal inhibition of the 2-AG response by CB₁ and CB₂ antagonists, SR141716 and SR144528 (IC₅₀ 5 ± 1 µM) (Maccarrone *et al.*, 2001). In contrast, CB₁ and CB₂ antagonists had no effect on 2-AG-induced aggregation in human whole blood (Keown *et al.*, 2010) and only inhibited washed platelets at a concentration above their known selectivity for cannabinoid receptors (Baldassarri *et al.*, 2008). The authors of these studies concluded that 2-AG produces

platelet aggregation through activation of an as yet unidentified cannabinoid receptor. This conclusion was supported by immunoblot and polymerase chain reaction (PCR) experiments which failed to detect CB₁ and CB₂ receptor protein or mRNA in human platelets (Baldassarri *et al.*, 2008).

2-AG and arachidonic acid produced a similar gradual aggregation response and concentration-response curve. Interestingly, the addition of 2-AG was followed by a lag period of ~2-3 minutes prior to a measurable aggregation response. This lag period was not observed following the addition of arachidonic acid. This observation suggests that 2-AG may need to be metabolised to form a pro-aggregatory substrate in order to produce platelet aggregation. This proposal is supported by experiments using inhibitors of COX metabolism and a thromboxane receptor antagonist. Platelet aggregation in response to 2-AG and arachidonic acid was inhibited by COX inhibitors, indomethacin (10 µM) and flurbiprofen, and abolished by the thromboxane receptor antagonist ICI 192,605. This data suggests that 2-AG-induced platelet aggregation involves metabolism of arachidonic acid via COX and formation of thromboxane A₂. These results are in agreement with data from human whole blood and washed platelets (Keown *et al.*, 2010; Baldassarri *et al.*, 2008), although, an earlier study in human platelet-rich plasma did not show any sensitivity of the 2-AG response to the COX inhibitor aspirin (Maccarrone *et al.*, 2001). It is of interest to note that the lower concentration of indomethacin (3 µM) reduced the response to 2-AG but did not affect arachidonic acid. Indomethacin has been shown to inhibit COX in rat whole blood with an IC₅₀ of 7.0 ± 1.2 µM (Lad *et al.*, 1987). As such, indomethacin at 3 µM may produce insufficient COX inhibition to significantly

affect the response to arachidonic acid. The reason for the different effect of indomethacin (3 μM) on 2-AG and arachidonic acid-induced platelet aggregation is not known. In additional experiments indomethacin (10 μM) and flurbiprofen were used to confirm the role of COX metabolism in the aggregation response to 2-AG and arachidonic acid. The effect of the higher concentration of indomethacin and flurbiprofen on the ADP response has not been examined. It is possible that these antagonists may affect the ADP response through inhibition of the release reaction during the second phase of platelet aggregation (Armstrong *et al.*, 1985). However, as ADP can produce platelet aggregation through several mechanisms inhibition of COX may not influence the overall aggregation response. This proposal is supported by the absence of any inhibition of the ADP response by the thromboxane receptor antagonist ICI 192,605.

The mechanism responsible for the metabolism of 2-AG to form arachidonic acid was investigated. The fatty acid amide hydrolase and monoacylglycerol lipase inhibitors URB597 and JZL184 at 0.3 μM and 0.1 μM , respectively, did not cause a significant reduction in the response to 2-AG or arachidonic acid. JZL184 produces time-dependent inhibition of monoacylglycerol lipase (80% maximal at 40 minutes) (Kathuria *et al.*, 2003). It is possible that the efficacy of JZL184 at 0.1 μM may be reduced by the low concentration or short incubation period (10 minutes) used. As such, the experiment was repeated using a higher concentration of JZL184 (1 μM) and extending the incubation period to 30 minutes. JZL184 (1 μM) significantly reduced the response to arachidonic acid and appeared to reduce 2-AG-induced aggregation; however, the effect on the 2-AG response was not significant. These

experiments were performed in a small number of animals (n=4) and the control response, especially for 2-AG, was variable as shown by the large error bars. As such, analysis of this data has a low statistical power and is unlikely to identify any differences between groups. It is unlikely that 2-AG produces platelet aggregation through metabolism of this mediator by fatty acid amide hydrolase or monoacylglycerol lipase to form arachidonic acid. This conclusion is in contrast with previous studies in human platelets which have shown inhibition of the 2-AG response by the monoacylglycerol lipase inhibitor URB602 (300 μ M; IC₅₀ of 75 μ M) (Keown *et al.*, 2010; Vandevoorde *et al.*, 2007). However, this inhibition was not observed with the more potent monoacylglycerol lipase inhibitor, N-arachidonyl maleimide (NAM) (up to 3 μ M; IC₅₀ of 140 nM) (Baldassarri *et al.*, 2008; Saario *et al.*, 2005). This experiment also suggests that JZL184 may not be entirely selective for monoacylglycerol lipase and can inhibit the aggregation response to arachidonic acid at micromolar concentrations.

2-AG has been shown to be highly labile in rat plasma (half-life of 1 minute vs. 16 minutes in human plasma) (Kozak *et al.*, 2001). This represents an important species difference between rat and human plasma. There are considerable differences in plasma esterases between species. There is higher esterase activity in rat whole blood compared to humans (100-400 times higher in rat) (Minagawa *et al.*, 1995). Rat plasma also contains carboxylesterases which are not found in human plasma (Li *et al.*, 2005). In this study, neostigmine, a selective cholinesterase inhibitor, was used to examine the involvement of plasma esterases in 2-AG-induced platelet aggregation. Spontaneous degradation of 2-AG in the plasma will produce

arachidonic acid which may cause platelet aggregation through COX metabolism and formation of thromboxane A₂. Neostigmine (1 μM) appeared to reduce the aggregation response to 2-AG and arachidonic acid; however, this effect did not reach significance. As with JZL184, the non-significant effect of neostigmine may be associated with the small sample number and low statistical power of this analysis. This finding suggests that 2-AG spontaneously breaks down in rat whole blood to form arachidonic acid which can produce platelet aggregation. This process can complicate interpretation of results from aggregometry experiments in whole blood as this mechanism does not reflect a direct effect of 2-AG on platelets and would not be observed in washed platelets. The reason for inhibition of the arachidonic acid response by neostigmine is unclear. A previous study has demonstrated that reactivation of acetylcholinesterases can inhibit arachidonic acid-induced aggregation in human platelet-rich plasma (Jun *et al.*, 2006).

The interaction of 2-AG and ADP was reduced by the thromboxane receptor antagonist ICI 192,605 and prevented by the COX inhibitor flurbiprofen. Potentiation of the ADP response by arachidonic acid was similarly prevented by flurbiprofen but no inhibition was observed with ICI 192,605. This suggests that the agonist interactions involved enhanced secretion of a pro-aggregatory prostanoid produced through COX metabolism. It is unclear why the interaction of arachidonic acid and ADP is sensitive to COX inhibition but not the thromboxane receptor antagonist ICI 192,605. The agonist interactions were more sensitive to COX inhibition by flurbiprofen compared to indomethacin. This effect was not related to differences in the potency of these inhibitors. Flurbiprofen may produce greater

inhibition of the aggregation response through its actions on NOS which result in enhanced synthesis and release of nitric oxide from leukocytes (De La Cruz *et al.*, 2010). This effect has not been shown with indomethacin (Fierro *et al.*, 1999). This effect may also account for inhibition of the interaction of arachidonic acid and ADP by flurbiprofen which is not caused by reduced production of thromboxane A₂. Indomethacin at 3 μ M had the opposite effect to ICI 192,605 on the interaction of 2-AG and ADP resulting in a small increase in the aggregation response. This increase was not observed with the higher concentration of indomethacin which showed a trend towards inhibition. This implies that the interaction of 2-AG and ADP involves production of anti-aggregatory prostanoids which can inhibit the aggregation response. The production of anti-aggregatory prostanoids may be more sensitive to the COX inhibitor indomethacin at 3 μ M. Additional experiments are required to assess the involvement of additional mechanisms in the agonist interactions.

Whole blood represents the most physiological preparation used to study the aggregatory effects of 2-AG. Platelets and leukocytes are known to express cannabinoid receptors and are involved in the synthesis and metabolism of endocannabinoids. As such, it is possible that leukocytes may be able to modulate the response to 2-AG and its interactions with other agonists. Additionally, spontaneous breakdown of 2-AG in plasma to form arachidonic acid will result in production of pro-aggregatory prostanoids which will contribute to the aggregation response in whole blood. In summary, whole blood aggregometry allows the aggregatory effects of 2-AG to be studied in the presence of plasma and other cell types which can

influence the effect of 2-AG on platelets. Thus, this preparation can be considered to provide more accurate information on the likely effect of 2-AG on platelet aggregation *in vivo* compared to platelet-rich plasma or washed platelets.

In conclusion, 2-AG is pro-aggregatory in rat whole blood and interacts with ADP to enhance platelet aggregation. 2-AG produces aggregation through CB₂ receptor-mediated activation of phospholipase A₂ which promotes the release of arachidonic acid from the phospholipid membrane and production of thromboxane A₂ via COX. Metabolism by COX and formation of thromboxane A₂ are also involved in mediating the interaction of 2-AG and ADP.

CHAPTER 6

GENERAL DISCUSSION

6.1 Novel Findings

The main novel findings in this thesis are that both anandamide and 2-AG can modify either injury volume or topography at 4 hours after middle cerebral artery occlusion. Exogenous anandamide and the metabolism inhibitor URB597 changed the topography of the injury with reduced cortical and increased subcortical injury. In contrast, 2-AG and the metabolism inhibitor JZL184 exacerbated injury development with greater injury observed in the cortex. Treatment with JZL184 also increased total injury volume at 4 hours post-occlusion. However, neither anandamide nor 2-AG caused a significant change in microglia number or activation following injury. This thesis also demonstrated for the first time that 2-AG is pro-aggregatory in rat whole blood at micromolar concentrations and can potentiate the aggregation response to ADP. In these experiments 2-AG-induced aggregation was shown to be mediated through activation of CB₂ receptors and production of arachidonic acid via COX metabolism.

6.2 Was a Model of Transient Cerebral Ischaemia Established?

In the initial stage of this work several attempts were made to establish a reproducible rat model of transient cerebral ischaemia. Unfortunately, these experiments were complicated by variable injury development, high mortality and severe functional deficits during the recovery period. This work examined several experimental protocols; including different ventilation settings, 100% oxygen or 30% oxygen:70% nitrous oxide, and varying duration of occlusion and reperfusion. In these experiments it was shown that the severity of the neurological deficits and post-operative mortality were related to the duration of the occlusion period. It was

also demonstrated that the ventilation settings used in each experiment could affect physiological parameters, such as blood gases and blood pressure, and influenced injury development and post-operative mortality. In the 4 hour permanent middle cerebral artery occlusion studies physiological parameters were continuously monitored during the surgery and occlusion period to establish the appropriate ventilation settings necessary to maintain normal physiological blood gases. These settings were used in the final transient middle cerebral artery occlusion study and resulted in improved survival to the 24 hour end-point and reduced neurological deficits. However, due to time limitations this study was not continued and this protocol has not been used for the study of endocannabinoids.

This work demonstrates the importance of using appropriate ventilation settings for each animal and monitoring as many physiological parameters as possible in order to maintain normal physiological measurements. Proper control of physiological parameters within the normal range is essential to produce a reproducible animal model of cerebral ischaemia in which to study potential therapeutic agents. The use of a combined pulse-oximeter / capnograph is a useful technique for non-invasive monitoring of artificially ventilated animals providing continuous measurements of oxygen saturation and end-tidal carbon dioxide. The non-invasive nature of this technique makes it ideal for monitoring physiological parameters in transient cerebral ischaemia models involving recovery where invasive monitoring would not be possible. A pulse-oximeter / capnograph can provide a reasonably accurate indication of blood gas values, described in chapter 4, and can identify potential problems with the ventilation settings or anaesthesia. These conclusions are

supported by guidelines from the Stroke therapy academic and industry roundtable (STAIR) which stated that physiological parameters, including blood pressure, temperature, blood gases and blood glucose, should be routinely monitored in animal models of cerebral ischaemia to improve the reliability of these models (Fisher, 2009).

6.3 Do Endocannabinoids Modify Injury Development in Acute Cerebral Ischaemia?

Endocannabinoid treatment modified injury development as measured at 4 hours after middle cerebral artery occlusion. These effects are not in line with the initial hypothesis that endocannabinoids could exert a neuroprotective effect and reduce injury development at 4 hours after middle cerebral artery occlusion. Exogenous anandamide and the metabolism inhibitor URB597 exerted a limited protective effect in this model. Anandamide did not reduce total injury volume but did modify injury topography with a reduction in cortical injury and a corresponding increase in the subcortical tissue. The absence of a reduction in total injury volume may be related to the early time-point studied post-occlusion or the cerebral ischaemia model used (permanent vs. transient). In contrast to the initial hypothesis and effect of anandamide treatment, 2-AG and JZL184 exacerbated cortical injury development while the metabolism inhibitor JZL184 alone increased total injury volume. The opposing effects of anandamide and 2-AG on injury development may be influenced by the different route of administration and treatment protocol (s.c. bolus vs. i.v. infusion, respectively) used in these studies. Administration of 2-AG (i.v.) may produce more potent cardiovascular effects compared to other routes of

administration and affected injury development following cerebral ischaemia. As such, the differences in the treatment protocols can make it difficult directly compare the results of these studies. In retrospect, it may have been better to give anandamide and URB597 as an i.v. infusion to limit the possible influence of the route of administration. These findings emphasise the importance of proper experimental design. As part of a complete body of work, the anandamide and 2-AG studies (chapters 3 and 4) should have been designed together to minimise differences between the experimental protocols and allow easier comparison of results.

6.4 Do Endocannabinoids Modify Haemodynamic Measurements and Cerebral Blood Flow During Acute Cerebral Ischaemia?

Exogenous anandamide and 2-AG have previously been shown to produce widespread vasodilation *in vivo* following i.v. administration (Lake *et al.*, 1997; Járαι *et al.*, 2000). Exogenous anandamide (i.p.) produced a small transient reduction in blood pressure following administration. Treatment with exogenous anandamide and URB597 did not produce a significant change in heart rate or cerebral blood flow. The absence of a significant effect of anandamide on haemodynamic measurements may be due to the route of administration used in these experiments. In contrast, exogenous 2-AG and JZL184 (i.v.) produced a significant reduction in cerebral blood flow but did not affect haemodynamic measurements during the occlusion period compared to vehicle treated animals. This change in cerebral blood flow may explain the increase in cortical injury volume in these animals as a reduction in blood flow to the penumbra would result in expansion of the injury boundary.

6.5 Do Endocannabinoids Modify the Microglia Response Following Injury in Acute Cerebral Ischaemia?

A significant part of this thesis focused on examining the effect of endocannabinoid treatment on the response of microglia following middle cerebral artery occlusion. In the anandamide study microglia number was not increased in any of the treatment groups at 4 hours post-occlusion. In contrast, in the 2-AG study microglia number was increased in the ipsilateral hemisphere in untreated and vehicle (PEG-300) treated animals. Interestingly, there was no increase in microglia number in the ipsilateral hemisphere in animals receiving 2-AG and JZL184 compared to the corresponding contralateral region. The difference in the effect of injury on microglia number in the vehicle treated groups in the anandamide and 2-AG studies is unclear. As different vehicles were administered in these studies, tocrisolve and 5% DMSO in the anandamide study and PEG-300 in the 2-AG study, it is possible that the difference in the effect of injury on microglia number may be caused by the specific vehicle used. It has been shown that DMSO administration can be protective in cerebral ischaemia (discussed in **section 6.7**) and, as such, may influence the microglia response following injury. This finding emphasises the importance of including a group of animals which did not receive any treatment to exclude possible vehicle effects.

In the anandamide and 2-AG studies microglia activation was increased in the ipsilateral hemisphere vs. contralateral in all groups following middle cerebral artery occlusion. Anandamide and URB597 produced greater microglia activation in the ipsilateral hemisphere vs. contralateral at the level of the globus pallidus. This was a

small effect which was only observed at one of the coronal levels examined. This effect is most likely due to reduced microglia activation in the contralateral hemisphere in anandamide and URB597 treated animals compared to the vehicle rather than an increase in microglia activation in the ipsilateral hemisphere. In contrast, neither 2-AG nor JZL184 treatment caused any change in microglia number or the extent of microglia activation in the ipsilateral hemisphere following injury.

6.6 Do Endocannabinoids Produce Platelet Aggregation in Rat Whole Blood?

This thesis has for the first time characterised the aggregatory effect of endocannabinoids in rat whole blood. This work demonstrated that the endocannabinoid 2-AG produced aggregation in rat whole blood at high micromolar concentrations (75-300 μ M). This response was similar to that observed in human whole blood (Keown *et al.*, 2010) and platelet-rich plasma (maximal at 200 μ M) (Maccarrone *et al.*, 2001). 2-AG produced slowly developing platelet aggregation which peaked at 10 minutes through activation of CB₂ receptors and COX metabolism. 2-AG also interacted with the physiological agonist ADP to potentiate the aggregatory response through COX metabolism. In contrast, anandamide did not produce platelet aggregation at concentrations up to 30 μ M and did not modify the response to other agonists, such as ADP and 5-HT (Shearer *et al.*, 2009).

6.7 Potential Limitations

There are several limitations in the studies described in this thesis. The primary limitation in all of these studies is the inherent difficulty in working with endocannabinoids. Endocannabinoids are highly lipophilic compounds which do not

readily dissolve in aqueous solvents. Most stock solutions were formed in non-aqueous solvents and diluted with saline immediately prior to use. As such, the use of endocannabinoids is often complicated by high solvent concentrations which may exert biological effects. In aggregometry experiments the highest concentration of ethanol vehicle used (0.4% ethanol f.b.c) reduced the aggregation response to the physiological agonist ADP. Due to these biological effects the high solvent concentrations can limit the range of endocannabinoid concentrations which can be studied. The solvent used has been shown to be of particular importance in models of cerebral ischaemia. Ethanol administration exacerbated infarct and oedema development (Zhao *et al.*, 1997; Shapira *et al.*, 1997), whereas, DMSO reduced infarct volume following cerebral ischaemia (Bardutzky *et al.*, 2005). DMSO (5%) was used as a vehicle for the anandamide metabolism inhibitor URB597 and may have influenced injury development or the microglia response after middle cerebral artery occlusion. It is not possible to clarify the effect of DMSO in these animals as a group that underwent middle cerebral artery occlusion without treatment was not included in this study. PEG, which was used as the vehicle in the 2-AG study, has been shown to be neuroprotective in animal models of spinal cord and traumatic brain injury (Baptiste *et al.*, 2009; Luo *et al.*, 2004; Borgens and Bohnert, 2001; Koob *et al.*, 2008). As such, it is necessary to include an additional group that underwent middle cerebral artery occlusion without treatment in order to exclude any effect of the vehicle. In contrast to previous studies, in the 2-AG study PEG alone did not exert a neuroprotective effect on injury volume at 4 hours post-occlusion compared to untreated animals. In summary, findings in other studies have emphasised the importance of the choice of vehicle and the necessity of including

animals that receive no treatment, where required, to exclude possible effects of the vehicle.

Endocannabinoids are rapidly metabolized *in vivo* and have been shown to be extremely labile in rat plasma (Kozak *et al.*, 2001). The instability of endocannabinoids, particularly 2-AG, in rat plasma can complicate the use of rats as an animal model in which to study these compounds. Due to the highly labile nature of 2-AG the experimental protocol in the cerebral ischaemia study was designed to include direct i.v. administration and continuous infusion of the treatment to ensure that the exogenous 2-AG can reach the desired tissue. However, i.v. administration may affect the experimental outcome through direct effects of 2-AG on the cardiovascular system. Degradation of endocannabinoids *in vivo* also produces active metabolites which can exert several biological effects and may influence the outcome of these experiments.

The acute cerebral ischaemia studies used a rat model of 4 hour permanent middle cerebral artery occlusion to investigate the effect of endocannabinoids. This model has the benefit of allowing invasive monitoring to examine the cardiovascular effects of endocannabinoids throughout the experimental period. As described previously, monitoring of physiological measurements is important as these parameters can influence injury development in cerebral ischaemia. However, the use of this model limits the histological end-points which can be examined to early injury development and the acute inflammatory response. At this early time-point it is not possible to determine if changes in injury volume or topography represent an actual effect or,

simply, a delay in injury development. Permanent middle cerebral artery occlusion performed in this model may limit the ability of the treatment to enter the ischaemic region as perfusion of this tissue will be dependent on collateral blood vessels. Middle cerebral artery occlusion studies are also very demanding in terms of the cost and time required to perform these experiments. These considerations limit the number of groups which can be included in each study.

Aggregation studies were performed in rat whole blood. This preparation is considered to be more physiological, in comparison to platelet-rich plasma, as red blood cells and leukocytes are present at physiological concentrations. However, in whole blood there are several different cell types which can degrade and release anti- or pro-aggregatory mediators and may influence the aggregation response. As such, it is not possible to identify platelet-specific effects involved in the aggregation response in whole blood. This is particularly relevant in the study of endocannabinoids as leukocytes express both CB₁ and CB₂ receptors and can metabolise these mediators through fatty acid amide hydrolase to produce arachidonic acid (Randall, 2007). Additionally, as these studies are performed *in vitro* using small aliquots of blood it is not possible to determine if the aggregatory effect of 2-AG described in this thesis is physiologically relevant *in vivo*, especially as rapid degradation in plasma and cellular metabolism will reduce the concentration present.

6.8 Future Work

The current work has demonstrated that endocannabinoids can influence injury

development at 4 hours after cerebral ischaemia. In these studies the endocannabinoids and appropriate metabolism inhibitors produced a similar pattern of effects in cerebral ischaemia. However, high pressure liquid chromatography (HPLC) analysis of brains from treated animals is required to confirm successful treatment and enhancement of endocannabinoid levels in the brain by metabolism inhibitors. This technique will also allow comparison of endocannabinoid concentrations in the brain following administration of exogenous endocannabinoids and metabolism inhibitors. This experiment may identify differences in the 2-AG concentration in the brain present in 2-AG and JZL184 treated animals and explain the difference in the effect of these treatments on total injury volume. These studies examined the effect of the endocannabinoids anandamide and 2-AG and metabolism inhibitors on injury at 4 hours after permanent middle cerebral artery occlusion and investigated the mechanisms involved. Future studies should investigate the effect of these drugs on injury development and the inflammatory response at a later time-point after middle cerebral artery occlusion. These studies should also examine the effect of the time-point when treatment is administered (pre- or post-occlusion) and compare transient and permanent cerebral ischaemia models. Future studies should include an additional treatment group which will receive anandamide or 2-AG in combination with the corresponding metabolism inhibitor. This protocol may enhance the effect of the endocannabinoids in cerebral ischaemia compared to administration of the exogenous endocannabinoid alone.

In the current study, 2-AG was administered i.v. and exerted a pronounced effect on cerebral blood flow. Additional experiments should be performed to compare

different routes of administration, including i.v. vs. i.p. This information will be important for future experiments as vessel cannulation for i.v. administration is not feasible in animal models that involve recovery from anaesthesia. This study demonstrated that 2-AG produced platelet aggregation in rat whole blood. It is possible that 2-AG may exert pro-aggregatory effects *in vivo* which could promote the development of thrombi in the cerebral vasculature and exacerbate injury development. To establish the involvement of 2-AG-induced aggregation in mediating the effect of 2-AG and JZL184 on injury after cerebral ischaemia immunohistochemistry should be performed in brain sections from these treatment groups to examine microthrombi formation. Platelet aggregates may be identified in sectioned tissue using platelet membrane surface markers, including fibrinogen receptor complex GP IIb/IIIa (CD41/CD61) (Denes *et al.*, 2010; Galindo *et al.*, 2009). Platelet activation may also be identified by co-expression of membrane surface markers and markers of activation, such as CD62 (P-selectin) which is released from α -granules and expressed on the surface of activated platelets (Burdess *et al.*, 2012; Winocour *et al.*, 1992).

6.9 Clinical Relevance

In an animal model of cerebral ischaemia there was a change in cannabinoid receptor expression, increased CB₁ and reduced CB₂ receptors, and increased anandamide concentrations in the brain within a few hours of injury (Muthian *et al.*, 2004). Several studies in animal models have also demonstrated that both synthetic and endogenous cannabinoids can affect injury development following cerebral ischaemia. In human patients a recent study has shown an increase in the

concentration of anandamide in plasma at ~6 hours after cerebral ischaemia in comparison to healthy volunteers (Naccarato *et al.*, 2010). This finding supports the involvement of the endocannabinoid system in cerebral ischaemia, as described previously in animal models. Endocannabinoids can exert numerous physiological effects, including neurological and cardiovascular effects and immunomodulation, which may influence injury development in cerebral ischaemia. This work suggests that endocannabinoids represent an important area of study in the pathophysiology of cerebral ischaemia. Currently, further work is required to provide more information on the role of endocannabinoids in cerebral ischaemia. This information will be essential for the development of future therapies.

This thesis supports a role for endocannabinoids in the pathophysiology of cerebral ischaemia. The endocannabinoid mediators studied exerted opposing effects on injury development in acute cerebral ischaemia. Anandamide produced a small reduction in the extent of cortical injury, whereas, 2-AG and JZL184 increased cortical injury and JZL184 also increased total injury volume. Anandamide treatment had a limited effect on injury at 4 hours post-occlusion and, as such, it is necessary to examine the effect of anandamide on injury development at a later time-point to confirm a neuroprotective effect and identify the mechanisms involved. It is possible that the difference in the effect of these mediators may be related to the route of administration used, or the receptor selectivity or mechanisms of action of the individual endocannabinoids studied. The detrimental effect of 2-AG and JZL184 on injury may be caused by a difference in the route of administration used as i.v. infusion may produce more potent cardiovascular effects through direct actions on

vascular cannabinoid receptors or pro-aggregatory effects on platelets. This finding emphasises the important role of the treatment protocol, including the route and timing of administration, and study design in influencing the experimental outcome following cerebral ischaemia. This thesis provides useful information on the potential role of the endocannabinoids, anandamide and 2-AG, in cerebral ischaemia. Further work is required to fully elucidate the mechanisms involved and identify possible targets for intervention. This information will be essential before the therapeutic potential of these mediators can be determined.

Cannabinoid based therapies have been controversial due to the neurological side effects associated with the CB₁ antagonist rimonabant which has since been withdrawn from the market. Endocannabinoid treatment may be associated with fewer side effects as these compounds are rapidly metabolised *in vivo* which will regulate their effects. However, it is still important to consider possible effects of endocannabinoids on other tissues, including the cardiovascular system, which may influence the outcome following cerebral ischaemia and could be detrimental in certain patient groups. This thesis has demonstrated that 2-AG, but not anandamide, is pro-aggregatory in rat whole blood *in vitro* and administration of 2-AG may have caused microthrombi formation *in vivo* exacerbating injury development in acute cerebral ischaemia. This pro-aggregatory effect was not observed with anandamide but remains a potential risk of endocannabinoid treatment, particularly in cerebral ischaemia which promotes a pro-thrombotic environment in the vasculature. Metabolism inhibitors are gaining attention for their therapeutic potential. These drugs act by enhancing the effects of endogenously synthesised endocannabinoids

and avoid the use of unstable exogenously administered endocannabinoids. This thesis demonstrated similar effects of exogenously administered and increased endogenous endocannabinoids using metabolism inhibitors on injury volume after acute cerebral ischaemia. This observation re-enforces the therapeutic potential of using these inhibitors to target the endocannabinoid system. However, the safety profile of endocannabinoids, particularly the pro-thrombotic effects, remains the greatest obstacle to the therapeutic use of cannabinoid based treatments.

REFERENCES

Arevalo-Martin A, Garcia-Ovejero D and Molina-Holgado E (2010). The endocannabinoid 2-arachidonoylglycerol reduces lesion expansion and white matter damage after spinal cord injury. *Neurobiol Dis* **38**(2):304-312.

Armstrong RA, Jones RL, Peesapati V, Will SG and Wilson NH (1985). Competitive antagonism at thromboxane receptors in human platelets. *Br J Pharmacol* **84**(3):595-607.

Ashton JC and Glass M (2007). The cannabinoid CB₂ receptor as a target for inflammation-dependent neurodegeneration. *Curr Neuropharmacol* **5**(2):73-80.

Baldassarri S, Bertoni A, Bagarotti A, Sarasso C, Zanfa M, Catani MV, Avigliano L, Maccarrone M, Torti M and Sinigaglia F (2008). The endocannabinoid 2-arachidonoylglycerol activates human platelets through non-CB₁/CB₂ receptors. *J Thromb Haemost* **6**(10):1772-1779.

Baptiste DC, Austin JW, Zhao W, Nahirny A, Sugita S and Fehlings MG (2009). Systemic polyethylene glycol promotes neurological recovery and tissue sparing in rats after cervical spinal cord injury. *J Neuropathol Exp Neurol* **68**(6):661-676.

Bardutzky J, Meng X, Bouley J, Duong TQ, Ratan R and Fisher M (2005). Effects of intravenous dimethyl sulfoxide on ischemia evolution in a rat permanent occlusion model. *J Cereb Blood Flow Metab* **25**(8):968-977.

Barzó P, Marmarou A, Fatouros P, Hayasaki K and Corwin F (1997). Contribution of vasogenic and cellular edema to traumatic brain swelling measured by diffusion-weighted imaging. *J Neurosurg* **87**(6):900-907.

Belayev L, Alonso OF, Busto R, Zhao W and Ginsberg MD (1996). Middle cerebral artery occlusion in the rat by intraluminal suture. Neurological and pathological evaluation of an improved model. *Stroke* **27**(9):1616-1623.

Berdyshev EV (2000). Cannabinoid receptors and the regulation of immune response. *Chem Phys Lipids* **108**(1-2):169-190.

Blackwell GJ, Flower RJ, Russell-Smith N, Salmon JA, Thorogood PB and Vane JR (1978). Prostacyclin is produced in whole blood. *Br J Pharmacol* **64**(3):436P.

Borgens RB and Bohnert D (2001). Rapid recovery from spinal cord injury after subcutaneously administered polyethylene glycol. *J Neurosci Res* **66**(6):1179-1186.

Born GV (1962a). Aggregation of blood platelets by adenosine diphosphate and its reversal. *Nature* **194**:927-929.

Born GV (1962b). Quantitative investigations into the aggregation of blood platelets. *J Physiol* **162**:67-68P.

Bronner G, Mitchell K and Welsh FA (1998). Cerebrovascular adaptation after unilateral carotid artery ligation in the rat: preservation of blood flow and ATP during forebrain ischemia. *J Cereb Blood Flow Metab* 18(1):118-121.

Burdess A, Michelsen AE, Brosstad F, Fox KA, Newby DE and Nimmo AF (2012). Platelet activation in patients with peripheral vascular disease: reproducibility and comparability of platelet markers. *Thromb Res* 129(1):50-55.

Cabral GA and Marciano-Cabral F (2005). Cannabinoid receptors in microglia of the central nervous system: immune functional relevance. *J Leukoc Biol* 78(6):1192-1197.

Cadenas E and Davies KJ (2000). Mitochondrial free radical generation, oxidative stress, and aging. *Free Radic Biol Med* 29(3-4):222-230.

Cardinal DC and Flower RJ (1980). The electronic aggregometer: a novel device for assessing platelet behavior in blood. *J Pharmacol Methods* 3(2):135-158.

Carmichael ST (2005). Rodent models of focal stroke: size, mechanism, and purpose. *NeuroRx* 2(3):396-409.

Carrier EJ, Kearns CS, Barkmeier AJ, Breese NM, Yang W, Nithipatikom K, Pfister SL, Campbell WB and Hillard CJ (2004). Cultured rat microglial cells synthesize the endocannabinoid 2-arachidonoylglycerol, which increases proliferation via a CB₂ receptor-dependent mechanism. *Mol Pharmacol* **65**(4):999-1007.

Chaitanya GV and Babu PP (2008). Activation of calpain, cathepsin-b and caspase-3 during transient focal cerebral ischemia in rat model. *Neurochem Res* **33**(11):2178-2186.

Chemin J, Monteil A, Perez-Reyes E, Nargeot J and Lory P (2001). Direct inhibition of T-type calcium channels by the endogenous cannabinoid anandamide. *EMBO J* **20**(24):7033-7040.

Cherian P, Hankey GJ, Eikelboom JW, Thom J, Baker RI, McQuillan A, Staton J and Yi Q (2003). Endothelial and platelet activation in acute ischemic stroke and its etiological subtypes. *Stroke* **34**(9):2132-2137.

Clark WM, Lessov NS, Dixon MP and Eckenstein F (1997). Monofilament intraluminal middle cerebral artery occlusion in the mouse. *Neurol Res* **19**(6):641-648.

Correa F, Hernangómez M, Mestre L, Loría F, Spagnolo A, Docagne F, Di Marzo V and Guaza C (2010). Anandamide enhances IL-10 production in activated microglia by targeting CB₂ receptors: roles of ERK_{1/2}, JNK, and NF-kappaB. *Glia* **58**(2):135-147.

Crack PJ and Taylor JM (2005). Reactive oxygen species and the modulation of stroke. *Free Radic Biol Med* **38**(11):1433-1444.

Crawley JN, Corwin RL, Robinson JK, Felder CC, Devane WA and Axelrod J (1993). Anandamide, an endogenous ligand of the cannabinoid receptor, induces hypomotility and hypothermia *in vivo* in rodents. *Pharmacol Biochem Behav* **46**(4):967-972.

Cuomo O, Pignataro G, Gala R, Scorziello A, Gravino E, Piazza O, Tufano R, Di Renzo G and Annunziato L (2007). Anti-thrombin reduces ischemic volume, ameliorates neurologic deficits, and prolongs animal survival in both transient and permanent focal ischemia. *Stroke* **38**(12):3272-3279.

Darmani NA (2002). The potent emetogenic effects of the endocannabinoid, 2-AG (2-arachidonoylglycerol) are blocked by Δ^9 -tetrahydrocannabinol and other cannabinoids. *J Pharmacol Exp Ther* **300**(1):34-42.

De la Cruz JP, Reyes JJ, Ruiz-Moreno MI, Lopez-Villodres JA, Jebrouni N and Gonzalez-Correa JA (2010). Differences in the *in vitro* antiplatelet effect of dexibuprofen, ibuprofen, and flurbiprofen in human blood. *Anesth Analg* **111**(6):1341-1346.

De Ley G, Nshimyumuremyi JB and Leusen I (1985). Hemispheric blood flow in the rat after unilateral common carotid occlusion: evolution with time. *Stroke* **16**(1):69-73.

De Petrocellis L, Cascio MG and Di Marzo V (2004). The endocannabinoid system: a general view and latest additions. *Br J Pharmacol* **141**(5):765-774.

Dénes A, Humphreys N, Lane TE, Grecis R and Rothwell N (2010). Chronic systemic infection exacerbates ischemic brain damage via a CCL5 (regulated on activation, normal T-cell expressed and secreted)-mediated pro-inflammatory response in mice. *J Neurosci* **30**(30):10086-10095.

Deng H, Han HS, Cheng D, Sun GH and Yenari MA (2003). Mild hypothermia inhibits inflammation after experimental stroke and brain inflammation. *Stroke* **34**(10):2495-2501.

Dereix L and Nighoghossian N (2008). Intracerebral haemorrhage after thrombolysis for acute ischaemic stroke: an update. *J Neurol Neurosurg Psychiatry* **79**(10):1093-1099.

Devane WA, Dysarz FA 3rd, Johnson MR, Melvin LS and Howlett AC (1988). Determination and characterization of a cannabinoid receptor in rat brain. *Mol Pharmacol* **34**(5):605-613.

Devane WA, Hanus L, Breuer A, Pertwee RG, Stevenson LA, Griffin G, Gibson D, Mandelbaum A, Etinger A and Mechoulam R (1992). Isolation and structure of a brain constituent that binds to the cannabinoid receptor. *Science* **258**(5090):1946-1949.

Di Marzo V, Bisogno T, De Petrocellis L, Melck D, Orlando P, Wagner JA and Kunos G (1999). Biosynthesis and inactivation of the endocannabinoid 2-arachidonoylglycerol in circulating and tumoral macrophages. *Eur J Biochem* **264**(1):258-267.

Dirnagl U, Iadecola C and Moskowitz MA (1999). Pathobiology of ischaemic stroke: an integrated view. *Trends Neurosci* **22**(9):391-397.

Dirnagl U and Pulsinelli W (1990). Autoregulation of cerebral blood flow in experimental focal brain ischemia. *J Cereb Blood Flow Metab* **10**(3):327-336.

Donnan GA, Fisher M, Macleod M and Davis SM (2008). Stroke. *Lancet* **371**(9624):1612-1623.

Dougherty JH Jr, Levy DE and Weksler BB (1977). Platelet activation in acute cerebral ischaemia. Serial measurements of platelet function in cerebrovascular disease. *Lancet* **1**(8016):821-824.

Durukan A and Tatlisumak T (2007). Acute ischemic stroke: overview of major experimental rodent models, pathophysiology, and therapy of focal cerebral ischemia. *Pharmacol Biochem Behav* **87**(1):179-197.

Dyszkiewicz-Korpanty AM, Frenkel EP and Sarode R. Approach to the assessment of platelet function: comparison between optical-based platelet-rich plasma and impedance-based whole blood platelet aggregation methods. *Clin Appl Thromb Hemost* **11**(1):25-35.

Ennis SR and Keep RF (2006). Effects of 2,4-dinitrophenol on ischemia-induced blood-brain barrier disruption. *Acta Neurochir Suppl* **96**:295-298.

Facchinetti F, Del Giudice E, Furegato S, Passarotto M and Leon A (2003). Cannabinoids ablate release of TNF- α in rat microglial cells stimulated with lipopolysaccharide. *Glia* **41**(2):161-168.

Fasia L, Karava V and Siafaka-Kapadai A (2003). Uptake and metabolism of [3 H]anandamide by rabbit platelets. Lack of transporter? *Eur J Biochem* **270**(17):3498-3506.

Fegley D, Gaetani S, Duranti A, Tontini A, Mor M, Tarzia G and Piomelli D (2005). Characterization of the fatty acid amide hydrolase inhibitor cyclohexyl carbamic acid 3'-carbamoyl-biphenyl-3-yl ester (URB597): effects on anandamide and oleylethanolamide deactivation. *J Pharmacol Exp Ther* **313**(1):352-358.

Felder CC, Dickason-Chesterfield AK and Moore SA (2006). Cannabinoids biology: the search for new therapeutic targets. *Mol Interv* **6**(3):149-161.

Fierro IM, Nascimento-DaSilva V, Arruda MA, Freitas MS, Plotkowski MC, Cunha FQ and Barja-Fidalgo C (1999). Induction of NOS in rat blood PMN *in vivo* and *in vitro*: modulation by tyrosine kinase and involvement in bactericidal activity. *J Leukoc Biol* **65**(4):508-514.

Fiori JL, Sanghvi M, O'Connell MP, Krzysik-Walker SM, Moaddel R and Bernier M (2011). The cannabinoid receptor inverse agonist AM251 regulates the expression of the EGF receptor and its ligands via destabilization of oestrogen-related receptor α protein. *Br J Pharmacol* **164**(3):1026-1040.

Fisher M and Zipser R (1985). Increased excretion of immunoreactive thromboxane B₂ in cerebral ischemia. *Stroke* **16**(1):10-14.

Fisher M, Feuerstein G, Howells DW, Hurn PD, Kent TA, Savitz SI and Lo EH (STAIR Group) (2009). Update of the stroke therapy academic industry roundtable preclinical recommendations. *Stroke* **40**(6):2244-2250.

Flecknell P (1996). Laboratory Animal Anaesthesia. *Academic Press Limited*.

Floch A and Cavero I (1990). Influence of plasma protein content and platelet number on the potency of PAF and its antagonist RP 59227 in rabbit platelet preparations. *Br J Pharmacol* **100**(1):163-167.

Forman MB, Puett DW and Virmani R (1989). Endothelial and myocardial injury during ischemia and reperfusion: pathogenesis and therapeutic implications. *J Am Coll Cardiol* **13**(2):450-459.

Freund TF, Katona I and Piomelli D (2003). Role of endogenous cannabinoids in synaptic signaling. *Physiol Rev* **83**(3):1017-1066.

Galiègue S, Mary S, Marchand J, Dussossoy D, Carrière D, Carayon P, Bouaboula M, Shire D, Le Fur G and Casellas P (1995). Expression of central and peripheral cannabinoid receptors in human immune tissues and leukocyte subpopulations. *Eur J Biochem* **232**(1):54-61.

Galindo M, Gonzalo E, Martinez-Vidal MP, Montes S, Redondo N, Santiago B, Loza E and Pablos JL (2009). Immunohistochemical detection of intravascular platelet microthrombi in patients with lupus nephritis and anti-phospholipid antibodies. *Rheumatology* **48**(8):1003-1007.

Garcia JH, Yoshida Y, Chen H, Li Y, Zhang ZG, Lian J, Chen S and Chopp M (1993). Progression from ischemic injury to infarct following middle cerebral artery occlusion in the rat. *Am J Pathol* **142**(2):623-635.

Gasche Y, Fujimura M, Morita-Fujimura Y, Copin JC, Kawase M, Massengale J and Chan PH (1999). Early appearance of activated matrix metalloproteinase-9 after focal cerebral ischemia in mice: a possible role in blood-brain barrier dysfunction. *J Cereb Blood Flow Metab* **19**(9):1020-1028.

Gauthier KM, Baewer DV, Hittner S, Hillard CJ, Nithipatikom K, Reddy DS, Falck JR and Campbell WB (2005). Endothelium-derived 2-arachidonylglycerol: an intermediate in vasodilatory eicosanoid release in bovine coronary arteries. *Am J Physiol Heart Circ Physiol* **288**(3):H1344-1351.

Gebremedhin D, Lange AR, Campbell WB, Hillard CJ and Harder DR (1999). Cannabinoid CB₁ receptor of cat cerebral arterial muscle functions to inhibit L-type Ca²⁺ channel current. *Am J Physiol* **276**(6 Pt 2):H2085-2093.

Gehrmann J, Banati RB, Wiessner C, Hossmann KA and Kreutzberg GW (1995). Reactive microglia in cerebral ischaemia: an early mediator of tissue damage? *Neuropathol Appl Neurobiol* **21**(4):277-289.

González RG (2006). Imaging-guided acute ischemic stroke therapy: From "time is brain" to "physiology is brain". *AJNR Am J Neuroradiol* **27**(4):728-735.

Grainger J and Boachie-Ansah G (2001). Anandamide-induced relaxation of sheep coronary arteries: the role of the vascular endothelium, arachidonic acid metabolites and potassium channels. *Br J Pharmacol* **134**(5):1003-1012.

Gürsoy-Özdemir Y, Bolay H, Saribaş O and Dalkara T (2000). Role of endothelial nitric oxide generation and peroxynitrite formation in reperfusion injury after focal cerebral ischemia. *Stroke* **31**(8):1974-1981.

Hall L, Clarke K, and Trim C (2002). *Veterinary Anesthesia. Saunders Publishing.*

Hancock JT, Desikan R and Neill SJ (2001). Role of reactive oxygen species in cell signalling pathways. *Biochem Soc Trans* **29**(Pt 2):345-350.

Harris AK, Ergul A, Kozak A, Machado LS, Johnson MH and Fagan SC (2005). Effect of neutrophil depletion on gelatinase expression, edema formation and hemorrhagic transformation after focal ischemic stroke. *BMC Neurosci* **6**:49.

Hatcher MA and Starr JA (2011). Role of tissue plasminogen activator in acute ischemic stroke. *Ann Pharmacother* **45**(3):364-371.

Heo JH, Han SW and Lee SK (2005). Free radicals as triggers of brain edema formation after stroke. *Free Radic Biol Med* **39**(1):51-70.

Hertz L (2008). Bioenergetics of cerebral ischemia: a cellular perspective. *Neuropharmacology* **55**(3):289-309.

Herz RC, Gaillard PJ, de Wildt DJ and Versteeg DH (1996). Differences in striatal extracellular amino acid concentrations between Wistar and Fischer 344 rats after middle cerebral artery occlusion. *Brain Res* **715**(1-2):163-171.

Hillard CJ (2000). Endocannabinoids and vascular function. *J Pharmacol Exp Ther* **294**(1):27-32.

Hillard CJ, Ho WS, Thompson J, Gauthier KM, Wheelock CE, Huang H and Hammock BD (2007). Inhibition of 2-arachidonoylglycerol catabolism modulates vasoconstriction of rat middle cerebral artery by the thromboxane mimetic, U-46619. *Br J Pharmacol* **152**(5):691-698.

Hossmann KA (2008). Cerebral ischemia: models, methods and outcomes. *Neuropharmacology* **55**(3):257-270.

Howlett AC, Qualy JM and Khachatrian LL (1986). Involvement of G_i in the inhibition of adenylate cyclase by cannabimimetic drugs. *Mol Pharmacol* **29**(3):307-313.

Ito D, Imai Y, Ohsawa K, Nakajima K, Fukuuchi Y and Kohsaka S (1998). Microglia-specific localisation of a novel calcium binding protein, Iba1. *Brain Res Mol Brain Res* **57**(1):1-9.

Ito D, Tanaka K, Suzuki S, Dembo T and Fukuuchi Y (2001). Enhanced expression of Iba1, ionized calcium-binding adapter molecule 1, after transient focal cerebral ischemia in rat brain. *Stroke* **32**(5):1208-1215.

Járai Z, Wagner JA, Varga K, Lake KD, Compton DR, Martin BR, Zimmer AM, Bonner TI, Buckley NE, Mezey E, Razdan RK, Zimmer A and Kunos G (1999). Cannabinoid-induced mesenteric vasodilation through an endothelial site distinct from CB₁ or CB₂ receptors. *Proc Natl Acad Sci USA* **96**(24):14136-14141.

Járai Z, Wagner JA, Goparaju SK, Wang L, Razdan RK, Sugiura T, Zimmer AM, Bonner TI, Zimmer A and Kunos G (2000). Cardiovascular effects of 2-arachidonoylglycerol in anesthetized mice. *Hypertension* **35**(2):679-684.

Jørgensen HS, Nakayama H, Raaschou HO and Olsen TS (1994). Effect of blood pressure and diabetes on stroke in progression. *Lancet* **344**(8916):156-159.

Joseph R, D'Andrea G, Oster SB and Welch KM (1989). Whole blood platelet function in acute ischemic stroke. Importance of dense body secretion and effects of antithrombotic agents. *Stroke* **20**(1):38-44.

Jun D, Kuca K, Hronek M and Opletal L (2006). Effect of some acetylcholinesterase reactivators on human platelet aggregation *in vitro*. *J Appl Toxicol* **26**(3):258-261.

Kalinichev M, Robbins MJ, Hartfield EM, Maycox PR, Moore SH, Savage KM, Austin NE and Jones DN (2008). Comparison between intraperitoneal and subcutaneous phencyclidine administration in Sprague-Dawley rats: a locomotor activity and gene induction study. *Prog Neuropsychopharmacol Biol Psychiatry* **32**(2):414-422.

Kaliszewski C, Fernandez LA, Wicke JD (1988). Differences in mortality rate between abrupt and progressive carotid ligation in the gerbil: role of endogenous angiotensin II. *J Cereb Blood Flow Metab* **8**(2):149-154.

Kaminski KA, Bonda TA, Korecki J and Musial WJ (2002). Oxidative stress and neutrophil activation--the two keystones of ischemia/reperfusion injury. *Int J Cardiol* **86**(1):41-59.

Kathuria S, Gaetani S, Fegley D, Valiño F, Duranti A, Tontini A, Mor M, Tarzia G, La Rana G, Calignano A, Giustino A, Tattoli M, Palmery M, Cuomo V and Piomelli D (2003). Modulation of anxiety through blockade of anandamide hydrolysis. *Nat Med* **9**(1):76-81.

Katona I, Sperlagh B, Magloczky Z, Santha E, Kofalvi A, Czirjak S, Mackie K, Vizi ES and Freund TF (2000). GABAergic interneurons are the targets of cannabinoid actions in the human hippocampus. *Neuroscience* **100**(4):797-804.

Kawamura S, Yasui N, Shirasawa M and Fukasawa H (1990). Therapeutic effects of hyperbaric oxygenation on acute focal cerebral ischemia in rats. *Surg Neurol* **34**(2):101-106.

Keown OP, Winterburn TJ, Wainwright CL, Macrury SM, Neilson I, Barrett F, Leslie SJ and Megson IL (2010). 2-Arachidonylglycerol activates platelets via conversion to arachidonic acid and not by direct activation of cannabinoid receptors. *Br J Clin Pharmacol* **70**(2):180-188.

Kimura M, Sawada K, Miyagawa T, Kuwada M, Katayama K and Nishizawa Y (1998). Role of glutamate receptors and voltage-dependent calcium and sodium channels in the extracellular glutamate/aspartate accumulation and subsequent neuronal injury induced by oxygen/glucose deprivation in cultured hippocampal neurons. *J Pharmacol Exp Ther* **285**(1):178-185.

Kitagawa K, Matsumoto M, Yang G, Mabuchi T, Yagita Y, Hori M and Yanagihara T (1998). Cerebral ischemia after bilateral carotid artery occlusion and intraluminal suture occlusion in mice: evaluation of the patency of the posterior communicating artery. *J Cereb Blood Flow Metab* **18**(5):570-579.

Koizumi J, Yoshida Y, Nazakawa T and Ooneda G (1986). Experimental studies of ischemic brain edema, I: a new experimental model of cerebral embolism in rats in which recirculation can be introduced in the ischemic area. *Jpn J Stroke* **8**:1-8.

Koob AO, Colby JM and Borgens RB (2008). Behavioral recovery from traumatic brain injury after membrane reconstruction using polyethylene glycol. *J Biol Eng* **2**:9.

Kozak KR, Crews BC, Ray JL, Tai HH, Morrow JD and Marnett LJ (2001). Metabolism of prostaglandin glycerol esters and prostaglandin ethanolamides *in vitro* and *in vivo*. *J Biol Chem* **276**(40):36993-36998.

Kozak KR, Prusakiewicz JJ and Marnett LJ (2004). Oxidative metabolism of endocannabinoids by COX-2. *Curr Pharm Des* **10**(6):659-667.

Kurata M, Ishizuka N, Matsuzawa M, Haruta K and Takeda K (1995). A comparative study of whole-blood platelet aggregation in laboratory animals: its species differences and comparison with turbidimetric method. *Comp Biochem Physiol C Pharmacol Toxicol Endocrinol* **112**(3):359-365.

Lad N, Lunt DO and Tuffin DP (1987). The effect of thromboxane A₂ synthesis inhibitors on platelet aggregation in whole blood. *Thromb Res* **46**(4):555-566.

Lake KD, Martin BR, Kunos G and Varga K (1997). Cardiovascular effects of anandamide in anesthetized and conscious normotensive and hypertensive rats. *Hypertension* **29**(5):1204-1210.

Lakhan SE, Kirchgessner A and Hofer M (2009). Inflammatory mechanisms in ischemic stroke: therapeutic approaches. *J Transl Med* **7**:97.

Lalancette-Hébert M, Gowing G, Simard A, Weng YC and Kriz J (2007). Selective ablation of proliferating microglial cells exacerbates ischemic injury in the brain. *J Neurosci* **27**(10):2596-2605.

Lansberg MG, Thijs VN, Bammer R, Kemp S, Wijman CA, Marks MP and Albers GW (2007). Risk factors of symptomatic intracerebral hemorrhage after tPA therapy for acute stroke. *Stroke* **38**(8):2275-2278.

Landsman RS, Makriyannis A, Deng H, Consroe P, Roeske WR and Yamamura HI (1998). AM630 is an inverse agonist at the human cannabinoid CB₁ receptor. *Life Sci* **62**(9):PL109-113.

Lefkovits J, Plow EF and Topol EJ (1995). Platelet glycoprotein IIb/IIIa receptors in cardiovascular medicine. *N Engl J Med* **332**(23):1553-1559.

Leker RR, Gai N, Mechoulam R and Ovadia H (2003). Drug-induced hypothermia reduces ischemic damage: effects of the cannabinoid HU-210. *Stroke* **34**(8):2000-2006.

Li B, Sedlacek M, Manoharan I, Boopathy R, Duysen EG, Masson P and Lockridge O (2005). Butyrylcholinesterase, paraoxonase, and albumin esterase, but not carboxylesterase, are present in human plasma. *Biochem Pharmacol* **70**(11):1673-1684.

Li Z, Delaney MK, O'Brien KA and Du X (2010). Signaling during platelet adhesion and activation. *Arterioscler Thromb Vasc Biol* **30**(12):2341-2349.

Liebeskind DS (2003). Collateral circulation. *Stroke* **34**(9):2279-2284.

Lo EH, Rogowska J, Bogorodzki P, Trocha M, Matsumoto K, Saffran B and Wolf GL (1996). Temporal correlation analysis of penumbral dynamics in focal cerebral ischemia. *J Cereb Blood Flow Metab* **16**(1):60-68.

Long JZ, Li W, Booker L, Burston JJ, Kinsey SG, Schlosburg JE, Pavón FJ, Serrano AM, Selley DE, Parsons LH, Lichtman AH and Cravatt BF (2009). Selective blockade of 2-arachidonoylglycerol hydrolysis produces cannabinoid behavioral effects. *Nat Chem Biol* **5**(1):37-44.

Longa EZ, Weinstein PR, Carlson S and Cummins R (1989). Reversible middle cerebral artery occlusion without craniectomy in rats. *Stroke* **20**(1):84-91.

Lopez-Bresnahan MV, Kearse LA Jr, Yanez P and Young TI (1993). Anterior communicating artery collateral flow protection against ischemic change during carotid endarterectomy. *J Neurosurg* **79**(3):379-382.

Luo J, Borgens R and Shi R (2004). Polyethylene glycol improves function and reduces oxidative stress in synaptosomal preparations following spinal cord injury. *J Neurotrauma* **21**(8):994-1007.

McIlvoy LH (2005). The effect of hypothermia and hyperthermia on acute brain injury. *AACN Clin Issues* **16**(4):488-500.

Mabuchi T, Kitagawa K, Ohtsuki T, Kuwabara K, Yagita Y, Yanagihara T, Hori M and Matsumoto M (2000). Contribution of microglia/macrophages to expansion of infarction and response of oligodendrocytes after focal cerebral ischemia in rats. *Stroke* **31**(7):1735-1743.

Maccarrone M, Bari M, Menichelli A, Del Principe D and Agrò AF (1999). Anandamide activates human platelets through a pathway independent of the arachidonate cascade. *FEBS Lett* **447**(2-3):277-282.

Maccarrone M, Bari M, Menichelli A, Giuliani E, Del Principe D and Finazzi-Agrò A (2001). Human platelets bind and degrade 2-arachidonoylglycerol, which activates these cells through a cannabinoid receptor. *Eur J Biochem* **268**(3):819-825.

Maccarrone M, Bari M, Battista N and Finazzi-Agrò A (2002). Estrogen stimulates arachidonoylethanolamide release from human endothelial cells and platelet activation. *Blood* **100**(12):4040-4048.

Maccarrone M, Bari M, Del Principe D and Finazzi-Agrò A (2003). Activation of human platelets by 2-arachidonoylglycerol is enhanced by serotonin. *Thromb Haemost* **89**(2):340-347.

Mackie K (2005). Distribution of cannabinoid receptors in the central and peripheral nervous system. *Handb Exp Pharmacol* (168):299-325.

Macrae IM (1992). New models of focal cerebral ischaemia. *Br J Clin Pharmacol* **34**(4): 302–308.

Mannucci L, Redaelli R and Tremoli E (1988). Effects of aggregating agents and of blood cells on the aggregation of whole blood by impedance technique. *Thromb Res* **52**(2):143-151.

Marrs WR, Blankman JL, Horne EA, Thomazeau A, Lin YH, Coy J, Bodor AL, Muccioli GG, Hu SS, Woodruff G, Fung S, Lafourcade M, Alexander JP, Long JZ, Li W, Xu C, Möller T, Mackie K, Manzoni OJ, Cravatt BF and Stella N (2010). The serine hydrolase ABHD6 controls the accumulation and efficacy of 2-AG at cannabinoid receptors. *Nat Neurosci* **13**(8):951-957.

Mauler F, Mittendorf J, Horváth E and De Vry J (2002). Characterization of the diarylether sulfonylester (-)-(R)-3-(2-hydroxymethylindanyl-4-oxy)phenyl-4,4,4-trifluoro-1-sulfonate (BAY 38-7271) as a potent cannabinoid receptor agonist with neuroprotective properties. *J Pharmacol Exp Ther* **302**(1):359-368.

Matalon S, Hardiman KM, Jain L, Eaton DC, Kotlikoff M, Eu JP, Sun J, Meissner G and Stamler JS (2003). Regulation of ion channel structure and function by reactive oxygen-nitrogen species. *Am J Physiol Lung Cell Mol Physiol* **285**(6):L1184-1189.

Mergenthaler P, Dirnagl U and Meisel A (2004). Pathophysiology of stroke: lessons from animal models. *Metab Brain Dis* **19**(3-4):151-167.

Minagawa T, Kohno Y, Suwa T and Tsuji A (1995). Species differences in hydrolysis of isocarbacyclin methyl ester (TEI-9090) by blood esterases. *Biochem Pharmacol* **49**(10):1361-1365.

Molina CA, Alvarez-Sabín J, Montaner J, Abilleira S, Arenillas JF, Coscojuela P, Romero F and Codina A (2002). Thrombolysis-related hemorrhagic infarction: a marker of early reperfusion, reduced infarct size, and improved outcome in patients with proximal middle cerebral artery occlusion. *Stroke* **33**(6):1551-1556.

Molina-Holgado F, Pinteaux E, Moore JD, Molina-Holgado E, Guaza C, Gibson RM and Rothwell NJ (2003). Endogenous interleukin-1 receptor antagonist mediates anti-inflammatory and neuroprotective actions of cannabinoids in neurons and glia. *J Neurosci* **23**(16):6470-6474.

Morley P, Hogan MJ and Hakim AM (1994). Calcium-mediated mechanisms of ischemic injury and protection. *Brain Pathol* **4**(1):37-47.

Schomacher M, Müller HD, Sommer C, Schwab S and Schäbitz WR (2008). Endocannabinoids mediate neuroprotection after transient focal cerebral ischemia. *Brain Res* **1240**:213-220.

Munro S, Thomas KL and Abu-Shaar M (1993). Molecular characterization of a peripheral receptor for cannabinoids. *Nature* **365**(6441):61-65.

Muthian S, Rademacher DJ, Roelke CT, Gross GJ and Hillard CJ (2004). Anandamide content is increased and CB₁ cannabinoid receptor blockade is protective during transient, focal cerebral ischemia. *Neuroscience* **129**(3):743-750.

Naccarato M, Pizzuti D, Petrosino S, Simonetto M, Ferigo L, Grandi FC, Pizzolato G and Di Marzo V (2010). Possible Anandamide and Palmitoylethanolamide involvement in human stroke. *Lipids Health Dis* **9**:47.

Nagasawa H and Kogure K (1989). Correlation between cerebral blood flow and histologic changes in a new rat model of middle cerebral artery occlusion. *Stroke* **20**(8):1037-1043.

Nagayama T, Sinor AD, Simon RP, Chen J, Graham SH, Jin K and Greenberg DA (1999). Cannabinoids and neuroprotection in global and focal cerebral ischemia and in neuronal cultures. *J Neurosci* **19**(8):2987-2995.

Neumann J, Gunzer M, Gutzeit HO, Ullrich O, Reymann KG and Dinkel K (2006). Microglia provide neuroprotection after ischemia. *FASEB J* **20**(6):714-716.

New DC and Wong YH (2003). BML-190 and AM251 act as inverse agonists at the human cannabinoid CB₂ receptor: signalling via cAMP and inositol phosphates. *FEBS Lett* **536**(1-3):157-60.

Nicotera P, Leist M and Ferrando-May E (1998). Intracellular ATP, a switch in the decision between apoptosis and necrosis. *Toxicol Lett* **102-103**:139-142.

Nishizawa Y (2001). Glutamate release and neuronal damage in ischemia. *Life Sci* **69**(4):369-381.

Olah L, Franke C, Schwindt W and Hoehn M (2000). CO₂ reactivity measured by perfusion MRI during transient focal cerebral ischemia in rats. *Stroke* **31**(9):2236-2244.

Oliff HS, Coyle P and Weber E (1997). Rat strain and vendor differences in collateral anastomoses. *J Cereb Blood Flow Metab* **17**(5):571-576.

Omae T, Mayzel-Oreg O, Li F, Sotak CH and Fisher M (2000). Inapparent hemodynamic insufficiency exacerbates ischemic damage in a rat microembolic stroke model. *Stroke* **31**(10):2494-2499.

Osborne KA, Shigeno T, Balarsky AM, Ford I, McCulloch J, Teasdale GM and Graham DI (1987). Quantitative assessment of early brain damage in a rat model of focal cerebral ischaemia. *J Neurol Neurosurg Psychiatry* **50**(4):402-410.

Pacher P, Batkai S and Kunos G (2005). Cardiovascular pharmacology of cannabinoids. *Handb Exp Pharmacol* (168):599-625.

Pacher P, Batkai S and Kunos G (2006). The endocannabinoid system as an emerging target of pharmacotherapy. *Pharmacol Rev* **58**(3):389-462.

Pacher P, Mukhopadhyay P, Mohanraj R, Godlewski G, Batkai S and Kunos G (2008). Modulation of the endocannabinoid system in cardiovascular disease: therapeutic potential and limitations. *Hypertension* **52**(4):601-607.

Pan B, Wang W, Long JZ, Sun D, Hillard CJ, Cravatt BF and Liu QS (2009). Blockade of 2-arachidonoylglycerol hydrolysis by selective monoacylglycerol lipase inhibitor 4-nitrophenyl 4-(dibenzo[d][1,3]dioxol-5-yl(hydroxy)methyl)piperidine-1-carboxylate (JZL184) Enhances retrograde endocannabinoid signaling. *J Pharmacol Exp Ther* **331**(2):591-597.

Panikashvili D, Simeonidou C, Ben-Shabat S, Hanus L, Breuer A, Mechoulam R and Shohami E (2001). An endogenous cannabinoid (2-AG) is neuroprotective after brain injury. *Nature* **413**(6855):527-531.

Panikashvili D, Shein NA, Mechoulam R, Trembovler V, Kohen R, Alexandrovich A and Shohami E (2006). The endocannabinoid 2-AG protects the blood-brain barrier after closed head injury and inhibits mRNA expression of proinflammatory cytokines. *Neurobiol Dis* **22**(2):257-264.

Pardridge WM (2003). Blood-brain barrier drug targeting: the future of brain drug development. *Mol Interv* **3**(2):90-105.

Park CK, Mendelow AD, Graham DI, McCulloch J and Teasdale GM. (1988). Correlation of triphenyltetrazolium chloride perfusion staining with conventional neurohistology in the detection of early brain ischemia. *Neuropathol Appl Neurobiol* **14**:289–298.

Pelagalli A, Lombardi P, d'Angelo D, Della Morte R, Avallone L and Staiano N (2002). Species variability in platelet aggregation response to different agonists. *J Comp Pathol* **127**(2-3):126-132.

Peng TI and Jou MJ (2010). Oxidative stress caused by mitochondrial calcium overload. *Ann N Y Acad Sci* **1201**:183-8.

Peroni RN, Orliac ML, Becu-Villalobos D, Huidobro-Toro JP, Adler-Graschinsky E and Celuch SM (2004). Sex-linked differences in the vasorelaxant effects of anandamide in vascular mesenteric beds: role of oestrogens. *Eur J Pharmacol* **493**(1-3):151-160.

Pertwee RG (2005). Inverse agonism and neutral antagonism at cannabinoid CB₁ receptors. *Life Sci* **76**(12):1307-1324.

Pertwee RG, Howlett AC, Abood ME, Alexander SP, Di Marzo V, Elphick MR, Greasley PJ, Hansen HS, Kunos G, Mackie K, Mechoulam R and Ross RA (2010). International Union of Basic and Clinical Pharmacology. LXXIX. Cannabinoid receptors and their ligands: beyond CB₁ and CB₂. *Pharmacol Rev* **62**(4):588-631.

Pettit DA, Harrison MP, Olson JM, Spencer RF and Cabral GA (1998). Immunohistochemical localization of the neural cannabinoid receptor in rat brain. *J Neurosci Res* **51**(3):391-402.

Phan TG, Wright PM, Markus R, Howells DW, Davis SM and Donnan GA (2002). Salvaging the ischaemic penumbra: more than just reperfusion? *Clin Exp Pharmacol Physiol* **29**(1-2):1-10.

Pignataro G, Gala R, Cuomo O, Tortiglione A, Giaccio L, Castaldo P, Sirabella R, Matrone C, Canitano A, Amoroso S, Di Renzo G and Annunziato L (2004). Two sodium/calcium exchanger gene products, NCX1 and NCX3, play a major role in the development of permanent focal cerebral ischemia. *Stroke* **35**(11):2566-2570.

Pratt PF, Hillard CJ, Edgmond WS and Campbell WB (1998). N-arachidonylethanolamide relaxation of bovine coronary artery is not mediated by CB₁ cannabinoid receptor. *Am J Physiol* **274**(1 Pt 2):H375-381.

Puffenbarger RA, Boothe AC and Cabral GA (2000). Cannabinoids inhibit LPS-inducible cytokine mRNA expression in rat microglial cells. *Glia* **29**(1):58-69.

Racz I, Nadal X, Alferink J, Baños JE, Rehnelt J, Martín M, Pintado B, Gutierrez-Adan A, Sanguino E, Manzanares J, Zimmer A and Maldonado R (2008). Crucial role of CB₂ cannabinoid receptor in the regulation of central immune responses during neuropathic pain. *J Neurosci* **28**(46):12125-12135.

Randall MD (2007). Endocannabinoids and the haematological system. *Br J Pharmacol* **152**(5):671-675.

Romano MR and Lograno MD (2006). Cannabinoid agonists induce relaxation in the bovine ophthalmic artery: evidences for CB₁ receptors, nitric oxide and potassium channels. *Br J Pharmacol* **147**(8):917-925.

Romero-Sandoval EA, Horvath R, Landry RP and DeLeo JA (2009). Cannabinoid receptor type 2 activation induces a microglial anti-inflammatory phenotype and reduces migration via MKP induction and ERK dephosphorylation. *Mol Pain* **5**:25.

Rordorf G, Cramer SC, Efird JT, Schwamm LH, Buonanno F and Koroshetz WJ (1997). Pharmacological elevation of blood pressure in acute stroke. Clinical effects and safety. *Stroke* **28**(11):2133-2138.

Ross RA, Brockie HC, Stevenson LA, Murphy VL, Templeton F, Makriyannis A and Pertwee RG (1999). Agonist-inverse agonist characterization at CB₁ and CB₂ cannabinoid receptors of L759633, L759656, and AM630. *Br J Pharmacol* **126**(3):665-672.

Rupalla K, Allegrini PR, Sauer D and Wiessner C (1998). Time course of microglia activation and apoptosis in various brain regions after permanent focal cerebral ischemia in mice. *Acta Neuropathol* **96**(2):172-178.

Ryberg E, Larsson N, Sjögren S, Hjorth S, Hermansson NO, Leonova J, Elebring T, Nilsson K, Drmota T and Greasley PJ (2007). The orphan receptor GPR55 is a novel cannabinoid receptor. *Br J Pharmacol* **152**(7):1092-1101.

Saario SM, Salo OM, Nevalainen T, Poso A, Laitinen JT, Järvinen T and Niemi R (2005). Characterization of the sulfhydryl-sensitive site in the enzyme responsible for hydrolysis of 2-arachidonoylglycerol in rat cerebellar membranes. *Chem Biol* **12**(6):649-656.

Schmid-Elsaesser R, Zausinger S, Hungerhuber E, Baethmann A and Reulen HJ (1998). A critical reevaluation of the intraluminal thread model of focal cerebral ischemia: evidence of inadvertent premature reperfusion and subarachnoid hemorrhage in rats by laser Doppler flowmetry. *Stroke* **29**(10):2162-2170.

Scremin OU (2004). The human nervous system (2nd edition). Chapter 37. Cerebral vascular system. *Elsevier (USA)*.

Shapira Y, Lam AM, Paez A, Artru AA, Laohaprasit V and Donato T (1997). The influence of acute and chronic alcohol treatment on brain edema, cerebral infarct volume and neurological outcome following experimental head trauma in rats. *J Neurosurg Anesthesiol* **9**(2):118-127.

Shearer J, Kane K, Carswell H and Coker S (2009). Does gender modify the effect of 2-arachidonoylglycerol on platelet aggregation in rat whole blood? <http://pa2online.org>.

Shin HK, Dunn AK, Jones PB, Boas DA, Lo EH, Moskowitz MA and Ayata C (2007). Normobaric hyperoxia improves cerebral blood flow and oxygenation, and inhibits peri-infarct depolarizations in experimental focal ischaemia. *Brain* **130**(Pt 6):1631-1642.

Sims NR and Muyderman H (2010). Mitochondria, oxidative metabolism and cell death in stroke. *Biochim Biophys Acta* **1802**(1):80-91.

Singhal AB, Wang X, Sumii T, Mori T and Lo EH (2002). Effects of normobaric hyperoxia in a rat model of focal cerebral ischemia-reperfusion. *J Cereb Blood Flow Metab* **22**(7):861-8.

Sleator A and Allen G (2000). Research paper: Cannabis. *House of Commons Library* (00/74).

Slivka A, Murphy E and Horrocks L (1995). Cerebral edema after temporary and permanent middle cerebral artery occlusion in the rat. *Stroke* **26**(6):1061-1066.

Solenski NJ, diPierro CG, Trimmer PA, Kwan AL and Helm GA (2002). Ultrastructural changes of neuronal mitochondria after transient and permanent cerebral ischemia. *Stroke* **33**(3):816-824.

Spigelman MK, Zappulla RA, Johnson J, Goldsmith SJ, Malis LI and Holland JF (1984). Etoposide-induced blood-brain barrier disruption. Effect of drug compared with that of solvents. *J Neurosurg* **61**(4):674-678.

Stella N, Schweitzer P and Piomelli D (1997). A second endogenous cannabinoid that modulates long-term potentiation. *Nature* **388**(6644):773-778.

Sugiura T, Kishimoto S, Oka S and Gokoh M (2006). Biochemistry, pharmacology and physiology of 2-arachidonoylglycerol, an endogenous cannabinoid receptor ligand. *Prog Lipid Res* **45**(5):405-446.

Sugiura T, Kondo S, Sukagawa A, Nakane S, Shinoda A, Itoh K, Yamashita A and Waku K (1995). 2-Arachidonoylglycerol: a possible endogenous cannabinoid receptor ligand in brain. *Biochem Biophys Res Commun* **215**(1):89-97.

Svíženská I, Dubový P and Sulcová A (2008). Cannabinoid receptors 1 and 2 (CB₁ and CB₂), their distribution, ligands and functional involvement in nervous system structures--a short review. *Pharmacol Biochem Behav* **90**(4):501-511.

Szydłowska K and Tymianski M (2010). Calcium, ischemia and excitotoxicity. *Cell Calcium* **47**(2):122-129.

Tamura A, Graham DI, McCulloch J and Teasdale GM (1981). Focal cerebral ischaemia in the rat: 1. Description of technique and early neuropathological consequences following middle cerebral artery occlusion. *J Cereb Blood Flow Metab* **1**(1):53-60.

Tohgi H, Suzuki H, Tamura K and Kimura B (1991). Platelet volume, aggregation, and adenosine triphosphate release in cerebral thrombosis. *Stroke* **22**(1):17-21.

Twitchell W, Brown S and Mackie K (1997). Cannabinoids inhibit N- and P/Q-type calcium channels in cultured rat hippocampal neurons. *J Neurophysiol* **78**(1):43-50.

Uchiyama S, Takeuchi M, Osawa M, Kobayashi I, Maruyama S, Aosaki M and Hirosawa K (1983). Platelet function tests in thrombotic cerebrovascular disorders. *Stroke* **14**(4):511-517.

Van der Stelt M, Veldhuis WB, Maccarrone M, Bär PR, Nicolay K, Veldink GA, Di Marzo V and Vliegthart JF (2002). Acute neuronal injury, excitotoxicity, and the endocannabinoid system. *Mol Neurobiol* **26**(2-3):317-346.

Vandevorde S, Jonsson KO, Labar G, Persson E, Lambert DM and Fowler CJ (2007). Lack of selectivity of URB602 for 2-oleoylglycerol compared to anandamide hydrolysis *in vitro*. *Br J Pharmacol* **150**(2):186-191.

Varga K, Wagner JA, Bridgen DT and Kunos G (1998). Platelet- and macrophage-derived endogenous cannabinoids are involved in endotoxin-induced hypotension. *FASEB J* **12**(11):1035-1044.

Wagner JA, Járαι Z, Bátkai S and Kunos G (2001). Hemodynamic effects of cannabinoids: coronary and cerebral vasodilation mediated by cannabinoid CB₁ receptors. *Eur J Pharmacol* **423**(2-3):203-210.

Waksman Y, Olson JM, Carlisle SJ and Cabral GA (1999). The central cannabinoid receptor (CB₁) mediates inhibition of nitric oxide production by rat microglial cells. *J Pharmacol Exp Ther* **288**(3):1357-1366.

Walter L, Franklin A, Witting A, Wade C, Xie Y, Kunos G, Mackie K and Stella N (2003). Nonpsychotropic cannabinoid receptors regulate microglial cell migration. *J Neurosci* **23**(4):1398-1405.

Wang Q, Tang XN and Yenari MA (2007). The inflammatory response in stroke. *J Neuroimmunol* **184**(1-2):53-68.

White R, Ho WS, Bottrill FE, Ford WR and Hiley CR (2001). Mechanisms of anandamide-induced vasorelaxation in rat isolated coronary arteries. *Br J Pharmacol* **134**(4):921-929.

Winocour PD, Chignier E, Parmentier S and McGregor JL (1992). A member of the selectin family (GMP-140/PADGEM) is expressed on thrombin-stimulated rat platelets *in vitro*. *Comp Biochem Physiol Comp Physiol* **102**(2):265-271.

Zeller JA, Tschoepe D and Kessler C (1999). Circulating platelets show increased activation in patients with acute cerebral ischemia. *Thromb Haemost* **81**(3):373-377.

Zhang M, Martin BR, Adler MW, Razdan RK, Ganea D and Tuma RF (2008). Modulation of the balance between cannabinoid CB₁ and CB₂ receptor activation during cerebral ischemic/reperfusion injury. *Neuroscience* **152**(3):753-760.

Zhao YJ, Yang GY and Domino EF (1997). Acute ethanol effects on focal cerebral ischemia in non-fasted rats. *Alcohol Clin Exp Res* **21**(4):745-748.

Zhuang SY, Bridges D, Grigorenko E, McCloud S, Boon A, Hampson RE and Deadwyler SA (2005). Cannabinoids produce neuroprotection by reducing intracellular calcium release from ryanodine-sensitive stores. *Neuropharmacology* **48**(8):1086-1096.

APPENDICES

APPENDIX A: EQUIPMENT AND MATERIALS

Suppliers of Equipment and Materials:

Equipment and Materials	Supplier
3-way stopcock	B. Braun Melsungen, Melsungen, Germany
25G hypodermic needle	BD UK, Oxford, UK
23G hypodermic needle	BD UK, Oxford, UK
Tracheal cannula (Anicath I.V. Cannula 16G)	Dunlops Veterinary Supplies, Dumfries, UK
Blood gas analyser (i-STAT) and consumables	Abbott Laboratories, Berkshire, UK
Bead Steriliser (Germinator 500)	Cellpoint Scientific, Gaithersburg, US
Blood pressure recorder (Gould, Easygraf)	Data Sciences International, Hertogenbosch, Netherlands
Confocal microscope	Leica Microsystems (UK) Ltd, Milton Keynes, UK
Data acquisition and analysis system: MCID Po-Ne-Mah Volocity	InterFocus Imaging Ltd, Linton, Cambridge, UK Linton, Diss, Norfolk, UK PerkinElmer, Cambridge, UK
Dental drill	Nakanishi Inc, Stevenage, UK
Diathermy unit (TDB60 Bipolar Coagulation Unit)	Eschmann Equipment, Lancing, West Sussex, UK
Disposable stir bars	Labmedics, Stockport, UK
Fibre optic lamp (Volpi Intralux)	Stemmer Imaging Ltd, Tongham, UK
Glass coverslips	VWR Ltd, Leicestershire, UK
Glass slides	VWR Ltd, Leicestershire, UK
Glass thermometer	VWR Ltd, Leicestershire, UK
Heat lamp	RS Components, Northamptonshire, UK
Homeothermic blanket	Harvard Apparatus, Kent, UK
Hydrophobic barrier pen	Vector Laboratories, Peterborough, UK

Suppliers of Equipment and Materials (continued):

Equipment and Materials	Supplier
Intraluminal filament: Nylon Monofilament (3-0; Dermalon) Silicon coated filaments (4-0)	Tyco Healthcare, Gosport, UK Docol Corporation, California, UK
Laser Doppler	Moor Instruments, Axminster, UK
Low temperature cautery pen	Royem Scientific Ltd, Bedfordshire, UK
Plastic cuvettes	Labmedics, Stockport, UK
Polythene tubing (non-sterile)	SIMS Portex, Hythe, Kent, UK
Pulse-oximeter / capnograph (Medair Lifesense)	Kruuse Ltd, Leeds, UK
Rectal thermometer (Physitemp, thermalert)	Linton, Diss, Norfolk, UK
Surgical microscope (Zeiss S21)	Microscope Systems Scotland, Glasgow, UK
Suture (4-0; Ethicon, mersilk)	Southern Syringe Services, London, UK
Syringes (1, 2 and 5 ml)	BD UK, Oxford, UK
Syringe infusion pump	Harvard Apparatus, Kent, UK
Triangular swabs	Royem Scientific Ltd, Bedfordshire, UK
Rodent Ventilator	Harvard Apparatus, Kent, UK
Chrono-log whole blood aggregometer	Labmedics, Stockport, UK

Materials for *In Vivo* Experiments

The trachea was cannulated using the plastic cover from a 16G i.v. cannula that was 45 mm in length and the blunted needle was used as a guide. The tracheal cannula was coated in lignocaine (2%) prior to intubation in order to prevent bronchospasm during manipulation of the trachea. For carotid artery cannulation, polyethylene tubing (0.58 mm ID and 0.96 mm OD) of approximately 30 cm in length was prepared and connected to a 3-way stopcock with a 23 G hypodermic needle. For cannulation of the femoral artery and vein, polyethylene tubing (0.4 mm ID and 0.8 mm OD) of 40 cm in length was prepared in order to reach the blood pressure transducer and drug infusion pump, respectively. The cannulae for the femoral artery and vein were connected to a 3-way stopcock with a 25 G needle. The end of the cannulae not connected to the needle was cut with a scalpel to form a bevelled edge which was inserted into the vessel.

APPENDIX B: SUPPLIERS OF DRUGS

Suppliers and Storage Information:

Drugs and Materials	Supplier	Storage
2-Arachidonoyl glycerol (2-AG)	Tocris Cookson, Bristol, UK	-20 °C or -80 °C (depending on solvent)
Adenosine diphosphate (ADP)	Sigma Aldrich, Poole, Dorset, UK	-20 °C
AM251	Tocris Cookson, Bristol, UK	-20 °C
AM630	Tocris Cookson, Bristol, UK	-20 °C
Anandamide	Tocris Cookson, Bristol, UK	4 °C
<u>Antibodies:</u> Anti-Iba-1 (raised in goat) FITC-conjugated anti-goat	Abcam, Cambridge, UK Vector Laboratories, Peterborough, UK	-20 °C 4 °C
Arachidonic acid	Labmedics, Stockport, UK	-20 °C (undiluted) -80 °C (in solution)
Atropine Sulfate	Sigma Aldrich, Poole, Dorset, UK	Room temperature
Betadine (alcoholic solution)	Seton Healthcare Group, Lancashire, UK	Room temperature
Chromium potassium sulfate	Sigma Aldrich, Poole, Dorset, UK	Room temperature
Collagen	Labmedics, Stockport, UK	4 °C
Dimethyl sulfoxide (DMSO)	Sigma Aldrich, Poole, Dorset, UK	Room temperature
Di-sodium hydrogen phosphate	Sigma Aldrich, Poole, Dorset, UK	Room temperature
Embedding matrix	Thermo Fisher Scientific, Loughborough, UK	4 °C
Eosin (aqueous)	Leica Microsystems Ltd, Milton Keynes, UK	Room temperature
Euthatal (sodium pentobarbital)	Merial Animal Health Ltd, Harlow, UK	Room temperature
Flurbiprofen	Sigma Aldrich, Poole, Dorset, UK	Room temperature

Suppliers and Storage Information (continued):

Drugs and Materials	Supplier	Storage
Formaldehyde	Thermo Fisher Scientific, Loughborough, UK	Room temperature
Gelatin	Sigma Aldrich, Poole, Dorset, UK	Room temperature
Haematoxylin	Leica Microsystems (UK) Ltd, Milton Keynes, UK	Room temperature
Heparin	Leo Laboratories Ltd, Princes Risborough, UK	4 °C
Histoclear	National Diagnostics, Hessle, UK	Room temperature
Histomount mounting medium	National Diagnostics, Hessle, UK	Room temperature
HU-210	Tocris Cookson, Bristol, UK	-20 °C
Hydrochloride	Sigma Aldrich, Poole, Dorset, UK	Room temperature
ICI 192,605	Gift from Astra Zeneca, Macclesfield, UK	Room temperature
Indomethacin	Sigma Aldrich, Poole, Dorset, UK	Room temperature
Isoflurane	Abbott Laboratories, Berkshire, UK	Room temperature
Isopentane	VWR Ltd, Leicestershire, UK	Room temperature
JZL184	Cayman Chemicals; Cambridge Bioscience, Cambridge, UK	-20 °C
Lignocaine (2%)	Hameln Pharmaceuticals, Gloucester, UK	Room temperature
Magnesium sulfate	Sigma Aldrich, Poole, Dorset, UK	Room temperature
Normal rabbit serum	Vector Laboratories, Peterborough, UK	4 °C
Neostigmine bromide	Sigma Aldrich, Poole, Dorset, UK	Room temperature
Paraformaldehyde	Sigma Aldrich, Poole, Dorset, UK	Room temperature

Suppliers and Storage Information (continued):

Drugs and Materials	Supplier	Storage
Polyethylene glycol (PEG-300)	Sigma Aldrich, Poole, Dorset, UK	Room temperature
Potassium chloride	Sigma Aldrich, Poole, Dorset, UK	Room temperature
Potassium di-hydrogen phosphate	Thermo Fisher Scientific, Loughborough, UK	Room temperature
Sodium bicarbonate	Sigma Aldrich, Poole, Dorset, UK	Room temperature
Sodium chloride	Sigma Aldrich, Poole, Dorset, UK	Room temperature
Sucrose	Sigma Aldrich, Poole, Dorset, UK	Room temperature
Tocrisolve	Tocris Cookson, Bristol, UK	4 °C
Triton X-100	Sigma Aldrich, Poole, Dorset, UK	Room temperature
Tween-80	Sigma Aldrich, Poole, Dorset, UK	Room temperature
URB597	Cayman Chemicals; Cambridge Bioscience, Cambridge, UK	-20 °C
Vectashield aqueous mounting medium with DAPI	Vector Laboratories, Peterborough, UK	4 °C (in the dark)